Demographic buffering in natural populations: multi-level perspective

Gabriel Santos[1], Samuel Gascoigne[2], André Dias[3], Maja Kajin[2], and Roberto Salguero-Gomez[2]

[1]National Institute of the Atlantic Forest (INMA)
[2]University of Oxford
[3]Universidade Federal do Rio de Janeiro

December 03, 2024

Abstract

Environmental stochasticity impacts population dynamics and their viability. As such, understanding how organisms cope with this variability is crucial. Here, we investigate demographic buffering, the ability of populations to maintain stable growth despite environmental fluctuations. We integrate well-established stochastic and deterministic approaches to investigate characteristics of demographic buffering, analysing stochastic elasticities and self-second derivatives of deterministic population growth rate. We test the hypothesis that buffered species exhibit low stochastic elasticity to temporal variability and signs of concave selection (i.e. negative second derivatives of population growth rate with respect to demographic processes), reducing variance in key demographic processes. Analysing 43 natural populations of 37 mammal species, we find limited support for this hypothesis. Indeed, while primates often show low stochastic elasticity, concave selection is less prevalent than expected. Our findings highlight the complex and dynamic relationship between demographic processes, environmental variability, and selection pressures in determining population persistence.

Demographic buffering in natural populations: multi-level perspective

A manuscript in preparation for submission to ECOLOGY LETTERS

Type of article: METHOD

Gabriel Silva Santos [1,2*], Samuel J L Gascoigne[3*], André Tavares Corrêa Dias[4], Maja Kajin[3,5**], Roberto Salguero-Gomez[3]

[1] National Institute of the Atlantic Forest (INMA), 29650-000, Santa Teresa, Espirito Santo, Brazil. ssantos.gabriel@gmail.com

[2] Department of Ecology, Graduate Program in Ecology and Evolution, Rio de Janeiro

State University, 524 Sao Francisco Xavier Street, 20550-900, Maracana, Rio de Janeiro, Brazil.

[3] Department of Biology, University of Oxford, South Parks Road, OX1 3RB, Oxford, UK. samuel.gascoigne@pmb.ox.ac.uk, rob.salguero@biology.ox.ac.uk

[4] Department of Ecology, Institute of Biology, Universidade Federal do Rio de Janeiro, Avenida Carlos Chagas Filho 373, 21941-590 Rio de Janeiro, RJ, Brazil. atcdias@gmail.com

[5] Chair of Zoology, Department of Biology, Biotechnical Faculty, University of Ljubljana, Večna pot 111, 1000 Ljubljana, Slovenia. maja.kajin@bf.uni-lj.si

[*]Shared first authorship

[**]Corresponding author

Shared senior authorship

AUTHOR CONTRIBUTIONS: GSS developed the initial concept, performed the statistical analyses, and contributed to the first draft of the manuscript. SJLG developed the initial concept, contributed to the first draft and all other versions of the manuscript, and generated final figures. ATCD co-advised the project and contributed significantly to final versions of the manuscript. MK developed and managed the project, contributed to the first draft and all other versions of the manuscript, and generated final figures. RSG developed and managed the project and contributed to the first draft and all other versions of the manuscript. All authors made substantial contributions to editing the manuscript and further refining ideas and interpretations.

RUNNING TITLE: Demographic buffering framework (32/45 characters)

KEYWORDS: COMADRE Animal Matrix Database, elasticity, life-history evolution, natural selection, second-order derivative, sensitivity, stochasticity, variance.

NUMBER OF WORDS: Abstract – 147/150 words, main text (excluding abstract, acknowledgements, references, table, and figure legends) – 5134/5000 words

NUMBER OF REFERENCES: 93

NUMBER OF TABLES: 2 (in Supplementary Material)

NUMBER OF FIGURES: 3

Abstract (147/150 words)

Environmental stochasticity impacts population dynamics and their viability. As such, understanding how organisms cope with this variability is crucial. Here, we investigate demographic buffering, the ability of populations to maintain stable growth despite environmental fluctuations. We integrate well-established stochastic and deterministic approaches to investigate characteristics of demographic buffering, analysing stochastic elasticities and self-second derivatives of deterministic population growth rate. We test the hypothesis that buffered species exhibit low stochastic elasticity to temporal variability and signs of concave selection (*i.e.* negative second derivatives of population growth rate with respect to demographic processes), reducing variance in key demographic processes. Analysing 43 natural populations of 37 mammal species, we find limited support for this hypothesis. Indeed, while primates often show low stochastic elasticity, concave selection is less prevalent than expected. Our findings highlight the complex and dynamic relationship between demographic processes, environmental variability, and selection pressures in determining population persistence.

Introduction

Environmental stochasticity shapes organisms' life histories (Bonsall & Klug 2011; Stearns 1992; Tuljapurkar 1990, 2010). Nonetheless, how organisms will cope with the changing variation in environmental conditions (Bathiany *et al.* 2018; Boyce *et al.* 2006; Morris *et al.* 2008) remains an intriguing ecological and evolutionary question (Sutherland *et al.* 2013). Evolutionary demography offers a range of explanations for how evolutionary processes influence demographic responses to environmental variability (Charlesworth 1994; Healy *et al.* 2019; Hilde *et al.* 2020; Pfister 1998; Tuljapurkar *et al.* 2009). However, it is stochastic demography that explicitly addresses the impacts of fluctuating environments on wild populations of plants and animals (Boyce *et al.* 2006).

Stochastic demography is grounded in the powerful approximation introduced by Tuljapurkar (Tuljapurkar 1982). This approximation posits that the long-term stochastic population growth rate (λ_ς) is directly related to the geometric mean of population growth rates over time (λ_τ) and the variance-covariance structure of demographic processes (Boyce *et al.* 2006; Tuljapurkar 1982). *An increase in* the geometric mean of λ_τ over time leads to a corresponding rise inλ_ς . Conversely, higher variance inλ_τ reduces λ_ς (Morris & Doak 2004; Tuljapurkar 1982), thereby influencing population persistence (Lefèvre *et al.* 2016).

The ability of a population to diminish the effects of environmental stochasticity on λ_ς — *βψ κεεπινγ σομε δεμογραπηις προςεσσες (ας μυςη ας ποσσιβλε) ςονσταντ οερ τιμε — ις ςαλλεδ δεμογραπηις βυφφερινγ* (Bjørkvoll *et al.* 2016; Gascoigne*et al.* 2023a, 2024b, a; Hilde *et al.* 2020; McDonald*et al.* 2016; Reed & Slade 2012; Rodríguez-Caro *et al.* 2021). *A way to test for demographic buffering is outlined by the* demographic buffering hypothesis (Pfister 1998) (Box 1). The demographic buffering hypothesis extends Tuljapurkar's approximation to state that negative covariance between *τηε ιμπαςτ οφ α δεμογραπηις προςεσς ον* λ_τ (see Box 1 for details) and *how much a demographic process varies* through time would be optimal if such negative covariance could evolve (Le Coeur *et al.* 2022; Gaillard & Yoccoz 2003; Morris & Doak 2004; Pélabon *et al.* 2020; Pfister 1998). Evidence exists supporting the demographic buffering hypothesis (e.g., Gaillard & Yoccoz 2003; Rotella et al. 2012) or not (McDonald et al. 2017). However, generalisation of demographic buffering patterns across species remains challenging for several reasons (Doak *et al.* 2005; Morris & Doak 2004).

One of the challenges surrounding demographic buffering are the different interpretations of results from correlational analyses, as in Pfister (1998) and Hilde *et al.* (2020). Some authors rank species' life histories along a continuum from buffered to labile (see Box 1 for definition) using the correlation coefficient (Spearman's correlation ρ) between the impact of demographic processes on the population growth rate and the temporal variance of said demographic processes (McDonald *et al.* 2017; Salguero-Gómez 2021). There, negative correlation coefficient values indicate demographic buffering. Alternatively, the absence of statistical support for buffering may suggest a preference for demographic variance to track environmental conditions, a phenomenon coined demographic lability (Drake 2005; Hilde*et al.* 2020; Jäkäläniemi *et al.* 2013; Koons *et al.* 2009; Reed & Slade 2012) (Box 1).

Demographic buffering can be measured in different ways (Gascoigne*et al.* 2023a, 2024a; Haridas & Tuljapurkar 2005; Hilde *et al.* 2020). One way to address demographic buffering is based on the 'penalisation term' of Tuljapurkar's approximation (Box 1), the variance-covariance structure (Tuljapurkar 1982). This approach measures how much temporal variability in demographic processes penalises the population relative to the value of its arithmetic population growth rate. This method uses stochastic elasticities ($E^S_{a_{\mathrm{ij}}}$, Haridas & Tuljapurkar 2005) and, as such, explicitly considers temporal variation in demographic processes. We use this method to compare the demographic buffering patterns across species and identify the populations displaying buffering signatures.

A buffered population is one where λ_ς is robust to penalty attributable to temporal variation of demographic processes. Assessing the said robustness relies on a *summed* effect of temporal variability. The summed effect of demographic process variability on population growth rate is related to the extent of impact that a demographic process has over λ_ς (Haridas & Tuljapurkar 2005). Given so, we might expect for buffered populations — robust to the aforementioned penalty — to exhibit evidence of restricted temporal variability in the most impacting demographic process for λ_τ.

To address this prediction, here we propose that, in addition to measuring the $\Sigma \mathrm{E}^S_{a_{\mathrm{ij}}}$ *for each population, one should also examine the effects of each* demographic process within a population's life cycle on λ_τ (*e.g.* , Caswell 1978, 1996, 2001; Ebert 1999; de Kroon et al. 1986). Furthermore, we propose that alongside this step, an analysis of nonlinear selection pressures acting on the temporal variance of each demographic process (Box 1) is essential.

The sign (>0, <0) of the self-second derivatives determines the type of nonlinear selection acting on demographic process temporal variability. Negative values (concave selection, [?]-shaped) reduce temporal variance, characteristic of buffering (Caswell 1996, 2001; Shyu & Caswell 2014). Positive values (convex selection, [?]-shaped) indicate selection forces that amplify the temporal variance, revealing a lack of selection pressures on demographic process variance (Bruijning *et al.* 2020; Caswell 1996, 2001; Le Coeur *et al.* 2022;

Koons *et al.* 2009; Shyu & Caswell 2014; Vinton*et al.* 2022).

Here, we show a novel combination of existing demographic methods to test the following hypothesis: buffered species with low summed effect of temporal variability on their fitness should show signatures of concave selection acting to reduce the variance in their most impacting demographic process(es) (see Box 1 for definitions). Concave selection pressures favour features that contribute to reducing temporal variance (Caswell 2001; Shyu & Caswell 2014), thereby enhancing population persistence in the face of environmental stochasticity. We test our hypothesis and demonstrate the applicability and challenges of our framework using 43 populations of 37 mammal species.

Methods

The summed effects of demographic process variability measured by stochastic elasticities

Current evidence for demographic buffering has primarily been assessed using Matrix Population Models (*MPMs* , hereafter) (Pfister 1998; Rotella *et al.* 2012). However, Integral Projection Models (*IPMs*) (Easterling *et al.* 2000; Ellner *et al.* 2016; Gascoigne *et al.* 2023b; Rodríguez-Caro *et al.* 2021; Wang*et al.* 2023) can also identify demographic buffering. MPMs and IPMs are structured, discrete-time demographic models (Caswell 2001; Ellner *et al.* 2016). For simplicity, here we focus on MPMs, but note that the same proposed approach applies to IPMs (Doak *et al.* 2021; Griffith 2017). Hereafter, we refer to demographic processes in the MPM A as its entries a_{ij} (*i.e.,* upper-level parameters *sensu* Zuidema & Franco 2001) and the vital rates composing those matrix elements (*i.e.,* lower-level parameters, *ditto*). The conversion between matrix elements and vital rates is straightforward (Franco & Silvertown 2004).

We obtain the stochastic elasticities (Haridas & Tuljapurkar 2005) ofλ_s to place species on a variance continuum. The variance continuum represents the *summed* effects of proportional increases in temporal variability across all demographic processes (a_{ij}) of the MPM A on the population growth rate λ_ς , operating at the*between-populations level.* The $\Sigma \mathrm{E}^{S}_{a_{\mathrm{ij}}}$can be partitioned into two components: i) the sum of stochastic elasticities with respect to variability11Standard deviation (σ) stands for a measure of variability.*($\Sigma E^{S^\sigma}_{a_{\mathrm{ij}}}$) — assessing how variability in a_{ij} affectsλ_ς —and ii) the sum of stochastic elasticities with respect to the arithmetic mean of demographic processes ($\Sigma E^{S^\mu}_{a_{\mathrm{ij}}}$) — assessing the impact of a change in mean values of demographic processes onλ_ς (Haridas & Tuljapurkar 2005). A weak (*i.e.,* near zero) summed effect of variability means that the population growth rate is relatively unaffected by the variability in demographic processes (Haridas & Tuljapurkar 2005), and this lack of effect by demographic process variability is consistent with demographic buffering. As such, a summed effect of variability offers a good proxy to evidence demographic buffering (Gascoigne *et al.* 2024b; Haridas & Tuljapurkar 2005) and enables the classification of populations along a continuum.

Species or populations are positioned along the variance continuum based on the impact of demographic process variance onλ_ς . Species highly sensitive to environmental variability are on the left (potentially unbuffered22^{1}Increased variance does not necessarily imply demographic lability, defined as an increase in *mean value* of a demographic process in response to improved environmental conditions (Le Coeur *et al.* 2022). By examining stochastic elasticities, we can assess changes in the contribution of demographic process variability toλ_ς , while mean values remain unchanged.), while species less sensitive are on the right (potentially buffered) end (Fig. 1A). Although the position on the continuum provides insight into how environmental variation affects λ_ς ,$\Sigma E^{S^\sigma}_{a_{\mathrm{ij}}}$does not consider covariances between demographic processes and serial correlations, crucial for a full comprehension of demographic buffering (Haridas & Tuljapurkar 2005). Thus, species' position at the buffered end of the variance continuum is a *necessary but not sufficient* condition for evidence of demographic buffering. To address this second criterion, as well as to test our hypothesis, we use second derivatives of population growth rate with respect to demographic processes to elucidate the impact of selection on the temporal variability of said demographic processes.

Δεμογραπηις προςεσσες, τηειρ φιρστ- ανδ σεςονδ-ορδερ εφφεςτς ονλ_ς, ανδ τψπες οφ σελεςτιον ον τεμποραλ αριανςε

The following method delves into within-population level by calculating the partial derivatives of λ_1 (obtained by averaging sequential MPMs across the study duration) concerning each separate matrix element a_{ij} of the MPMA (Fig. 1B). This step reveals a first-order effect of demographic process variation on fitness — the elasticities ofλ_1 to changes in demographic processes. We then evaluate a second-order effect using self-second derivatives ofλ_1 for each a_{ij} (Fig. 1C) (Caswell 1996; Shyu & Caswell 2014).

First- and second-order effects of the variation in demographic processes on fitness are evidence of *average* selection pressures over time (Carslake *et al.* 2008; Caswell 2001; Kajin *et al.* 2023; Shyu & Caswell 2014; Tuljapurkar *et al.* 2023). While elasticities can be considered a proxy for selection gradients (Lande 1982), a second-order effect (measured as a self-second derivative of

λ_1 *ωιτη ρεσπεςτ το εαςη δεμογραπηις προςεσς) ρεεαλς τηε τψπε οφ σελεςτιον αςτινγ ον τεμποραλ αριαβιλιτψ οφ δεμογραπηις παττερνς.*

A strong first-order effect of variation on fitness implies in a linear relationship between a demographic process and fitness. When linearity is assumed, the self-second derivatives are near zero, which means selection changes the mean of demographic processes, but not their variance (Shyu & Caswell 2014). Nonzero self-second derivatives indicate *nonlinear* relationships between fitness and a demographic process, revealing additional aspects of selection on the variances and covariances of demographic processes (Brodie *et al.* 1995; Carslake *et al.* 2008; Shyu & Caswell 2014). Furthermore, the second-order derivatives measure how sensitive the population growth rate is to temporal autocorrelation of demographic processes.

We argue that the joint interpretation of first- and second-order effects of variation on λ_1 provides the needed platform to address our prediction of demographically buffered populations displaying concave selection pressures. To address our hypothesis, we:

1. Place populations along a continuum defined by$\Sigma E_{a_{\mathrm{ij}}}^{S^{\sigma}}$ values.
2. Identify the demographic processes with highest elasticities for each population.
3. Associate the same demographic processes identified in (2) with negative self-second derivatives, indicating concave selection.

We showcase these steps on an imaginary wolf population (Fig. 1B). In this wolf population, individuals remaining in the fourth stage (MPM element $a_{4,4}$) have the most impact overλ_1 , with the highest elasticity value (Fig. 1B, yellow square). However, Figure 1C reveals a weak second-order effect of element $a_{4,4}$ on λ_1 , thus implying a weak selection pressure to reduce $a_{4,4}$ temporal variance. A combination of a strong first-order and near zero second-order effects on fitness coincides with a strong linear influence of a change in the mean of $a_{4,4}$ onλ_1 . However, in this example, there is no evidence of concave selection on $a_{4,4}$, as we expected based on the positioning of wolf population on the left (unbuffered) side of the variance continuum (Fig. 1A).

We found evidence of concave selection in the fertility of individuals in the second and third stages of the hypothetical wolf species (*Fig. 3C,* MPM elements $a_{1,2}$ *and* $a_{1,3}$ *, respectively, large black dots). Both fertility elements in this wolf population reveal low elasticities (Fig. 3B), but highly negative self-second derivatives. Such a pattern coincides with strong concave selection acting to reduce temporal variance in wolves' second- and third- stage fertilities. These patterns also reveal that temporal autocorrelation in second- and third- stage fertilities affect population fitness. Nonetheless, the absence of concave selection in the fertility of individuals in the fourth stage (Fig. 3C,* MPM element $a_{1,4}$*, small black dot) might suggests a pattern consistent with senescence.*

Although not our primary goal, we briefly introduce steps to evidence demographic lability. Compelling lability evidence requires sufficient data across environments [over time or space; but see Perret et al. (2024)] to construct reaction norms depicting demographic responses to environmental changes (Drake 2005; Koons *et al.* 2009; Morris*et al.* 2008). Non-linear relationships between demographic processes and the environment must be established based on the reaction norms. Demographic processes where an increase in the mean value has a stronger positive impact on population growth rate than the detrimental effect of increased variance need to be identified. The latter condition is only met when the process-environment reaction norms are convex (Drake 2005, Koons *et al* . 2009, Morris *et al* . 2008). However, Barraquand & Yoccoz (2013) show that even with log-concave reaction norms, environmental variability can positively affect population growth under certain conditions, such as constant survival or density-dependent growth. Importantly, species may not be purely buffered or labile some processes may be buffered, others labile, and others insensitive to environmental variability (*e.g.* , Doak*et al* . 2005). Deciphering these patterns is a primary research interest in the field.

Demographic buffering in mammals: A case study

We examine the performance of our framework and test the hypothesis, that is that species at the buffered end of the variance continuum display highly negative self-second derivatives for the governing demographic processes. We use 43 MPMs from 37 mammal species (16 species at the within-populations level). Mammals are of special interest in the context of demographic buffering for two reasons: (1) mammalian life histories have been well studied (Beccari *et al.* 2024; Bielby*et al.* 2007; Gillespie 1977; Jones 2011; Stearns 1983) and (2) some of their populations have already been assessed in terms of demographic buffering, particularly for primates (Campos *et al.* 2017; Morris *et al.* 2008, 2011; Reed & Slade 2012; Rotella*et al.* 2012). Together, the well-studied life histories and previous information about the occurrence of buffering in mammals allow us to make accurate predictions and validate the performance of our framework.

We used MPMs (Caswell 2001) from 43 out of 139 studies with mammals available in the COMADRE Animal Matrix Database v.3.0.0 (Salguero-Gómez*et al.* 2016). These 43 populations encompass 37 species from eight taxonomic orders. We carefully selected these MPMs in our analyses because their models contain values of demographic processes (a_{ij}) for three or more contiguous time periods, thus allowing us to obtain the stochastic elasticity of eacha_{ij}. Although we are aware that not all possible temporal variation in demographic processes may have been expressed within this period, we assumed three or more transitions are enough to provide sufficient variation for population comparison (Compagnoni *et al.* 2023). To mitigate bias in variance estimates, we randomly extracted three MPMs from the existing data for each species (Supplementary Material, Table S1), calculated the mean of these three MPMs, and repeated this process 50 times to obtain estimates of$\Sigma E^{S^{\sigma}}_{a_{\mathrm{ij}}}$ and their corresponding standard errors. A detailed description of the analysed data and their original sources are detailed in Table S1. *Finally, we included MPMs of Homo sapiens* to cross-check our estimates of second-order derivatives, as it is the only mammalian species where these have been calculated (Caswell 1996). The data for *H. sapiens* were gathered from 26 modern populations (Keyfitz & Flieger 1990).

At the within-populations level, we used a subset of 16 populations (including *H. sapiens*) whose MPMs were age-based. We specifically selected these populations because their life cycles can be summarised by two main demographic processes: survival and contribution to the recruitment of new individuals (Caswell 2010; Ebert 1999).

To quantify the variance continuum and calculate$\Sigma E^{S^{\sigma}}_{a_{\mathrm{ij}}}$ for between-populations level comparisons, we followed Tuljapurkar *et al.* (2003) and Haridas & Tuljapurkar (2005). Next, at the within-populations level, we calculated the deterministic elasticities to each demographic process using the *popbio* package (Stubben *et al.* 2020). The self-second derivatives were adapted from *demogR* (Jones 2007) following (Caswell 1996) and applied to the mean MPM of each study. All analyses were performed using R version 4.4.1 (R Core Team 2024).

Results

We ranked 43 populations from 37 mammal species into a continuum of variance according to the summed impact of variation in demographic processes on λ_s (Fig. 2). Most of the analysed taxonomic orders were placed on the low or zero variance end of the variance continuum (Fig. 2), coinciding with demographically buffered populations. The smallest contributions of variability in demographic processes (note that $\Sigma E^{S^{\sigma}}_{a_{\mathrm{ij}}}$ ranges from 0 to -1), suggesting buffered populations, were assigned to Primates: northern muriqui (*Brachyteles hyphoxantus* ,$\Sigma E^{S^{\sigma}}_{a_{\mathrm{ij}}} = -5.31 \times 10^{-5} \pm 2.09 \times 10^{-5}$) (mean ± S.E.) (Fig. 2 silhouette a), mountain gorilla (*Gorilla beringei* ,$\Sigma E^{S^{\sigma}}_{a_{\mathrm{ij}}}$ = -1.28 × 10^{-5} ± 1.32 × 10^{-5}) (Fig. 2 silhouette b), followed by the blue monkey (*Cercopithecus mitis* ,$\Sigma E^{S^{\sigma}}_{a_{\mathrm{ij}}}$ = -4.43 × 10^{-5} ± 1.18 × 10^{-5}) (Fig. 2 silhouette c). The first non-primate species placed near the buffered end of the continuum was the Columbian ground squirrel (*Urocitellus columbianus* , Rodentia,$\Sigma E^{S^{\sigma}}_{a_{\mathrm{ij}}}$ = -3.38 × 10^{-3} ± 6.96 × 10^{-4}) (Fig. 2 silhouette d). On the other opposite, the species with the highest contribution of variation in demographic processes – placed at the high-variance end of the continuum – was the stoat (*Mustela erminea* , Carnivora, $\Sigma E^{S^{\sigma}}_{a_{\mathrm{ij}}}$ = -0.310 ± 0.0162) (Fig. 2 silhouette e). All the 14 primate populations occupied the buffered side of the variance continuum, with the exception of the Patas monkey (*Erythrocebus patas* , Primates,$\Sigma E^{S^{\sigma}}_{a_{\mathrm{ij}}}$ = -0.0521 ± 5.38 × 10^{-3}) (Fig. 2 silhouette f). The snowshoe hare (*Lepus americanus* , Lagomorpha,$\Sigma E^{S^{\sigma}}_{a_{\mathrm{ij}}}$ = -0.262 ± 0.0233) (Fig. 2 silhouette g) and the Bush rat (*Rattus fuscipes* , Rodentia,$\Sigma E^{S^{\sigma}}_{a_{\mathrm{ij}}}$ = -0.245 ± 4.29 × 10^{-3}) (Fig. 2 silhouette h) were positioned on the non-buffered end of the variance continuum. Additional information (including standard errors of the elasticity estimates) is provided in Table S1. *A posteriori* , we quantified the impact of phylogenetic relatedness on the estimates of the sum of stochastic elasticities (Fig. 2), and then for the correlation between those estimates and the number of MPMs available per species. For the former, we estimated Blomberg's K, a measure of phylogenetic signal that ranges between 0 (weak signal) to positive values 1 (strong) (Münkemüller *et al.* 2012).*Blomberg's K in our analyses was 0.23. The correlation between the* number of available MPMs per study and the sum of stochastic elasticities (post jack-knifing) raised a weakly negative coefficient (-0.002), though significant (P = 0.017).

We found evidence in support of our hypothesis in only one of the studied species, the Columbian ground squirrel (*Urocitellus columbianus*). This species *is placed near the buffered end of the variance continuum (Fig. 2, silhouette d) and its most impactful demographic process shows signs of concave selection. The strongly negative self-second derivative with respect to growth from first to the second stage (Fig. 3B, MPM element $a_{2,1}$)* indicates that$a_{2,1}$ is both important, and at the same time, kept constant through time in this population of *U. columbianus* .

In humans, the support for our hypothesis was present, but weaker, as humans are placed further away from the buffered end of the variance continuum (Fig. 2, silhouette j). However, the demographic parameters representing growth from the first to second age class and growth from second to third age class (matrix elements $a_{2,1}$ and $a_{3,2}$, respectively) displayed high elasticities alongside negative self-second derivatives (Fig. 3D), corroborating with demographically buffered population.

For the remaining studied species the demographic processes with the highest elasticity values did not display strong negative self-second derivatives (Fig. 3). Particularly for the majority of primates, placed on the buffered end of the variance continuum, demographic processes with high elasticities had positive values for the self-second derivatives (indicated by yellow squares with white dots in Figure 3). Examples of primate species exhibiting high elasticities and positive values for their self-second derivatives include northern muriqui (*Brachyteles hypoxanthus*), mountain gorilla (*Gorilla beringei*), white-faced capuchin monkey (*Cebus capucinus*), rhesus monkey (*Macaca mulatta*), blue monkey (*Cercopithecus mitis*), Verreaux's sifaka (*Propithecus verreauxi*) and olive baboon (*Papio cynocephalus*) (Fig. 3). This implies that the key demographic processes influencing λ_1 do not show evidence of selective pressure for reducing their variability.

The killer whale (*Orcinus orca*) showed similar lack of support for our hypothesis as primates. Indeed, *O. orca* was positioned at the buffered end of the variance continuum (Cetacea,$\Sigma E^{S^{\sigma}}_{a_{\mathrm{ij}}}$ = -4.72 × 10^{-4} ± 1.53 × 10^{-4}) (Fig. 2 silhouette not shown). However, the first- and second-order effects show that the governing three demographic processes in the killer whale life cycle (namely, matrix elements $a_{2,2}$,$a_{3,3}$, and $a_{4,4}$) are not under selection pressures for reducing their temporal variance, but the opposite (yellow and green squares with white dots, Fig. 3).

The primary governing demographic process for Soay sheep (*Ovis aries*) displayed convex selection signatures. For *O. aries* (Fig. 2, silhouette i), remaining in the third age class (Fig. 3,$a_{3,3}$,) impacts λ_τ most and is under selection pressure to have its variance increased. These characteristics suggest potential conditions for lability, despite the species being positioned closer to the buffered end of the variance continuum.

Adding the second-order effect of variation on fitness to the toolbox for demographic buffering is an important addition. The high absolute values of self-second derivatives (large dots, either black or white, Fig. 3) suggest λ_τ is sensitive to autororrelation in those demographic processes. This pattern also means that if, for example, the mean value of $a_{5,4}$ for *U. maritimus* increased, the sensitivity of λ_τ to $a_{5,4}$ would decrease because the self-second derivative of $a_{5,4}$ is highly negative (depicted by the largest black dot in polar bear, Fig. 3 silhouette j). The opposite holds for the $a_{4,4}$, where an increase in the value of $a_{4,4}$ would increase the sensitivity of λ_τ to $a_{4,4}$, because the self-second derivative of $a_{4,4}$ is highly positive (the largest white dot in the polar bear MPM).

Discussion

We explore demographic buffering patterns through the integration of established demographic techniques. Our framework merges insights from both stochastic and deterministic demographic approaches, which revealed only limited support for our hypothesis. Specifically, we had anticipated that species exhibiting minimal influence from temporal variability in demographic processes on their stochastic growth rates would demonstrate concave selection affecting the demographic processes with the highest deterministic elasticities. However, using stochastic elasticities alongside the first- and second- order perturbation analysis of the deterministic population growth rate and applying these analyses to mammal species, we found that only the Columbian ground squirrel fully supported our hypothesis; humans showed partial support; other species did not.

Evidencing demographic buffering is not straightforward. Indeed, through the analysis of stochastic population growth rate (λ_ς) in our application of the framework to 43 populations of 37 mammal species, we identify the highest density of natural populations near the buffered end of the variance continuum. However, we show that most of the species then fail to exhibit signs of concave ([?]-shaped) selection on impacting demographic parameters, opposed to our hypothesis. Such results suggest discordance between two features of demographic buffering, namely: 1) the stochastic population growth rate having a low sensitivity to temporal variability in demographic processes, and 2) demographic processes having their temporal variability reduced by selection.

The lack of association between the non-linear selection patterns (concave/convex) and species positioning on the variance continuum for the studied mammal species may have several explanations. Firstly, non-linear selection on demographic process variability is *dynamic* (Kajin *et al.* 2023). Within a life cycle, even minor changes in key demographic processes can trigger a domino effect, affecting not only the process itself but also the sensitivity of λ_1 to changes in said process (Stearns 1992). Consequently, correlations between demographic processes (negative correlations known as trade-offs) are influenced by minor alterations in the governing demographic processes (Doak *et al.* 2005). Because of these characteristics, second-order derivatives reveal “fine scale” fitness behaviour compared to sums of stochastic elasticities. Evolutionary demography still requires new tools to connect second-order fitness effects with stochastic elasticities in a biologically interpretable manner similar as in Tuljapurkar *et al.* 2023.

The stochastic elasticities explicitly account for the demographic process variation in time, while the first- and second- order effects on fitness are obtained from temporally averaged population matrices. Because a mean environment rarely characterizes the natural variation in demographic process typical of stochastic environments (Boyce *et al.* 2006), any metric derived from averaged matrix population models represent only an averaged realisation and could only rarely be representative of a pattern emerged from explicitly accounting for temporal variation.

Our original assumptions regarding demographically buffered populations, however, remain valid. We assumed that: 1) a buffered population is one with a weak summed effect of temporal variability on the long-term stochastic population growth rate, and 2) if a population is buffered, there should be signs of concave selection acting on the demographic process with the highest deterministic elasticity. The lack of support for our hypothesis supports the idea that the patterns of first- and second-order effects of demographic process variation on fitness are dynamic and can change rapidly in natural environments. Even if a given demographic process is primarily governing the population growth rate in one year, a different one might take over next year (Evers *et al.* 2021).

When placing our study species along a variance continuum, primates tend to be located on the buffered end. However, most primates displayed convex – instead of the expected concave – selection on adult survival. Similar results, where the key demographic process failed to display reduced temporal variability, have been reported for long-lived seabirds (Doherty *et al.* 2004). One explanation for the unexpected convex selection on adult survival involves trade-offs, as suggested by (Doak *et al.* 2005). When two demographic parameters are negatively correlated, the variance of population growth rate can be increased or decreased (Compagnoni *et al.* 2016; Evans & Holsinger 2012).

Correlations among demographic processes (positive and negative) inherently influence the biological limits of variance (Haridas & Tuljapurkar 2005). This is because the magnitude of variation in a particular demographic process is restrained by the variation of other demographic processes. Not surprisingly, correlations among demographic processes have been shown to be strongly subjected to ecological factors (Fay *et al.* 2022). Therefore, future studies may benefit from deeper insights using *cross* -second derivatives (Caswell 1996, 2001) to investigate correlations among demographic processes.

Biological variance estimates are inevitably subjected to several sources of bias (Simmonds & Jones 2024). To minimise bias, we randomly sampled the available matrices before obtaining the estimates. Despite the significant correlation between$\Sigma E^{S^{\sigma}}_{a_{\mathrm{ij}}}$ and the number of available matrices per species, the relative positioning of species remains meaningful for between-population level comparisons, as the correlation is very weak (-0.002). *Still, researchers carrying out macroecological comparisons of demographic buffering might want to be even more stringent than we have been here with their datasets, as these grow longer with time* (Compagnoni *et al.* 2021; Salguero-Gómez*et al.* 2021).

Regarding phylogenetic effects, our tests revealed a mild signal, but we note that future work regressing $\Sigma E^{S^{\sigma}}_{a_{\mathrm{ij}}}$ *values against potential independent variables (e.g., climate values) may want to correct for this phylogenetic dependence.* By having carefully chosen studies from a database that contains >400 species and retained only those that passed through a set of selection criteria (Che-Castaldo *et al.* 2020; Gascoigne *et al.* 2023b; Kendall *et al.* 2019; Römer *et al.* 2024; Simmonds & Jones 2024), we mitigate those biases *a priori* . Furthermore, we are using an elasticity-based approach, meaning we are comparing proportional variances. At present, the available methods still do not account for constraints in variance nor performing a perturbation approach disproportionately.

The analyses at both between- and within-populations levels are fundamentally interconnected. This connection is grounded on the fact that large summed elasticities to variability are intrinsically linked to high elasticity values, as demonstrated in equation 6 in (Haridas & Tuljapurkar 2005). This finding robustly endorses the perspective that species' positions along the variance continuum should be interpreted with consideration of first and second-order effects, and additionally, in the context of selection pressures acting on the variability of demographic processes, as revealed by second-order derivatives.

Demographic processes within our study populations often face a mix of convex and concave selection. This mix of selection patterns was suggested by Doak et al. (2005), who noted that dramatic changes in population growth rate sensitivities are influenced by correlations among demographic processes. Here, only two of the 16 mammal species revealed concave selection on the key demographic processes: Columbian ground squirrel (*Urocitellus columbianus*), and humans (*Homo sapiens*). These two species were placed near (or relatively near) the buffered end of the variance continuum, supporting (partially) our hypothesis. Evidence of buffering has been reported across 22 ungulate species (Gaillard & Yoccoz 2003). However, in the one ungulate we examined, the moose (*Alces alces*), we found only partial support for our hypothesis, as it is near the buffered end of the variance continuum but lacks concave selection pressures on the most important demographic process.

Our overall findings reveal varying levels of support for the notion that adult survival in long-lived species tends to be buffered. Indeed, Gaillard et al. (1998) found that adult female survival varied considerably less than juvenile survival in large herbivores. This finding was also supported by further studies in ungulates (Gaillard & Yoccoz 2003), turtles (Heppell 1998), vertebrates and plants (Pfister 1998), and more recently across nine species of plants (McDonald*et al.* 2017). Gaillard and Yoccoz (2003) reported unexpectedly high adult survival in small mammals, even though the studied small mammals were annual, and as such, comparable to large mammal model. Seasonality, frequency and method of sampling all influence survival estimates and their estimated variability, thus, when comparing multiple species/studies, all the latter characteristics should be taken into account when interpreting the results.

Examining the drivers of demographic buffering has become an important piece of the ecological and evolutionary puzzle of demography. As such, understanding buffering can help us better predict population responses to environmental variability, climate change, and direct anthropogenic disturbances (Boyce *et al.* 2006; Gascoigne *et al.* 2024a; McDonald *et al.* 2017; Pfister 1998; Vázquez *et al.* 2017). By setting demographic buffering into a broader and more integrated frameworks, we hope to enhance comprehension and prediction of the implications of heightened environmental stochasticity on the evolution of life history traits. This understanding is crucial in mitigating the risk of extinction for the most vulnerable species.

Acknowledgements

This study was financed in part by the *Coordenação de Aperfeiçoamento de Pessoal de Nível Superior* - Brasil (CAPES) - Finance Code 001. GSS was supported by CAPES and CNPq (301343/2023-3). MK was supported by the European Commission through the Marie Skłodowska-Curie fellowship (MSCA Max-Persist #101032484) hosted by RSG. RS-G was supported by a NERC Independent Research Fellowship (NE/M018458/1) and a NERC Pushing the Frontiers (NE/X013766/1).

Data availability The demographic data used in this paper are open-access and available in the COMADRE Animal Matrix Database (https://compadre-db.org/Data/Comadre). A list of the studies and species used here is available in Supplementary Material (Table S1). The data and code supporting the results can be accessed here: https://github.com/SamuelGascoigne/Demographic_buffering_

References

Barraquand, F. & Yoccoz, N.G. (2013). When can environmental variability benefit population growth? Counterintuitive effects of nonlinearities in vital rates. *Theor Popul Biol* , 89, 1–11.

Bathiany, S., Dakos, V., Scheffer, M. & Lenton, T.M. (2018). Climate models predict increasing temperature variability in poor countries.*Sci Adv* , 4.

Beccari, E., Capdevila, P., Salguero-Gómez, R. & Carmona, C.P. (2024). Worldwide diversity in mammalian life histories: Environmental realms and evolutionary adaptations. *Ecol Lett* , 27.

Bielby, J., Mace, G.M., Bininda-Emonds, O.R.P., Cardillo, M., Gittleman, J.L., Jones, K.E., *et al.* (2007). The Fast-Slow Continuum in Mammalian Life History: An Empirical Reevaluation. *Am Nat* , 169, 748–757.

Bjorkvoll, E., Lee, A.M., Grotan, V., Saether, B.-E., Stien, A., Engen, S., *et al.* (2016). Demographic buffering of life histories? Implications of the choice of measurement scale. *Ecology* , 97, 40–47.

Bonsall, M.B. & Klug, H. (2011). The evolution of parental care in stochastic environments. *J Evol Biol* , 24, 645–655.

Boyce, M., Haridas, C., Lee, C. & The NCEAS Stochastic Demography Working Group. (2006). Demography in an increasingly variable world.*Trends Ecol Evol* , 21, 141–148.

Campos, F.A., Morris, W.F., Alberts, S.C., Altmann, J., Brockman, D.K., Cords, M., *et al.* (2017). Does climate variability influence the demography of wild primates? Evidence from long-term life-history data in seven species. *Glob Chang Biol* , 23, 4907–4921.

Carslake, D., Townley, S. & Hodgson, D.J. (2008). Nonlinearity in eigenvalue-perturbation curves of simulated population projection matrices. *Theor Popul Biol* , 73, 498–505.

Caswell, H. (1978). A general formula for the sensitivity of population growth rate to changes in life history parameters. *Theor Popul Biol* , 14, 215–230.

Caswell, H. (1996). Second Derivatives of Population Growth Rate: Calculation and Applications. *Ecology* , 77, 870–879.

Caswell, H. (2001). *Matrix Population Models: Construction, Analysis, and Interpretation* . Sinauer Associates Inc. Publishers, Sunderland, Massachusetts, USA.

Charlesworth, B. (1994). *Evolution in age-structured populations* . second edi. Cambridge University Press.

Che-Castaldo, J., Jones, O.R., Kendall, B.E., Burns, J.H., Childs, D.Z., Ezard, T.H.G., *et al.* (2020). Comments to "Persistent problems in the construction of matrix population models." *Ecol Modell* , 416.

Le Coeur, C., Yoccoz, N.G., Salguero-Gomez, R. & Vindenes, Y. (2022). Life history adaptations to fluctuating environments: Combined effects of demographic buffering and lability. *Ecol Lett* , 25, 2107–2119.

Compagnoni, A., Bibian, A.J., Ochocki, B.M., Rogers, H.S., Schultz, E.L., Sneck, M.E., *et al.* (2016). The effect of demographic correlations on the stochastic population dynamics of perennial plants.*Ecol Monogr* , 86, 480–494.

Compagnoni, A., Evers, S. & Knight, T. (2023). Spatial replication can best advance our understanding of population responses to climate.*bioRxiv* , https://doi.org/10.1101/2022.06.24.497542.

Compagnoni, A., Levin, S., Childs, D.Z., Harpole, S., Paniw, M., Romer, G., *et al.* (2021). Herbaceous perennial plants with short generation time have stronger responses to climate anomalies than those with longer generation time. *Nat Commun* , 12, 1824.

Doak, D.F., Morris, W.F., Pfister, C., Kendall, B.E. & Bruna, E.M. (2005). Correctly Estimating How Environmental Stochasticity Influences Fitness and Population Growth. *Am Nat* , 166, E14–E21.

Doak, D.F., Waddle, E., Langendorf, R.E., Louthan, A.M., Isabelle Chardon, N., Dibner, R.R., *et al.* (2021). A critical comparison of integral projection and matrix projection models for demographic analysis. *Ecol Monogr* , 91, e01447.

Doherty, P.F., Schreiber, E.A., Nichols, J.D., Hines, J.E., Link, W.A., Schenk, G.A., *et al.* (2004). Testing life history predictions in a long-lived seabird: A population matrix approach with improved parameter estimation. *Oikos* , 105, 606–618.

Drake, J.M. (2005). Population effects of increased climate variation.*Proceedings of the Royal Society B: Biological Sciences* , 272, 1823–1827.

Easterling, M.R., Ellner, S.P. & Dixon, P.M. (2000). Size-Specific Sensitivity: Applying a New Structured Population Model. *Ecology* , 81, 694–708.

Ebert, T. (1999). *Plant and animal populations: Methods in demography* . Academis Press, San Diego, CA, USA.

Ellner, S.P., Childs, D.Z. & Rees, M. (2016). *Data-driven Modelling of Structured Populations. A practical guide to the Integral Projection Model* . Lecture Notes on Mathematical Modelling in the Life Sciences. Springer International Publishing, Cham.

Evans, M.E.K. & Holsinger, K.E. (2012). Estimating covariation between vital rates : A simulation study of connected vs . separate generalized linear mixed models (GLMMs). *Theor Popul Biol* , 82, 299–306.

Evers, S.M., Knight, T.M., Inouye, D.W., Miller, T.E.X., Salguero-Gomez, R., Iler, A.M., *et al.* (2021). Lagged and dormant season climate better predict plant vital rates than climate during the growing season.*Glob Chang Biol* , 27, 1927–1941.

Fay, R., Hamel, S., van de Pol, M., Gaillard, J.M., Yoccoz, N.G., Acker, P., *et al.* (2022). Temporal correlations among demographic parameters are ubiquitous but highly variable across species. *Ecol Lett* , 25, 1640–1654.

Franco, M. & Silvertown, J. (2004). A comparative demography of plants based upon elasticities of vital rates. *Ecology* , 85, 531–538.

Gaillard, J.M., Festa-Bianchet, M. & Yoccoz, N.G. (1998). Population dynamics of large herbivores: Variable recruitment with constant adult survival. *Trends Ecol Evol* , 13, 58–63.

Gaillard, J.-M. & Yoccoz, N. (2003). Temporal Variation in Survival of Mammals: a Case of Environmental Canalization? *Ecology* , 84, 3294–3306.

Gascoigne, S.J.L., Kajin, M. & Salguero-Gomez, R. (2024a). Criteria for buffering in ecological modeling. *Trends Ecol Evol* , 39, 116–118.

Gascoigne, S.J.L., Kajin, M., Sepil, I. & Salguero-Gomez, R. (2024b). Testing for efficacy in four measures of demographic buffering.*EcoEvoRxiv* , 0–2.

Gascoigne, S.J.L., Kajin, M., Tuljapurkar, S.D., Silva Santos, G., Compagnoni, A., Steiner, U.K., *et al.* (2023a). Structured demographic buffering: A framework to explore the environment drivers and demographic mechanisms underlying demographic buffering.*bioRxiv* .

Gascoigne, S.J.L., Rolph, S., Sankey, D., Nidadavolu, N., Stell Pičman, A.S., Hernández, C.M., *et al.* (2023b). A standard protocol to report discrete stage-structured demographic information. *Methods Ecol Evol* , 14, 2065–2083.

Gillespie, J.H. (1977). Natural Selection for Variances in Offspring Numbers: A New Evolutionary Principle. *Am Nat* , 111, 1010–1014.

Grant, A., Benton, T.G. & Mar, N. (2007). Elasticity Analysis for Density-Dependent Populations in Stochastic Environments, 81, 680–693.

Griffith, A.B. (2017). Perturbation approaches for integral projection models. *Oikos* , 126, 1675–1686.

Haridas, C. V. & Tuljapurkar, S. (2005). Elasticities in Variable Environments: Properties and Implications. *Am Nat* , 166, 481–495.

Haridas, C. V & Tuljapurkar, S. (2007). Time, transients and elasticity. *Ecol Lett* , 10, 1143–53.

Haridas, C. V., Tuljapurkar, S. & Coulson, T. (2009). Estimating stochastic elasticities directly from longitudinal data. *Ecol Lett* , 12, 806–812.

Healy, K., Ezard, T.H.G., Jones, O.R., Salguero-Gómez, R. & Buckley, Y.M. (2019). Animal life history is shaped by the pace of life and the distribution of age-specific mortality and reproduction. *Nat Ecol Evol* , 3, 1217–1224.

Heppell, S.S. (1998). Application of Life-History Theory and Population Model Analysis to Turtle Conservation. *Copeia* , 1998, 367.

Hilde, C.H., Gamelon, M., Sæther, B.-E., Gaillard, J.-M., Yoccoz, N.G. & Pélabon, C. (2020). The Demographic Buffering Hypothesis: Evidence and Challenges. *Trends Ecol Evol* , 35, 523–538.

Jäkäläniemi, A., Ramula, S. & Tuomi, J. (2013). Variability of important vital rates challenges the demographic buffering hypothesis.*Evol Ecol* , 27, 533–545.

Jones, J.H. (2007). demogR: A Package for the Construction and Analysis of Age-structured Demographic Models in R. *J Stat Softw* , 22, 1–28.

Jones, J.H. (2011). Primates and the evolution of long, slow life histories. *Current Biology* , 21, R708–R717.

Jongejans, E., De Kroon, H., Tuljapurkar, S. & Shea, K. (2010). Plant populations track rather than buffer climate fluctuations. *Ecol Lett* , 13, 736–743.

Kajin, M., Gentile, R., Almeida, P.J.A.L. de, Vieira, M.V. & Cerqueira, R. (2023). Vital rates, their variation and natural selection: a case for an Atlantic forest marsupial. *Oecologia Australis* , 27.

Kendall, B.E., Fujiwara, M., Diaz-Lopez, J., Schneider, S., Voigt, J. & Wiesner, S. (2019). Persistent problems in the construction of matrix population models. *Ecol Modell* , 406, 33–43.

Keyfitz, N. & Flieger, W. (1990). *World Population Growth and Aging: Demographic Trends in the Late Twentieth Century* . University of Chicago Press, Chicago.

Koons, D.N., Pavard, S., Baudisch, A. & Jessica E. Metcalf, C. (2009). Is life-history buffering or lability adaptive in stochastic environments? *Oikos* , 118, 972–980.

Kroon, H. De, Groenendael, J. Van & Ehrlen, J. (2000). Elasticities: A review of methods and model limitations. *Ecology* , 81, 607–618.

de Kroon, H., Plaisier, A., van Groenendael, J. & Caswell, H. (1986). Elasticity: The Relative Contribution of Demographic Parameters to Population Growth Rate. *Ecology* , 67, 1427–1431.

Lande, R. (1982). A Quantitative Genetic Theory of Life History Evolution. *Ecology* , 63, 607–615.

Lawler, R.R., Caswell, H., Richard, A.F., Ratsirarson, J., Dewar, R.E. & Schwartz, M. (2009). Demography of Verreaux's sifaka in a stochastic rainfall environment. *Oecologia* , 161, 491–504.

Lefèvre, C.D., Nash, K.L., González-Cabello, A. & Bellwood, D.R. (2016). Consequences of extreme life history traits on population persistence: do short-lived gobies face demographic bottlenecks? *Coral Reefs* , 35, 399–409.

McDonald, J.L., Bailey, T., Delahay, R.J., McDonald, R.A., Smith, G.C. & Hodgson, D.J. (2016). Demographic buffering and compensatory recruitment promotes the persistence of disease in a wildlife population. *Ecol Lett* , 19, 443–449.

McDonald, J.L., Franco, M., Townley, S., Ezard, T.H.G., Jelbert, K. & Hodgson, D.J. (2017). Divergent demographic strategies of plants in variable environments. *Nat Ecol Evol* , 1, 0029.

Morris, W.F., Altmann, J., Brockman, D.K., Cords, M., Fedigan, L.M., Pusey, A.E., *et al.* (2011). Low Demographic Variability in Wild Primate Populations: Fitness Impacts of Variation, Covariation, and Serial Correlation in Vital Rates. *Am Nat* , 177, E14–E28.

Morris, W.F. & Doak, D.F. (2004). Buffering of Life Histories against Environmental Stochasticity: Accounting for a Spurious Correlation between the Variabilities of Vital Rates and Their Contributions to Fitness. *Am Nat* , 163, 579–590.

Morris, W.F., Pfister, C.A., Tuljapurkar, S., Haridas, C. V., Boggs, C.L., Boyce, M.S., *et al.* (2008). Longevity can buffer plant and animal populations against changing climatic variability. *Ecology* , 89, 19–25.

Münkemüller, T., Lavergne, S., Bzeznik, B., Dray, S., Jombart, T., Schiffers, K., *et al.* (2012). How to measure and test phylogenetic signal. *Methods Ecol Evol* , 3, 743–756.

Pélabon, C., Hilde, C.H., Einum, S. & Gamelon, M. (2020). On the use of the coefficient of variation to quantify and compare trait variation. *Evol Lett* , 4, 180–188.

Perret, D.L., Evans, M.E.K. & Sax, D.F. (2024). A species' response to spatial climatic variation does not predict its response to climate change. *Proc Natl Acad Sci U S A* , 121, e2304404120.

Pfister, C. (1998). Patterns of variance in stage-structured populations: Evolutionary predictions and ecological implications. *Proceedings of the National Academy of Sciences* , 95, 213–218.

R Core Team. (2024). R: A Language and Environment for Statistical Computing.

Reed, A.W. & Slade, N.A. (2012). Buffering and plasticity in vital rates of oldfield rodents. *Journal of Animal Ecology* , 81, 953–959.

Rodríguez-Caro, R.C., Capdevila, P., Gracia, E., Barbosa, J.M., Gimenez, A. & Salguero-Gomez, R. (2021). The limits of demographic buffering in coping with environmental variation. *Oikos* , 130, 1346–1358.

Rodriguez-Caro, R.C., Capdevila, P., Gracia, E., Barbosa, J.M., Gimenez, A. & Salguero-Gomez, R. (2021). The limits of demographic buffering in coping with environmental variation. *Oikos* , 130, 1346–1358.

Romer, G., Dahlgren, J.P., Salguero-Gomez, R., Stott, I.M. & Jones, O.R. (2024). Plant demographic knowledge is biased towards short-term studies of temperate-region herbaceous perennials. *Oikos* , 2024.

Rotella, J.J., Link, W.A., Chambert, T., Stauffer, G.E. & Garrott, R.A. (2012). Evaluating the demographic buffering hypothesis with vital rates estimated for Weddell seals from 30 years of mark-recapture data. *Journal of Animal Ecology* , 81, 162–173.

Salguero-Gomez, R. (2021). Commentary on the life history special issue: The fast-slow continuum is not the end-game of life history evolution, human or otherwise. *Evolution and Human Behavior* , 42, 281–283.

Salguero-Gomez, R. (2024). More social species live longer, have higher generation times, and longer reproductive windows. *bioRxiv; https://doi.org/10.1101/2024.01.22.575897* .

Salguero-Gomez, R., Jackson, J. & Gascoigne, S.J.L. (2021). Four key challenges in the open-data revolution. *Journal of Animal Ecology* , 90, 2000–2004.

Salguero-Gomez, R., Jones, O.R., Archer, C.R., Bein, C., de Buhr, H., Farack, C., *et al.* (2016). COMADRE: A global data base of animal demography. *Journal of Animal Ecology* , 85, 371–384.

Sanghvi, K., Vega-Trejo, R., Nakagawa, S., Gascoigne, S.J.L., Johnson, S.L., Salguero-Gomez, R., *et al.* (2024). Meta-analysis shows no consistent evidence for senescence in ejaculate traits across animals. *Nat Commun* , 15, 558.

Shyu, E. & Caswell, H. (2014). Calculating second derivatives of population growth rates for ecology and evolution. *Methods Ecol Evol* , 5, 473–482.

Simmonds, E.G. & Jones, O.R. (2024). Uncertainty propagation in matrix population models: Gaps, importance and guidelines. *Methods Ecol Evol* , 15, 427–438.

Stearns, S. (1992). *The Evolution of Life Histories* . Oxford University Press, New York, USA.

Stearns, S.C. (1983). The Influence of Size and Phylogeny on Patterns of Covariation among Life-History Traits in the Mammals. *Oikos* , 41, 173.

Stubben, C., Milligan, B., Nantel, P. & Stubben, M.C. (2020). Package 'popbio.'

Sutherland, W.J., Freckleton, R.P., Godfray, H.C.J., Beissinger, S.R., Benton, T., Cameron, D.D., *et al.* (2013). Identification of 100 fundamental ecological questions. *Journal of Ecology* , 101, 58–67.

Van Tienderen, P.H. (2000). Elasticities and the link between demographic and evolutionary dynamics. *Ecology* , 81, 666–679.

Tuljapurkar, S. (1990). Population Dynamics in Variable Environments. In: *Lecture notes in Biomathematics* , Lecture Notes in Biomathematics (ed. Levin, S.). Springer Berlin Heidelberg.

Tuljapurkar, S. (2010). Environmental variance, population growth and evolution. *J Anim Ecol* , 79, 1–3.

Tuljapurkar, S., Gaillard, J.-M. & Coulson, T. (2009). From stochastic environments to life histories and back. *Philosophical Transactions of the Royal Society B: Biological Sciences* , 364, 1499–1509.

Tuljapurkar, S., Horvitz, C.C. & Pascarella, J.B. (2003). The Many Growth Rates and Elasticities of Populations in Random Environments. *Am Nat* , 162, 489–502.

Tuljapurkar, S., Jaggi, H., Gascoigne, S.J.L., Zuo, W., Kajin, M. & Salguero-Gomez, R. (2023). From disturbances to nonlinear fitness and back. *bioRxiv* , 2023.10.20.563360.

Tuljapurkar, S.D. (1982). Population dynamics in variable environments. III. Evolutionary dynamics of r-selection. *Theor Popul Biol* , 21, 141–165.

Vazquez, D.P., Gianoli, E., Morris, W.F. & Bozinovic, F. (2017). Ecological and evolutionary impacts of changing climatic variability.*Biological Reviews* , 92, 22–42.

Wang, J., Yang, X., Silva Santos, G., Ning, H., Li, T., Zhao, W.,*et al.* (2023). Flexible demographic strategies promote the population persistence of a pioneer conifer tree (Pinus massoniana) in ecological restoration. *For Ecol Manage* , 529, 120727.

Zuidema, P.A. & Franco, M. (2001). Integrating vital rate variability into perturbation analysis: an evaluation for matrix population models of six plant species. *Journal of Ecology* , 89, 995–1005.

Figure 1

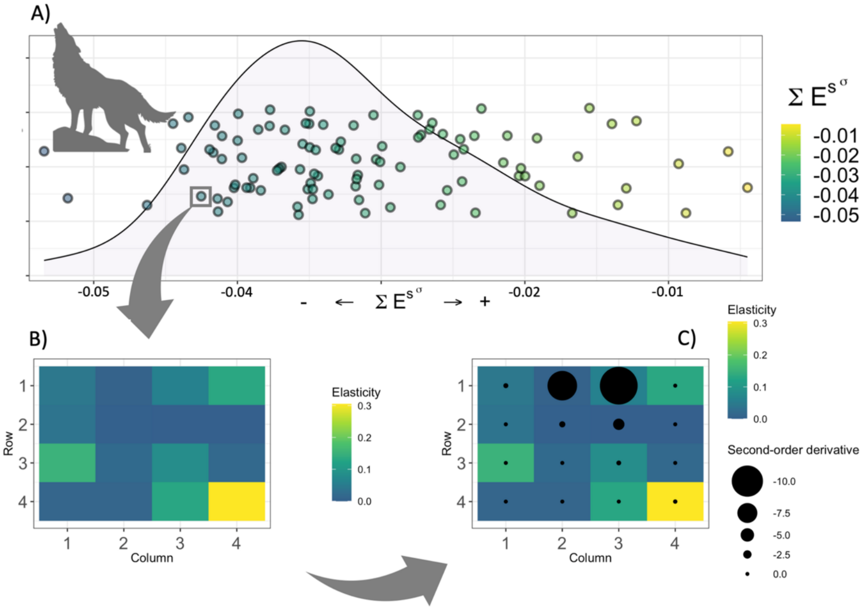

Figure 2

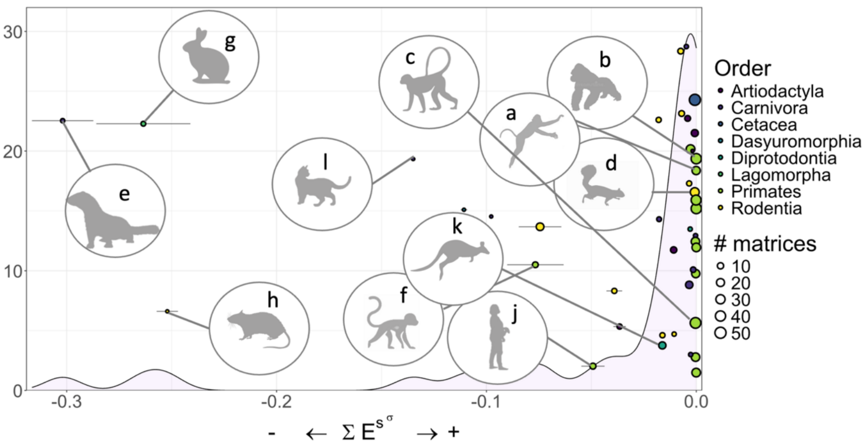

Figure 3

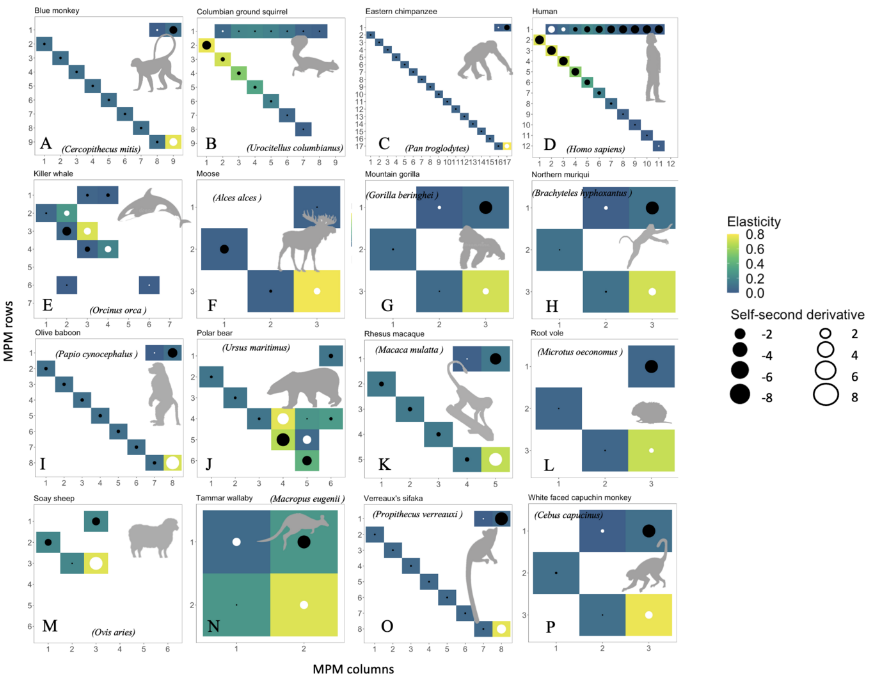

Figure legends

Figure 1 . A) The variance continuum for 37 hypothetical species based on the summed stochastic elasticities ($\Sigma E^{S^\sigma}_{a_{ij}}$) at the between populations hierarchical level. The closer the$\Sigma E^{S^\sigma}_{a_{ij}}$ is to zero, the weaker the impact of variation in demographic processes on the stochastic population growth rate, λ_ς . The variance continuum ranges from potentially buffered (right-hand side) to less buffered (left-hand side) populations. The yellow-dotted populations can be classified as having potentially *buffered life cycles* . The left-hand side of the graph represents populations where variability in demographic processes results in strong impact onλ_ς (blue dots). Thus, the blue-dotted populations can be classified as having potentially *unbuffered life cycles* . The vertical axis delineates the values of the probability density function, indicating the frequency of populations at each value of$\Sigma E^{S^\sigma}_{a_{ij}}$. The placement of data points (species/populations) along the horizontal axis corresponds

to their calculated values of $\Sigma E_{a_{ij}}^{S^{\sigma}}$ and is arranged linearly, while the placement along the y-axis is random for improved visual comprehension. B) First-order effects or elasticities for separate populations at within-species level. Shown are the elasticities of the deterministic population growth rate (λ_1) for a hypothetical population of wolves and revealing the most important demographic process(es) in the life cycle (yellow cells: high elasticity, blue cells: low elasticity). C) Combined results for first- (yellow and blue cells) and second-order effects (black dots), where the latter reveals the nonlinear selection pressures at the within-species level.

Figure 2 . The variance continuum for 43 populations from 37 species of mammals from the COMADRE database based on the summed stochastic elasticities of λ_S to temporal variability in demographic processes ($\Sigma E_{a_{ij}}^{S^{\sigma}}$) at the between-populations hierarchical level. Colors represent different taxonomic orders with Primates occupying the right-hand side. Silhouettes: a)*Brachyteles hyphoxantus* , b) *Gorilla beringhei* , c)*Cercopithecus mitis* , d) *Urocitellus columbianus,* e)*Mustela erminea* , f) *Erythrocebus patas* , g) *Lepus americanus* , h) *Rattus fuscipes* , i) *Ovis aries* , j)*Homo sapiens* , k) *Macropus eugenii* , and l) *Felis catus* . The vertical axis delineates the values of the probability density function, indicating the frequency of populations at each value of $\Sigma E_{a_{ij}}^{S^{\sigma}}$. The placement of data points (species/populations) along the horizontal axis corresponds to their calculated values of $\Sigma E_{a_{ij}}^{S^{\sigma}}$ and is arranged linearly, while the placement along the y-axis is random for improved visual comprehension.

Figure 3: First- and second-order effects on population growth rate, λ_1 (corresponding to elasticities and self-second derivatives of population growth rate, respectively) for 16 mammal species. The 16 plots represent populations where the MPMs built by ages were available in the COMADRE Animal Matrix Database. The yellow-blue colour scale represents elasticity values for each of the demographic processes in the MPM, where yellow cells represent high and blue cells low elasticity of deterministic population growth rate to changes in demographic processes. No colour means elasticity=0. The black dots represent negative self-second derivatives ofλ_1 - corresponding to concave selection - and the white dots represent positive self-second derivatives ofλ_1 - ditto convex selection. The dot sizes are scaled by the absolute value of self-second derivatives, where the smaller the dot, the closer a self-second derivative is to 0, indicating weak or no nonlinearity. Thus, large dots indicate strong nonlinear selection forces, either concave (black) or convex (white). Since the derivatives of population growth rate are confounded by eigen-structure (Kroon *et al.* 2000), the scaling of the elasticity values and second-derivative values is species specific - *i.e.* , each plot has its own scale. Species-specific scales can be found in Supplementary material (Table S2).

BOX 1:

The demographic buffering hypothesis : Stemming from Tuljapurkar's approximation (Tuljapurkar 1982), Pfister (1998) showed that the penalisation term representing the variance-covariance structure, tends to be reduced when elasticities of demographic processes and their coefficients of variation covary negatively.*However, the term demographic buffering was only coined later* (*sensu* Morris & Doak 2004). The demographic buffering hypothesis is also referred to as "adaptive buffering" (*sensu* Le Coeur et al. 2022), suggesting that *selection* acts to minimize the negative impacts of environmental variation by reducing the temporal variance of key demographic processes (*e.g.* , survival, development, reproduction) that have the highest sensitivity/elasticity to population growth rate, a fitness proxy (Gaillard & Yoccoz 2003; Pfister 1998).

Demographic buffering is a broader concept than the demographic buffering hypothesis; it refers to a population's capacity to withstand environmental variability by keeping essential demographic processes stable over time (Gascoigne *et al.* 2024a, b; Hilde *et al.* 2020; Morris & Doak 2004; Pfister 1998). It is worth noting that this term does not explicit allude to the evolutionary mechanisms that include selection, which are predicted by the demographic buffering hypothesis (Le Coeur *et al.* 2022).

Demographic lability : A population's ability to accommodate fluctuations in demographic processes in response to temporal variations in environmental conditions (Le Coeur *et al.* 2022; Jäkäläniemi*et al.* 2013; Koons *et al.* 2009). The relationship between the labile demographic process and the environment can be convex, concave, or linear. A labile vital rate in a variable environment will have an average value that is greater than, less than, or equal to the vital rate estimated in the mean environment, depending on the shape of the relationship. Similar as for the demographic buffering hypothesis, the demographic lability hypothesis relies on *selection* for demographic process to track environmental fluctuations in a way that increases the long-term fitness (λ_{ς}). This process occurs when the increase in demographic process mean — due to convexity — overcomes the detrimental effect of temporal variance in annual population growth rates (Le Coeur *et al.* 2022).

Sensitivity : Represented by a first-order partial derivative of population growth rate with respect to each demographic process (Caswell 1978, 2001; Ebert 1999), sensitivity measures the absolute change in fitness that a change in a demographic process would cause.

Elasticity : Proportional sensitivity. A measure of proportional change in fitness caused by a proportional change in demographic process. Elasticities can be of different types (Grant *et al.* 2007; Haridas *et al.* 2009; Haridas & Tuljapurkar 2005, 2007; de Kroon *et al.* 1986; Kroon *et al.* 2000; Van Tienderen 2000; Tuljapurkar *et al.* 2003) and with respect to both, the stochastic and the deterministic population growth rates.

Tuljapurkar's approximation : To overcome dealing with complex probability distributions that describe demographic fluctuations through time, the approximation captures the essence of the effect of temporal variability, at least for small amounts of variability (*i.e.* small noise). It states that the logarithm of the long-term stochastic population growth rate equals the geometric mean growth rate plus a penalty term containing the demographic process variance-covariance structure (Tuljapurkar 1982).

Supplementary material – Data available in COMADRE Version 3.0.0 and results from Step 1 of the framework

Table S1. The metadata used and the respective results presented in the main text. The first four columns represent the information from where Matrix Populations Models (MPMs) were extract precisely as presented in COMADRE 3.0.0.

Species	**Common name**	**Species (COMADRE)**	**Order**
Homo sapiens sapiens	Human	Homo_sapiens_subsp._sapiens	Primat
Alces alces	Moose	Alces_alces	Artioda
Antechinus agilis	Agile antechinus	Antechinus_agilis	Dasyur
Bos primigenius	Cattle	Bos_primigenius	Artioda
Brachyteles hypoxanthus	Northern muriqui	Brachyteles_hypoxanthus	Primat
Callospermophilus lateralis	Golden-mantled ground squirrel	Callospermophilus_lateralis	Rodent
Cebus capucinus	White faced capuchin monkey	Cebus_capucinus	Primat
Cercopithecus mitis	Blue monkey	Cercopithecus_mitis	Primat
Cervus canadensis subsp. nelsoni	Rocky Mountain elk	Cervus_canadensis_subsp._nelsoni	Artioda
Eumetopias jubatus	Northern sea lion; Steller sea lion	Eumetopias_jubatus	Carniv
Felis catus	Feral cat	Felis_catus	Carniv
Gorilla beringei	Mountain gorilla	Gorilla_beringei	Primat
Hippocamelus bisulcus	Huemul deer	Hippocamelus_bisulcus	Artioda
Leopardus pardalis	Ocelot	Leopardus_pardalis	Carniv
Lepus americanus	Snowshoe hare	Lepus_americanus	Lagom
Lycaon pictus	African wild dog	Lycaon_pictus	Carniv
Macaca mulatta	Rhesus macaque	Macaca_mulatta_3	Primat
Macropus eugenii	Tammar wallaby	Macropus_eugenii	Diprot
Marmota flaviventris	Yellow-bellied marmot	Marmota_flaviventris_2	Rodent
Marmota flaviventris	Yellow-bellied marmot	Marmota_flaviventris_3	Rodent
Microtus oeconomus	Root vole	Microtus_oeconomus	Rodent
Mustela erminea	Stoat	Mustela_erminea	Carniv

Orcinus orca	Killer whale	Orcinus_orca_2	Cetace
Ovis aries	Soay sheep	Ovis_aries_2	Artioda
Pan troglodytes subsp. schweinfurthii	Eastern chimpanzee	Pan_troglodytes_subsp._schweinfurthii	Primat
Papio cynocephalus	Olive baboon	Papio_cynocephalus	Primat
Peromyscus maniculatus	Deer mouse	Peromyscus_maniculatus_2	Rodent
Phascolarctos cinereus	Koala	Phascolarctos_cinereus_2	Diprot
Phocarctos hookeri	New Zealand sea lion	Phocarctos_hookeri	Carniv
Propithecus verreauxi	Verreaux's sifaka	Propithecus_verreauxi	Primat
Rattus fuscipes	Bush rat	Rattus_fuscipes	Rodent
Urocitellus armatus	Uinta ground squirrel	Spermophilus_armatus	Rodent
Urocitellus armatus	Uinta ground squirrel	Spermophilus_armatus_2	Rodent
Urocitellus columbianus	Columbian ground squirrel	Spermophilus_columbianus	Rodent
Urocitellus columbianus	Columbian ground squirrel	Spermophilus_columbianus_3	Rodent
Ursus americanus subsp. floridanus	Florida black bear	Ursus_americanus_subsp._floridanus	Carniv
Ursus arctos subsp. horribilis	Grizzly bear	Ursus_arctos_subsp._horribilis_5	Carniv
Ursus maritimus	Polar bear	Ursus_maritimus_2	Carniv
Brachyteles hypoxanthus	Northern muriqui	Brachyteles_hypoxanthus_2	Primat
Cebus capucinus	White-faced capuchin monkey	Cebus_capucinus_2	Primat
Chlorocebus aethiops	Vervet	Chlorocebus_aethiops_2	Primat
Erythrocebus patas	Patas monkey	Erythrocebus_patas	Primat
Gorilla beringei subsp. beringei	Mountain gorilla	Gorilla_beringei_subsp._beringei	Primat

Table S2 . The species-specific scales for the elasticity ofλ_1 to changes in demographic processes and for the self-second derivatives of λ_1 with respect to demographic processes for the 16 mammal species studied.

Figure 3 reference	Species common name	E_{min}=elasticity minimum value	E_{max}=elasticity maximum value	S
A	Blue monkey	0	0.52	-
B	Columbian ground squirrel	0	0.23	-
C	Eastern chimpanzee	0	0.60	-
D	Human	0	0.18	-0
E	Killer whale	0	0.55	-
F	Moose	0	0.55	-0
G	Mountain gorilla	0	0.81	-
H	Northern muriqui	0	0.72	-
I	Olive baboon	0	0.54	-0
J	Polar bear	0	0.26	-0
K	Rhesus macaque	0	0.51	-0
L	Root vole	0	0.86	-
M	Soay sheep	0	0.56	-0
N	Tammar wallaby	0	0.55	-0
O	Verreaux's sifaka	0	0.60	-
P	White faced capuchin monkey	0	0.66	-

Hosted file

`Santos Gascoigne_Towards a unified framework for buffering _FINAL_TRACKED.docx` available at `https://authorea.com/users/640983/articles/1247163-demographic-buffering-in-natural-populations-multi-level-perspective`

Towards an integrated framework for evidencing demographic buffering in natural populations

A manuscript in preparation for submission to ECOLOGY LETTERS
Type of article: METHOD

Gabriel Silva Santos [1,2*], Samuel J L Gascoigne[3*], André Tavares Corrêa Dias[4], Maja Kajin [3,5**♦], Roberto Salguero-Gómez[3♦]

[1] National Institute of the Atlantic Forest (INMA), 29650-000, Santa Teresa, Espírito Santo, Brazil. ssantos.gabriel@gmail.com
[2] Department of Ecology, Graduate Program in Ecology and Evolution, Rio de Janeiro State University, 524 São Francisco Xavier Street, 20550-900, Maracanã, Rio de Janeiro, Brazil.
[3] Department of Biology, University of Oxford, South Parks Road, OX1 3RB, Oxford, UK. samuel.gascoigne@pmb.ox.ac.uk, rob.salguero@biology.ox.ac.uk
[4] Department of Ecology, Institute of Biology, Universidade Federal do Rio de Janeiro, Avenida Carlos Chagas Filho 373, 21941-590 Rio de Janeiro, RJ, Brazil. atcdias@gmail.com
[5] Chair of Zoology, Department of Biology, Biotechnical Faculty, University of Ljubljana, Večna pot 111, 1000 Ljubljana, Slovenia. maja.kajin@bf.uni-lj.si

[*] Shared first authorship
[**] Corresponding author
♦ Shared senior authorship

AUTHOR CONTRIBUTIONS: GSS developed the initial concept, performed the statistical analyses, and contributed to the first draft of the manuscript. SJLG developed the initial concept, contributed to the first draft and all other versions of the manuscript, and generated final figures. ATCD co-advised the project and contributed significantly to final versions of the manuscript. MK developed and managed the project, contributed to the first draft and all other versions of the manuscript, and generated final figures. RSG developed and managed the project and contributed to the first draft and all other versions of the manuscript. All authors made substantial contributions to editing the manuscript and further refining ideas and interpretations.

RUNNING TITLE: Demographic buffering framework (32/45 characters)

KEYWORDS: COMADRE Animal Matrix Database, elasticity, life-history evolution, natural selection, second-order derivative, sensitivity, stochasticity, variance.

NUMBER OF WORDS: Abstract – 146/150 words, main text (excluding abstract, acknowledgements, references, table, and figure legends) – 4979/5000 words

NUMBER OF REFERENCES: 86

NUMBER OF TABLES: 2 (in Supplementary Material)

NUMBER OF FIGURES: 3

Abstract (146/150 words)

The demographic buffering hypothesis predicts that natural selection reduces the temporal fluctuations in demographic processes (survival, development, and reproduction) due to their negative impacts of temporal variation on population dynamics. However, evidencing buffering patterns at different hierarchical levels – between and within populations – and understanding how selection shapes those patterns, remains a challenge in Ecology and Evolution. Here, we introduce a framework that allows for the evidencing of demographic buffering between and within populations. The framework uses the sum of stochastic elasticities for between-populations comparisons along with first- and second-order effects of demographic process variability on fitness for within-population comparisons. We apply this framework to 43 populations of 37 mammal species to test the hypothesis that buffered species are under strong concave selection pressures. Using our framework, we show that demographically buffered species do not necessarily have strong concave selection pressures in their most impactful demographic processes.

Environmental stochasticity shapes organisms' life histories (Bonsall & Klug 2011; Stearns 1992; Tuljapurkar 1990, 2010). Nonetheless, how organisms will cope with the changing variation in environmental conditions (Bathiany *et al.* 2018; Boyce *et al.* 2006; Morris *et al.* 2008) remains an intriguing ecological and evolutionary question (Sutherland *et al.* 2013). Evolutionary demography provides diverse explanations for how evolutionary processes shape demographic responses to environmental stochasticity (Charlesworth 1994; Healy *et al.* 2019; Hilde *et al.* 2020; Pfister 1998; Tuljapurkar *et al.* 2009). The long-term stochastic population growth rate (λ_s) representing the geometric mean of population growth rates over time (λ_t; Tuljapurkar 1982), forms the basis of the Demographic Buffering Hypothesis (Morris & Doak 2004; Pélabon *et al.* 2020).

Increasing the geometric mean of λ_t over time corresponds to a rise in the long-term stochastic population growth rate. Conversely, higher variance in λ_t reduces λ_s (Morris & Doak 2004; Tuljapurkar 1982), impacting population persistence (Lefèvre *et al.* 2016). The demographic buffering hypothesis (Pfister 1998) suggests life histories are selected to minimize the negative impacts of environmental variation by constraining the temporal variance of key demographic processes (*e.g.*, survival, development, reproduction) that have the highest sensitivity/elasticity to population growth rate, a fitness proxy (Gaillard & Yoccoz 2003; Pfister 1998). Demographic buffering describes the selection-driven constraint on the temporal variance of these key demographic processes (Gascoigne *et al.* 2024a, b; Hilde *et al.* 2020; Morris & Doak 2004; Pfister 1998). Here, we focus on the emerging patterns of demographic buffering in different animal life histories rather than on the demographic buffering hypothesis itself.

An integrative approach to evidence demographic buffering is still missing. Indeed, identifying demographic buffering remains challenging (Doak *et al.* 2005; Morris & Doak 2004) for several reasons, one of them being different interpretations of results from correlational analyses, as in Pfister (1998) and Hilde *et al.* (2020). Some authors rank species' life histories on a continuum from buffered to labile using the correlation coefficient (Spearman's correlation ρ) between the impact of demographic processes on the population growth rate and the temporal variance of said demographic processes (McDonald *et al.* 2017; Salguero-Gómez 2021). There, negative correlation coefficient values indicate buffering. Alternatively, the absence of statistical support for buffering may suggest a preference for demographic variance to track environmental conditions, a phenomenon supported by the Demographic Lability Hypothesis (Drake 2005; Hilde *et al.* 2020; Jäkäläniemi *et al.* 2013; Koons *et al.* 2009; Reed & Slade 2012). However, increased variability alone is not enough to constitute demographic lability; it must also result in significant changes in the mean value of the demographic process (Le Coeur *et al.* 2022).

Another obstacle to generalising a measure of demographic buffering across populations and species is the targeted hierarchical level of examination. Some studies focus on characteristics drawn from the *entire population model* (McDonald *et al.* 2017; Reed & Slade 2012). At this *between-populations level* (hereafter), a life history is considered demographically buffered if the governing demographic processes have low temporal variance (Le Coeur *et al.* 2022; Hilde *et al.* 2020; Morris & Doak 2004; Pfister 1998). However, to fully grasp how and why demographic buffering occurs, and how patterns might change in response to the environment, we must also consider characteristics within an individual population model (*within-populations level* hereafter). Within a population, one demographic process may be buffered against climatic variability while another may be labile (Barraquand & Yoccoz 2013; Jongejans *et al.* 2010; Koons *et al.* 2009). Furthermore, even if a given demographic process is primarily governing the population growth rate in one year, a different one might take over next year (Evers *et al.* 2021). Despite the relevance of within- and between-populations level processes, thus far studies have focused on evidencing demographic buffering at the within- and between-population levels separately. To integrate these two levels of analysis, here we investigate demographic buffering signatures together.

To examine demographic buffering at the between-populations level, we use the *summed* effect of the variability of all demographic processes on the population growth rate. A weak summed effect means that the population growth rate is relatively unaffected by the variability in demographic processes (Haridas & Tuljapurkar 2005), and this lack of effect by demographic process variability is consistent with demographic buffering. As such, a summed effect of variability offers a good proxy to evidence demographic buffering (Gascoigne *et al.* 2024b; Haridas & Tuljapurkar 2005) and enables the classification of populations along a continuum. The within-populations level requires a separate approach. Thus, there we use the relative contribution of each demographic process and how variability in the governing demographic process(es) affects the population growth rate (*e.g.*, Caswell 1978, 1996, 2001; Ebert 1999; de Kroon et al. 1986). Importantly, by exploring the governing demographic processes, we also investigate how natural selection affects them (*e.g.*, Caswell 1996; Shyu & Caswell 2014). Understanding the interplay between demographic variability and natural selection thus not only elucidates population dynamics but also provides insight into the evolutionary pressures shaping the life-history strategies (Charlesworth 1994; Salguero-Gómez 2024; Sanghvi *et al.* 2024).

A powerful approach to reveal the role of natural selection acting on the variability of demographic processes is through measuring a first and second order effect on population growth rate (Carslake *et al.* 2008). First-order effects of demographic processes on population growth rate, such as elasticities, show how *variation* in demographic processes affects population growth rate, and relies on the *linear* relation between demographic processes and the growth rate. A second-order effect, on the other hand, reveals the sensitivity of population growth rate to temporal *autocorrelation* in variable environments (Tuljapurkar 1990), and identifies where demographic processes have a *nonlinear* effect on population growth rate. Combining both approaches into a single framework consolidates our understanding of fitness behaviour near local maxima and minima, among other advantages discussed below. This approach and has started to pave its way into Ecology (Kajin *et al.* 2023; Tuljapurkar *et al.* 2023).

Here, we propose that an additional metric to examine demographic buffering: the second-order effect of demographic process variation on population growth rate. We show that each hierarchical level is best studied with a different method. Moreover, we hypothesise that buffered species, those where perturbing the variance of demographic processes has little impact on their fitness, are under strong concave selection pressures (*i.e.*, the force that aims to diminish temporal variance of a trait, sensu Shyu & Caswell 2014) on the governing demographic processes. Indeed, the summed effect of demographic process variability on population growth rate and elasticities are related (Haridas & Tuljapurkar 2005). Concave selection pressures favour traits that contribute to reducing temporal variance, thereby enhancing population stability and resilience in the face of environmental volatility. We discuss the validity of our hypothesis and demonstrate the applicability and advantages of our framework by testing it with 43 populations of 37 mammal species.

Towards an integrated framework to assess evidence of demographic buffering

Current evidence for demographic buffering has primarily been assessed using Matrix Population Models (*MPMs*) (Pfister 1998; Rotella *et al.* 2012). However, Integral Projection Models (*IPMs*) (Easterling *et al.* 2000; Ellner *et al.* 2016; Gascoigne *et al.* 2023a, 2024b; Rodríguez-Caro *et al.* 2021; Wang *et al.* 2023) can also identify demographic buffering. MPMs and IPMs are structured, discrete-time demographic models (Caswell 2001; Ellner *et al.* 2016). For simplicity, here we focus on MPMs, but the same approaches apply to IPMs

(Doak *et al.* 2021; Griffith 2017). We refer to demographic processes as MPM ***A*** entries a_{ij} (*i.e.,* upper-level parameters *sensu* Zuidema & Franco 2001) and the vital rates composing the matrix elements (*i.e.,* lower-level parameters, *ditto*). The conversion between matrix elements and vital rates is straightforward (Franco & Silvertown 2004).

We first place species on a variance continuum. The variance continuum represents the *summed* effects of proportional increases in temporal variance across all demographic processes (a_{ij}) of the MPM ***A*** on the population growth rate λ_s, operating at the *between-populations level.* It is based on partitioning the sum of all the stochastic elasticities ($\Sigma E_{a_{ij}}^{S}$) into two components: i) the sum of stochastic elasticities with respect to the variance ($\Sigma E_{a_{ij}}^{S^\sigma}$), which assesses how variability in a_{ij} affects λ_s, and ii) the sum of stochastic elasticities with respect to the arithmetic mean of demographic processes ($\Sigma E_{a_{ij}}^{S^\mu}$), which evaluates the impact of a change in mean values of demographic processes on λ_s (Haridas & Tuljapurkar 2005).

The equal perturbation of both $\Sigma E_{a_{ij}}^{S}$components assumes that the CV of demographic processes remains constant (Haridas & Tuljapurkar 2005). Higher absolute value of $\Sigma E_{a_{ij}}^{S^\sigma}$ indicates greater sensitivity of λ_s to demographic process variability, suggesting the absence of demographic buffering. Conversely, lower $\Sigma E_{a_{ij}}^{S^\sigma}$ values support the demographic buffering hypothesis, with λ_s being is less sensitive to variability (Haridas & Tuljapurkar 2005; Tuljapurkar *et al.* 2003) (Fig. 1A).

Species or populations are positioned along the variance continuum based on the impact of variance on the stochastic population growth rate. Species highly sensitive to environmental variability are on the left (potentially unbuffered[1]), while species less sensitive

---

[1] Unconstrained variance does not necessarily imply demographic lability, defined as an increase in *mean value* of a demographic process in response to improved environmental conditions (Le Coeur *et al.* 2022). By examining stochastic elasticities, we can assess changes in the contribution of demographic process variance to λ_s, while mean values remain unchanged.

are on the right (potentially buffered) end (Fig. 1A). We expect buffered species to exhibit concave selection signatures. Although the position on the continuum provides insight into how environmental variation affects λ_s, $\Sigma E^{S^{\sigma}}_{a_{ij}}$does not consider covariances between demographic processes and serial correlations, crucial for fully diagnosing buffering (Haridas & Tuljapurkar 2005). Thus, species' position at the buffered end of the variance continuum is a *necessary but not sufficient* condition for evidence of demographic buffering. To address this second criterion, we use second derivatives of population growth rate with respect to demographic processes to elucidate the impact of selection on variance (below).

Next, we delve into within-population level by calculating the partial derivatives of λ_1 (obtained by averaging sequential MPMs across the study duration) concerning all matrix elements a_{ij} of the MPM $\boldsymbol{A}$ (Fig. 1B). This step reveals a first-order effect on fitness – how each demographic process influences λ_1. We then evaluate nonlinear selection patterns using self-second derivatives of λ_1 for each a_{ij} (Fig. 1C), revealing potential nonlinear selection pressures (Brodie *et al.* 1995). Failure to consider these evolutionary processes may lead to misinterpretation of patterns (*e.g.*, Lawler et al. 2009).

First- and second-order effects on fitness show average selection pressures over time. Self-second derivatives of population growth rate with respect to demographic processes measure second-order effects (Carslake *et al.* 2008; Caswell 2001; Kajin *et al.* 2023; Shyu & Caswell 2014; Tuljapurkar *et al.* 2023). Linear fitness relationships (zero self-second derivatives) mean selection changes mean demographic values, not variance (Shyu & Caswell 2014). Nonzero self-second derivatives indicate nonlinear relationships between fitness and a demographic process, revealing additional aspects of selection on the variances and covariances of demographic processes (Brodie *et al.* 1995; Carslake *et al.* 2008; Shyu & Caswell 2014). Interpreting both first- and second-order effects offers insights into population placement on the variance continuum.

The sign (>0, =0, <0) of the self-second derivatives determines the selection type. Negative values (concave selection, ∩-shaped) reduce temporal variance, providing evidence of buffering (Caswell 1996, 2001; Shyu & Caswell 2014). Positive values (convex selection, ∪-shaped) indicate amplified variance, revealing a lack of selection constraints on demographic variance (Bruijning *et al.* 2020; Caswell 1996, 2001; Le Coeur *et al.* 2022; Koons *et al.* 2009; Shyu & Caswell 2014; Vinton *et al.* 2022).

Following the above steps allows evidencing demographic buffering at the between- and within-populations levels. The joint interpretation of first- and second-order effects offers insights into why a population is on either end of the variance continuum. Evidence supporting buffering includes:

1. A population positioned near the 0 end of the $\Sigma E_{a_{ij}}^{S^{\sigma}}$ continuum.
2. Identifying the demographic processes with highest elasticity values within the life cycle.
3. The same processes from (2) associated with negative self-second derivatives, indicating concave selection.

Figure 1B shows that, for an imaginary wolf population, the governing demographic process is the fourth stage stasis (MPM element $a_{4,4}$), with the highest elasticity value (Fig. 1B yellow square). However, Figure 1C reveals little selection on $a_{4,4}$ for variance reduction. Hence, there is no concave selection on $a_{4,4}$, explaining the positioning on the left-side variance continuum (Fig. 1A).

Although not our primary goal, we briefly introduce steps to evidence demographic lability. Compelling lability evidence requires sufficient data across environments [over time or space; but see Perret et al. (2024)] to construct reaction norms depicting demographic responses to environmental changes (Drake 2005; Koons *et al.* 2009; Morris *et al.* 2008). Non-linear relationships between demographic processes and the environment must be established based on the reaction norms. Demographic processes where an increase in the mean value has a stronger positive impact on population growth rate than the detrimental effect of increased variance need to be identified. The latter condition is only met when the process-environment reaction norms are convex (Drake 2005, Koons *et al*. 2009, Morris *et al*. 2008) – but see Barraquand & Yoccoz (2013) for an alternative result. Importantly, species may not be purely buffered or labile some processes may be buffered, others labile, and others insensitive to environmental variability (*e.g.*, Doak *et al*. 2005). Deciphering these patterns is a primary research interest in the field.

Demographic buffering in mammals: A case study

Here, we examine the performance of our framework and test our hypothesis, that is that species at the buffered end of the variance continuum display highly negative self-second derivatives for the governing demographic processes. We use 43 MPMs from 37 mammal species (16 species at the within-populations level). Mammals are of special interest in the context of demographic buffering for two reasons: (1) mammalian life histories have been well studied (Beccari *et al.* 2024; Bielby *et al.* 2007; Gillespie 1977; Jones 2011; Stearns 1983) and (2) some of their populations have already been assessed in terms of demographic buffering, particularly for primates (Campos *et al.* 2017; Morris *et al.* 2008, 2011; Reed & Slade 2012; Rotella *et al.* 2012). Together, the well-studied life histories and previous information about the occurrence of buffering in mammals allow us to make accurate predictions and validate the performance of our framework.

We used MPMs (Caswell 2001) from 43 out of 139 studies with mammals available in the COMADRE Animal Matrix Database v.3.0.0 (Salguero-Gómez *et al.* 2016). These 43 populations encompass 37 species from eight taxonomic orders. We carefully selected these MPMs in our analyses because their models contain values of demographic processes (a_{ij})

for three or more contiguous time periods, thus allowing us to obtain the stochastic elasticity of each a_{ij}. Although we are aware that not all possible temporal variation in demographic processes may have been expressed within this period, we assumed three or more transitions are enough to provide sufficient variation for population comparison (Compagnoni *et al.* 2023). To mitigate bias in variance estimates, we randomly extracted three MPMs from the existing data for each species (Supplementary Material, Table S1), calculated the mean of these three MPMs, and repeated this process 50 times to obtain estimates of $\Sigma E_{a_{ij}}^{S^{\sigma}}$ and their corresponding standard errors. A detailed description of the analysed data and their original sources are detailed in Table S1. Finally, we included MPMs of *Homo sapiens* to cross-check our estimates of second-order derivatives, as it is the only mammalian species where these have been calculated (Caswell 1996). The data for *H. sapiens* were gathered from 26 modern populations (Keyfitz & Flieger 1990).

At the within-populations level, we used a subset of 16 populations (including *H. sapiens*) whose MPMs were age-based. We specifically selected these populations because their life cycles can be summarised by two main demographic processes: survival and contribution to the recruitment of new individuals (Caswell 2010; Ebert 1999).

To quantify the variance continuum and calculate $\Sigma E_{a_{ij}}^{S^{\sigma}}$ for between-populations level comparisons, we followed Tuljapurkar *et al.* (2003) and Haridas & Tuljapurkar (2005). Next, at the within-populations level, we calculated the deterministic elasticities to each demographic process using the *popbio* package (Stubben *et al.* 2020). The self-second derivatives were adapted from *demogR* (Jones 2007) following (Caswell 1996) and applied to the mean MPM of each study. All analyses were performed using R version 4.4.1 (R Core Team 2024).

Results

We ranked 43 populations from the 37 identified mammal species into a variance continuum according to the cumulative impact of variation in demographic processes on λ_s (Fig. 2). Most of the analysed taxonomic orders were placed on the low or zero variance end of the variance continuum (Fig. 2), corroborating with demographically buffered populations. The smallest contributions of variation in demographic processes (note that $\Sigma E_{a_{ij}}^{S^\sigma}$ ranges from 0 to -1), suggesting buffered populations, were assigned to Primates: northern muriqui (*Brachyteles hyphoxantus*, $\Sigma E_{a_{ij}}^{S^\sigma} = -5.31 \times 10^{-5} \pm 2.09 \times 10^{-5}$) (mean ± S.E.) (Fig. 2 silhouette a), mountain gorilla (*Gorilla beringei*, $\Sigma E_{a_{ij}}^{S^\sigma} = -1.28 \times 10^{-5} \pm 1.32 \times 10^{-5}$) (Fig. 2 silhouette b), followed by the blue monkey (*Cercopithecus mitis*, $\Sigma E_{a_{ij}}^{S^\sigma} = -4.43 \times 10^{-5} \pm 1.18 \times 10^{-5}$) (Fig. 2 silhouette c). The first non-primate species placed near the buffered end of the continuum was the Columbian ground squirrel (*Urocitellus columbianus*, Rodentia, $\Sigma E_{a_{ij}}^{S^\sigma} = -3.38 \times 10^{-3} \pm 6.96 \times 10^{-4}$) (Fig. 2 silhouette d). On the other opposite, the species with the highest contribution of variation in demographic processes – placed at the high-variance end of the continuum – was the stoat (*Mustela erminea*, Carnivora, $\Sigma E_{a_{ij}}^{S^\sigma} = -0.310 \pm 0.0162$) (Fig. 2 silhouette e). All the 14 primate populations occupied the buffered side of the variance continuum, with the exception of the Patas monkey (*Erythrocebus patas*, Primates, $\Sigma E_{a_{ij}}^{S^\sigma} = -0.0521 \pm 5.38 \times 10^{-3}$) (Fig. 2 silhouette f). The snowshoe hare (*Lepus americanus*, Lagomorpha, $\Sigma E_{a_{ij}}^{S^\sigma} = -0.262 \pm 0.0233$) (Fig. 2 silhouette g) and the Bush rat (*Rattus fuscipes*, Rodentia, $\Sigma E_{a_{ij}}^{S^\sigma} = -0.245 \pm 4.29 \times 10^{-3}$) (Fig. 2 silhouette h) were positioned on the non-buffered end of the variance continuum. Additional information (including standard errors of the elasticity estimates) is provided in Table S1. *A posteriori*, we quantified the impact of phylogenetic relatedness on the estimates of the sum of stochastic elasticities (Fig. 2), and then for the correlation between those estimates and the number of MPMs available per species. For the former, we estimated Blomberg's K, a measure of phylogenetic signal that ranges between 0 (weak signal) to positive values 1 (strong) (Münkemüller *et al.* 2012). Blomberg's K in our analyses was 0.23. The correlation between the number of available MPMs per study and the sum of stochastic elasticities (post jack-knifing) raised a weakly negative coefficient (-0.002), though significant ($P = 0.017$).

We found little evidence in support of our hypothesis. Specifically, the demographic processes with the highest elasticity values failed to display strong negative self-second derivatives (Fig. 3). Particularly for the majority of primates, demographic processes with high elasticities had positive values for the self-second derivatives (indicated by yellow squares with white dots in Figure 3). Examples of primate species exhibiting high elasticities and positive values for their self-second derivatives include northern muriqui (*Brachyteles hypoxanthus*), mountain gorilla (*Gorilla beringei*), white-faced capuchin monkey (*Cebus capucinus*), rhesus monkey (*Macaca mulatta*), blue monkey (*Cercopithecus mitis*), Verreaux's sifaka (*Propithecus verreauxi*) and olive baboon (*Papio cynocephalus*) (Fig. 3). This implies that the key demographic processes influencing λ_1 do not show evidence of selective pressure for reducing their variability.

The killer whale (*Orcinus orca*) showed similar lack of support for our hypothesis as primates. Indeed, *O. orca* was positioned at the buffered end of the variance continuum (Cetacea, $\Sigma E^{S^{\sigma}}_{a_{ij}} = -4.72 \times 10^{-4} \pm 1.53 \times 10^{-4}$) (Fig. 2 silhouette not shown). However, the first- and second-order effects show that the governing three demographic processes in the killer whale life cycle (namely, matrix elements $a_{2,2}$, $a_{3,3}$, and $a_{4,4}$) are not under selection pressures for reducing their temporal variance, but the opposite (yellow and green squares with white dots, Fig. 3).

Only two species supported our hypothesis: humans and the Columbian ground squirrel (*Urocitellus columbianus*). In humans, demographic parameters representing survival from the first to second age class (matrix element $a_{2,1}$) displayed high elasticities and negative self-second derivatives (depicted as yellow squares with black dots in Fig. 3). In *U. columbianus*, survival from the first to the second age class ($a_{2,1}$) too showed evidence of selection reducing the variance of this demographic process. Accordingly, *U. columbianus* was positioned near the buffered end of the variance continuum, providing consistent evidence supporting our hypothesis by displaying first- and second-order effects indicative of temporal variance reduction in the key demographic process. Conversely, the primary governing demographic process for Soay sheep (*Ovis aries*) displayed convex selection signatures. For *O. aries* (Fig. 2, silhouette i), remaining in the third age class ($a_{3,3}$, Fig. 3) governs the influence on λ_t and is under selection pressure to have its variance increased. These characteristics suggest potential conditions for lability, despite the species being positioned closer to the buffered end of the variance continuum.

The first- and second-order effects illustrate the importance of examining buffering evidence at the within-populations level. These effects can identify the simultaneous contributions of concave and convex selection on different demographic processes within a single life cycle. In the polar bear (*Ursus maritimus*), the key demographic process ($a_{4,4}$) is under convex selection, as depicted by a yellow square with a white dot in Figure 3. However, the demographic process with the second highest elasticity value ($a_{5,4}$) is under strong concave selection (depicted by a light green square with a black dot in Figure. 3).

By adding the second-order effect to the toolbox for demographic buffering, another important inference was made possible. The high absolute values of self-second derivatives (large dots, either black or white, Fig. 3) indicate where the sensitivity of λ_1 to demographic parameters is itself prone to environmental changes. For instance, if the value of $a_{5,4}$ for *U. maritimus* increased, the sensitivity of λ_t to $a_{5,4}$ would decrease because the self-second derivative of $a_{5,4}$ is highly negative (depicted by the largest black dot in polar bear, Fig. 3 silhouette j). The opposite holds for the $a_{4,4}$ demographic process, where an increase in the value of $a_{4,4}$ would increase the sensitivity of λ_t to $a_{4,4}$, because the self-second derivative of $a_{4,4}$ is highly positive (the largest white dot in the polar bear MPM). Thus, sensitivities (or equally elasticities) of demographic processes with high absolute values for self-second derivatives are dynamic and can easily change.

Discussion

We report evidence of demographic buffering assessed at the between and within populations level. We used stochastic elasticities alongside the first- and second- order perturbation analysis and applied these analyses to mammal species to test our hypothesis. Here, we find weak support for said hypothesis, since most populations placed at the buffered end of variance continuum failed to display concave selection signatures.

Evidencing demographic buffering is not straightforward. Indeed, through the analysis of stochastic population growth rate (λ_s) in our application of the framework to 43 populations of 37 mammal species, we identify the highest density of natural populations near the buffered end of the variance continuum. However, we show that the same species then fail to exhibit signs of concave (∩-shaped) selection on key demographic parameters, opposed to our hypothesis. Such results suggest discordance between two features of demographic buffering, namely: 1) the stochastic population growth rate having a low sensitivity to temporal variability in demographic processes, and 2) demographic processes having variability constrained by selection.

The lack of correlation between non-linear selection patterns (concave/convex) and species positioning on the variance continuum for the studied mammal species may have several explanations. Firstly, non-linear selection on demographic process variability is *dynamic* (Kajin *et al.* 2023). Within a life cycle, even minor changes in key demographic processes can trigger a domino effect, affecting not only the process itself but also the sensitivity of λ_1 to changes in said process (Stearns 1992). Consequently, correlations between demographic processes (negative correlations known as trade-offs) are influenced by minor alterations in the governing demographic processes (Doak *et al.* 2005). Therefore, the observed self-second derivative of the population growth rate represents a momentum that can be influenced by small changes in any demographic process within the life cycle. Because of these characteristics, second-order derivatives reveal “fine scale” fitness behaviour compared to sums of stochastic elasticities. Evolutionary demography still requires a tool to connect second-order fitness effects with stochastic elasticities in a biologically interpretable manner (but see Tuljapurkar *et al.* 2023).

When placing our study species along a variance continuum, primates tend to be located on the buffered end. However, most primates displayed convex – instead of the expected concave – selection on adult survival. Similar results, where the key demographic process failed to display constrained temporal variability, have been reported for long-lived seabirds (Doherty *et al.* 2004). One explanation for the unexpected convex selection on adult survival involves trade-offs, as suggested by (Doak *et al.* 2005). When two demographic parameters are negatively correlated, the variance of population growth rate can be increased or decreased (Compagnoni *et al.* 2016; Evans & Holsinger 2012).

Correlations among demographic processes (positive and negative) inherently influence the biological limits of variance (Haridas & Tuljapurkar 2005). This is because the magnitude of variation in a particular demographic process is constrained by the variation of other demographic processes. Not surprisingly, correlations among demographic processes have been shown to be strongly subjected to ecological factors (Fay *et al.* 2022). Therefore, future studies may benefit from deeper insights using *cross*-second derivatives (Caswell 1996, 2001) to investigate correlations among demographic processes.

Biological variance estimates are inevitably subjected to several sources of bias (Simmonds & Jones 2024). To minimise bias, we randomly sampled the available matrices before obtaining the estimates. Despite the significant correlation between $\Sigma E_{a_{ij}}^{S^{\sigma}}$ and the number of available matrices per species, the relative positioning of species remains meaningful for between-population level comparisons, as the correlation is very weak (-0.002). Still, researchers carrying out macroecological comparisons of demographic buffering might want to be even more restringent than we have been here with their datasets, as these grow longer with time (Compagnoni *et al.* 2021; Salguero-Gómez *et al.* 2021).

Regarding phylogenetic effects, our tests revealed a mild signal, but we note that future work regressing $\Sigma E_{a_{ij}}^{S^{\sigma}}$ values against potential independent variables (*e.g.*, climate values) may want to correct for this phylogenetic dependence. By having carefully chosen studies from a database that contains >400 species and retained only those that passed through a set of selection criteria (Che-Castaldo *et al.* 2020; Gascoigne *et al.* 2023b; Kendall *et al.* 2019; Römer *et al.* 2024; Simmonds & Jones 2024), we mitigate those biases *a priori*. Furthermore, we are using an elasticity-based approach, meaning we are comparing proportional variances. At present, the available methods still do not account for constraints in variance nor performing a perturbation approach disproportionately.

The analyses at both between- and within-populations levels are fundamentally interconnected. This connection is grounded on the fact that large summed elasticities with respect to variance are intrinsically linked to high elasticity values, as demonstrated in equation 6 in (Haridas & Tuljapurkar 2005). This finding robustly endorses the perspective that species' positions along the variance continuum should be interpreted with consideration of first and second-order effects, and additionally, in the context of selection pressures acting on the variability of demographic processes, as revealed by a second order effect.

Combining first- and second-order analyses is crucial for understanding the factors shaping demographic buffering patterns. The second-order effect reveals that the role of natural selection in shaping temporal variation in demographic processes is more complex than initially thought. Indeed, demographic processes within our study populations often face a mix of convex and concave selection. This mix of selection patterns was suggested by Doak et al. (2005), who noted that dramatic changes in population growth rate sensitivities are influenced by correlations among demographic processes. Here, only two of the 16 mammal species revealed concave selection on the key demographic processes: Columbian ground squirrel (*Urocitellus columbianus*), and humans (*Homo sapiens*). These two species were placed near the buffered end of the variance continuum, supporting our hypothesis. Evidence of buffering has been reported across 22 ungulate species (Gaillard & Yoccoz 2003). However, in the one ungulate we examined, the moose (*Alces alces*), we found only partial support for our hypothesis, as it is near the buffered end of the variance continuum but lacks concave selection pressures.

Our overall findings reveal varying levels of support for the notion that adult survival in long-lived species tends to be buffered. Indeed, Gaillard et al. (1998) found that adult female survival varied considerably less than juvenile survival in large herbivores. This finding was also supported by further studies in ungulates (Gaillard & Yoccoz 2003), turtles (Heppell 1998), vertebrates and plants (Pfister 1998), and more recently across nine species of plants (McDonald *et al.* 2017). However, an alternative result was also reported by Gaillard and Yoccoz (2003) for small mammals, where variability in adult survival was unexpectedly high, even though the studied small mammals were annual, and as such comparable to large mammal model. Seasonality, frequency and method of sampling all influence survival estimates and their estimated variability, thus, when comparing multiples species/studies, all of the latter characteristics should be taken into account when interpreting the results.

Examining the drivers of demographic buffering has become an important piece of the ecological and evolutionary puzzle of demography. As such, understanding buffering can help us better predict population responses to environmental variability, climate change, and direct anthropogenic disturbances (Boyce *et al.* 2006; Gascoigne *et al.* 2024a; McDonald *et al.* 2017; Pfister 1998; Vázquez *et al.* 2017). By setting demographic buffering into a broader and integrated framework, we hope to enhance comprehension and prediction of the implications of heightened environmental stochasticity on the evolution of life history traits. This understanding is crucial in mitigating the risk of extinction for the most vulnerable species.

Acknowledgements

This study was financed in part by the *Coordenação de Aperfeiçoamento de Pessoal de Nível Superior* - Brasil (CAPES) - Finance Code 001. GSS was supported by CAPES and CNPq (301343/2023-3). MK was supported by the European Commission through the Marie Skłodowska-Curie fellowship (MSCA MaxPersist #101032484) hosted by RSG. RS-G was supported by a NERC Independent Research Fellowship (NE/M018458/1) and a NERC Pushing the Frontiers (NE/X013766/1).

Data availability

The demographic data used in this paper are open-access and available in the COMADRE Animal Matrix Database (https://compadre-db.org/Data/Comadre). A list of the studies and species used here is available in Supplementary Material (Table S1). The data and code supporting the results can be accessed here:

https://github.com/SamuelGascoigne/Demographic_buffering_unified_framework.

References

Barraquand, F. & Yoccoz, N.G. (2013). When can environmental variability benefit population growth? Counterintuitive effects of nonlinearities in vital rates. *Theor Popul Biol*, 89, 1–11.

Bathiany, S., Dakos, V., Scheffer, M. & Lenton, T.M. (2018). Climate models predict increasing temperature variability in poor countries. *Sci Adv*, 4.

Beccari, E., Capdevila, P., Salguero-Gómez, R. & Carmona, C.P. (2024). Worldwide diversity in mammalian life histories: Environmental realms and evolutionary adaptations. *Ecol Lett*, 27.

Bielby, J., Mace, G.M., Bininda-Emonds, O.R.P., Cardillo, M., Gittleman, J.L., Jones, K.E., *et al.* (2007). The Fast-Slow Continuum in Mammalian Life History: An Empirical Reevaluation. *Am Nat*, 169, 748–757.

Bonsall, M.B. & Klug, H. (2011). The evolution of parental care in stochastic environments. *J Evol Biol*, 24, 645–655.

Boyce, M., Haridas, C., Lee, C. & The NCEAS Stochastic Demography Working Group. (2006). Demography in an increasingly variable world. *Trends Ecol Evol*, 21, 141–148.

Brodie, E.I., Moore, A. & Janzen, F. (1995). Visualizing and quantifying natural selection. *Trends Ecol Evol*, 10, 313–318.

Campos, F.A., Morris, W.F., Alberts, S.C., Altmann, J., Brockman, D.K., Cords, M., *et al.* (2017). Does climate variability influence the demography of wild primates? Evidence from long-term life-history data in seven species. *Glob Chang Biol*, 23, 4907–4921.

Carslake, D., Townley, S. & Hodgson, D.J. (2008). Nonlinearity in eigenvalue-perturbation curves of simulated population projection matrices. *Theor Popul Biol*, 73, 498–505.

Caswell, H. (1978). A general formula for the sensitivity of population growth rate to changes in life history parameters. *Theor Popul Biol*, 14, 215–230.

Caswell, H. (1996). Second Derivatives of Population Growth Rate: Calculation and Applications. *Ecology*, 77, 870–879.

Caswell, H. (2001). *Matrix Population Models: Construction, Analysis, and Interpretation*. Sinauer Associates Inc. Publishers, Sunderland, Massachusetts, USA.

Charlesworth, B. (1994). *Evolution in age-structured populations*. second edi. Cambridge University Press.

Che-Castaldo, J., Jones, O.R., Kendall, B.E., Burns, J.H., Childs, D.Z., Ezard, T.H.G., *et al.* (2020). Comments to "Persistent problems in the construction of matrix population models." *Ecol Modell*, 416.

Le Coeur, C., Yoccoz, N.G., Salguero-Gómez, R. & Vindenes, Y. (2022). Life history adaptations to fluctuating environments: Combined effects of demographic buffering and lability. *Ecol Lett*, 25, 2107–2119.

Compagnoni, A., Bibian, A.J., Ochocki, B.M., Rogers, H.S., Schultz, E.L., Sneck, M.E., *et al.* (2016). The effect of demographic correlations on the stochastic population dynamics of perennial plants. *Ecol Monogr*, 86, 480–494.

Compagnoni, A., Evers, S. & Knight, T. (2023). Spatial replication can best advance our understanding of population responses to climate. *bioRxiv*, https://doi.org/10.1101/2022.06.24.497542.

Compagnoni, A., Levin, S., Childs, D.Z., Harpole, S., Paniw, M., Römer, G., *et al.* (2021). Herbaceous perennial plants with short generation time have stronger responses to climate anomalies than those with longer generation time. *Nat Commun*, 12, 1824.

Doak, D.F., Morris, W.F., Pfister, C., Kendall, B.E. & Bruna, E.M. (2005). Correctly Estimating How Environmental Stochasticity Influences Fitness and Population Growth. *Am Nat*, 166, E14–E21.

Doak, D.F., Waddle, E., Langendorf, R.E., Louthan, A.M., Isabelle Chardon, N., Dibner, R.R., *et al.* (2021). A critical comparison of integral projection and matrix projection models for demographic analysis. *Ecol Monogr*, 91, e01447.

Doherty, P.F., Schreiber, E.A., Nichols, J.D., Hines, J.E., Link, W.A., Schenk, G.A., *et al.* (2004). Testing life history predictions in a long-lived seabird: A population matrix approach with improved parameter estimation. *Oikos*, 105, 606–618.

Drake, J.M. (2005). Population effects of increased climate variation. *Proceedings of the Royal Society B: Biological Sciences*, 272, 1823–1827.

Easterling, M.R., Ellner, S.P. & Dixon, P.M. (2000). Size-Specific Sensitivity: Applying a New Structured Population Model. *Ecology*, 81, 694–708.

Ebert, T. (1999). *Plant and animal populations: Methods in demography*. Academis Press, San Diego, CA, USA.

Ellner, S.P., Childs, D.Z. & Rees, M. (2016). *Data-driven Modelling of Structured Populations. A practical guide to the Integral Projection Model*. Lecture Notes on Mathematical Modelling in the Life Sciences. Springer International Publishing, Cham.

Evans, M.E.K. & Holsinger, K.E. (2012). Estimating covariation between vital rates : A simulation study of connected vs . separate generalized linear mixed models (GLMMs). *Theor Popul Biol*, 82, 299–306.

Evers, S.M., Knight, T.M., Inouye, D.W., Miller, T.E.X., Salguero-Gómez, R., Iler, A.M., *et al.* (2021). Lagged and dormant season climate better predict plant vital rates than climate during the growing season. *Glob Chang Biol*, 27, 1927–1941.

Fay, R., Hamel, S., van de Pol, M., Gaillard, J.M., Yoccoz, N.G., Acker, P., *et al.* (2022). Temporal correlations among demographic parameters are ubiquitous but highly variable across species. *Ecol Lett*, 25, 1640–1654.

Franco, M. & Silvertown, J. (2004). A comparative demography of plants based upon elasticities of vital rates. *Ecology*, 85, 531–538.

Gaillard, J.M., Festa-Bianchet, M. & Yoccoz, N.G. (1998). Population dynamics of large herbivores: Variable recruitment with constant adult survival. *Trends Ecol Evol*, 13, 58–63.

Gaillard, J.-M. & Yoccoz, N. (2003). Temporal Variation in Survival of Mammals: a Case of Environmental Canalization? *Ecology*, 84, 3294–3306.

Gascoigne, S.J.L., Kajin, M. & Salguero-Gómez, R. (2024a). Criteria for buffering in ecological modeling. *Trends Ecol Evol*, 39, 116–118.

Gascoigne, S.J.L., Kajin, M., Sepil, I. & Salguero-Gómez, R. (2024b). Testing for efficacy in four measures of demographic buffering. *EcoEvoRxiv*, 0–2.

Gascoigne, S.J.L., Kajin, M., Tuljapurkar, S.D., Silva Santos, G., Compagnoni, A., Steiner, U.K., *et al.* (2023a). Structured demographic buffering: A framework to explore the environment drivers and demographic mechanisms underlying demographic buffering. *bioRxiv*.

Gascoigne, S.J.L., Rolph, S., Sankey, D., Nidadavolu, N., Stell Pičman, A.S., Hernández, C.M., *et al.* (2023b). A standard protocol to report discrete stage-structured demographic information. *Methods Ecol Evol*, 14, 2065–2083.

Gillespie, J.H. (1977). Natural Selection for Variances in Offspring Numbers: A New Evolutionary Principle. *Am Nat*, 111, 1010–1014.

Griffith, A.B. (2017). Perturbation approaches for integral projection models. *Oikos*, 126, 1675–1686.

Haridas, C. V. & Tuljapurkar, S. (2005). Elasticities in Variable Environments: Properties and Implications. *Am Nat*, 166, 481–495.

Healy, K., Ezard, T.H.G., Jones, O.R., Salguero-Gómez, R. & Buckley, Y.M. (2019). Animal life history is shaped by the pace of life and the distribution of age-specific mortality and reproduction. *Nat Ecol Evol*, 3, 1217–1224.

Heppell, S.S. (1998). Application of Life-History Theory and Population Model Analysis to Turtle Conservation. *Copeia*, 1998, 367.

Hilde, C.H., Gamelon, M., Sæther, B.-E., Gaillard, J.-M., Yoccoz, N.G. & Pélabon, C. (2020). The Demographic Buffering Hypothesis: Evidence and Challenges. *Trends Ecol Evol*, 35, 523–538.

Jäkäläniemi, A., Ramula, S. & Tuomi, J. (2013). Variability of important vital rates challenges the demographic buffering hypothesis. *Evol Ecol*, 27, 533–545.

Jones, J.H. (2007). demogR: A Package for the Construction and Analysis of Age-structured Demographic Models in R. *J Stat Softw*, 22, 1–28.

Jones, J.H. (2011). Primates and the evolution of long, slow life histories. *Current Biology*, 21, R708–R717.

Jongejans, E., De Kroon, H., Tuljapurkar, S. & Shea, K. (2010). Plant populations track rather than buffer climate fluctuations. *Ecol Lett*, 13, 736–743.

Kajin, M., Gentile, R., Almeida, P.J.A.L. de, Vieira, M.V. & Cerqueira, R. (2023). Vital rates, their variation and natural selection: a case for an Atlantic forest marsupial. *Oecologia Australis*, 27.

Kendall, B.E., Fujiwara, M., Diaz-Lopez, J., Schneider, S., Voigt, J. & Wiesner, S. (2019). Persistent problems in the construction of matrix population models. *Ecol Modell*, 406, 33–43.

Keyfitz, N. & Flieger, W. (1990). *World Population Growth and Aging: Demographic Trends in the Late Twentieth Century*. University of Chicago Press, Chicago.

Koons, D.N., Pavard, S., Baudisch, A. & Jessica E. Metcalf, C. (2009). Is life-history buffering or lability adaptive in stochastic environments? *Oikos*, 118, 972–980.

Kroon, H. De, Groenendael, J. Van & Ehrlen, J. (2000). Elasticities: A review of methods and model limitations. *Ecology*, 81, 607–618.

de Kroon, H., Plaisier, A., van Groenendael, J. & Caswell, H. (1986). Elasticity: The Relative Contribution of Demographic Parameters to Population Growth Rate. *Ecology*, 67, 1427–1431.

Lawler, R.R., Caswell, H., Richard, A.F., Ratsirarson, J., Dewar, R.E. & Schwartz, M. (2009). Demography of Verreaux's sifaka in a stochastic rainfall environment. *Oecologia*, 161, 491–504.

Lefèvre, C.D., Nash, K.L., González-Cabello, A. & Bellwood, D.R. (2016). Consequences of extreme life history traits on population persistence: do short-lived gobies face demographic bottlenecks? *Coral Reefs*, 35, 399–409.

McDonald, J.L., Franco, M., Townley, S., Ezard, T.H.G., Jelbert, K. & Hodgson, D.J. (2017). Divergent demographic strategies of plants in variable environments. *Nat Ecol Evol*, 1, 0029.

Morris, W.F., Altmann, J., Brockman, D.K., Cords, M., Fedigan, L.M., Pusey, A.E., *et al.* (2011). Low Demographic Variability in Wild Primate Populations: Fitness Impacts of Variation, Covariation, and Serial Correlation in Vital Rates. *Am Nat*, 177, E14–E28.

Morris, W.F. & Doak, D.F. (2004). Buffering of Life Histories against Environmental Stochasticity: Accounting for a Spurious Correlation between the Variabilities of Vital Rates and Their Contributions to Fitness. *Am Nat*, 163, 579–590.

Morris, W.F., Pfister, C.A., Tuljapurkar, S., Haridas, C. V., Boggs, C.L., Boyce, M.S., *et al.* (2008). Longevity can buffer plant and animal populations against changing climatic variability. *Ecology*, 89, 19–25.

Münkemüller, T., Lavergne, S., Bzeznik, B., Dray, S., Jombart, T., Schiffers, K., *et al.* (2012). How to measure and test phylogenetic signal. *Methods Ecol Evol*, 3, 743–756.

Pélabon, C., Hilde, C.H., Einum, S. & Gamelon, M. (2020). On the use of the coefficient of variation to quantify and compare trait variation. *Evol Lett*, 4, 180–188.

Perret, D.L., Evans, M.E.K. & Sax, D.F. (2024). A species' response to spatial climatic variation does not predict its response to climate change. *Proc Natl Acad Sci U S A*, 121, e2304404120.

Pfister, C. (1998). Patterns of variance in stage-structured populations: Evolutionary predictions and ecological implications. *Proceedings of the National Academy of Sciences*, 95, 213–218.

R Core Team. (2024). R: A Language and Environment for Statistical Computing.

Reed, A.W. & Slade, N.A. (2012). Buffering and plasticity in vital rates of oldfield rodents. *Journal of Animal Ecology*, 81, 953–959.

Rodríguez-Caro, R.C., Capdevila, P., Graciá, E., Barbosa, J.M., Giménez, A. & Salguero-Gómez, R. (2021). The limits of demographic buffering in coping with environmental variation. *Oikos*, 130, 1346–1358.

Römer, G., Dahlgren, J.P., Salguero-Gómez, R., Stott, I.M. & Jones, O.R. (2024). Plant demographic knowledge is biased towards short-term studies of temperate-region herbaceous perennials. *Oikos*, 2024.

Rotella, J.J., Link, W.A., Chambert, T., Stauffer, G.E. & Garrott, R.A. (2012). Evaluating the demographic buffering hypothesis with vital rates estimated for Weddell seals from 30 years of mark-recapture data. *Journal of Animal Ecology*, 81, 162–173.

Salguero-Gómez, R. (2021). Commentary on the life history special issue: The fast-slow continuum is not the end-game of life history evolution, human or otherwise. *Evolution and Human Behavior*, 42, 281–283.

Salguero-Gómez, R. (2024). More social species live longer, have higher generation times, and longer reproductive windows. *bioRxiv; https://doi.org/10.1101/2024.01.22.575897*.

Salguero-Gómez, R., Jackson, J. & Gascoigne, S.J.L. (2021). Four key challenges in the open-data revolution. *Journal of Animal Ecology*, 90, 2000–2004.

Salguero-Gómez, R., Jones, O.R., Archer, C.R., Bein, C., de Buhr, H., Farack, C., *et al.* (2016). COMADRE: A global data base of animal demography. *Journal of Animal Ecology*, 85, 371–384.

Sanghvi, K., Vega-Trejo, R., Nakagawa, S., Gascoigne, S.J.L., Johnson, S.L., Salguero-Gómez, R., *et al.* (2024). Meta-analysis shows no consistent evidence for senescence in ejaculate traits across animals. *Nat Commun*, 15, 558.

Shyu, E. & Caswell, H. (2014). Calculating second derivatives of population growth rates for ecology and evolution. *Methods Ecol Evol*, 5, 473–482.

Simmonds, E.G. & Jones, O.R. (2024). Uncertainty propagation in matrix population models: Gaps, importance and guidelines. *Methods Ecol Evol*, 15, 427–438.

Stearns, S. (1992). *The Evolution of Life Histories*. Oxford University Press, New York, USA.

Stearns, S.C. (1983). The Influence of Size and Phylogeny on Patterns of Covariation among Life-History Traits in the Mammals. *Oikos*, 41, 173.

Stubben, C., Milligan, B., Nantel, P. & Stubben, M.C. (2020). Package 'popbio.'

Sutherland, W.J., Freckleton, R.P., Godfray, H.C.J., Beissinger, S.R., Benton, T., Cameron, D.D., *et al.* (2013). Identification of 100 fundamental ecological questions. *Journal of Ecology*, 101, 58–67.

Tuljapurkar, S. (1990). Population Dynamics in Variable Environments. In: *Lecture notes in Biomathematics*, Lecture Notes in Biomathematics (ed. Levin, S.). Springer Berlin Heidelberg.

Tuljapurkar, S. (2010). Environmental variance, population growth and evolution. *J Anim Ecol*, 79, 1–3.

Tuljapurkar, S., Gaillard, J.-M. & Coulson, T. (2009). From stochastic environments to life histories and back. *Philosophical Transactions of the Royal Society B: Biological Sciences*, 364, 1499–1509.

Tuljapurkar, S., Horvitz, C.C. & Pascarella, J.B. (2003). The Many Growth Rates and Elasticities of Populations in Random Environments. *Am Nat*, 162, 489–502.

Tuljapurkar, S., Jaggi, H., Gascoigne, S.J.L., Zuo, W., Kajin, M. & Salguero-Gómez, R. (2023). From disturbances to nonlinear fitness and back. *bioRxiv*, 2023.10.20.563360.

Tuljapurkar, S.D. (1982). Population dynamics in variable environments. III. Evolutionary dynamics of r-selection. *Theor Popul Biol*, 21, 141–165.

Vázquez, D.P., Gianoli, E., Morris, W.F. & Bozinovic, F. (2017). Ecological and evolutionary impacts of changing climatic variability. *Biological Reviews*, 92, 22–42.

Wang, J., Yang, X., Silva Santos, G., Ning, H., Li, T., Zhao, W., *et al.* (2023). Flexible demographic strategies promote the population persistence of a pioneer conifer tree (Pinus massoniana) in ecological restoration. *For Ecol Manage*, 529, 120727.

Zuidema, P.A. & Franco, M. (2001). Integrating vital rate variability into perturbation analysis: an evaluation for matrix population models of six plant species. *Journal of Ecology*, 89, 995–1005.

701 **Figure 1**

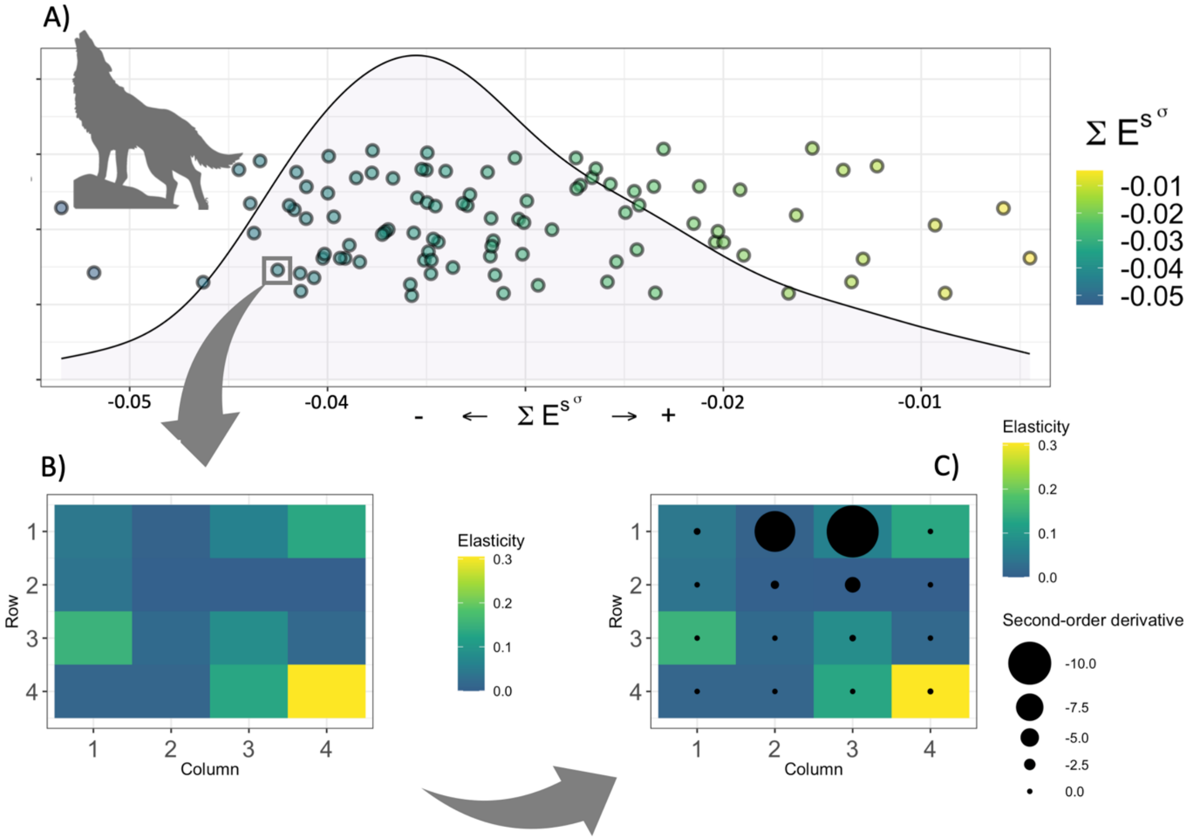

702

Figure 2

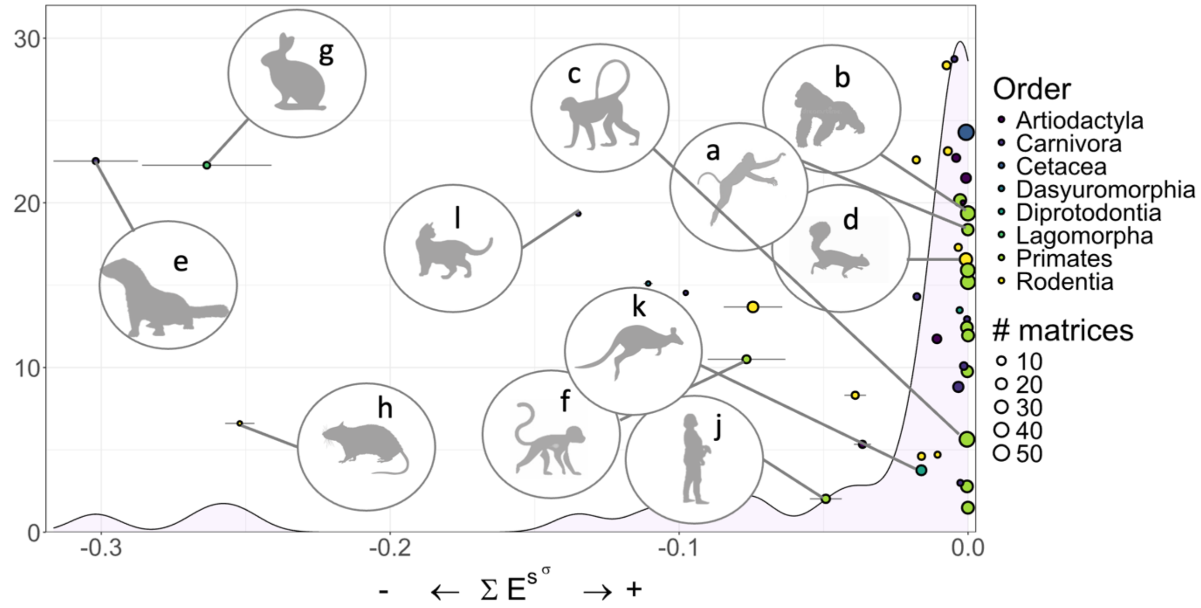
30
20
10
0
-0.3
-0.2
-0.1
0.0
- ← Σ E^s σ → +
g
c
b
a
e
l
d
k
h
f
j
Order
Artiodactyla
Carnivora
Cetacea
Dasyuromorphia
Diprotodontia
Lagomorpha
Primates
Rodentia
matrices
10
20
30
40
50

Figure 3

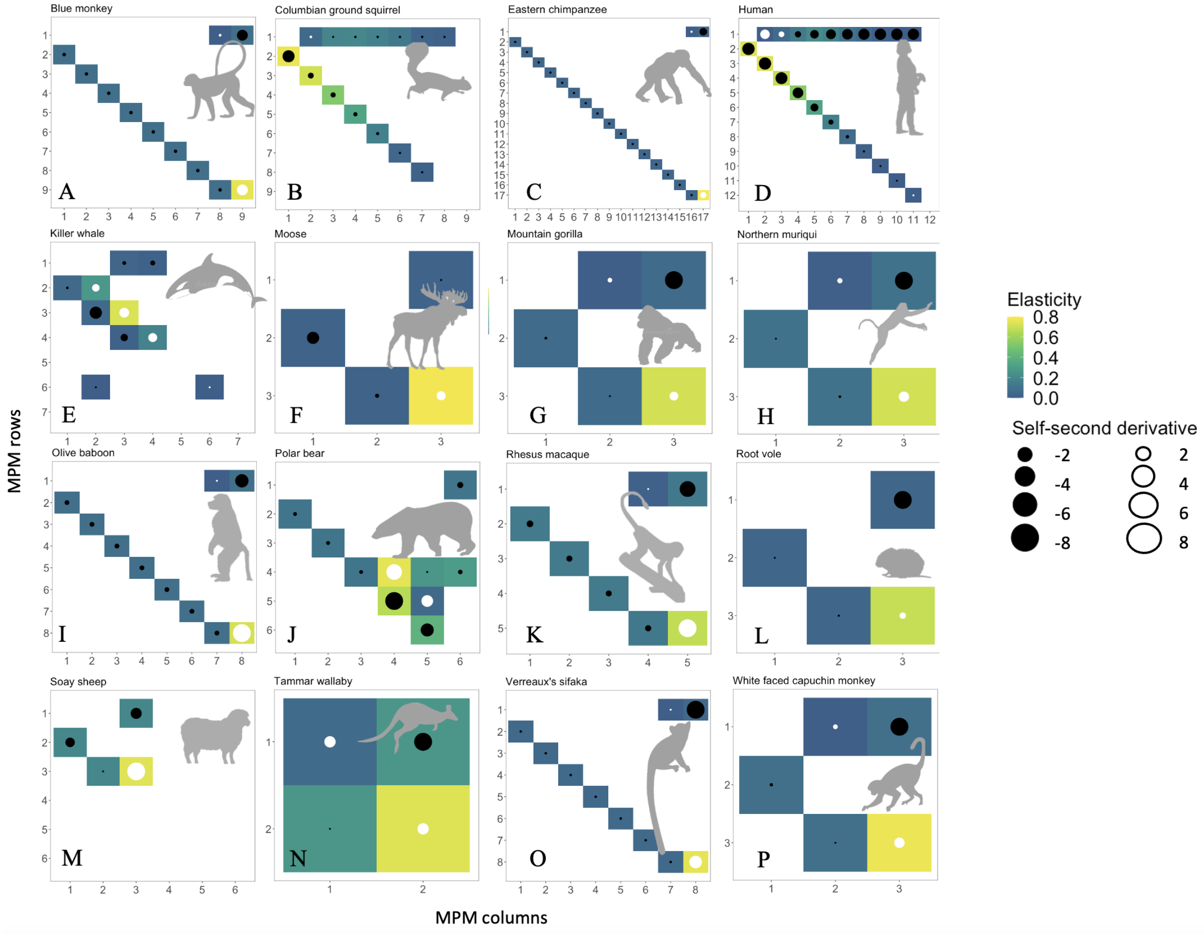
Blue monkey
A
Columbian ground squirrel
B
Eastern chimpanzee
C
Human
D
Killer whale
E
Moose
F
Mountain gorilla
G
Northern muriqui
H
Olive baboon
I
Polar bear
J
Rhesus macaque
K
Root vole
L
Soay sheep
M
Tammar wallaby
N
Verreaux's sifaka
O
White faced capuchin monkey
P
MPM rows
MPM columns
Elasticity
0.8
0.6
0.4
0.2
0.0
Self-second derivative
-2
-4
-6
-8
2
4
6
8

Figure legends

Figure 1. A) The variance continuum for 37 hypothetical species based on the summed stochastic elasticities ($\Sigma E_{a_{ij}}^{S\sigma}$) at the between populations hierarchical level. The closer the $\Sigma E_{a_{ij}}^{S\sigma}$ is to zero, the weaker the impact of variation in demographic processes on the stochastic population growth rate, λ_s. The variance continuum ranges from potentially buffered (right-hand side) to less buffered (left-hand side) species/populations. The yellow-dotted species/populations can be classified as having potentially *buffered life cycles*. The left-hand side of the graph represents species/populations where variability in demographic processes results in strong impact on λ_s (blue dots). Thus, the blue-dotted species/populations can be classified as having potentially *unbuffered life cycles*. The vertical axis delineates the values of the probability density function, indicating the number of species/populations at each value of $\Sigma E_{a_{ij}}^{S\sigma}$. The placement of data points (species/populations) along the horizontal axis corresponds to their calculated values of $\Sigma E_{a_{ij}}^{S\sigma}$ and is arranged linearly, while the placement along the y-axis is random for improved visual comprehension. B) First-order effects or linear selection pressures for individual species/populations at within-species level (see text). Shown are the elasticities of the deterministic population growth rate (λ_1) for a hypothetical population of wolves and revealing the governing demographic process(es) in the life cycle (yellow cells: high elasticity, blue cells: low elasticity). C) Combined results for first (yellow and blue cells) and second order effects (black dots), where the latter reveals the nonlinear selection pressures at the within-species level.

Figure 2. The variance continuum for 43 populations from 37 species of mammals from the COMADRE database based on the summed stochastic elasticities ($\Sigma E_{a_{ij}}^{S\sigma}$) at the between populations hierarchical level. Colors represent different taxonomic orders with Primates occupying the right-hand side. Silhouettes: a) *Brachyteles hyphoxantus*, b) *Gorilla beringhei*,

c) *Cercopithecus mitis*, d) *Urocitellus columbianus,* e) *Mustela erminea*, f) *Erythrocebus patas*, g) *Lepus americanus*, h) *Rattus fuscipes*, i) *Ovis aries*, j) *Homo sapiens*, k) *Macropus eugenii*, and l) *Felis catus*. The vertical axis delineates the values of the probability density function, indicating the number of species/populations at each value of $\Sigma E_{a_{ij}}^{S^{\sigma}}$. The placement of data points (species/populations) along the horizontal axis corresponds to their calculated values of $\Sigma E_{a_{ij}}^{S^{\sigma}}$ and is arranged linearly, while the placement along the y-axis is random for improved visual comprehension.

Figure 3: First- and second-order effects on population growth rate, λ_1 (corresponding to elasticities and self-second derivatives of population growth rate, respectively) for 16 mammal species. The 16 plots represent populations where the MPMs built by ages were available in the COMADRE Animal Matrix Database. The yellow-blue colour scale represents elasticity values for each of the demographic processes in the MPM, where yellow cells represent high and blue cells low elasticity of population growth rate to changes in demographic processes. No colour means elasticity=0. The black dots represent negative self-second derivatives of λ_1 - corresponding to concave selection - and the white dots represent positive self-second derivatives of λ_1 - ditto convex selection. The dot sizes are scaled by the absolute value of self-second derivatives, where the smaller the dot, the closer a self-second derivative is to 0, indicating weak or no nonlinearity. Thus, large dots indicate strong nonlinear selection forces, either concave (black) or convex (white). Since the derivatives of population growth rate are confounded by eigen-structure (Kroon *et al.* 2000), the scaling of the elasticity values and second-derivative values is species specific - *i.e.*, each plot has its own scale. Species-specific scales can be found in Supplementary material (Table S2).

Supplementary material – Data available in COMADRE Version 3.0.0 and results from Step 1 of the framework

Table S1. The metadata used and the respective results presented in the main text. The first four columns represent the information from where Matrix Populations Models (MPMs) were extract precisely as presented in COMADRE 3.0.0.

Species	**Common name**	**Species (COMADRE)**	**Order**	**# matrices**	λ_1	λ_s	$\Sigma \boldsymbol{E}^{S^\sigma}_{a_{ij}}$	$\Sigma \boldsymbol{E}^{S^\sigma}_{a_{ij}}$**(SE)**
Homo sapiens sapiens	Human	Homo_sapiens_subsp._sapiens	Primates	26	1.063707	1.061537	-2.24E-03	3.15E-04
Alces alces	Moose	Alces_alces	Artiodactyla	14	1.205368	1.205161	-6.69E-04	8.42E-05
Antechinus agilis	Agile antechinus	Antechinus_agilis	Dasyuromorphia	3	0.931076	0.885919	-1.11E-01	1.62E-03
Bos primigenius	Cattle	Bos_primigenius	Artiodactyla	8	1.002505	1.000493	-2.83E-03	2.96E-04
Brachyteles hypoxanthus	Northern muriqui	Brachyteles_hypoxanthus	Primates	25	1.05122	1.051273	-5.31E-05	2.09E-05
Callospermophilus lateralis	Golden-mantled ground squirrel	Callospermophilus_lateralis	Rodentia	18	2.052345	1.970253	-6.68E-02	8.72E-03
Cebus capucinus	White faced capuchin monkey	Cebus_capucinus	Primates	22	1.020887	1.020868	-2.04E-04	4.75E-05
Cercopithecus mitis	Blue monkey	Cercopithecus_mitis	Primates	28	1.036082	1.036075	-4.43E-05	1.18E-05

Cervus canadensis subsp. nelsoni	Rocky Mountain elk	Cervus_canadensis_subsp._nelsoni	Artiodactyla	10	1.107412	1.099838	-8.55E-03	1.09E-03
Eumetopias jubatus	Northern sea lion; Steller sea lion	Eumetopias_jubatus	Carnivora	4	0.904383	0.902155	-4.52E-03	2.44E-04
Felis catus	Feral cat	Felis_catus	Carnivora	3	1.948471	1.8259	-1.34E-01	1.89E-03
Gorilla beringei	Mountain gorilla	Gorilla_beringei	Primates	41	1.026827	1.02682	-1.28E-05	1.32E-05
Hippocamelus bisulcus	Huemul deer	Hippocamelus_bisulcus	Artiodactyla	3	0.996197	0.995462	-1.80E-03	1.09E-04
Leopardus pardalis	Ocelot	Leopardus_pardalis	Carnivora	4	1.086146	1.086122	-2.94E-04	3.89E-05
Lepus americanus	Snowshoe hare	Lepus_americanus	Lagomorpha	5	0.811904	0.707678	-2.62E-01	2.33E-02
Lycaon pictus	African wild dog	Lycaon_pictus	Carnivora	3	1.500429	1.430517	-9.70E-02	9.91E-04
Macaca mulatta	Rhesus macaque	Macaca_mulatta_3	Primates	24	1.127496	1.12735	-3.84E-04	6.83E-05
Macropus eugenii	Tammar wallaby	Macropus_eugenii	Diprotodontia	15	0.981097	0.970794	-1.43E-02	1.62E-03
Marmota flaviventris	Yellow-bellied marmot	Marmota_flaviventris_2	Rodentia	8	0.89031	0.886098	-8.80E-03	6.98E-04
Marmota flaviventris	Yellow-bellied marmot	Marmota_flaviventris_3	Rodentia	8	0.920541	0.916392	-7.00E-03	7.04E-04

Microtus oeconomus	Root vole	Microtus_oeconomus	Rodentia	28	1.027531	1.027095	-5.60E-04	1.06E-04
Mustela erminea	Stoat	Mustela_erminea	Carnivora	4	1.258462	1.074391	-3.10E-01	1.62E-02
Orcinus orca	Killer whale	Orcinus_orca_2	Cetacea	50	0.998658	0.998351	-4.72E-04	1.53E-04
Ovis aries	Soay sheep	Ovis_aries_2	Artiodactyla	6	1.09877	1.080656	-3.45E-02	2.96E-03
Pan troglodytes subsp. schweinfurthii	Eastern chimpanzee	Pan_troglodytes_subsp._schweinfurthii	Primates	45	0.982286	0.982191	-1.94E-04	5.06E-05
Papio cynocephalus	Olive baboon	Papio_cynocephalus	Primates	37	1.053872	1.053789	-2.41E-04	6.97E-05
Peromyscus maniculatus	Deer mouse	Peromyscus_maniculatus_2	Rodentia	4	1.10686	1.101117	-9.41E-03	6.88E-04
Phascolarctos cinereus	Koala	Phascolarctos_cinereus_2	Diprotodontia	4	1.064011	1.062744	-2.53E-03	2.16E-04
Phocarctos hookeri	New Zealand sea lion	Phocarctos_hookeri	Carnivora	16	1.023016	1.020083	-3.56E-03	4.15E-04
Propithecus verreauxi	Verreaux's sifaka	Propithecus_verreauxi	Primates	24	0.985592	0.985399	-3.06E-04	6.29E-05
Rattus fuscipes	Bush rat	Rattus_fuscipes	Rodentia	3	1.304662	1.188931	-2.45E-01	4.29E-03
Urocitellus armatus	Uinta ground squirrel	Spermophilus_armatus	Rodentia	6	1.125011	1.113416	-1.73E-02	1.68E-03

Urocitellus armatus	Uinta ground squirrel	Spermophilus_armatus_2	Rodentia	6	1.094693	1.084304	-1.47E-02	1.56E-03
Urocitellus columbianus	Columbian ground squirrel	Spermophilus_columbianus	Rodentia	6	1.008949	0.984575	-3.80E-02	3.26E-03
Urocitellus columbianus	Columbian ground squirrel	Spermophilus_columbianus_3	Rodentia	6	1.200353	1.197473	-3.38E-03	6.96E-04
Ursus americanus subsp. floridanus	Florida black bear	Ursus_americanus_subsp._floridanus	Carnivora	4	1.01989	1.018094	-3.68E-03	3.97E-04
Ursus arctos subsp. horribilis	Grizzly bear	Ursus_arctos_subsp._horribilis_5	Carnivora	7	1.025712	1.024785	-1.38E-03	1.26E-04
Ursus maritimus	Polar bear	Ursus_maritimus_2	Carnivora	5	0.940646	0.931697	-1.91E-02	9.23E-04
Brachyteles hypoxanthus	Northern muriqui	Brachyteles_hypoxanthus_2	Primates	25	1.110953	1.110983	1.22E-05	5.05E-06
Cebus capucinus	White-faced capuchin monkey	Cebus_capucinus_2	Primates	22	1.059311	1.059248	-1.03E-04	2.85E-05
Chlorocebus aethiops	Vervet	Chlorocebus_aethiops_2	Primates	8	1.187136	1.148862	-8.03E-02	1.31E-02
Erythrocebus patas	Patas monkey	Erythrocebus_patas	Primates	9	1.127974	1.092178	-5.21E-02	5.38E-03
Gorilla beringei subsp. beringei	Mountain gorilla	Gorilla_beringei_subsp._beringei	Primates	41	1.052588	1.05255	-6.81E-05	1.11E-05

Table S2. The species-specific scales for the elasticity of λ_1 to changes in demographic processes and for the self-second derivatives of λ_1 with respect to demographic processes for the 16 mammal species studied.

Figure 3 reference	Species common name	E_{min}=elasticity minimum value	E_{max}=elasticity maximum value	SSD_{min}=self-second derivative minimum value	SSD_{max}=self-second derivative maximum value
A	Blue monkey	0	0.52	-1.25	1.27
B	Columbian ground squirrel	0	0.23	-1.48	0.01
C	Eastern chimpanzee	0	0.60	-4.39	2.59
D	Human	0	0.18	-0.15	0.08
E	Killer whale	0	0.55	-5.72	3.43
F	Moose	0	0.55	-0.66	0.36
G	Mountain gorilla	0	0.81	-1.46	0.28
H	Northern muriqui	0	0.72	-1.17	0.35
I	Olive baboon	0	0.54	-0.57	1.13
J	Polar bear	0	0.26	-0.73	0.54
K	Rhesus macaque	0	0.51	-0.54	0.71
L	Root vole	0	0.86	-2.54	0.22
M	Soay sheep	0	0.56	-0.22	0.40
N	Tammar wallaby	0	0.55	-0.64	0.34
O	Verreaux's sifaka	0	0.60	-2.64	1.34
P	White faced capuchin monkey	0	0.66	-2.66	1.21

Towards an integrated framework for evidencing demographic buffering in natural populations

Deleted: A
Deleted: unified
Deleted: to
Deleted: quantify

A manuscript in preparation for submission to ECOLOGY LETTERS
Type of article: METHOD

Gabriel Silva Santos[1,2*], Samuel J L Gascoigne[3*], André Tavares Corrêa Dias[4], Maja Kajin[3,5**♦], Roberto Salguero-Gómez[3♦]

[1] National Institute of the Atlantic Forest (INMA), 29650-000, Santa Teresa, Espírito Santo, Brazil. ssantos.gabriel@gmail.com
[2] Department of Ecology, Graduate Program in Ecology and Evolution, Rio de Janeiro State University, 524 São Francisco Xavier Street, 20550-900, Maracanã, Rio de Janeiro, Brazil.
[3] Department of Biology, University of Oxford, South Parks Road, OX1 3RB, Oxford, UK. samuel.gascoigne@pmb.ox.ac.uk, rob.salguero@biology.ox.ac.uk

Deleted: , maja.kajin@biology.ox.ac.uk

[4] Department of Ecology, Institute of Biology, Universidade Federal do Rio de Janeiro, Avenida Carlos Chagas Filho 373, 21941-590 Rio de Janeiro, RJ, Brazil. atcdias@gmail.com
[5] Chair of Zoology, Department of Biology, Biotechnical Faculty, University of Ljubljana, Večna pot 111, 1000 Ljubljana, Slovenia. maja.kajin@bf.uni-lj.si

*Shared first authorship
**Corresponding author
♦ Shared senior authorship

AUTHOR CONTRIBUTIONS: GSS developed the initial concept, performed the statistical analyses, and contributed to the first draft of the manuscript. SJLG developed the initial concept, contributed to the first draft and all other versions of the manuscript, and generated final figures. ATCD co-advised the project and contributed significantly to final versions of the manuscript. MK developed and managed the project, contributed to the first draft and all other versions of the manuscript, and generated final figures. RSG developed and managed the project and contributed to the first draft and all other versions of the manuscript. All authors made substantial contributions to editing the manuscript and further refining ideas and interpretations.

RUNNING TITLE: Demographic buffering framework (32/45 characters)

KEYWORDS: COMADRE Animal Matrix Database, elasticity, life-history evolution, natural selection, second-order derivative, sensitivity, stochasticity, variance.

NUMBER OF WORDS: Abstract – 146/150 words, main text (excluding abstract, acknowledgements, references, table, and figure legends) – 4979/5000 words

Deleted: 3
Deleted: 4966

NUMBER OF REFERENCES: 86

Deleted: 60

NUMBER OF TABLES: 2 (in Supplementary Material)

Deleted: 1

NUMBER OF FIGURES: 3

Abstract (146/150 words)

The demographic buffering hypothesis predicts that natural selection reduces the temporal fluctuations in demographic processes (survival, development, and reproduction) due to their negative impacts of temporal variation on population dynamics. However, evidencing buffering patterns at different hierarchical levels – between and within populations – and understanding how selection shapes those patterns, remains a challenge in Ecology and Evolution. Here, we introduce a framework that allows for the evidencing of demographic buffering between and within populations. The framework uses the sum of stochastic elasticities for between-populations comparisons along with first- and second-order effects of demographic process variability on fitness for within-population comparisons. We apply this framework to 43 populations of 37 mammal species to test the hypothesis that buffered species are under strong concave selection pressures. Using our framework, we show that demographically buffered species do not necessarily have strong concave selection pressures in their most impactful demographic processes.

Deleted: ¶

Deleted: 43

Deleted: D

Deleted: B

Deleted: H

Deleted: (DBH)

Deleted: *such as*

Deleted: ,

Deleted: a comprehensive approach that allows for the examination of demographic buffering patterns across multiple species is still lacking

Deleted: propose

Deleted: that an additional metric - a second-order effect on population growth rate – be added to the framework for evidencing demographic buffering.

Deleted: Firstly, w

Deleted: categorize species along a continuum of variance based on the sums of stochastic elasticities. Secondly, we examine the linear selection gradients, followed by the examination of nonlinear selection gradients as the third step. With these three steps, our framework overcomes existing limitations of conventional approaches to quantify demographic buffering, allows for multi-species comparisons, and offers insight into the evolutionary forces that shape demographic buffering. We apply this framework to mammal species and discuss both the shortagesadvantages and potential of our framework.¶

Environmental stochasticity shapes organisms' life histories (Bonsall & Klug 2011; Stearns 1992; Tuljapurkar 1990, 2010). Nonetheless, how organisms will cope with the changing variation in environmental conditions (Bathiany *et al.* 2018; Boyce *et al.* 2006; Morris *et al.* 2008) remains an intriguing ecological and evolutionary question (Sutherland *et al.* 2013). Evolutionary demography provides diverse explanations for how evolutionary processes shape demographic responses to environmental stochasticity (Charlesworth 1994; Healy *et al.* 2019; Hilde *et al.* 2020; Pfister 1998; Tuljapurkar *et al.* 2009). The long-term stochastic population growth rate (${\lambda_s}$) representing the geometric mean of population growth rates over time (λ_t; Tuljapurkar 1982), forms the basis of the Demographic Buffering Hypothesis (Morris & Doak 2004; Pélabon *et al.* 2020).

Increasing the geometric mean of λ_t over time corresponds to a rise in the long-term stochastic population growth rate. Conversely, higher variance in λ_t reduces λ_s (Morris & Doak 2004; Tuljapurkar 1982), impacting population persistence (Lefèvre *et al.* 2016). The demographic buffering hypothesis (Pfister 1998) suggests life histories are selected to minimize the negative impacts of environmental variation by constraining the temporal variance of key demographic processes (*e.g.*, survival, development, reproduction) that have the highest sensitivity/elasticity to population growth rate, a fitness proxy (Gaillard & Yoccoz 2003; Pfister 1998). Demographic buffering describes the selection-driven constraint on the temporal variance of these key demographic processes (Gascoigne *et al.* 2024a, b; Hilde *et al.* 2020; Morris & Doak 2004; Pfister 1998). Here, we focus on the emerging patterns of demographic buffering in different animal life histories rather than on the demographic buffering hypothesis itself.

An integrative approach to evidence demographic buffering is still missing. Indeed, identifying demographic buffering remains challenging (Doak *et al.* 2005; Morris & Doak 2004) for several reasons, one of them being different interpretations of results from

Deleted: increasing

Deleted: ,

Deleted: expressed

Deleted: as

Deleted: annual

Deleted: ,

Deleted: ,

Deleted: (DBH)

Deleted: (λ_s, hereafter)

Deleted: DBH

Deleted: predicts that life histories are under selection pressure to minimise the negative impacts of environmental variation by constraining the temporal variance of those demographic processes (*e.g.*, survival, development, reproduction) to which population growth rate (*i.e.*, a proxy for fitness)

Deleted: is most sensitive

Deleted: to

Deleted:

Deleted: The *demographic pattern strategy* operating the DBH, *i.e.,* demographic buffering, describes the selection-driven constraint on the temporal variance of the most impacting demographic processes for the population growth rate …

Deleted: .

Deleted: latter - on the

Deleted: –

Deleted: DBH

Deleted: unified

Deleted: unambiguously

Deleted: quantify

correlational analyses, as in Pfister (1998) and Hilde *et al.* (2020). Some authors rank species' life histories on a continuum from buffered to labile using the correlation coefficient (Spearman's correlation ρ) between the impact of demographic processes on the population growth rate and the temporal variance of said demographic processes (McDonald *et al.* 2017; Salguero-Gómez 2021). There, negative correlation coefficient values indicate buffering Alternatively, the absence of statistical support for buffering may suggest a preference for demographic variance to track environmental conditions, a phenomenon supported by the Demographic Lability Hypothesis (Drake 2005; Hilde *et al.* 2020; Jäkäläniemi *et al.* 2013; Koons *et al.* 2009; Reed & Slade 2012). However, increased variability alone is not enough to constitute demographic lability; it must also result in significant changes in the mean value of the demographic process (Le Coeur *et al.* 2022).

Another obstacle to generalising a measure of demographic buffering across populations and species is the targeted hierarchical level of examination. Some studies focus on characteristics drawn from the *entire population model* (McDonald *et al.* 2017; Reed & Slade 2012). At this *between-populations level* (hereafter), a life history is considered demographically buffered if the governing demographic processes have low temporal variance (Le Coeur *et al.* 2022; Hilde *et al.* 2020; Morris & Doak 2004; Pfister 1998). However, to fully grasp how and why demographic buffering occurs, and how patterns might change in response to the environment, we must also consider characteristics within an individual population model (*within-populations level* hereafter). Within a population, one demographic process may be buffered against climatic variability while another may be labile (Barraquand & Yoccoz 2013; Jongejans *et al.* 2010; Koons *et al.* 2009). Furthermore, even if a given demographic process is primarily governing the population growth rate in one year, a different one might take over next year (Evers *et al.* 2021). Despite the relevance of within- and between-populations level processes, thus far studies have focused on evidencing

Deleted: (*e.g.*,

Deleted: Some authors rank species' life histories on a continuum from buffered to labile using the correlation coefficient (Spearman's correlation ρ), where negative values indicate buffering (McDonald *et al.* 2017)

Deleted: known as

Deleted: (DLH)

Deleted: temporal variance

Deleted: achieving

Deleted: z

Deleted: ation

Deleted: '

Deleted: populations regarding demographic buffering

Deleted: typical

Deleted: (*between-populations level*)

Deleted: level

Deleted: key

Deleted: at the level of separate *components of*

Deleted: the

Deleted: one

demographic buffering at the within- and between-population levels separately. To integrate these two levels of analysis, here we investigate demographic buffering signatures together.

To examine demographic buffering at the between-populations level, we use the *summed* effect of the variability of all demographic processes on the population growth rate. A weak summed effect means that the population growth rate is relatively unaffected by the variability in demographic processes (Haridas & Tuljapurkar 2005), and this lack of effect by demographic process variability is consistent with demographic buffering. As such, a summed effect of variability offers a good proxy to evidence demographic buffering (Gascoigne *et al.* 2024b; Haridas & Tuljapurkar 2005) and enables the classification of populations along a continuum. The within-populations level requires a separate approach. Thus, there we use the relative contribution of each demographic process and how variability in the governing demographic process(es) affects the population growth rate (*e.g.*, Caswell 1978, 1996, 2001; Ebert 1999; de Kroon et al. 1986). Importantly, by exploring the governing demographic processes, we also investigate how natural selection affects them (*e.g.*, Caswell 1996; Shyu & Caswell 2014). Understanding the interplay between demographic variability and natural selection thus not only elucidates population dynamics but also provides insight into the evolutionary pressures shaping the life-history strategies (Charlesworth 1994; Salguero-Gómez 2024; Sanghvi *et al.* 2024).

A powerful approach to reveal the role of natural selection acting on the variability of demographic processes is through measuring a first and second order effect on population growth rate (Carslake *et al.* 2008). First-order effects of demographic processes on population growth rate, such as elasticities, show how *variation* in demographic processes affects population growth rate, and relies on the *linear* relation between demographic processes and the growth rate. A second-order effect, on the other hand, reveals the sensitivity of population growth rate to temporal *autocorrelation* in variable environments (Tuljapurkar 1990), and

Deleted: focus

Deleted: o

Deleted: ' variability

Deleted: . Thus far, studies have focused on either one of the hierarchical levels, however, for a mechanistic understanding of how environmental stochasticity shapes life histories, both between- and within-population levels need to be addressed at the same time.

Deleted: here

Deleted: focus

Deleted: Namely, our interest was i

Deleted: o

Deleted: every

Deleted: ¶

Deleted: The complexity of examining the underlying mechanisms of demographic buffering presents additional challenge. Evidence suggests buffering in both long-lived , and short-lived species . However, these patterns alone do not fully reveal how life histories are shaped by natural selection. One useful way

Deleted: variance

Deleted: second-order

Deleted: of variation

identifies where demographic processes have a *nonlinear* effect on population growth rate. Combining both approaches into a single framework consolidates our understanding of fitness behaviour near local maxima and minima, among other advantages discussed below. This approach and has started to pave its way into Ecology (Kajin *et al.* 2023; Tuljapurkar *et al.* 2023).

Here, we propose that an additional metric to examine demographic buffering: the second-order effect of demographic process variation on population growth rate. We show that each hierarchical level is best studied with a different method. Moreover, we hypothesise that buffered species, those where perturbing the variance of demographic processes has little impact on their fitness, are under strong concave selection pressures (*i.e.*, the force that aims to diminish temporal variance of a trait, sensu Shyu & Caswell 2014) on the governing demographic processes. Indeed, the summed effect of demographic process variability on population growth rate and elasticities are related (Haridas & Tuljapurkar 2005). Concave selection pressures favour traits that contribute to reducing temporal variance, thereby enhancing population stability and resilience in the face of environmental volatility. We discuss the validity of our hypothesis and demonstrate the applicability and advantages of our framework by testing it with 43 populations of 37 mammal species.

Towards an integrated framework to assess evidence of demographic buffering

Current evidence for demographic buffering has primarily been assessed using Matrix Population Models (*MPMs*) (Pfister 1998; Rotella *et al.* 2012). However, Integral Projection Models (*IPMs*) (Easterling *et al.* 2000; Ellner *et al.* 2016; Gascoigne *et al.* 2023a, 2024b; Rodríguez-Caro *et al.* 2021; Wang *et al.* 2023) can also identify demographic buffering. MPMs and IPMs are structured, discrete-time demographic models (Caswell 2001; Ellner *et al.* 2016). For simplicity, here we focus on MPMs, but the same approaches apply to IPMs

Deleted: A second-order effect can be measured by self-second derivatives of population growth rate with respect to every demographic process . While fFirst-order effectss on population growth rate, such as elasticities, show how *variation* in demographic processes affects population growth rate, while the second-order effects reveal sensitivity to *autocorrelation* . Integrating both approaches into a single framework enables an integrativeallows a better understanding of fitness function behaviour near local maxima and minima

Deleted: -

Deleted: -

Deleted: finally

Deleted: e

Deleted: ¶
In linear relationships between fitness and demographic processes, second-order derivatives of population growth rate (measuring a second-order effect on ∠) are zero, indicating natural selection acts on changing the mean values of demographic processes . Nonzero second derivatives suggest nonlinear relationships between fitness and a demographic process, revealing additional aspects of selection on the variances and covariances of demographic processes . Thus, it is of biological interest to join the information on first-order effect with the information on second-order effect. Furthermore, tThe sign (>0, =0, <0) of the self-second derivative of λ with respect to demographic processes determines the type of selection. Negative values describe concave (∩-shaped) selection, reducing temporal variance , providing information regarding the selection processes that might have led to an observed pattern of demographic ... [1]

Deleted: - a

Deleted: – be added to the framework for evidencing ... [2]

Deleted: z

Deleted: integrated proposal

Deleted: applying

Deleted: to

Deleted: 0

Deleted: 4

Deleted: sourced from the COMADRE database (Salg ... [3]

Deleted: Here, we introduce a framework to quantify ... [4]

Deleted:]). First, species or populations are positioned ... [5]

Deleted: . We showcase how the framework can provid ... [6]

Deleted: A

Deleted: unified

Deleted: framework

Deleted: The

Deleted: has been mainly assessed using Matrix Popula ... [7]

Deleted:

Deleted: be equally applied for identifying signatures o ... [8]

Deleted:

Deleted: note that

Deleted: are as equally applicable

(Doak *et al.* 2021; Griffith 2017). We refer to demographic processes as MPM ***A*** entries, a_{ij} (*i.e.,* upper-level parameters *sensu* Zuidema & Franco 2001) and the vital rates composing the matrix elements (*i.e.,* lower-level parameters, *ditto*). The conversion between matrix elements and vital rates is straightforward (Franco & Silvertown 2004).

We first place species on a variance continuum. The variance continuum represents the *summed* effects of proportional increases in temporal variance across all demographic processes (a_{ij}) of the MPM ***A*** on the population growth rate λ_s, operating at the *between-populations level.* It is based on partitioning the sum of all the stochastic elasticities ($\Sigma E^{S}_{a_{ij}}$) into two components: i) the sum of stochastic elasticities with respect to the variance ($\Sigma E^{S^{\sigma}}_{a_{ij}}$), which assesses how variability in a_{ij} affects λ_s, and ii) the sum of stochastic elasticities with respect to the arithmetic mean of demographic processes ($\Sigma E^{S^{\mu}}_{a_{ij}}$), which evaluates the impact of a change in mean values of demographic processes on λ_s (Haridas & Tuljapurkar 2005).

The equal perturbation of both $\Sigma E^{S}_{a_{ij}}$ components assumes that the CV of demographic processes remains constant (Haridas & Tuljapurkar 2005). Higher absolute value of $\Sigma E^{S^{\sigma}}_{a_{ij}}$ indicates greater sensitivity of λ_s to demographic process variability, suggesting the absence of demographic buffering. Conversely, lower $\Sigma E^{S^{\sigma}}_{a_{ij}}$ values support the demographic buffering hypothesis, with λ_s being is less sensitive to variability (Haridas & Tuljapurkar 2005; Tuljapurkar *et al.* 2003) (Fig. 1A).

Species or populations are positioned along the variance continuum based on the impact of variance on the stochastic population growth rate. Species highly sensitive to environmental variability are on the left (potentially unbuffered[1]), while species less sensitive

---

[1] Unconstrained variance does not necessarily imply demographic lability, defined as an increase in *mean value* of a demographic process in response to improved environmental conditions (Le Coeur *et al.* 2022). By examining stochastic elasticities, we can assess changes in the contribution of demographic process variance to λ_s, while mean values remain unchanged.

Deleted: Throughout this manuscript, w

Deleted: both

Deleted: matrix entries

Formatted: Font: Italic

Deleted: that underline

Deleted: , and note that their

Deleted: and described elsewhere

Deleted: The framework operates on three steps.¶

Deleted: In the first step of our framework, we

Deleted: start by

Deleted: calculatinge the impact of variation in demographic processes on the stochastic growth rate, λ_s, known as stochastic elasticities E^{S}_{ij} (Figure 1A). This calculation separates the sum of all stochastic elasticities into two components: one for assessing how temporal variance affects λ_s ( ), and the other for assessing the impact of mean values of demographic processes on λ_s, (

Deleted: A h

Deleted: the sum of stochastic elasticity with respect to variance (

Deleted:),

Deleted: changes in

Deleted: demographic process varianc

Deleted: e,

Deleted: ting

Deleted: a

Deleted: absolute value

Deleted: suggests

Deleted: where

Deleted: less

Deleted: such perturbations

Deleted:

Deleted: ¶

Deleted: Stochastic elasticities (E^{S}) are calculated through equal perturbations to mean and variances in demographic processes across . This equal perturbation is an important assumption as the impacts of means and variances in demographic processes are inferred under the assumption that the coefficient of variaton of said processes remains constant. Importantly, stochastic elasticities can be decomposed into contributions from means ($\Sigma E^{S^{\mu}}_{a_{ij}}$) and variances ($E^{S^{\sigma}}_{a_{ij}}$) of demographic process.

Deleted: This

are on the right (potentially buffered) end (Fig. 1A). We expect buffered species to exhibit concave selection signatures. Although the position on the continuum provides insight into how environmental variation affects λ_s, $\Sigma E^{S^{\sigma}}_{a_{ij}}$ does not consider covariances between demographic processes and serial correlations, crucial for fully diagnosing buffering (Haridas & Tuljapurkar 2005). Thus, species' position at the buffered end of the variance continuum is a *necessary but not sufficient* condition for evidence of demographic buffering. To address this second criterion, we use second derivatives of population growth rate with respect to demographic processes to elucidate the impact of selection on variance (below).

Next, we delve into within-population level by calculating the partial derivatives of λ_t (obtained by averaging sequential MPMs across the study duration) concerning all matrix elements a_{ij} of the MPM $\boldsymbol{A}$ (Fig. 1B). This step reveals a first-order effect on fitness – how each demographic process influences λ_t. We then evaluate nonlinear selection patterns using self-second derivatives of λ_t for each a_{ij} (Fig. 1C), revealing potential nonlinear selection pressures (Brodie *et al.* 1995). Failure to consider these evolutionary processes may lead to misinterpretation of patterns (*e.g.*, Lawler et al. 2009).

First- and second-order effects on fitness show average selection pressures over time. Self-second derivatives of population growth rate with respect to demographic processes measure second-order effects (Carslake *et al.* 2008; Caswell 2001; Kajin *et al.* 2023; Shyu & Caswell 2014; Tuljapurkar *et al.* 2023). Linear fitness relationships (zero self-second derivatives) mean selection changes mean demographic values, not variance (Shyu & Caswell 2014). Nonzero self-second derivatives indicate nonlinear relationships between fitness and a demographic process, revealing additional aspects of selection on the variances and covariances of demographic processes (Brodie *et al.* 1995; Carslake *et al.* 2008; Shyu & Caswell 2014). Interpreting both first- and second-order effects offers insights into population placement on the variance continuum.

Deleted: step places species or populations along a continuum based on variance in demographic processes, with unconstrained variance on the left (possibly unbuffered) and constrained variance on the right (possibly buffered)^2

Deleted: .

Deleted: However, unconstrained variance does not necessarily imply demographic lability, defined as an increase in *mean value* of a demographic process in response to improved environmental conditions . By examining, we can assess changes in the contribution of demographic process variance to λ_s, while mean values remain unchanged.

Deleted: this step

Deleted: which are important

Deleted: Instead

Deleted: these

Deleted: a

Deleted: To address these criteria

Deleted: our approach focuses utilizeson

Deleted: selection's

Deleted: step 3,

Deleted: Steps 2 and 3 of the framework

Deleted: analyseis

Deleted: . After step 1 positions species or populations along the $\Sigma E^{S^{\sigma}}_{a_{ij}}$ variance continuum for λ_s, each life cycle undergoes scrutiny. Step 2

Deleted: (Fig. 1B) involves calculating

Deleted: $_t$

Deleted: $_t$

Deleted: .

Deleted: $_t$

Deleted: In step 3

Deleted: , one

Deleted: s

Deleted: $_t$

Deleted: demographic process

Deleted: . This step unveils

Deleted: on demographic processes

Deleted: (Brodie *et al.* 1995)

Deleted: , crucial for understanding their evolutionary dynamics

Deleted: in step 1

Deleted: Lawler et al. 2009)

Deleted:)

Deleted: Steps 2 and 3

Deleted: of the framework analyse averaged selection pressures over time periods. They These steps offer insights into how perturbations in demographic processes affect λ_t, obtained by averaging sequential Matrix Population Models (MPMs) across the study duration. Therefore, they step ... [9]

The sign (>0, =0, <0) of the self-second derivatives determines the selection type. Negative values (concave selection, ∩-shaped) reduce temporal variance, providing evidence of buffering (Caswell 1996, 2001; Shyu & Caswell 2014). Positive values (convex selection, ∪-shaped) indicate amplified variance, revealing a lack of selection constraints on demographic variance (Bruijning *et al.* 2020; Caswell 1996, 2001; Le Coeur *et al.* 2022; Koons *et al.* 2009; Shyu & Caswell 2014; Vinton *et al.* 2022).

Following the above steps allows evidencing demographic buffering at the between- and within-populations levels. The joint interpretation of first- and second-order effects offers insights into why a population is on either end of the variance continuum. Evidence supporting buffering includes:

1. A population positioned near the 0 end of the $\Sigma E^{S^{\sigma}}_{a_{ij}}$ continuum.
2. Identifying the demographic processes with highest elasticity values within the life cycle.
3. The same processes from (2) associated with negative self-second derivatives, indicating concave selection.

Figure 1B shows that, for an imaginary wolf population, the governing demographic process is the fourth stage stasis (MPM element $a_{4,4}$), with the highest elasticity value (Fig. 1B yellow square). However, Figure 1C reveals little selection on $a_{4,4}$ for variance reduction. Hence, there is no concave selection on $a_{4,4}$, explaining the positioning on the left-side variance continuum (Fig. 1A).

Although not our primary goal, we briefly introduce steps to evidence demographic lability. Compelling lability evidence requires sufficient data across environments [over time or space; but see Perret et al. (2024)] to construct reaction norms depicting demographic responses to environmental changes (Drake 2005; Koons *et al.* 2009; Morris *et al.* 2008). Non-linear relationships between demographic processes and the environment must be

Deleted: In step 3, it is important to note that the importance of demographic processes shifts with changing environments . This dynamic sensitivity of λ_t to specific processes , indicated by self-second derivatives, helps pinpoint which processes are most likely to induce changes in λ_s. For instance, in the hypothetical wolf species (Fig. 1), a decline in reproduction among third age-class individuals (matrix element $a_{1,3}$) would heighten sensitivity to that process. Consequently, with increased environmental variability, the key demographic process might change from remaining in the fourth age class (matrix element $a_{4,4}$, Fig. 1B) to reproduction of the third age-class (matrix element $a_{1,3}$, Fig. 1C).¶
Combining

Deleted: three

Deleted: of our framework

Deleted: a quantitative identification

Deleted: of

Deleted: Steps 2 and 3

Deleted: -- offer key insights as to *why* a given species or population is placed on either the buffered ($\Sigma E^{S^{\sigma}}_{a_{ij}}$ ~ 0) or the non-buffered end ($\Sigma E^{S^{\sigma}}_{a_{ij}}$ ~ -1) of the variance continuum. A clear and unequivocal evidence for support towards buffering consists of:

Deleted: (1)

Deleted: Aa species or population being positioned near the 0 end of the

Deleted: (the right-hand side) in step 1

Deleted: ; (2) this species' or populations' life cycle having one or more

Deleted: of population growth rate

Deleted: species' or populations'

Deleted: in step 2

Deleted: ;

Deleted: ¶

Deleted: the chosen

Deleted: of a hypothetical wolf species

Deleted: most important

Deleted: remaining in

Deleted: as this demographic process results inis associated

Deleted: .

Deleted: that $a_{4,4}$ is under

Deleted: pressure

Deleted: Thus, there is no clear evidence of buffering ... [10]

Deleted:).

Deleted: This way, the lack of concave selection force ... [11]

Deleted: here,

Deleted: said

Deleted: 4

Deleted: To establish compelling evidence of lability, ... [12]

Deleted: However, we note that c, which can be challe ... [13]

established based on the reaction norms. Demographic processes where an increase in the mean value has a stronger positive impact on population growth rate than the detrimental effect of increased variance need to be identified. The latter condition is only met when the process-environment reaction norms are convex (Drake 2005, Koons *et al.* 2009, Morris *et al.* 2008) – but see Barraquand & Yoccoz (2013) for an alternative result. Importantly, species may not be purely buffered or labile some processes may be buffered, others labile, and others insensitive to environmental variability (*e.g.*, Doak *et al.* 2005). Deciphering these patterns is a primary research interest in the field.

Demographic buffering in mammals: A case study

Here, we examine the performance of our framework and test our hypothesis, that is that species at the buffered end of the variance continuum display highly negative self-second derivatives for the governing demographic processes. We use 43 MPMs from 37 mammal species (16 species at the within-populations level). Mammals are of special interest in the context of demographic buffering for two reasons: (1) mammalian life histories have been well studied (Beccari *et al.* 2024; Bielby *et al.* 2007; Gillespie 1977; Jones 2011; Stearns 1983) and (2) some of their populations have already been assessed in terms of demographic buffering, particularly for primates (Campos *et al.* 2017; Morris *et al.* 2008, 2011; Reed & Slade 2012; Rotella *et al.* 2012). Together, the well-studied life histories and previous information about the occurrence of buffering in mammals allow us to make accurate predictions and validate the performance of our framework.

We used MPMs (Caswell 2001) from 43 out of 139 studies with mammals available in the COMADRE Animal Matrix Database v.3.0.0 (Salguero-Gómez *et al.* 2016). These 43 populations encompass 37 species from eight taxonomic orders. We carefully selected these MPMs in our analyses because their models contain values of demographic processes (a_{ij})

Deleted: demographic process-environment

Deleted: Lastly, d

Deleted: s

Deleted: demographic

Deleted: takes a convex shape

Deleted: (resembling a "∪" shape), as described by

Deleted: and

Deleted: . However, a study by

Deleted: reported

Deleted: diverging

Deleted: s in this regard

Deleted: demographically demographic processes

Deleted: Importantly, we note that more likely than previously thought (*e.g.*, Pfister 1998), species do not exist as purely buffering or labile, but that within populations, some vital rates may be buffered, others labile, and others insensitive to the environment (*e.g.*, (Doak *et al.* 2005). Deciphering generality in this likely complex pattern should attract much research attention going forward, in our opinion.¶

Deleted: **using the unified framework**

Deleted: W

Deleted: demonstrate

Deleted: framework

Deleted: integrated approach

Deleted: validate

Deleted: -

Deleted: using

Deleted: 44

Deleted: 34

Deleted: here

Deleted: provide the necessary information

Deleted: the proposed

Deleted: Matrix Population Models (

Deleted:

Deleted: ,

Deleted: 0

Deleted: d

Deleted:

Deleted: 0

Deleted: 4

Deleted: included

Deleted: ,

Deleted: y

Deleted: provide

for three or more contiguous time periods, thus allowing us to obtain the stochastic elasticity of each a_{ij}. Although we are aware that not all possible temporal variation in demographic processes may have been expressed within this period, we assumed three or more transitions are enough to provide sufficient variation for population comparison (Compagnoni *et al.* 2023). To mitigate bias in variance estimates, we randomly extracted three MPMs from the existing data for each species (Supplementary Material, Table S1), calculated the mean of these three MPMs, and repeated this process 50 times to obtain estimates of $\Sigma E^{S^{\sigma}}_{a_{ij}}$ and their corresponding standard errors. A detailed description of the analysed data and their original sources are detailed in Table S1. Finally, we included MPMs of *Homo sapiens* to cross-check our estimates of second-order derivatives, as it is the only mammalian species where these have been calculated (Caswell 1996). The data for *H. sapiens* were gathered from 26 modern populations (Keyfitz & Flieger 1990).

At the within-populations level, we used a subset of 16 populations (including *H. sapiens*) whose MPMs were age-based. We specifically selected these populations because their life cycles can be summarised by two main demographic processes: survival and contribution to the recruitment of new individuals (Caswell 2010; Ebert 1999).

To quantify the variance continuum and calculate $\Sigma E^{S^{\sigma}}_{a_{ij}}$ for between-populations level comparisons, we followed Tuljapurkar *et al.* (2003) and Haridas & Tuljapurkar (2005). Next, at the within-populations level, we calculated the deterministic elasticities to each demographic process using the *popbio* package (Stubben *et al.* 2020). The self-second derivatives were adapted from *demogR* (Jones 2007) following (Caswell 1996) and applied to the mean MPM of each study. All analyses were performed using R version 4.4.1 (R Core Team 2024).

Results

Deleted:

Deleted: matrices

Deleted: number of matrices detailed in

Deleted: matrices

Deleted: Fortunately, several long-lived species, characteriszed by low variation in their demographic processes, were studied for a long time (*e.g.,* some primates in our dataset have been studied for over 20 years – Morris *et al.* 2011). We removed the populations where either only survival or only reproduction rates were reported, because of the impossibility to calculate the stochastic growth rate.

Deleted: available in supplementary material (Supplem ... [14]

Deleted:)

Deleted: ¶

Deleted: as a way

Deleted: was included in our analyses because

Deleted: before

Deleted: in which second-order derivatives have been applied

Deleted: Therefore, *Homo sapiens* provides an ideal b ... [15]

Deleted: *omo*

Deleted: located in various cities, allowing us to const ... [16]

Deleted: For steps 2 and 3 of our framework,

Deleted: utilized

Deleted: *Homo*

Deleted: population projection matrices (

Deleted:)

Deleted: organiszed by

Deleted: z

Deleted: .

Deleted: The contribution to recruitment can be interp ... [17]

Deleted: One advantage of using such matrices MPMs ... [18]

Deleted: perform the step 1 of our framework

Deleted: obtain

Deleted: the

Deleted: (and $\Sigma E^{S^{\mu}}_{a_{ij}}$)

Deleted: (

Deleted: (

Deleted: To perform step 2 of our framework

Deleted: -

Deleted: -

Deleted: ,

Deleted: of

Deleted: extracted

Deleted: All analyses were performed using R version ... [19]

Deleted: to perform the step 3 of our framework t

Deleted: for

We ranked 43 populations from the 37 identified mammal species into a variance continuum according to the cumulative impact of variation in demographic processes on λ_s (Fig. 2). Most of the analysed taxonomic orders were placed on the low or zero variance end of the variance continuum (Fig. 2), corroborating with demographically buffered populations. The smallest contributions of variation in demographic processes (note that $\Sigma E_{a_{ij}}^{S^{\sigma}}$ ranges from 0 to -1), suggesting buffered populations, were assigned to Primates: northern muriqui (*Brachyteles hyphoxantus*, $\Sigma E_{a_{ij}}^{S^{\sigma}}$ = -5.31 × 10^{-5} ± 2.09 × 10^{-5}) (mean ± S.E.) (Fig. 2 silhouette a), mountain gorilla (*Gorilla beringei*, $\Sigma E_{a_{ij}}^{S^{\sigma}}$ = -1.28 × 10^{-5} ± 1.32 × 10^{-5}) (Fig. 2 silhouette b), followed by the blue monkey (*Cercopithecus mitis*, $\Sigma E_{a_{ij}}^{S^{\sigma}}$ = -4.43 × 10^{-5} ± 1.18 × 10^{-5}) (Fig. 2 silhouette c). The first non-primate species placed near the buffered end of the continuum was the Columbian ground squirrel (*Urocitellus columbianus*, Rodentia, $\Sigma E_{a_{ij}}^{S^{\sigma}}$ = -3.38 × 10^{-3} ± 6.96 × 10^{-4}) (Fig. 2 silhouette d). On the other opposite, the species with the highest contribution of variation in demographic processes – placed at the high-variance end of the continuum – was the stoat (*Mustela erminea*, Carnivora, $\Sigma E_{a_{ij}}^{S^{\sigma}}$ = -0.310 ± 0.0162) (Fig. 2 silhouette e). All the 14 primate populations occupied the buffered side of the variance continuum, with the exception of the Patas monkey (*Erythrocebus patas*, Primates, $\Sigma E_{a_{ij}}^{S^{\sigma}}$ = -0.0521 ± 5.38 × 10^{-3}) (Fig. 2 silhouette f). The snowshoe hare (*Lepus americanus*, Lagomorpha, $\Sigma E_{a_{ij}}^{S^{\sigma}}$ = -0.262 ± 0.0233) (Fig. 2 silhouette g) and the Bush rat (*Rattus fuscipes*, Rodentia, $\Sigma E_{a_{ij}}^{S^{\sigma}}$ = -0.245 ± 4.29 × 10^{-3}) (Fig. 2 silhouette h) were positioned on the non-buffered end of the variance continuum. Additional information (including standard errors of the elasticity estimates) is provided in Table S1. *A posteriori*, we quantified the impact of phylogenetic relatedness on the estimates of the sum of stochastic elasticities (Fig. 2), and then for the correlation between those estimates and the number of MPMs available per species. For the former, we estimated Blomberg's K, a measure of phylogenetic signal that ranges between 0 (weak

Deleted: 40 …opulations from the 37 34 ... [20]

Deleted: using the step 1 of our framework …Fig. 2). Additional information (including standard deviations of the deviations of the elasticity estimates and number of matrices available) is provided in the supplementary material (Table S1). …ost of the analysed taxonomic orders were placed on the low-…or zero variance end of the variance continuum 2), corroborating with demographifically…emographically buffered populations. The smallest contributions of variation in demographic processes (*i.e.,* maximum value o, ... [21]

Deleted: more

Deleted: 0.09…× 10^{-54}…± 2.090.12…× 10^{-54} ... [22]

Deleted: standard ….E.error ... [23]

Deleted: deviation

Deleted: *h*

Deleted: 0.24…× 10^{-54}…± 1.320.08…× 10^{-54} ... [24]

Deleted: 0.63…× 10^{-54}…± 1.180.06…× 10^{-54} ... [25]

Deleted: low-variance

Deleted: -0.003…3.38 × 10^{-3} ± 6.96 -4.430.63…× 10 ... [26]

Deleted: T

Deleted: -… placed at the high-variance end of the continuum –- ... [27]

Deleted: 5…± 0.01622 ... [28]

Deleted: displayed potential evidence of buffering, occupiedying…the right-hand ... [29]

Deleted: 0.03

Deleted: 9…± 0.023316 ... [30]

Deleted: 0.03

Deleted: appear …ere positioned on the high-variance ... [31]

Deleted: the Supplementary material (…able S1)… *A posteriori*, we tested…uantified for ... [32]

Deleted: strength…mpact of phylogenetic relatedness on the estimates of the sum of stochastic elasticities (Fig. 2), and then for the correlation between those estimates and the number of MPMs available per species. For the former, we estimated Blomberg's K, (…n…estimate ... [33]

Deleted: [

signal) to positive values 1 (strong) (Münkemüller *et al.* 2012). Blomberg's K in our analyses was 0.23. The correlation between the number of available MPMs per study and the sum of stochastic elasticities (post jack-knifing) raised a weakly negative coefficient (-0.002), though significant (P = 0.017).

We found little evidence in support of our hypothesis. Specifically, the demographic processes with the highest elasticity values failed to display strong negative self-second derivatives (Fig. 3). Particularly for the majority of primates, demographic processes with high elasticities had positive values for the self-second derivatives (indicated by yellow squares with white dots in Figure 3). Examples of primate species exhibiting high elasticities and positive values for their self-second derivatives include northern muriqui (*Brachyteles hypoxanthus*), mountain gorilla (*Gorilla beringei*), white-faced capuchin monkey (*Cebus capucinus*), rhesus monkey (*Macaca mulatta*), blue monkey (*Cercopithecus mitis*), Verreaux's sifaka (*Propithecus verreauxi*) and olive baboon (*Papio cynocephalus*) (Fig. 3). This implies that the key demographic processes influencing λ_1 do not show evidence of selective pressure for reducing their variability.

The killer whale (*Orcinus orca*) showed similar lack of support for our hypothesis as primates. Indeed, *O. orca* was positioned at the buffered end of the variance continuum (Cetacea, $\Sigma E^{S\sigma}_{a_{ij}}$ = -4.72 × 10^{-4} ± 1.53 × 10^{-4}) (Fig. 2 silhouette not shown). However, the first- and second-order effects show that the governing three demographic processes in the killer whale life cycle (namely, matrix elements $a_{2,2}$, $a_{3,3}$ and $a_{4,4}$) are not under selection pressures for reducing their temporal variance, but the opposite (yellow and green squares with white dots, Fig. 3).

Only two species supported our hypothesis: humans and the Columbian ground squirrel (*Urocitellus columbianus*). In humans, demographic parameters representing survival from the first to second age class (matrix element $a_{2,1}$) displayed high elasticities and negative

Deleted: even

Deleted:

Deleted: As predicted for the steps 2 and 3,

Deleted: w

Deleted: could not observe a clear pattern in support of buffering

Deleted: Indeed

Deleted: This finding means that

Deleted: ly

Deleted: - with the a lack or minor temporal variation in demographic processes -

Deleted: .

Deleted: and

Deleted: ,

Deleted: are

Deleted: not subject to

Deleted: temporal

Deleted: However, even though the primates were positioned closer to the low-variance end of the continuum in step 1, the evidence from steps 2 and 3 does do not support the occurrence of buffering in the most influential demographic processes.

Deleted: controversy between the results of step 1 and steps 2-3 results as most primates. In step 1, t

Deleted: The

Deleted: killer whale

Formatted: Font: Italic

Deleted: *Orcinus orca*,

Deleted: 0.70

Deleted: 04

Deleted: ^{5}

Deleted: steps 2 and 3

Deleted:

Deleted: with highest elasticity values

Deleted:

Deleted: depicted by

Deleted: The only primate species exhibiting evidence of buffering in steps 2 and 3corroborating our hypothesis was the human self-second derivatives (depicted as yellow squares with black dots in Fig. 3). In *U. columbianus*, survival from the first to the second age class ($a_{2,1}$) too showed evidence of selection reducing the variance of this demographic process. Accordingly, *U. columbianus* was positioned near the buffered end of the variance continuum, providing consistent evidence supporting our hypothesis by displaying first- and second-order effects indicative of temporal variance reduction in the key demographic process. Conversely, the primary governing demographic process for Soay sheep (*Ovis aries*) displayed convex selection signatures. For *O. aries* (Fig. 2, silhouette i), remaining in the third age class ($a_{3,3}$, Fig. 3) governs the influence on λ_t and is under selection pressure to have its variance increased. These characteristics suggest potential conditions for lability, despite the species being positioned closer to the buffered end of the variance continuum.

The first- and second-order effects illustrate the importance of examining buffering evidence at the within-populations level. These effects can identify the simultaneous contributions of concave and convex selection on different demographic processes within a single life cycle. In the polar bear (*Ursus maritimus*), the key demographic process ($a_{4,4}$) is under convex selection, as depicted by a yellow square with a white dot in Figure 3. However, the demographic process with the second highest elasticity value ($a_{5,4}$) is under strong concave selection (depicted by a light green square with a black dot in Figure. 3).

By adding the second-order effect to the toolbox for demographic buffering, another important inference was made possible. The high absolute values of self-second derivatives (large dots, either black or white, Fig. 3) indicate where the sensitivity of λ_t to demographic parameters is itself prone to environmental changes. For instance, if the value of $a_{5,4}$ for *U. maritimus* increased, the sensitivity of λ_t to $a_{5,4}$ would decrease because the self-second derivative of $a_{5,4}$ is highly negative (depicted by the largest black dot in polar bear, Fig. 3 silhouette j). The opposite holds for the $a_{4,4}$ demographic process, where an increase in the

Deleted: Evidence supporting buffering our hypothesis was also found in the Columbian ground squirrel

Deleted: (*Urocitellus columbianus*), where, similar tolike in humans

Deleted: matrix element

Deleted: indications

Deleted: acting to reduce

Deleted: $a_{2,1}$ variance

Deleted: the Columbian ground squirrel

Deleted: was positioned close to the buffered end of the variance continuum in step 1. Hence, this speciese Columbian ground squirrel was the sole species was the only one with consistent evidence of buffering -- across all three steps of the framework.

Deleted: ¶

Deleted: The Soay sheep (*Ovis aries*) was the species furthest from the buffered end of the variance continuum that enabled to perform steps 2 and 3.

Deleted: *the Soay sheep*

Deleted: matrix element

Deleted: has

Deleted: major

Deleted: The latter characteristics reveal potential conditions for lability even though the species is placed closer to the buffered end of the variance continuum.¶

Deleted: Steps 2 and 3

Deleted:

Deleted: on

Deleted: two steps of the framework

Deleted: acting

Deleted: s

Deleted: matrix element

Deleted: .

Deleted: matrix element

Deleted: step 3

Deleted: framework

Deleted: information

Deleted: was accessed

Deleted: $_t$

Deleted: *polar bear*

Deleted:

Deleted: MPM

Deleted: Vice versa

value of $a_{4,4}$ would increase the sensitivity of λ_s to $a_{4,4}$, because the self-second derivative of $a_{4,4}$ is highly positive (the largest white dot in the polar bear MPM). Thus, sensitivities (or equally elasticities) of demographic processes with high absolute values for self-second derivatives are dynamic and can easily change.

Discussion

We report evidence of demographic buffering assessed at the between and within populations level. We used stochastic elasticities alongside the first- and second- order perturbation analysis and applied these analyses to mammal species to test our hypothesis. Here, we find weak support for said hypothesis, since most populations placed at the buffered end of variance continuum failed to display concave selection signatures.

Evidencing demographic buffering is not straightforward. Indeed, through the analysis of stochastic population growth rate (λ_s) in our application of the framework to 43 populations of 37 mammal species, we identify the highest density of natural populations near the buffered end of the variance continuum. However, we show that the same species then fail to exhibit signs of concave (∩-shaped) selection on key demographic parameters, opposed to our hypothesis. Such results suggest discordance between two features of demographic buffering, namely: 1) the stochastic population growth rate having a low sensitivity to temporal variability in demographic processes, and 2) demographic processes having variability constrained by selection.

The lack of correlation between non-linear selection patterns (concave/convex) and species positioning on the variance continuum for the studied mammal species may have several explanations. Firstly, non-linear selection on demographic process variability is *dynamic* (Kajin *et al.* 2023). Within a life cycle, even minor changes in key demographic processes can trigger a domino effect, affecting not only the process itself but also the

Deleted: ’s sensitivity

Deleted: $_s$

Deleted: depicted by

Deleted: can

Deleted: In the Anthropocene, identifying and quantifying mechanisms of species responses to stochastic environments holds crucial importance. This importance is particularly tangible in the context of the unprecedented environmental changes and uncertainties that impact the dynamics and persistence of natural populations . Correlational demographic analysis, whereby the importance of demographic processes and their temporal variability is examined , has attempted to identify how species may buffer against the negative effects of environmental stochasticity. However, these widely used approaches have important limitations (see Introduction and Hilde *et al.* 2020). One significant limitation is the issue of measurement scale concerning demographic processes . Demographic processes, such as birth rates, death rates, immigration, and emigration, operate at various temporal and spatial scales. The choice of scale at which these processes are measured can impact the outcomes of correlational demographic analysis . Our novel framework overcomes said limitations by providing a rigorous approach to quantify demographic buffering (. ¶

Deleted: 44

Deleted: 34

Deleted: (step 1)

Deleted: the

Deleted:

Deleted: swhen further analyses are performed averaging the variation across the duration of each study (steps 2 and 3)

Deleted: This

sensitivity of λ_1 to changes in said process (Stearns 1992). Consequently, correlations between demographic processes (negative correlations known as trade-offs) are influenced by minor alterations in the governing demographic processes (Doak *et al.* 2005). Therefore, the observed self-second derivative of the population growth rate represents a momentum that can be influenced by small changes in any demographic process within the life cycle. Because of these characteristics, second-order derivatives reveal “fine scale” fitness behaviour compared to sums of stochastic elasticities. Evolutionary demography still requires a tool to connect second-order fitness effects with stochastic elasticities in a biologically interpretable manner (but see Tuljapurkar *et al.* 2023).

When placing our study species along a variance continuum, primates tend to be located on the buffered end. However, most primates displayed convex – instead of the expected concave – selection on adult survival. Similar results, where the key demographic process failed to display constrained temporal variability, have been reported for long-lived seabirds (Doherty *et al.* 2004). One explanation for the unexpected convex selection on adult survival involves trade-offs, as suggested by (Doak *et al.* 2005). When two demographic parameters are negatively correlated, the variance of population growth rate can be increased or decreased (Compagnoni *et al.* 2016; Evans & Holsinger 2012).

Correlations among demographic processes (positive and negative) inherently influence the biological limits of variance (Haridas & Tuljapurkar 2005). This is because the magnitude of variation in a particular demographic process is constrained by the variation of other demographic processes. Not surprisingly, correlations among demographic processes have been shown to be strongly subjected to ecological factors (Fay *et al.* 2022). Therefore, future studies may benefit from deeper insights using *cross*-second derivatives (Caswell 1996, 2001) to investigate correlations among demographic processes.

Deleted: finding confirms that placing the species near the buffered end of the variance continuum is *necessary* but not *sufficient* to diagnose demographic buffering. Indeed, buffering occurs when concave selection forces act on the key demographic parameter . ¶

Biological variance estimates are inevitably subjected to several sources of bias (Simmonds & Jones 2024). To minimise bias, we randomly sampled the available matrices before obtaining the estimates. Despite the significant correlation between $\Sigma E^{S^{\sigma}}_{a_{ij}}$ and the number of available matrices per species, the relative positioning of species remains meaningful for between-population level comparisons, as the correlation is very weak (-0.002). Still, researchers carrying out macroecological comparisons of demographic buffering might want to be even more restringent than we have been here with their datasets, as these grow longer with time (Compagnoni *et al.* 2021; Salguero-Gómez *et al.* 2021).

Regarding phylogenetic effects, our tests revealed a mild signal, but we note that future work regressing $\Sigma E^{S^{\sigma}}_{a_{ij}}$ values against potential independent variables (*e.g.*, climate values) may want to correct for this phylogenetic dependence. By having carefully chosen studies from a database that contains >400 species and retained only those that passed through a set of selection criteria (Che-Castaldo *et al.* 2020; Gascoigne *et al.* 2023b; Kendall *et al.* 2019; Römer *et al.* 2024; Simmonds & Jones 2024), we mitigate those biases *a priori*. Furthermore, we are using an elasticity-based approach, meaning we are comparing proportional variances. At present, the available methods still do not account for constraints in variance nor performing a perturbation approach disproportionately.

The analyses at both between- and within-populations levels are fundamentally interconnected. This connection is grounded on the fact that large summed elasticities with respect to variance are intrinsically linked to high elasticity values, as demonstrated in equation 6 in (Haridas & Tuljapurkar 2005). This finding robustly endorses the perspective that species' positions along the variance continuum should be interpreted with consideration of first and second-order effects, and additionally, in the context of selection pressures acting on the variability of demographic processes, as revealed by a second order effect.

Combining first- and second-order analyses is crucial for understanding the factors shaping demographic buffering patterns. The second-order effect reveals that the role of natural selection in shaping temporal variation in demographic processes is more complex than initially thought. Indeed, demographic processes within our study populations often face a mix of convex and concave selection. This mix of selection patterns was suggested by Doak et al. (2005), who noted that dramatic changes in population growth rate sensitivities are influenced by correlations among demographic processes. Here, only two of the 16 mammal species revealed concave selection on the key demographic processes: Columbian ground squirrel (*Urocitellus columbianus*), and humans, (*Homo sapiens*). These two species were placed near the buffered end of the variance continuum, supporting our hypothesis. Evidence of buffering has been reported across 22 ungulate species (Gaillard & Yoccoz 2003). However, in the one ungulate we examined, the moose (*Alces alces*), we found only partial support for our hypothesis, as it is near the buffered end of the variance continuum but lacks concave selection pressures.

Our overall findings reveal varying levels of support for the notion that adult survival in long-lived species tends to be buffered. Indeed, Gaillard et al. (1998) found that adult female survival varied considerably less than juvenile survival in large herbivores. This finding was also supported by further studies in ungulates (Gaillard & Yoccoz 2003), turtles (Heppell 1998), vertebrates and plants (Pfister 1998), and more recently across nine species of plants (McDonald *et al.* 2017). However, an alternative result was also reported by Gaillard and Yoccoz (2003) for small mammals, where variability in adult survival was unexpectedly high, even though the studied small mammals were annual, and as such comparable to large mammal model. Seasonality, frequency and method of sampling all influence survival estimates and their estimated variability, thus, when comparing multiples

Deleted: Combining the three steps into a unified framework is of outmost importance. In steps 2 and 3 of the framework, we find relatively limited overall evidence of buffering in the examination of our 16 (out of 34 in step 1) studied animal species (out of 34 in step 1). Step 3 of our framework reveals that the role of natural selection shaping temporal variation in demographic processes is more complex than expected. Indeed, demographic processes within our study populations are often under a mix of convex and concave selection. This mix of selection patterns was already suggested by Doak *et al.* (2005).

Deleted: out

Deleted: acting

Deleted: (Columbian ground squirrel [*Urocitellus columbianus*], and humans, [*Homo sapiens sapiens*])

Deleted: also

Deleted: therefore

Deleted: meeting all the necessary conditions to diagnose buffering

Deleted: However, finding 12.5% (two out of 16) species that meet the criteria for demographic buffering is not in concordance with previous studies.

Deleted: I

Deleted: find

Deleted: buffering in adult survival

Deleted: since this species is placed

Deleted: in step 1

Deleted: does not show

Deleted: on adult survival in step 2/3, as would be necessary to confirm the occurrence of buffering

Deleted: It is worth noting that a varying number of matrices per species were employed, ranging from 1 to 21, with an average of 8.1 matrices per species (as shown in Table S1). Naturally, having a greater number of matrices is preferred in such analyses. Furthermore, while the size of matrices (matrix dimensions) does not directly bias the results of our framework in any way – since steps 2 and 3 are shown for all the demographic processes independent of matrix dimension – potential implications of varying matrix dimensions should be further investigated in the future. ¶

species/studies, all of the latter characteristics should be taken into account when interpreting the results.

Examining the drivers of demographic buffering has become an important piece of the ecological and evolutionary puzzle of demography. As such, understanding buffering can help us better predict population responses to environmental variability, climate change, and direct anthropogenic disturbances (Boyce *et al.* 2006; Gascoigne *et al.* 2024a; McDonald *et al.* 2017; Pfister 1998; Vázquez *et al.* 2017). By setting demographic buffering into a broader and integrated framework, we hope to enhance comprehension and prediction of the implications of heightened environmental stochasticity on the evolution of life history traits. This understanding is crucial in mitigating the risk of extinction for the most vulnerable species.

Acknowledgements

This study was financed in part by the *Coordenação de Aperfeiçoamento de Pessoal de Nível Superior* - Brasil (CAPES) - Finance Code 001. GSS was supported by CAPES and CNPq (301343/2023-3). MK was supported by the European Commission through the Marie Skłodowska-Curie fellowship (MSCA MaxPersist #101032484) hosted by RSG. RS-G was supported by a NERC Independent Research Fellowship (NE/M018458/1) and a NERC Pushing the Frontiers (NE/X013766/1).

Data availability

The demographic data used in this paper are open-access and available in the COMADRE Animal Matrix Database (https://compadre-db.org/Data/Comadre). A list of the studies and species used here is available in Supplementary Material (Table S1). The data and code

Deleted: When placing our study species along a variance continuum (step 1), primates tend to be located on the buffered end. However, most primates displayed convex – instead of the expected concave– selection on adult survival. Similar results, where the key demographic process failed to display constrained temporal variability, have been reported for long-lived seabirds . One explanation for the unexpected convex selection on adult survival involves trade-offs, as suggested by . When two demographic parameters are negatively correlated, the variance of population growth rate (/) can be increased or decreased . The well-established trade-off between survival and fecundity might explain the observed deviation of our results. Because variation in primate recruitment is already constrained by physiological limitations , when adult survival and recruitment are engaged in a trade-off, this trade-off might lead to our unexpected result. Correlations among demographic processes (positive and negative) inherently influence the biological limits of variance (Haridas & Tuljapurkar, 2005). This is because the magnitude of variation in a particular demographic process is constrained by (the variation of) other demographic processes that exert an influence on it. Not surprisingly, correlations among demographic processes have been shown to be strongly subjected to ecological factors . HereTherefore, future studies may benefit from deeper insights via using cross-second derivatives to investigate correlations among demographic processes. ¶

Deleted: quantifying

Deleted: In the Anthropocene, identifying and quantifying mechanisms of species responses to stochastic environments holds crucial importance. This importance is particularly tangible in the context of the unprecedented environmental changes and uncertainties that impact the dynamics and persistence of natural populations . Correlational demographic analysis, whereby the importance of demographic processes and their temporal variability is examined , has attempted to identify how species may buffer against the negative effects of environmental stochasticity. However, these widely used approaches have important limitations (see Introduction and Hilde *et al.* 2020). One significant limitation is the issue of measurement scale concerning demographic processes . Demographic processes, such as birth rates, death rates, immigration, and emigration, operate at various temporal and spatial scales. The choice of scale at which these processes are measured can impact the outcomes of correlational demographic analysis . Our novel framework overcomes said limitations by providing a rigorous approach to quantify demographic buffering (. ¶
¶

Moved (insertion) [1]

Moved up [1]: MK was supported by the European Commission through the Marie Skłodowska-Curie fellowship (MSCA MaxPersist #101032484) hosted by RSG.

supporting the results can be accessed here: https://github.com/SamuelGascoigne/Demographic_buffering_unified_framework.

References

Barraquand, F. & Yoccoz, N.G. (2013). When can environmental variability benefit population growth? Counterintuitive effects of nonlinearities in vital rates. *Theor Popul Biol*, 89, 1–11.

Bathiany, S., Dakos, V., Scheffer, M. & Lenton, T.M. (2018). Climate models predict increasing temperature variability in poor countries. *Sci Adv*, 4.

Beccari, E., Capdevila, P., Salguero-Gómez, R. & Carmona, C.P. (2024). Worldwide diversity in mammalian life histories: Environmental realms and evolutionary adaptations. *Ecol Lett*, 27.

Bielby, J., Mace, G.M., Bininda-Emonds, O.R.P., Cardillo, M., Gittleman, J.L., Jones, K.E., *et al.* (2007). The Fast-Slow Continuum in Mammalian Life History: An Empirical Reevaluation. *Am Nat*, 169, 748–757.

Bonsall, M.B. & Klug, H. (2011). The evolution of parental care in stochastic environments. *J Evol Biol*, 24, 645–655.

Boyce, M., Haridas, C., Lee, C. & The NCEAS Stochastic Demography Working Group. (2006). Demography in an increasingly variable world. *Trends Ecol Evol*, 21, 141–148.

Brodie, E.I., Moore, A. & Janzen, F. (1995). Visualizing and quantifying natural selection. *Trends Ecol Evol*, 10, 313–318.

Campos, F.A., Morris, W.F., Alberts, S.C., Altmann, J., Brockman, D.K., Cords, M., *et al.* (2017). Does climate variability influence the demography of wild primates? Evidence from long-term life-history data in seven species. *Glob Chang Biol*, 23, 4907–4921.

Carslake, D., Townley, S. & Hodgson, D.J. (2008). Nonlinearity in eigenvalue-perturbation curves of simulated population projection matrices. *Theor Popul Biol*, 73, 498–505.

Caswell, H. (1978). A general formula for the sensitivity of population growth rate to changes in life history parameters. *Theor Popul Biol*, 14, 215–230.

Caswell, H. (1996). Second Derivatives of Population Growth Rate: Calculation and Applications. *Ecology*, 77, 870–879.

Caswell, H. (2001). *Matrix Population Models: Construction, Analysis, and Interpretation*. Sinauer Associates Inc. Publishers, Sunderland, Massachusetts, USA.

Charlesworth, B. (1994). *Evolution in age-structured populations*. second edi. Cambridge University Press.

Che-Castaldo, J., Jones, O.R., Kendall, B.E., Burns, J.H., Childs, D.Z., Ezard, T.H.G., *et al.* (2020). Comments to "Persistent problems in the construction of matrix population models." *Ecol Modell*, 416.

Le Coeur, C., Yoccoz, N.G., Salguero-Gómez, R. & Vindenes, Y. (2022). Life history adaptations to fluctuating environments: Combined effects of demographic buffering and lability. *Ecol Lett*, 25, 2107–2119.

Compagnoni, A., Bibian, A.J., Ochocki, B.M., Rogers, H.S., Schultz, E.L., Sneck, M.E., *et al.* (2016). The effect of demographic correlations on the stochastic population dynamics of perennial plants. *Ecol Monogr*, 86, 480–494.

Compagnoni, A., Evers, S. & Knight, T. (2023). Spatial replication can best advance our understanding of population responses to climate. *bioRxiv*, https://doi.org/10.1101/2022.06.24.497542.

Compagnoni, A., Levin, S., Childs, D.Z., Harpole, S., Paniw, M., Römer, G., *et al.* (2021). Herbaceous perennial plants with short generation time have stronger responses to climate anomalies than those with longer generation time. *Nat Commun*, 12, 1824.

Doak, D.F., Morris, W.F., Pfister, C., Kendall, B.E. & Bruna, E.M. (2005). Correctly Estimating How Environmental Stochasticity Influences Fitness and Population Growth. *Am Nat*, 166, E14–E21.

Doak, D.F., Waddle, E., Langendorf, R.E., Louthan, A.M., Isabelle Chardon, N., Dibner, R.R., *et al.* (2021). A critical comparison of integral projection and matrix projection models for demographic analysis. *Ecol Monogr*, 91, e01447.

Doherty, P.F., Schreiber, E.A., Nichols, J.D., Hines, J.E., Link, W.A., Schenk, G.A., *et al.* (2004). Testing life history predictions in a long-lived seabird: A population matrix approach with improved parameter estimation. *Oikos*, 105, 606–618.

Drake, J.M. (2005). Population effects of increased climate variation. *Proceedings of the Royal Society B: Biological Sciences*, 272, 1823–1827.

Easterling, M.R., Ellner, S.P. & Dixon, P.M. (2000). Size-Specific Sensitivity: Applying a New Structured Population Model. *Ecology*, 81, 694–708.

Ebert, T. (1999). *Plant and animal populations: Methods in demography*. Academis Press, San Diego, CA, USA.

Ellner, S.P., Childs, D.Z. & Rees, M. (2016). *Data-driven Modelling of Structured Populations. A practical guide to the Integral Projection Model*. Lecture Notes on Mathematical Modelling in the Life Sciences. Springer International Publishing, Cham.

Evans, M.E.K. & Holsinger, K.E. (2012). Estimating covariation between vital rates : A simulation study of connected vs . separate generalized linear mixed models (GLMMs). *Theor Popul Biol*, 82, 299–306.

Evers, S.M., Knight, T.M., Inouye, D.W., Miller, T.E.X., Salguero-Gómez, R., Iler, A.M., *et al.* (2021). Lagged and dormant season climate better predict plant vital rates than climate during the growing season. *Glob Chang Biol*, 27, 1927–1941.

Fay, R., Hamel, S., van de Pol, M., Gaillard, J.M., Yoccoz, N.G., Acker, P., *et al.* (2022). Temporal correlations among demographic parameters are ubiquitous but highly variable across species. *Ecol Lett*, 25, 1640–1654.

Franco, M. & Silvertown, J. (2004). A comparative demography of plants based upon elasticities of vital rates. *Ecology*, 85, 531–538.

Gaillard, J.M., Festa-Bianchet, M. & Yoccoz, N.G. (1998). Population dynamics of large herbivores: Variable recruitment with constant adult survival. *Trends Ecol Evol*, 13, 58–63.

Gaillard, J.-M. & Yoccoz, N. (2003). Temporal Variation in Survival of Mammals: a Case of Environmental Canalization? *Ecology*, 84, 3294–3306.

Gascoigne, S.J.L., Kajin, M. & Salguero-Gómez, R. (2024a). Criteria for buffering in ecological modeling. *Trends Ecol Evol*, 39, 116–118.

Gascoigne, S.J.L., Kajin, M., Sepil, I. & Salguero-Gómez, R. (2024b). Testing for efficacy in four measures of demographic buffering. *EcoEvoRxiv*, 0–2.

Gascoigne, S.J.L., Kajin, M., Tuljapurkar, S.D., Silva Santos, G., Compagnoni, A., Steiner, U.K., *et al.* (2023a). Structured demographic buffering: A framework to explore the environment drivers and demographic mechanisms underlying demographic buffering. *bioRxiv*.

Gascoigne, S.J.L., Rolph, S., Sankey, D., Nidadavolu, N., Stell Pičman, A.S., Hernández, C.M., *et al.* (2023b). A standard protocol to report discrete stage-structured demographic information. *Methods Ecol Evol*, 14, 2065–2083.

Gillespie, J.H. (1977). Natural Selection for Variances in Offspring Numbers: A New Evolutionary Principle. *Am Nat*, 111, 1010–1014.

Griffith, A.B. (2017). Perturbation approaches for integral projection models. *Oikos*, 126, 1675–1686.

Haridas, C. V. & Tuljapurkar, S. (2005). Elasticities in Variable Environments: Properties and Implications. *Am Nat*, 166, 481–495.

Healy, K., Ezard, T.H.G., Jones, O.R., Salguero-Gómez, R. & Buckley, Y.M. (2019). Animal life history is shaped by the pace of life and the distribution of age-specific mortality and reproduction. *Nat Ecol Evol*, 3, 1217–1224.

Heppell, S.S. (1998). Application of Life-History Theory and Population Model Analysis to Turtle Conservation. *Copeia*, 1998, 367.

Hilde, C.H., Gamelon, M., Sæther, B.-E., Gaillard, J.-M., Yoccoz, N.G. & Pélabon, C. (2020). The Demographic Buffering Hypothesis: Evidence and Challenges. *Trends Ecol Evol*, 35, 523–538.

Jäkäläniemi, A., Ramula, S. & Tuomi, J. (2013). Variability of important vital rates challenges the demographic buffering hypothesis. *Evol Ecol*, 27, 533–545.

Jones, J.H. (2007). demogR: A Package for the Construction and Analysis of Age-structured Demographic Models in R. *J Stat Softw*, 22, 1–28.

Jones, J.H. (2011). Primates and the evolution of long, slow life histories. *Current Biology*, 21, R708–R717.

Jongejans, E., De Kroon, H., Tuljapurkar, S. & Shea, K. (2010). Plant populations track rather than buffer climate fluctuations. *Ecol Lett*, 13, 736–743.

Kajin, M., Gentile, R., Almeida, P.J.A.L. de, Vieira, M.V. & Cerqueira, R. (2023). Vital rates, their variation and natural selection: a case for an Atlantic forest marsupial. *Oecologia Australis*, 27.

Kendall, B.E., Fujiwara, M., Diaz-Lopez, J., Schneider, S., Voigt, J. & Wiesner, S. (2019). Persistent problems in the construction of matrix population models. *Ecol Modell*, 406, 33–43.

Keyfitz, N. & Flieger, W. (1990). *World Population Growth and Aging: Demographic Trends in the Late Twentieth Century*. University of Chicago Press, Chicago.

Koons, D.N., Pavard, S., Baudisch, A. & Jessica E. Metcalf, C. (2009). Is life-history buffering or lability adaptive in stochastic environments? *Oikos*, 118, 972–980.

Kroon, H. De, Groenendael, J. Van & Ehrlen, J. (2000). Elasticities: A review of methods and model limitations. *Ecology*, 81, 607–618.

de Kroon, H., Plaisier, A., van Groenendael, J. & Caswell, H. (1986). Elasticity: The Relative Contribution of Demographic Parameters to Population Growth Rate. *Ecology*, 67, 1427–1431.

Lawler, R.R., Caswell, H., Richard, A.F., Ratsirarson, J., Dewar, R.E. & Schwartz, M. (2009). Demography of Verreaux's sifaka in a stochastic rainfall environment. *Oecologia*, 161, 491–504.

Lefèvre, C.D., Nash, K.L., González-Cabello, A. & Bellwood, D.R. (2016). Consequences of extreme life history traits on population persistence: do short-lived gobies face demographic bottlenecks? *Coral Reefs*, 35, 399–409.

McDonald, J.L., Franco, M., Townley, S., Ezard, T.H.G., Jelbert, K. & Hodgson, D.J. (2017). Divergent demographic strategies of plants in variable environments. *Nat Ecol Evol*, 1, 0029.

Morris, W.F., Altmann, J., Brockman, D.K., Cords, M., Fedigan, L.M., Pusey, A.E., *et al.* (2011). Low Demographic Variability in Wild Primate Populations: Fitness Impacts of Variation, Covariation, and Serial Correlation in Vital Rates. *Am Nat*, 177, E14–E28.

Morris, W.F. & Doak, D.F. (2004). Buffering of Life Histories against Environmental Stochasticity: Accounting for a Spurious Correlation between the Variabilities of Vital Rates and Their Contributions to Fitness. *Am Nat*, 163, 579–590.

Morris, W.F., Pfister, C.A., Tuljapurkar, S., Haridas, C. V., Boggs, C.L., Boyce, M.S., *et al.* (2008). Longevity can buffer plant and animal populations against changing climatic variability. *Ecology*, 89, 19–25.

Münkemüller, T., Lavergne, S., Bzeznik, B., Dray, S., Jombart, T., Schiffers, K., *et al.* (2012). How to measure and test phylogenetic signal. *Methods Ecol Evol*, 3, 743–756.

Pélabon, C., Hilde, C.H., Einum, S. & Gamelon, M. (2020). On the use of the coefficient of variation to quantify and compare trait variation. *Evol Lett*, 4, 180–188.

Perret, D.L., Evans, M.E.K. & Sax, D.F. (2024). A species' response to spatial climatic variation does not predict its response to climate change. *Proc Natl Acad Sci U S A*, 121, e2304404120.

Pfister, C. (1998). Patterns of variance in stage-structured populations: Evolutionary predictions and ecological implications. *Proceedings of the National Academy of Sciences*, 95, 213–218.

R Core Team. (2024). R: A Language and Environment for Statistical Computing.

Reed, A.W. & Slade, N.A. (2012). Buffering and plasticity in vital rates of oldfield rodents. *Journal of Animal Ecology*, 81, 953–959.

Rodríguez-Caro, R.C., Capdevila, P., Graciá, E., Barbosa, J.M., Giménez, A. & Salguero-Gómez, R. (2021). The limits of demographic buffering in coping with environmental variation. *Oikos*, 130, 1346–1358.

Römer, G., Dahlgren, J.P., Salguero-Gómez, R., Stott, I.M. & Jones, O.R. (2024). Plant demographic knowledge is biased towards short-term studies of temperate-region herbaceous perennials. *Oikos*, 2024.

Rotella, J.J., Link, W.A., Chambert, T., Stauffer, G.E. & Garrott, R.A. (2012). Evaluating the demographic buffering hypothesis with vital rates estimated for Weddell seals from 30 years of mark-recapture data. *Journal of Animal Ecology*, 81, 162–173.

Salguero-Gómez, R. (2021). Commentary on the life history special issue: The fast-slow continuum is not the end-game of life history evolution, human or otherwise. *Evolution and Human Behavior*, 42, 281–283.

Salguero-Gómez, R. (2024). More social species live longer, have higher generation times, and longer reproductive windows. *bioRxiv; https://doi.org/10.1101/2024.01.22.575897.*

Salguero-Gómez, R., Jackson, J. & Gascoigne, S.J.L. (2021). Four key challenges in the open-data revolution. *Journal of Animal Ecology*, 90, 2000–2004.

Salguero-Gómez, R., Jones, O.R., Archer, C.R., Bein, C., de Buhr, H., Farack, C., *et al.* (2016). COMADRE: A global data base of animal demography. *Journal of Animal Ecology*, 85, 371–384.

Sanghvi, K., Vega-Trejo, R., Nakagawa, S., Gascoigne, S.J.L., Johnson, S.L., Salguero-Gómez, R., *et al.* (2024). Meta-analysis shows no consistent evidence for senescence in ejaculate traits across animals. *Nat Commun*, 15, 558.

Shyu, E. & Caswell, H. (2014). Calculating second derivatives of population growth rates for ecology and evolution. *Methods Ecol Evol*, 5, 473–482.

Simmonds, E.G. & Jones, O.R. (2024). Uncertainty propagation in matrix population models: Gaps, importance and guidelines. *Methods Ecol Evol*, 15, 427–438.

Stearns, S. (1992). *The Evolution of Life Histories*. Oxford University Press, New York, USA.

Stearns, S.C. (1983). The Influence of Size and Phylogeny on Patterns of Covariation among Life-History Traits in the Mammals. *Oikos*, 41, 173.

Stubben, C., Milligan, B., Nantel, P. & Stubben, M.C. (2020). Package 'popbio.'

Sutherland, W.J., Freckleton, R.P., Godfray, H.C.J., Beissinger, S.R., Benton, T., Cameron, D.D., *et al.* (2013). Identification of 100 fundamental ecological questions. *Journal of Ecology*, 101, 58–67.

Tuljapurkar, S. (1990). Population Dynamics in Variable Environments. In: *Lecture notes in Biomathematics*, Lecture Notes in Biomathematics (ed. Levin, S.). Springer Berlin Heidelberg.

Tuljapurkar, S. (2010). Environmental variance, population growth and evolution. *J Anim Ecol*, 79, 1–3.

Tuljapurkar, S., Gaillard, J.-M. & Coulson, T. (2009). From stochastic environments to life histories and back. *Philosophical Transactions of the Royal Society B: Biological Sciences*, 364, 1499–1509.

Tuljapurkar, S., Horvitz, C.C. & Pascarella, J.B. (2003). The Many Growth Rates and Elasticities of Populations in Random Environments. *Am Nat*, 162, 489–502.

Tuljapurkar, S., Jaggi, H., Gascoigne, S.J.L., Zuo, W., Kajin, M. & Salguero-Gómez, R. (2023). From disturbances to nonlinear fitness and back. *bioRxiv*, 2023.10.20.563360.

Tuljapurkar, S.D. (1982). Population dynamics in variable environments. III. Evolutionary dynamics of r-selection. *Theor Popul Biol*, 21, 141–165.

Vázquez, D.P., Gianoli, E., Morris, W.F. & Bozinovic, F. (2017). Ecological and evolutionary impacts of changing climatic variability. *Biological Reviews*, 92, 22–42.

Wang, J., Yang, X., Silva Santos, G., Ning, H., Li, T., Zhao, W., *et al.* (2023). Flexible demographic strategies promote the population persistence of a pioneer conifer tree (Pinus massoniana) in ecological restoration. *For Ecol Manage*, 529, 120727.

Zuidema, P.A. & Franco, M. (2001). Integrating vital rate variability into perturbation analysis: an evaluation for matrix population models of six plant species. *Journal of Ecology*, 89, 995–1005.

Figure 1

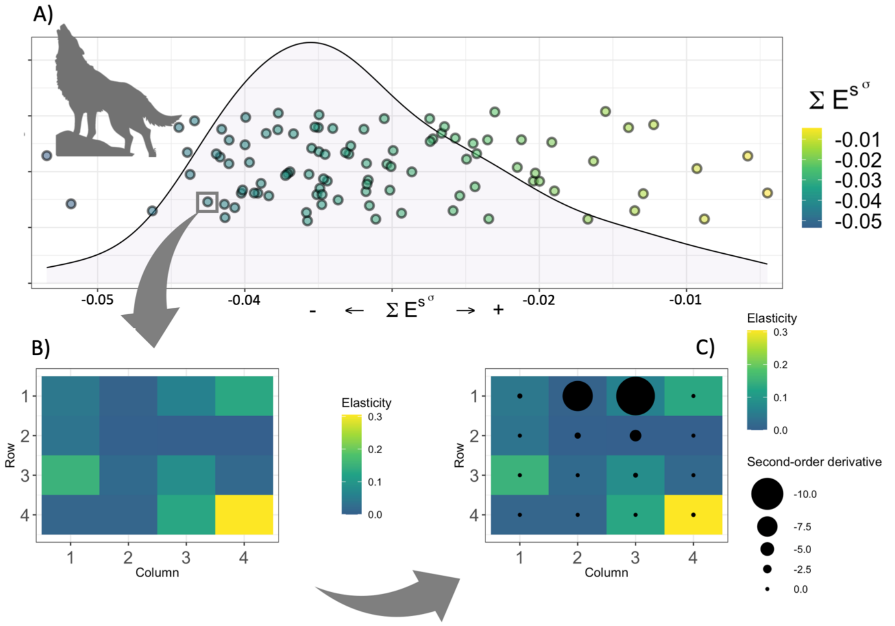

Deleted:

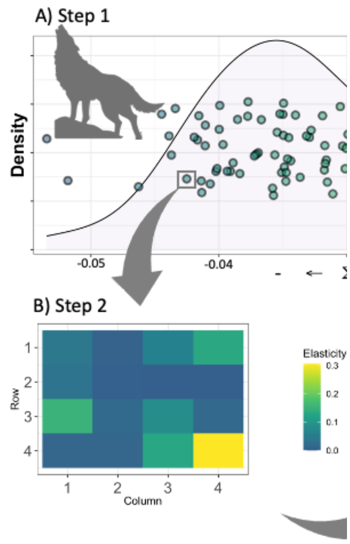

Figure 2

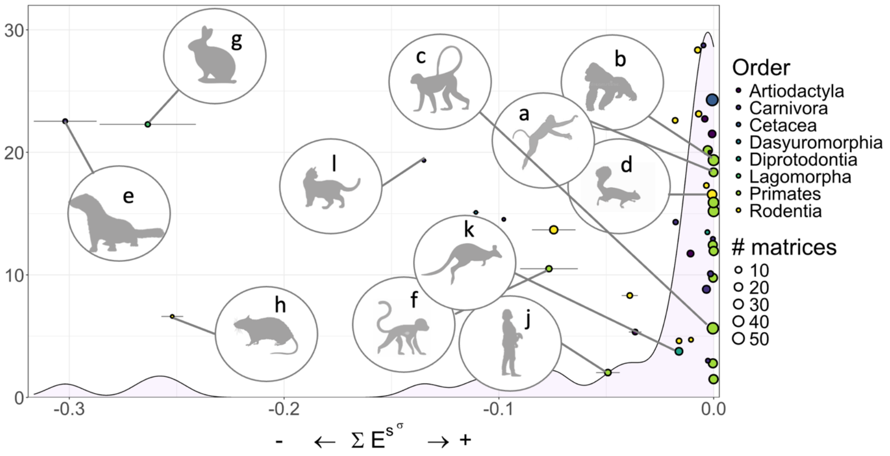

Deleted:

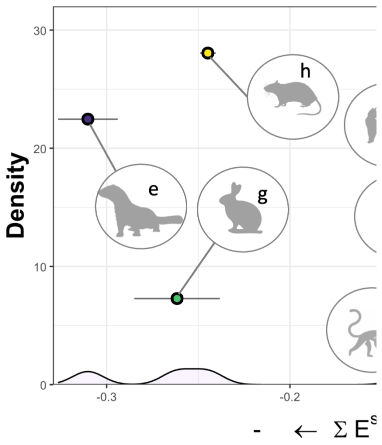

Figure 3

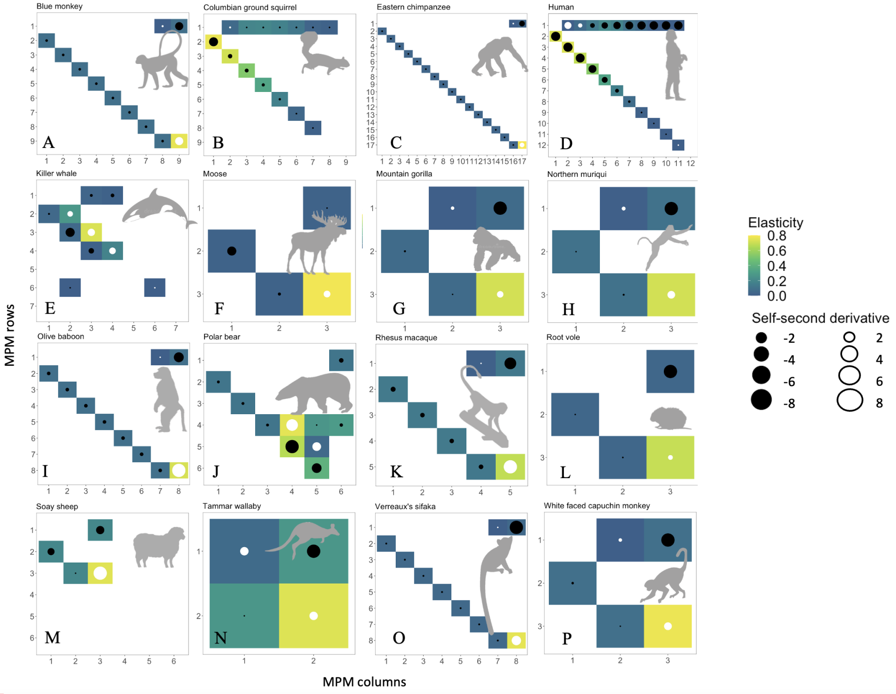

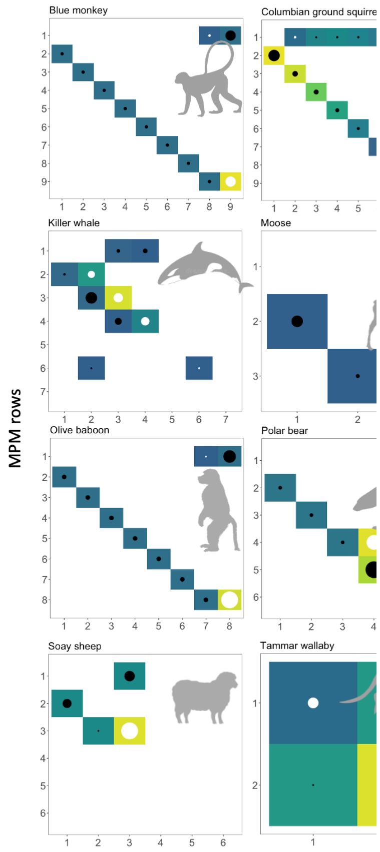

Deleted:

Figure legends

Figure 1. A) The variance continuum for 37 hypothetical species based on the summed stochastic elasticities ($\Sigma E^{S^{\sigma}}_{a_{ij}}$) at the between populations hierarchical level. The closer the $\Sigma E^{S^{\sigma}}_{a_{ij}}$ is to zero, the weaker the impact of variation in demographic processes on the stochastic population growth rate, λ_s. The variance continuum ranges from potentially buffered (right-hand side) to less buffered (left-hand side) species/populations. The yellow-dotted species/populations can be classified as having potentially *buffered life cycles*. The left-hand side of the graph represents species/populations where variability in demographic processes results in strong impact on λ_s (blue dots). Thus, the blue-dotted species/populations can be classified as having potentially *unbuffered life cycles*. The vertical axis delineates the values of the probability density function, indicating the number of species/populations at each value of $\Sigma E^{S^{\sigma}}_{a_{ij}}$. The placement of data points (species/populations) along the horizontal axis corresponds to their calculated values of $\Sigma E^{S^{\sigma}}_{a_{ij}}$ and is arranged linearly, while the placement along the y-axis is random for improved visual comprehension. B) First-order effects or linear selection pressures for individual species/populations at within-species level (see text). Shown are the elasticities of the deterministic population growth rate (λ_1) for a hypothetical population of wolves and revealing the governing demographic process(es) in the life cycle (yellow cells: high elasticity, blue cells: low elasticity). C) Combined results for first (yellow and blue cells) and second order effects (black dots), where the latter reveals the nonlinear selection pressures at the within-species level.

Figure 2. The variance continuum for 43 populations from 37 species of mammals from the COMADRE database based on the summed stochastic elasticities ($\Sigma E^{S^{\sigma}}_{a_{ij}}$) at the between populations hierarchical level. Colors represent different taxonomic orders with Primates occupying the right-hand side. Silhouettes: a) *Brachyteles hypoxantus*, b) *Gorilla beringhei*,

Deleted: A three-step framework proposed to: Step

Deleted: 1 - allocate species and/or populations on a

Deleted: (plot A, dots representing

Deleted: 50

Deleted:)

Deleted: The variance continuum operates at the between-populations level (see text) and is represented by partitioning the sum of all the stochastic elasticities into two compounds: i) sums of stochastic elasticities with resp ... [34]

Deleted: (or

Deleted:)

Deleted: -

Deleted: – based on all the demographic processes

Deleted: (or

Deleted:)

Deleted: a perturbation of the variance

Deleted: (or

Deleted:)

Deleted: – based on all the demographic processes

Deleted: distribution

Deleted: breadth

Deleted: solely

Deleted: Step

Deleted: 2 -

Deleted:

Deleted: Access the

Deleted: or

Deleted: (plot B)

Deleted: Step 2

Deleted: displays

Deleted: $_t$

Deleted: wolf

Deleted: s

Deleted: linear selection gradients

Deleted: ,

Deleted: and which demographic processes are the m ... [35]

Deleted: λ_t

Deleted: Step 3

Deleted: -

Deleted: Access the n

Deleted: (see text) (plot C)

Deleted: In the third step self-second derivatives for t ... [36]

Deleted: 40

Deleted: 34

Deleted: Results for step 1 of our framework showing ... [37]

c) *Cercopithecus mitis*, d) *Urocitellus columbianus,* e) *Mustela erminea*, f) *Erythrocebus patas*, g) *Lepus americanus*, h) *Rattus fuscipes*, i) *Ovis aries*, j) *Homo sapiens*, k) *Macropus eugenii*, and l) *Felis catus*. The vertical axis delineates the values of the probability density function, indicating the number of species/populations at each value of $\Sigma E^{S^{\sigma}}_{a_{ij}}$. The placement of data points (species/populations) along the horizontal axis corresponds to their calculated values of $\Sigma E^{S^{\sigma}}_{a_{ij}}$ and is arranged linearly, while the placement along the y-axis is random for improved visual comprehension.

Figure 3: First and second order effects on population growth rate, λ_1 (corresponding to elasticities and self-second derivatives of population growth rate, respectively) for 16 mammal species. The 16 plots represent populations where the MPMs built by ages were available in the COMADRE Animal Matrix Database. The yellow-blue colour scale represents elasticity values for each of the demographic processes in the MPM, where yellow cells represent high and blue cells low elasticity of population growth rate to changes in demographic processes. No colour means elasticity=0. The black dots represent negative self-second derivatives of λ_1 - corresponding to concave selection - and the white dots represent positive self-second derivatives of λ_1 - ditto convex selection. The dot sizes are scaled by the absolute value of self-second derivatives, where the smaller the dot, the closer a self-second derivative is to 0, indicating weak or no nonlinearity. Thus, large dots indicate strong nonlinear selection forces, either concave (black) or convex (white). Since the derivatives of population growth rate are confounded by eigen-structure (Kroon *et al.* 2000), the scaling of the elasticity values and second-derivative values is species specific - i.e., each plot has its own scale. Species-specific scales can be found in Supplementary material (Table S2).

Deleted: breadth

Deleted: solely

Deleted: Results from steps 2 and 3 of the proposed framework (see Fig. 2B, C).

Deleted: d

Deleted: (see text)

Deleted: color

Deleted: s

Deleted: values.

Deleted: color

Deleted: Because the aim of step 2 is to identify the most impacting demographic process within each species' life cycle (the within-populations level, see text) - not to compare the elasticity values among species - each plot has its own scale (see end of legend).

Deleted: The black dots represent negative self-second derivatives of λ_t - thus concave selection - and the white dots represent positive self-second derivatives of λ_t - thus convex selection. The dot sizes are scaled by the absolute value of self-second derivatives, where the smaller the dot, the closer a self-second derivative is to 0, indicating weak or no nonlinearity. Large dots indicate strong nonlinear selection forces. Scales ($E_{min-max}$=elasticity minimum and maximum value, $SSD_{min-max}$=self-second derivative minimum and maximum value): Blue monkey $E_{min-max}$=0.00-0.52, $SSD_{min-max}$=-1.25-1.27; Columbian ground squirrel: $E_{min-max}$=0.00-0.23, $SSD_{min-max}$=-1.48-0.01; Eastern chimpanzee: $E_{min-max}$=0.00-0.60, $SSD_{min-max}$=-4.39-2.59; Human: $E_{min-max}$=0.00-0.18, $SSD_{min-max}$=-0.15-0.08; Killer whale: $E_{min-max}$=0.00-0.55, $SSD_{min-max}$=-5.72-3.43; Moose: $E_{min-max}$=0.00-0.55, $SSD_{min-max}$=-0.66-0.36; Mountain gorilla: $E_{min-max}$=0.00-0.81, $SSD_{min-max}$=-1.46-0.28; Northern muriqui: $E_{min-max}$=0.00-0.72, $SSD_{min-max}$=-1.17-0.35; Olive baboon: $E_{min-max}$=0.00-0.54, $SSD_{min-max}$=-0.57-1.13; Polar bear: $E_{min-max}$=0.00-0.26, $SSD_{min-max}$=-0.73-0.54; Rhesus macaque: $E_{min-max}$=0.00-0.51, $SSD_{min-max}$=-0.54-0.71; Root vole: $E_{min-max}$=0.00-0.86, $SSD_{min-max}$=-2.54-0.22; Soay sheep: $E_{min-max}$=0.00-0.56, $SSD_{min-max}$=-0.22-0.40; Tammar wallaby: $E_{min-max}$=0.00-0.55, $SSD_{min-max}$=-0.64-0.34; Verreaux's sifaka: $E_{min-max}$=0.00-0.60, $SSD_{min-max}$=-2.64-1.34; White faced capuchin monkey: $E_{min-max}$=0.00-0.66, $SSD_{min-max}$=-2.66-1.21.¶

Supplementary material – Data available in COMADRE Version 3.0.0 and results from Step 1 of the framework

Table S1. The metadata used and the respective results presented in the main text. The first four columns represent the information from where Matrix Populations Models (MPMs) were extract precisely as presented in COMADRE 3.0.0.

Species	**Common name**	**Species (COMADRE)**	**Order**	**# matrices**	λ_1	λ_s	$\Sigma E^{S^\sigma}_{a_{ij}}$	$\Sigma E^{S^\sigma}_{a_{ij}}$ **(SE)**
Homo sapiens sapiens	Human	Homo_sapiens_subsp._sapiens	Primates	26	1.063707	1.061537	-2.24E-03	3.15E-04
Alces alces	Moose	Alces_alces	Artiodactyla	14	1.205368	1.205161	-6.69E-04	8.42E-05
Antechinus agilis	Agile antechinus	Antechinus_agilis	Dasyuromorphia	3	0.931076	0.885919	-1.11E-01	1.62E-03
Bos primigenius	Cattle	Bos_primigenius	Artiodactyla	8	1.002505	1.000493	-2.83E-03	2.96E-04
Brachyteles hypoxanthus	Northern muriqui	Brachyteles_hypoxanthus	Primates	25	1.05122	1.051273	-5.31E-05	2.09E-05
Callospermophilus lateralis	Golden-mantled ground squirrel	Callospermophilus_lateralis	Rodentia	18	2.052345	1.970253	-6.68E-02	8.72E-03
Cebus capucinus	White faced capuchin monkey	Cebus_capucinus	Primates	22	1.020887	1.020868	-2.04E-04	4.75E-05
Cercopithecus mitis	Blue monkey	Cercopithecus_mitis	Primates	28	1.036082	1.036075	-4.43E-05	1.18E-05

Deleted: in step 1 of our framework

Deleted: 2

Deleted: 1

Deleted: Column titles differ from the database as “SpeciesAuthorComadre” is equivalent to “SpeciesAuthor” and “SpeciesName” is equivalent to “SpeciesAccepted” in COMADRE 3.0.0. The remaining columns present the results of step 1, where we present the raw values o a, their respective standard deviation, the stochastic population growth rate λ_s, and the number of available matrices (# matrices).

Cervus canadensis subsp. nelsoni	Rocky Mountain elk	Cervus_canadensis_subsp._nelsoni	Artiodactyla	10	1.107412	1.099838	-8.55E-03	1.09E-03
Eumetopias jubatus	Northern sea lion; Steller sea lion	Eumetopias_jubatus	Carnivora	4	0.904383	0.902155	-4.52E-03	2.44E-04
Felis catus	Feral cat	Felis_catus	Carnivora	3	1.948471	1.8259	-1.34E-01	1.89E-03
Gorilla beringei	Mountain gorilla	Gorilla_beringei	Primates	41	1.026827	1.02682	-1.28E-05	1.32E-05
Hippocamelus bisulcus	Huemul deer	Hippocamelus_bisulcus	Artiodactyla	3	0.996197	0.995462	-1.80E-03	1.09E-04
Leopardus pardalis	Ocelot	Leopardus_pardalis	Carnivora	4	1.086146	1.086122	-2.94E-04	3.89E-05
Lepus americanus	Snowshoe hare	Lepus_americanus	Lagomorpha	5	0.811904	0.707678	-2.62E-01	2.33E-02
Lycaon pictus	African wild dog	Lycaon_pictus	Carnivora	3	1.500429	1.430517	-9.70E-02	9.91E-04
Macaca mulatta	Rhesus macaque	Macaca_mulatta_3	Primates	24	1.127496	1.12735	-3.84E-04	6.83E-05
Macropus eugenii	Tammar wallaby	Macropus_eugenii	Diprotodontia	15	0.981097	0.970794	-1.43E-02	1.62E-03
Marmota flaviventris	Yellow-bellied marmot	Marmota_flaviventris_2	Rodentia	8	0.89031	0.886098	-8.80E-03	6.98E-04
Marmota flaviventris	Yellow-bellied marmot	Marmota_flaviventris_3	Rodentia	8	0.920541	0.916392	-7.00E-03	7.04E-04

Microtus oeconomus	Root vole	Microtus_oeconomus	Rodentia	28	1.027531	1.027095	-5.60E-04	1.06E-04	
Mustela erminea	Stoat	Mustela_erminea	Carnivora	4	1.258462	1.074391	-3.10E-01	1.62E-02	
Orcinus orca	Killer whale	Orcinus_orca_2	Cetacea	50	0.998658	0.998351	-4.72E-04	1.53E-04	
Ovis aries	Soay sheep	Ovis_aries_2	Artiodactyla	6	1.09877	1.080656	-3.45E-02	2.96E-03	
Pan troglodytes subsp. schweinfurthii	Eastern chimpanzee	Pan_troglodytes_subsp._schweinfurthii	Primates	45	0.982286	0.982191	-1.94E-04	5.06E-05	
Papio cynocephalus	Olive baboon	Papio_cynocephalus	Primates	37	1.053872	1.053789	-2.41E-04	6.97E-05	
Peromyscus maniculatus	Deer mouse	Peromyscus_maniculatus_2	Rodentia	4	1.10686	1.101117	-9.41E-03	6.88E-04	
Phascolarctos cinereus	Koala	Phascolarctos_cinereus_2	Diprotodontia	4	1.064011	1.062744	-2.53E-03	2.16E-04	
Phocarctos hookeri	New Zealand sea lion	Phocarctos_hookeri	Carnivora	16	1.023016	1.020083	-3.56E-03	4.15E-04	
Propithecus verreauxi	Verreaux's sifaka	Propithecus_verreauxi	Primates	24	0.985592	0.985399	-3.06E-04	6.29E-05	
Rattus fuscipes	Bush rat	Rattus_fuscipes	Rodentia	3	1.304662	1.188931	-2.45E-01	4.29E-03	
Urocitellus armatus	Uinta ground squirrel	Spermophilus_armatus	Rodentia	6	1.125011	1.113416	-1.73E-02	1.68E-03	

Urocitellus armatus	Uinta ground squirrel	Spermophilus_armatus_2	Rodentia	6	1.094693	1.084304	-1.47E-02	1.56E-03
Urocitellus columbianus	Columbian ground squirrel	Spermophilus_columbianus	Rodentia	6	1.008949	0.984575	-3.80E-02	3.26E-03
Urocitellus columbianus	Columbian ground squirrel	Spermophilus_columbianus_3	Rodentia	6	1.200353	1.197473	-3.38E-03	6.96E-04
Ursus americanus subsp. floridanus	Florida black bear	Ursus_americanus_subsp._floridanus	Carnivora	4	1.01989	1.018094	-3.68E-03	3.97E-04
Ursus arctos subsp. horribilis	Grizzly bear	Ursus_arctos_subsp._horribilis_5	Carnivora	7	1.025712	1.024785	-1.38E-03	1.26E-04
Ursus maritimus	Polar bear	Ursus_maritimus_2	Carnivora	5	0.940646	0.931697	-1.91E-02	9.23E-04
Brachyteles hypoxanthus	Northern muriqui	Brachyteles_hypoxanthus_2	Primates	25	1.110953	1.110983	1.22E-05	5.05E-06
Cebus capucinus	White-faced capuchin monkey	Cebus_capucinus_2	Primates	22	1.059311	1.059248	-1.03E-04	2.85E-05
Chlorocebus aethiops	Vervet	Chlorocebus_aethiops_2	Primates	8	1.187136	1.148862	-8.03E-02	1.31E-02
Erythrocebus patas	Patas monkey	Erythrocebus_patas	Primates	9	1.127974	1.092178	-5.21E-02	5.38E-03
Gorilla beringei subsp. beringei	Mountain gorilla	Gorilla_beringei_subsp._beringei	Primates	41	1.052588	1.05255	-6.81E-05	1.11E-05

Table S2. The species-specific scales for the elasticity of λ_1 to changes in demographic processes and for the self-second derivatives of λ_1 with respect to demographic processes for the 16 mammal species studied.

Figure 3 reference	Species common name	E_{min}=elasticity minimum value	E_{max}=elasticity maximum value	SSD_{min}=self-second derivative minimum value	SSD_{max}=self-second derivative maximum value
A	Blue monkey	0	0.52	-1.25	1.27
B	Columbian ground squirrel	0	0.23	-1.48	0.01
C	Eastern chimpanzee	0	0.60	-4.39	2.59
D	Human	0	0.18	-0.15	0.08
E	Killer whale	0	0.55	-5.72	3.43
F	Moose	0	0.55	-0.66	0.36
G	Mountain gorilla	0	0.81	-1.46	0.28
H	Northern muriqui	0	0.72	-1.17	0.35
I	Olive baboon	0	0.54	-0.57	1.13
J	Polar bear	0	0.26	-0.73	0.54
K	Rhesus macaque	0	0.51	-0.54	0.71
L	Root vole	0	0.86	-2.54	0.22
M	Soay sheep	0	0.56	-0.22	0.40
N	Tammar wallaby	0	0.55	-0.64	0.34
O	Verreaux's sifaka	0	0.60	-2.64	1.34
P	White faced capuchin monkey	0	0.66	-2.66	1.21

A unified framework to quantify demographic buffering in natural populations

A manuscript in preparation for submission to ECOLOGY LETTERS
Type of article: METHOD

Gabriel Silva Santos [1,2*], Samuel J L Gascoigne[3*], André Tavares Corrêa Dias[4], Maja Kajin [3,5**♦], Roberto Salguero-Gómez[3♦]

1 National Institute of the Atlantic Forest (INMA), 29650-000, Santa Teresa, Espírito Santo, Brazil. ssantos.gabriel@gmail.com
2 Department of Ecology, Graduate Program in Ecology and Evolution, Rio de Janeiro State University, 524 São Francisco Xavier Street, 20550-900, Maracanã, Rio de Janeiro, Brazil
3 Department of Biology, University of Oxford, South Parks Road, OX1 3RB, Oxford, UK. samuel.gascoigne@pmb.ox.ac.uk, rob.salguero@biology.ox.ac.uk, maja.kajin@biology.ox.ac.uk
4 Department of Ecology, Institute of Biology, Universidade Federal do Rio de Janeiro, Avenida Carlos Chagas Filho 373, 21941-590 Rio de Janeiro, RJ, Brazil. atcdias@gmail.com
5 Department of Biology, Biotechnical Faculty, University of Ljubljana, Večna pot 111, 1000 Ljubljana, Slovenia

[*] Shared first authorship
[**] Corresponding author
[♦] Shared senior authorship

AUTHOR CONTRIBUTIONS: GSS developed the initial concept, performed the statistical analyses, and contributed to the first draft of the manuscript. SJLG developed the initial concept, contributed to the first draft and all other versions of the manuscript, and generated final figures. ATCD co-advised the project and contributed significantly to final versions of the manuscript. MK developed and managed the project, contributed to the first draft and all other versions of the manuscript, and generated final figures. RSG developed and managed the project and contributed to the first draft and all other versions of the manuscript. All authors made substantial contributions to editing the manuscript and further refining ideas and interpretations.

RUNNING TITLE: Demographic buffering framework (32/45 characters)

KEYWORDS: COMADRE Animal Matrix Database, elasticity, life-history evolution, natural selection, second-order derivative, sensitivity, stochasticity, variance.

NUMBER OF WORDS: Abstract – 143/150 words, main text (excluding abstract, acknowledgements, references, table, and figure legends) – 4966/5000 words

NUMBER OF REFERENCES: 60

NUMBER OF TABLES: 1 (in Supplementary Material)

NUMBER OF FIGURES: 3

Abstract (143/150 words)

The Demographic Buffering Hypothesis (DBH) predicts that natural selection reduces the temporal fluctuations in demographic processes (such as survival, development, and reproduction), due to their negative impacts on population dynamics. However, a comprehensive approach that allows for the examination of demographic buffering patterns across multiple species is still lacking. Here, we propose a three-step framework aimed at quantifying demographic buffering. Firstly, we categorize species along a continuum of variance based on the sums of stochastic elasticities. Secondly, we examine the linear selection gradients, followed by the examination of nonlinear selection gradients as the third step. With these three steps, our framework overcomes existing limitations of conventional approaches to quantify demographic buffering, allows for multi-species comparisons, and offers insight into the evolutionary forces that shape demographic buffering. We apply this framework to mammal species and discuss both the advantages and potential of our framework.

Environmental stochasticity shapes organisms' life histories (Bonsall & Klug 2011). Nonetheless, how organisms will cope with the increasing variation in environmental conditions (Boyce *et al.* 2006; Morris *et al.* 2008) remains an intriguing ecological and evolutionary question (Sutherland *et al.* 2013). Evolutionary demography provides diverse explanations for how evolutionary processes shape demographic responses to environmental stochasticity (Charlesworth 1994; Healy *et al.* 2019; Hilde *et al.* 2020; Pfister 1998; Tuljapurkar *et al.* 2009). The long-term stochastic population growth rate, expressed as the geometric mean of annual growth rates (Tuljapurkar 1982), forms the basis of the Demographic Buffering Hypothesis (DBH) (Morris & Doak 2004; Pélabon *et al.* 2020).

Increasing the geometric mean of λ corresponds to a rise in the long-term stochastic population growth rate (λ_s, hereafter). Conversely, higher variance in λ reduces λ_s (Morris & Doak 2004; Tuljapurkar 1982), impacting population persistence. The DBH predicts that life histories are under selection pressure to minimise the negative impacts of environmental variation by constraining the temporal variance of those demographic processes (*e.g.*, survival, development, reproduction) to which population growth rate (*i.e.*, fitness) is most sensitive to (Gaillard & Yoccoz 2003; Pfister 1998). The *demographic pattern* operating the DBH, *i.e.,* demographic buffering, describes the selection-driven constraint on the temporal variance of the most impacting demographic processes for the population growth rate (Hilde *et al.* 2020; Morris & Doak 2004; Pfister 1998). Here, we focus on the latter - on the emerging pattern of demographic buffering in different animal life histories – rather than on the DBH itself.

A unified approach to unambiguously quantify demographic buffering is still missing. Indeed, identifying demographic buffering remains challenging (Doak *et al.* 2005; Morris & Doak 2004) for several reasons, one of them being different interpretation of results from correlational analyses (*e.g.*, as in Pfister, 1998). Some authors rank species' life histories on a continuum from buffered to labile using the correlation coefficient (Spearman's correlation ρ), where negative values indicate buffering (McDonald *et al.* 2017). Alternatively, the absence of statistical support for buffering may suggest a preference for demographic variance to track environmental conditions, known as the Demographic Lability Hypothesis (DLH) (Hilde *et al.* 2020; Jäkäläniemi *et al.* 2013; Koons *et al.* 2009; Reed & Slade 2012). However, increased temporal variance alone is not enough to constitute demographic lability; it must also result in significant changes in the mean value of the demographic process (Le Coeur *et al.* 2022).

Another obstacle to achieving generalization across species' populations regarding demographic buffering is the typical hierarchical level of examination. Some studies focus on characteristics drawn from the *entire population model* (*between-populations level*) (McDonald *et al.* 2017; Reed & Slade 2012). At this level, a life history is considered demographically buffered if key demographic processes have low temporal variance (Le Coeur *et al.* 2022; Hilde *et al.* 2020; Morris & Doak 2004; Pfister 1998). However, to fully grasp how and why demographic buffering occurs, and how patterns might change in response to the environment, we must also consider characteristics at the level of separate *components of population model* (*within-populations level*). Within a population, one demographic process may be buffered while another may be labile (Barraquand & Yoccoz 2013; Jongejans *et al.* 2010; Koons *et al.* 2009). Thus far, studies have focused on either one of the hierarchical levels, however, for a mechanistic understanding of how environmental stochasticity shapes life histories, both between- and within-population levels need to be addressed at the same time.

The complexity of examining the underlying mechanisms of demographic buffering presents additional challenge. Evidence suggests buffering in both long-lived (Doak *et al.* 2005; Gaillard & Yoccoz 2003; McDonald *et al.* 2017; Pfister 1998; Rotella *et al.* 2012), and short-lived species (Ferreira *et al.* 2013; Pfister 1998; Reed & Slade 2012). However, these patterns alone do not fully reveal how life histories are shaped by natural selection. First-order effects, such as elasticities, show how variation in demographic processes affects population growth rate, while second-order effects reveal sensitivity to autocorrelation (Tuljapurkar 1990). Integrating both allows a better understanding of fitness function behaviour near local maxima and minima.

In linear relationships between fitness and demographic processes, second-order derivatives of population growth rate are zero, indicating natural selection acts on mean values (Shyu & Caswell 2014). Nonzero second derivatives suggest nonlinear relationships between fitness and a demographic process, revealing additional aspects of selection on the variances and covariances of demographic processes (Brodie *et al.* 1995; Carslake *et al.* 2008; Shyu & Caswell 2014). The sign (>0, =0, <0) of the self-second derivative of λ with respect to demographic processes determines the type of selection. Negative values describe concave (∩-shaped) selection, reducing temporal variance (Caswell 1996, 2001; Shyu & Caswell 2014) and thus, indicating demographic buffering. Positive values indicate convex (∪-shaped) selection, amplifying variance (Caswell 1996, 2001; Shyu & Caswell 2014) and potentially indicating demographic lability (Le Coeur *et al.* 2022; Koons *et al.* 2009). To confirm lability, increased variance must shift the mean value of a demographic process, outweighing its negative effect on population growth rate (Le Coeur *et al.* 2022).

The diverse demographic strategies across species result from evolutionary processes shaping variance in demographic processes over time. Integrating demographic buffering into the context of linear and nonlinear selection enables quantification of the evolutionary forces driving these patterns, shedding light on how environmental variability shapes existing and novel strategies. Despite this, a unified approach to characterize demographic buffering signatures remains lacking.

Here, we introduce a framework to quantify demographic buffering, offering insight into temporal variance patterns affected by environmental stochasticity. This framework involves categorizing species or populations along a variance continuum based on the degree of natural selection buffering key demographic processes, with three steps incorporating well-known methods applied to stage-structured demographic data (*e.g.*, matrix population models [Caswell 2001]; integral projection models [(Easterling et al. 2000]). First, species or populations are positioned on the continuum to assess cumulative effects of variance in demographic processes on population growth rate. Second, linear selection forces within the life cycle of each species or population are investigated at the within-populations level. Third, non-linear selection forces within the life cycle are explored at the within-populations level. These steps provide quantitative evidence of demographic buffering occurrence. Lastly, further analyses are proposed to identify demographic lability.

To demonstrate the applicability of our framework, we apply it to 40 populations of 34 mammal species sourced from the COMADRE database (Salguero-Gómez *et al.* 2016). We showcase how the framework can provide valuable insights into the patterns of demographic buffering across species. The framework offers novel, detailed insights into the selection pressures that act within species' life cycles, thus allowing for a thorough understanding of the evolutionary selection forces that shape the patterns of demographic buffering across species. Beyond providing a quantitative, systematic toolset to quantify buffering through three steps, we have also offered an alternative fourth step that briefly outlines how to evidence lability.

A unified framework to assess evidence of demographic buffering

The evidence for demographic buffering has been mainly assessed using Matrix Population Models (MPM; Pfister 1998; Rotella et al. 2012)). However, Integral Projection Models

(IPM; Rodríguez-Caro et al. 2020; Wang et al. 2023) can be equally applied for identifying the demographic buffering signatures. Both MPMs and IPMs are stage-structured, discrete-time demographic models (Caswell 2001; Ellner *et al.* 2016). For simplicity, here we focus on MPMs, but note that the same approaches are as equally applicable to IPMs (Doak *et al.* 2021; Griffith 2017). Throughout this manuscript, we refer to demographic processes as both matrix entries a_{ij} (*i.e.,* upper-level parameters) and the vital rates that underline the matrix elements (*i.e.,* lower-level parameters), and note that their conversion is straightforward and described elsewhere (Franco & Silvertown 2004). The framework operates on three steps.

In the first step of our framework, we calculate the impact of variation in demographic processes on the stochastic growth rate, λ_s, known as stochastic elasticities E_{ij}^{S} (Haridas & Tuljapurkar 2005) (Figure 1A). This calculation separates the sum of all stochastic elasticities ($\Sigma E_{a_{ij}}^{S}$) into two components: one for assessing how temporal variance affects λ_s ($\Sigma E_{a_{ij}}^{S\sigma}$), and the other for assessing the impact of mean values of demographic processes on λ_s, ($\Sigma E_{a_{ij}}^{S\mu}$) (Haridas & Tuljapurkar 2005). A higher absolute value of the sum of stochastic elasticity with respect to variance ($\Sigma E_{a_{ij}}^{S\sigma}$), indicates greater sensitivity of λ_s to changes in demographic process variance, suggesting absence of buffering. Conversely, a lower absolute value suggests demographic buffering, where λ_s is less sensitive to such perturbations (Haridas & Tuljapurkar 2005; Tuljapurkar *et al.* 2003) (Fig. 1A). This step places species or populations along a continuum based on variance in demographic processes, with unconstrained variance on the left (possibly unbuffered) and constrained variance on the right (possibly buffered). However, unconstrained variance does not necessarily imply demographic lability, defined as an increase in *mean value* of a demographic process in response to improved environmental conditions (Le Coeur *et al.* 2022). By examining $\Sigma E_{a_{ij}}^{S\sigma}$, we can assess changes in the contribution of demographic process variance to λ_s, while mean values remain unchanged.

Although this step provides insight into how environmental variation affects λ_s, it does not consider covariances between demographic processes and serial correlations, which are important for fully diagnosing buffering (Haridas & Tuljapurkar 2005). Instead, our approach focuses on second derivatives of population growth rate with respect to demographic processes to elucidate selection's impact on variance (step 3, below).

Steps 2 and 3 of the framework delve into within-population analysis. After step 1 positions species or populations along the variance continuum for λ_s, each life cycle undergoes scrutiny. Step 2 (Fig. 1B) involves calculating the partial derivatives of λ_t concerning all matrix elements of the MPM. This step reveals how each demographic process influences λ_t. In step 3, one evaluates nonlinear selection patterns using self-second derivatives of λ_t for each demographic process (Fig. 1C). This step unveils potential nonlinear selection pressures on demographic processes, crucial for understanding their evolutionary dynamics. Failure to consider these evolutionary processes in step 1 may lead to misinterpretation of patterns (*e.g.*, Lawler et al. 2009).

Steps 2 and 3 of the framework analyse averaged selection pressures over time periods. They offer insights into how perturbations in demographic processes affect λ_t, obtained by averaging sequential Matrix Population Models (MPMs) across the study duration. Therefore, they enhance our understanding of selection pressures' role in shaping demographic patterns across various species.

In step 3, it is important to note that the importance of demographic processes shifts with changing environments (Stearns 1992). This dynamic sensitivity of λ_t to specific processes (Kroon *et al.* 2000), indicated by self-second derivatives, helps pinpoint which processes are most likely to induce changes. For instance, in the hypothetical wolf species (Fig. 1), a decline in reproduction among third age-class individuals (matrix element $a_{1,3}$) would heighten sensitivity to that process. Consequently, with increased environmental variability, the key demographic process might change from remaining in the fourth age class (matrix element $a_{4,4}$, Fig. 1B) to reproduction of the third age-class (matrix element $a_{1,3}$, Fig. 1C).

Combining the three steps of our framework allows for a quantitative identification of buffering. Steps 2 and 3 offer key insights as to *why* a given species or population is placed on either the buffered or the non-buffered end of the variance continuum. A clear and unequivocal evidence for support towards buffering consists of: (1) a species or population being positioned near the 0 end of the continuum (the right-hand side) in step 1; (2) this species' or populations' life cycle having one or more demographic processes with highest elasticity values in step 2; and (3) the same demographic process displaying the highest elasticity in step 2 with negative self-second derivative values in step 3. In this sense, Figure 1B shows that, for the chosen population of a hypothetical wolf species, the most important demographic process is remaining in the fourth stage (MPM element $a_{4,4}$), as this demographic process results in highest elasticity value (Fig. 1B yellow square). However, Fig. 1C reveals that $a_{4,4}$ is under little selection pressure for variance reduction. Thus, there is no clear evidence of buffering from the third step of the framework (*i.e.,* no concave selection forces). This way, the lack of concave selection forces on the key demographic process within wolf's life cycle explains why this species is placed on the left-hand side of the variance continuum (Fig. 1A).

Although not our primary goal here, we briefly introduce said step 4. To establish compelling evidence of lability, it is essential to fulfil several further criteria. First, sufficient data across various environments (over time or space) are required to construct reaction norms that depict how a demographic process responds to environmental changes (Koons *et al.* 2009; Morris *et al.* 2008), which can be challenging in terms of sufficient and high-quality demographic and environmental data. Second, non-linear relationships between demographic processes and the environment must be established based on the demographic process-environment reaction norms. Lastly, demographic processes where an increase in the mean value has a stronger positive impact on population growth rate than the detrimental effect of increased variance needs to be identified. The latter condition is only met when the demographic process-environment reaction norm takes a convex shape (resembling a "U" shape), as described by Koons et al. (2009) and Morris et al. (2008). However, a study by Barraquand & Yoccoz (2013) reported diverging results in this regard. Importantly, we note that more likely than previously thought (*e.g.*, Pfister 1998), species do not exist as purely buffering or labile, but that within populations, some vital rates may be buffered, other labile, and others insensitive to the environment (*e.g.*, Doak et al. 2005). Deciphering generality in this likely complex pattern should attract much research attention going forward, in our opinion.

Demographic buffering in mammals: a case study using the unified framework

We demonstrate the performance of our framework using 44 MPMs from 34 mammal species. Mammals are of special interest here for two reasons: (1) mammalian life histories have been well studied (Bielby *et al.* 2007; Gillespie 1977; Jones 2011; Stearns 1983); and (2) some of their populations have already been assessed in terms of buffering, particularly for primates (Campos *et al.* 2017; Morris *et al.* 2008, 2011; Reed & Slade 2012; Rotella *et al.* 2012). Together, the well-studied life histories and previous information about the occurrence of buffering in mammals provide the necessary information to make accurate predictions and validate the performance of the proposed framework.

We used Matrix Population Models from 40 out of 139 studies with mammals available in the COMADRE database v.3.0.0 (Salguero-Gómez *et al.* 2016). These 40 populations encompass 34 species from eight taxonomic orders. We included these MPMs in our analyses because they provide values of demographic processes (a_{ij}) for three or more contiguous time periods, thus allowing us to obtain the stochastic elasticity of each a_{ij}. Although we are aware that not all possible temporal variation in demographic processes may have been expressed within this period, we assumed three or more transitions are enough to provide sufficient variation for population comparison. At least three contiguous time periods - a common selection criteria in comparative studies of stochastic demography (Compagnoni *et al.* 2023) - also allowed to test and showcase our framework. Fortunately, several long-lived species, characterized by low variation in their demographic processes, were studied for a long time (*e.g.,* some primates in our dataset have been studied for over 20 years – Morris *et al.* 2011). We removed the populations where either only survival or only reproduction rates were reported, because of the impossibility to calculate the stochastic growth rate. A detailed description of the analysed data and their original sources are available in supplementary material (Supplementary Material, Table S1).

Homo sapiens was included in our analyses because it is the only mammalian species in which second-order derivatives have been applied (Caswell 1996). Therefore, *Homo sapiens* provides an ideal basis for comparisons among species. The data for *Homo sapiens* were gathered from 26 modern populations located in various cities, allowing us to construct a spatiotemporal variance. It is important to note that in this case, we are not working with true temporal variance but rather a variance that encompasses both spatial and temporal aspects.

For steps 2 and 3 of our framework, we utilized a subset of 16 populations (including *Homo sapiens*) whose population projection matrices (MPMs) were organized by age. We specifically selected these populations because their life cycles can be summarized by two main demographic processes: survival and contribution to recruitment of new individuals. The contribution to recruitment can be interpreted as either the mean reproductive output for each age class or an approximation thereof, depending on how the matrices are structured

(Ebert 1999). One advantage of using such matrices is that they encompass only two types of demographic processes, namely survival and recruitment, eliminating the need to account for multiple transitions between different life stages.

To perform the step 1 of our framework and obtain the $\Sigma E_{a_{ij}}^{S^{\sigma}}$ (and $\Sigma E_{a_{ij}}^{S^{\mu}}$), we followed Tuljapurkar et al. (2003) and Haridas & Tuljapurkar (2005). To perform step 2 of our framework, we calculated the deterministic elasticities of each demographic process extracted using the *popbio* package. All analyses were performed using R version 3.5.1 (R Core team, 2018). Finally, to perform the step 3 of our framework the self-second derivatives were adapted from *demogR* (Jones 2007) following (Caswell 1996) and applied for the mean MPM.

Results

We ranked 40 populations from the 34 identified mammal species according to the cumulative impact of variation in demographic processes on λ_s using the step 1 of our framework (Fig. 2). Additional information (including standard deviations of the elasticity estimates and number of matrices available) is provided in the supplementary material (Table S1). Most of the analysed orders were placed on the low-variance end of the variance continuum (Fig. 2). The smallest contributions of variation in demographic processes (*i.e.,* maximum value of $\Sigma E_{a_{ij}}^{S^{\sigma}}$, note that $\Sigma E_{a_{ij}}^{S^{\sigma}}$ ranges from 0 to -1), suggesting more buffered populations, were assigned to Primates: northern muriqui (*Brachyteles hyphoxantus*, $\Sigma E_{a_{ij}}^{S^{\sigma}} = -0.09 \times 10^{-4} \pm 0.12 \times 10^{-4}$) (mean ± standard deviation) (Fig. 2 silhouette a), mountain gorilla (*Gorilla beringhei*, $\Sigma E_{a_{ij}}^{S^{\sigma}} = -0.24 \times 10^{-4} \pm 0.08 \times 10^{-4}$) (Fig. 2 silhouette b), followed by the blue monkey (*Cercopithecus mitis*, $\Sigma E_{a_{ij}}^{S^{\sigma}} = -0.63 \times 10^{-4} \pm 0.06 \times 10^{-4}$) (Fig. 2 silhouette c). The first non-primate species placed near the low-variance end of the continuum was the Columbian ground squirrel (*Urocitellus columbianus*, Rodentia, $\Sigma E_{a_{ij}}^{S^{\sigma}} = -0.003 \pm 0.002$) (Fig.

2 silhouette d). The species with the highest contribution of variation in demographic processes placed at the high-variance end of the continuum was the stoat (*Mustela erminea*, Carnivora, $\Sigma E^{S^{\sigma}}_{a_{ij}}$ = -0.35 ± 0.02) (Fig. 2 silhouette e). All the 14 primate populations displayed potential evidence of buffering, occupying the right-hand side of the variance continuum, with the exception of the Patas monkey (*Erythrocebus patas*, Primates, $\Sigma E^{S^{\sigma}}_{a_{ij}}$ = -0.05 ± 0.03) (Fig. 2 silhouette f). The snowshoe hare (*Lepus americanus*, Lagomorpha, $\Sigma E^{S^{\sigma}}_{a_{ij}}$ = -0.29 ± 0.16) (Fig. 2 silhouette g) and the Bush rat (*Rattus fuscipes*, Rodentia, $\Sigma E^{S^{\sigma}}_{a_{ij}}$ = -0.25 ± 0.03) (Fig. 2 silhouette h) appear on the high-variance end of the continuum.

As predicted for the steps 2 and 3, we could not observe a clear pattern in support of buffering. This finding means that the demographic processes with the highest elasticity values failed to display strongly negative self-second derivatives (Fig. 3). Particularly for majority of primates - with the lack or minor temporal variation in demographic processes - demographic processes with high elasticities had positive values for the self-second derivatives (indicated by yellow squares with white dots in Fig. 3). Examples of primate species exhibiting high elasticities and positive values for the self-second derivatives and include northern muriqui (*Brachyteles hypoxanthus*), mountain gorilla (*Gorilla beringei*), white-faced capuchin monkey (*Cebus capucinus*), rhesus monkey (*Macaca mulatta*), blue monkey (*Cercopithecus mitis*), Verreaux's sifaka (*Propithecus verreauxi*) and olive baboon (*Papio cynocephalus*) (Fig. 3). This implies that the key demographic processes influencing λ_t are not subject to selective pressure for reducing their temporal variability. However, even though the primates were positioned closer to the low-variance end of the continuum in step 1, the evidence from steps 2 and 3 does not support the occurrence of buffering in the most influential demographic processes.

The killer whale showed similar controversy between step 1 and steps 2-3 results as most primates. In step 1, the killer whale was positioned at the buffered end of the variance continuum (*Orcinus orca*, Cetacea, $\Sigma E^{S^{\sigma}}_{a_{ij}} = -0.70 \times 10^{-4} \pm 1.04 \times 10^{-5}$) (Fig. 2 silhouette not shown). However, steps 2 and 3 show that the three demographic processes in killer whale life cycle with highest elasticity values (matrix elements $a_{2,2}$, $a_{3,3}$ and $a_{4,4}$) are not under selection pressures for reducing their temporal variance, but the opposite (depicted by yellow and green squares with white dots, Fig. 3).

The only primate species exhibiting evidence of buffering in steps 2 and 3 was human. In human, demographic parameters representing survival from first to second age class (matrix element $a_{2,1}$) displayed high elasticities and negative self-second derivatives (depicted as yellow squares with black dots in Fig. 3). Evidence supporting buffering was also found in the Columbian ground squirrel (*Urocitellus columbianus*), where, similar to humans, survival from the first to the second age class (matrix element $a_{2,1}$) showed indications of selection acting to reduce $a_{2,1}$variance. Accordingly, the Columbian ground squirrel was positioned close to the buffered end of the variance continuum in step 1. Hence, the Columbian ground squirrel was the sole species with consistent evidence of buffering across all three steps of the framework.

The Soay sheep (*Ovis aries*) was the species furthest from the buffered end of the variance continuum that enabled to perform steps 2 and 3. For the Soay sheep, remaining in the third age class (matrix element $a_{3,3}$) has the major influence on λ_t and is under selection pressure to have its variance increased. The latter characteristics reveal potential conditions for lability even though the species is placed closer to the buffered end of the variance continuum.

Steps 2 and 3 illustrate the importance of examining buffering evidence on the within-populations level. These two steps of the framework identify the simultaneous acting of concave and convex selection on different demographic processes within a single life cycle. In polar bear (*Ursus maritimus*), the key demographic process (matrix element $a_{4,4}$) is under convex selection, as depicted by a yellow square with a white dot in Fig. 3. However, the demographic process with the second highest elasticity value (matrix element $a_{5,4}$) is under strong concave selection (depicted by a light green square with a black dot in Fig. 3).

By adding step 3 to the framework, another important information was accessed. The high absolute values of self-second derivatives (large dots, either black or white, Fig. 3) indicate where the sensitivity of λ_t to demographic parameters is itself prone to environmental changes. For instance, if the value of $a_{5,4}$ for polar bear increased, the sensitivity of λ_t to $a_{5,4}$ would decrease because the self-second derivative of $a_{5,4}$ is highly negative (depicted by the largest black dot in polar bear MPM). Vice versa holds for the $a_{4,4}$ demographic process, where an increase in the value of $a_{4,4}$ would increase λ_t's sensitivity to $a_{4,4}$, because the self-second derivative of $a_{5,4}$ is highly positive (depicted by the largest white dot in polar bear MPM). Thus, sensitivities (or equally elasticities) of demographic processes with high absolute values for self-second derivatives can easily change.

Discussion

In the Anthropocene, identifying and quantifying mechanisms of species responses to stochastic environments holds crucial importance. This importance is particularly tangible in the context of the unprecedented environmental changes and uncertainties that impact the dynamics and persistence of natural populations (Boyce *et al.* 2006). Correlational demographic analysis, whereby the importance of demographic processes and their temporal variability is examined (Pfister 1998), has attempted to identify how species may buffer against the negative effects of environmental stochasticity. However, these widely used approaches have important limitations (see Introduction and Hilde *et al*. 2020). One significant limitation is the issue of measurement scale concerning demographic processes (Hilde *et al.* 2020; Morris & Doak 2004). Demographic processes, such as birth rates, death rates, immigration, and emigration, operate at various temporal and spatial scales. The choice of scale at which these processes are measured can impact the outcomes of correlational demographic analysis (Bjørkvoll *et al.* 2016). Our novel framework overcomes said limitations by providing a rigorous approach to quantify demographic buffering (Hilde et al. 2020; Pfister 1998).

Evidencing demographic buffering is not straightforward. Indeed, through the analysis of stochastic population growth rate (λ_s) in our application of the framework to 44 populations of 34 species, we identify the highest density of natural populations near the buffered end of the variance continuum (step 1). However, we show that the same species then fail to exhibit signs of concave (∩-shaped) selection on the key demographic parameters when further analyses are performed averaging the variation across the duration of each study (steps 2 and 3). This finding confirms that placing the species near the buffered end of the variance continuum is *necessary* but not *sufficient* to diagnose demographic buffering. Indeed, buffering occurs when concave selection forces act on the key demographic parameter (Caswell 1996, 2001; Shyu & Caswell 2014).

Combining the three steps into a unified framework is of outmost importance. In steps 2 and 3 of the framework, we find relatively limited overall evidence of buffering in the examination of our 16 (out of 34 in step 1) studied animal species. Step 3 of our framework reveals that the role of natural selection shaping temporal variation in demographic processes is more complex than expected. Indeed, demographic processes within our study populations are often under a mix of convex and concave selection. This mix of selection patterns was already suggested by Doak *et al.* (2005). Here, only two out of 16 mammal species revealed concave selection acting on the key demographic processes (Columbian ground squirrel [*Urocitellus columbianus*], and humans, [*Homo sapiens sapiens*]). These two species were also placed near the buffered end of the variance continuum, therefore meeting all the necessary conditions to diagnose buffering. However, finding 12.5% (two out of 16) species that meet the criteria for demographic buffering is not in concordance with previous studies. Evidence of buffering has been reported across 22 ungulate species (Gaillard & Yoccoz 2003). In the one ungulate we examined, the moose (*Alces alces*), we find only partial support for buffering in adult survival, since this species is placed near the buffered end of the variance continuum in step 1 but does not show concave selection pressures on adult survival in step 2/3, as would be necessary to confirm the occurrence of buffering.

It is worth noting that a varying number of matrices per species were employed, ranging from 1 to 21, with an average of 8.1 matrices per species (as shown in Table S1). Naturally, having a greater number of matrices is preferred in such analyses. Furthermore, while the size of matrices (matrix dimensions) does not directly bias the results of our framework in any way – since steps 2 and 3 are shown for all the demographic processes independent of matrix dimension – potential implications of varying matrix dimensions should be further investigated in the future.

Our overall findings reveal varying levels of support for the notion that adult survival in long-lived species tends to be buffered. Indeed, (Gaillard *et al.* 1998) found that adult female survival varied considerably less than juvenile survival in large herbivores. This finding was also supported by further studies in ungulates and small rodents (Gaillard & Yoccoz 2003), turtles (Heppell 1998), vertebrates and plants (Pfister 1998), and more recently across nine (out of 73) species of plants (McDonald *et al.* 2017).

When placing our study species along a variance continuum (step 1), primates tend to be located on the buffered end. However, most primates displayed convex –instead of the expected concave– selection on adult survival. Similar results, where the key demographic process failed to display constrained temporal variability, have been reported for long-lived seabirds (Doherty *et al.* 2004). One explanation for the unexpected convex selection on adult survival involves trade-offs, as suggested by (Doak *et al.* 2005). When two demographic parameters are negatively correlated, the variance of population growth rate (λ) can be increased or decreased (Compagnoni *et al.* 2016; Evans & Holsinger 2012). The well-established trade-off between survival and fecundity (Roff & Fairbairn 2007; Stearns 1992) might explain the observed deviation of our results. Because variation in primate recruitment is already constrained by physiological limitations (Campos *et al.* 2017), when adult survival and recruitment are engaged in a trade-off, this trade-off might lead to our unexpected result. Correlations among demographic processes (positive and negative) inherently influence the biological limits of variance (Haridas & Tuljapurkar, 2005). This is because the magnitude of variation in a particular demographic process is constrained by (the variation of) other demographic processes that exert an influence on it. Not surprisingly, correlations among demographic processes have been shown to be strongly subjected to ecological factors (Fay *et al.* 2022). Here, future studies may benefit from deeper insights via cross-second derivatives (Caswell 1996, 2001) to investigate correlations among demographic processes.

Examining the drivers of demographic buffering has become an important piece of the ecological and evolutionary puzzle of demography. As such, quantifying buffering can help us better predict population responses to environmental variability, climate change, and direct anthropogenic disturbances (Boyce *et al.* 2006; McDonald *et al.* 2017; Pfister 1998; Vázquez *et al.* 2017). By setting demographic buffering into a broader and integrated framework, we hope to enhance comprehension and prediction of the implications of heightened environmental stochasticity on the evolution of life history traits. This understanding is crucial in mitigating the risk of extinction for the most vulnerable species.

Acknowledgements

This study was financed in part by the *Coordenação de Aperfeiçoamento de Pessoal de Nível Superior* - Brasil (CAPES) - Finance Code 001. GSS was supported by CAPES and CNPq (301343/2023-3). RS-G was supported by a NERC Independent Research Fellowship (NE/M018458/1). MK was supported by the European Commission through the Marie Skłodowska-Curie fellowship (MSCA MaxPersist #101032484) hosted by RSG.

Data availability

The demographic data used in this paper are open-access and available in the COMADRE Animal Matrix Database (https://compadre-db.org/Data/Comadre). A list of the studies and species used here is available in Supplementary Material (Table S1). The data and code supporting the results can be accessed here: https://github.com/SamuelGascoigne/Demographic_buffering_unified_framework.

References

Barraquand, F. & Yoccoz, N.G. (2013). When can environmental variability benefit population growth? Counterintuitive effects of nonlinearities in vital rates. *Theor Popul Biol*, 89, 1–11.

Bielby, J., Mace, G.M., Bininda-Emonds, O.R.P., Cardillo, M., Gittleman, J.L., Jones, K.E., *et al.* (2007). The Fast-Slow Continuum in Mammalian Life History: An Empirical Reevaluation. *Am Nat*, 169, 748–757.

Bjørkvoll, E., Lee, A.M., Grøtan, V., Saether, B.-E., Stien, A., Engen, S., *et al.* (2016). Demographic buffering of life histories? Implications of the choice of measurement scale. *Ecology*, 97, 40–47.

Bonsall, M.B. & Klug, H. (2011). The evolution of parental care in stochastic environments. *J Evol Biol*, 24, 645–655.

Boyce, M.S., Haridas, C. V., Lee, C.T., Boggs, C.L., Bruna, E.M., Coulson, T., *et al.* (2006). Demography in an increasingly variable world. *Trends Ecol Evol*, 21, 141–148.

Brodie, E.I., Moore, A. & Janzen, F. (1995). Visualizing and quantifying natural selection. *Trends Ecol Evol*, 10, 313–318.

Campos, F.A., Morris, W.F., Alberts, S.C., Altmann, J., Brockman, D.K., Cords, M., *et al.* (2017). Does climate variability influence the demography of wild primates? Evidence from long-term life-history data in seven species. *Glob Chang Biol*, 23, 4907–4921.

Carslake, D., Townley, S. & Hodgson, D.J. (2008). Nonlinearity in eigenvalue-perturbation curves of simulated population projection matrices. *Theor Popul Biol*, 73, 498–505.

Caswell, H. (1996). Second Derivatives of Population Growth Rate: Calculation and Applications. *Ecology*, 77, 870–879.

Caswell, H. (2001). *Matrix Population Models: Construction, Analysis, and Interpretation*. Sinauer Associates Inc. Publishers, Sunderland, Massachusetts, USA.

Charlesworth, B. (1994). *Evolution in age-structured populations*. second edi. Cambridge University Press.

Le Coeur, C., Yoccoz, N.G., Salguero-Gómez, R. & Vindenes, Y. (2022). Life history adaptations to fluctuating environments: Combined effects of demographic buffering and lability. *Ecol Lett*, 1–13.

Compagnoni, A., Bibian, A.J., Ochocki, B.M., Rogers, H.S., Schultz, E.L., Sneck, M.E., *et al.* (2016). The effect of demographic correlations on the stochastic population dynamics of perennial plants. *Ecol Monogr*, 86, 480–494.

Compagnoni, A., Evers, S. & Knight, T. (2023). Spatial replication can best advance our understanding of population responses to climate. *bioRxiv*, https://doi.org/10.1101/2022.06.24.497542.

Doak, D.F., Morris, W.F., Pfister, C., Kendall, B.E. & Bruna, E.M. (2005). Correctly Estimating How Environmental Stochasticity Influences Fitness and Population Growth. *Am Nat*, 166, E14–E21.

Doak, D.F., Waddle, E., Langendorf, R.E., Louthan, A.M., Isabelle Chardon, N., Dibner, R.R., *et al.* (2021). A critical comparison of integral projection and matrix projection models for demographic analysis. *Ecol Monogr*, 91, e01447.

Doherty, P.F., Schreiber, E.A., Nichols, J.D., Hines, J.E., Link, W.A., Schenk, G.A., *et al.* (2004). Testing life history predictions in a long-lived seabird: A population matrix approach with improved parameter estimation. *Oikos*, 105, 606–618.

Easterling, M.R., Ellner, S.P. & Dixon, P.M. (2000). Size-Specific Sensitivity: Applying a New Structured Population Model. *Ecology*, 81, 694–708.

Ebert, T. (1999). *Plant and animal populations: Methods in demography*. Academis Press, San Diego, CA, USA.

Ellner, S.P., Childs, D.Z. & Rees, M. (2016). *Data-driven Modelling of Structured Populations. A practical guide to the Integral Projection Model*. Lecture Notes on Mathematical Modelling in the Life Sciences. Springer International Publishing, Cham.

Evans, M.E.K. & Holsinger, K.E. (2012). Estimating covariation between vital rates : A simulation study of connected vs . separate generalized linear mixed models (GLMMs). *Theor Popul Biol*, 82, 299–306.

Fay, R., Hamel, S., van de Pol, M., Gaillard, J.M., Yoccoz, N.G., Acker, P., *et al.* (2022). Temporal correlations among demographic parameters are ubiquitous but highly variable across species. *Ecol Lett*, 25, 1640–1654.

Ferreira, M., Kajin, M., Vieira, M., Zangrandi, P., Cerqueira, R. & Gentile, R. (2013). Life history of a neotropical marsupial: Evaluating potential contributions of survival and reproduction to population growth rate. *Mamm Biol*, 78, 406–411.

Franco, M. & Silvertown, J. (2004). A comparative demography of plants based upon elasticities of vital rates. *Ecology*, 85, 531–538.

Gaillard, J.M., Festa-Bianchet, M. & Yoccoz, N.G. (1998). Population dynamics of large herbivores: Variable recruitment with constant adult survival. *Trends Ecol Evol*, 13, 58–63.

Gaillard, J.-M. & Yoccoz, N. (2003). Temporal Variation in Survival of Mammals: a Case of Environmental Canalization? *Ecology*, 84, 3294–3306.

Gillespie, J.H. (1977). Natural Selection for Variances in Offspring Numbers: A New Evolutionary Principle. *Am Nat*, 111, 1010–1014.

Griffith, A.B. (2017). Perturbation approaches for integral projection models. *Oikos*, 126, 1675–1686.

Haridas, C. V. & Tuljapurkar, S. (2005). Elasticities in variable environments: Properties and implications. *American Naturalist*, 166, 481–495.

Healy, K., Ezard, T.H.G., Jones, O.R., Salguero-Gómez, R. & Buckley, Y.M. (2019). Animal life history is shaped by the pace of life and the distribution of age-specific mortality and reproduction. *Nat Ecol Evol*, 3, 1217–1224.

Heppell, S.S. (1998). Application of Life-History Theory and Population Model Analysis to Turtle Conservation. *Copeia*, 1998, 367.

Hilde, C.H., Gamelon, M., Sæther, B.-E., Gaillard, J.-M., Yoccoz, N.G. & Pélabon, C. (2020). The Demographic Buffering Hypothesis: Evidence and Challenges. *Trends Ecol Evol*, 35, 523–538.

Jäkäläniemi, A., Ramula, S. & Tuomi, J. (2013). Variability of important vital rates challenges the demographic buffering hypothesis. *Evol Ecol*, 27, 533–545.

Jones, J.H. (2007). demogR: A Package for the Construction and Analysis of Age-structured Demographic Models in R. *J Stat Softw*, 22, 1–28.

Jones, J.H. (2011). Primates and the evolution of long, slow life histories. *Current Biology*, 21, R708–R717.

Jongejans, E., De Kroon, H., Tuljapurkar, S. & Shea, K. (2010). Plant populations track rather than buffer climate fluctuations. *Ecol Lett*, 13, 736–743.

Koons, D.N., Pavard, S., Baudisch, A. & Jessica E. Metcalf, C. (2009). Is life-history buffering or lability adaptive in stochastic environments? *Oikos*, 118, 972–980.

Kroon, H. De, Groenendael, J. Van & Ehrlen, J. (2000). Elasticities: A review of methods and model limitations. *Ecology*, 81, 607–618.

Lawler, R.R., Caswell, H., Richard, A.F., Ratsirarson, J., Dewar, R.E. & Schwartz, M. (2009). Demography of Verreaux's sifaka in a stochastic rainfall environment. *Oecologia*, 161, 491–504.

McDonald, J.L., Franco, M., Townley, S., Ezard, T.H.G., Jelbert, K. & Hodgson, D.J. (2017). Divergent demographic strategies of plants in variable environments. *Nat Ecol Evol*, 1, 0029.

Morris, W.F., Altmann, J., Brockman, D.K., Cords, M., Fedigan, L.M., Pusey, A.E., *et al.* (2011). Low Demographic Variability in Wild Primate Populations: Fitness Impacts of Variation, Covariation, and Serial Correlation in Vital Rates. *Am Nat*, 177, E14–E28.

Morris, W.F. & Doak, D.F. (2004). Buffering of Life Histories against Environmental Stochasticity: Accounting for a Spurious Correlation between the Variabilities of Vital Rates and Their Contributions to Fitness. *Am Nat*, 163, 579–590.

Morris, W.F., Pfister, C.A., Tuljapurkar, S., Haridas, C. V., Boggs, C.L., Boyce, M.S., *et al.* (2008). Longevity can buffer plant and animal populations against changing climatic variability. *Ecology*, 89, 19–25.

Pélabon, C., Hilde, C.H., Einum, S. & Gamelon, M. (2020). On the use of the coefficient of variation to quantify and compare trait variation. *Evol Lett*, 4, 180–188.

Pfister, C. (1998). Patterns of variance in stage-structured populations: Evolutionary predictions and ecological implications. *Proceedings of the National Academy of Sciences*, 95, 213–218.

Reed, A.W. & Slade, N.A. (2012). Buffering and plasticity in vital rates of oldfield rodents. *Journal of Animal Ecology*, 81, 953–959.

Rodríguez-Caro, R.C., Capdevila, P., Graciá, E., Barbosa, J.M., Giménez, A. & Salguero-Gómez, R. (2020). The demographic buffering strategy has a threshold of effectiveness to increases in environmental stochasticity. *bioRxiv*, 1–41.

Roff, D.A. & Fairbairn, D.J. (2007). The evolution of trade-offs: Where are we? *J Evol Biol*, 20, 433–447.

Rotella, J.J., Link, W.A., Chambert, T., Stauffer, G.E. & Garrott, R.A. (2012). Evaluating the demographic buffering hypothesis with vital rates estimated for Weddell seals from 30 years of mark – recapture data, 162–173.

Salguero-Gómez, R., Jones, O.R., Archer, C.R., Bein, C., de Buhr, H., Farack, C., *et al.* (2016). COMADRE: A global data base of animal demography. *Journal of Animal Ecology*, 85, 371–384.

Shyu, E. & Caswell, H. (2014). Calculating second derivatives of population growth rates for ecology and evolution. *Methods Ecol Evol*, 5, 473–482.

Stearns, S. (1992). *The Evolution of Life Histories*. Oxford University Press, New York, USA.

Stearns, S.C. (1983). The Influence of Size and Phylogeny on Patterns of Covariation among Life-History Traits in the Mammals. *Oikos*, 41, 173.

Sutherland, W.J., Freckleton, R.P., Godfray, H.C.J., Beissinger, S.R., Benton, T., Cameron, D.D., *et al.* (2013). Identification of 100 fundamental ecological questions. *Journal of Ecology*, 101, 58–67.

Tuljapurkar, S. (1990). Population Dynamics in Variable Environments. In: *Lecture notes in Biomathematics*, Lecture Notes in Biomathematics (ed. Levin, S.). Springer Berlin Heidelberg.

Tuljapurkar, S., Gaillard, J.-M. & Coulson, T. (2009). From stochastic environments to life histories and back. *Philosophical Transactions of the Royal Society B: Biological Sciences*, 364, 1499–1509.

Tuljapurkar, S., Horvitz, C.C. & Pascarella, J.B. (2003). The Many Growth Rates and Elasticities of Populations in Random Environments. *Am Nat*, 162, 489–502.

Tuljapurkar, S.D. (1982). Population dynamics in variable environments. III. Evolutionary dynamics of r-selection. *Theor Popul Biol*, 21, 141–165.

Vázquez, D.P., Gianoli, E., Morris, W.F. & Bozinovic, F. (2017). Ecological and evolutionary impacts of changing climatic variability. *Biological Reviews*, 92, 22–42.

Wang, J., Yang, X., Silva Santos, G., Ning, H., Li, T., Zhao, W., *et al.* (2023). Flexible demographic strategies promote the population persistence of a pioneer conifer tree (Pinus massoniana) in ecological restoration. *For Ecol Manage*, 529, 120727.

Figure 1

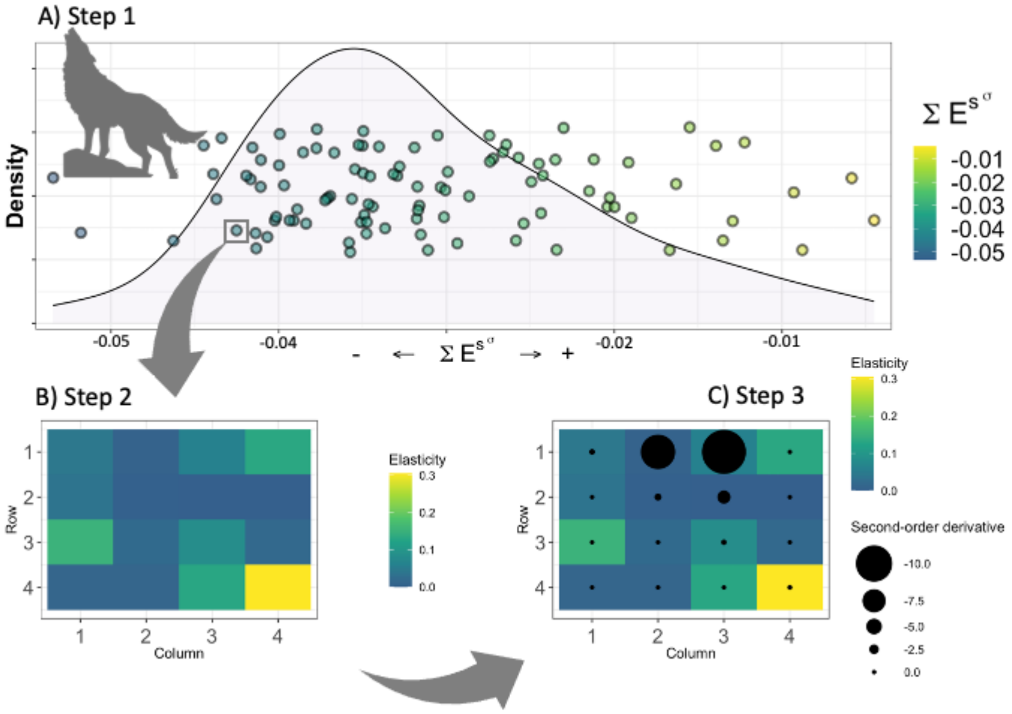
A) Step 1
Density
-0.05
-0.04
-0.02
-0.01
- ← Σ E^s^σ → +
Σ E^s^σ
-0.01
-0.02
-0.03
-0.04
-0.05
B) Step 2
Row
1
2
3
4
Column
1
2
3
4
Elasticity
0.3
0.2
0.1
0.0
C) Step 3
Row
1
2
3
4
Column
1
2
3
4
Elasticity
0.3
0.2
0.1
0.0
Second-order derivative
-10.0
-7.5
-5.0
-2.5
0.0

Figure 2

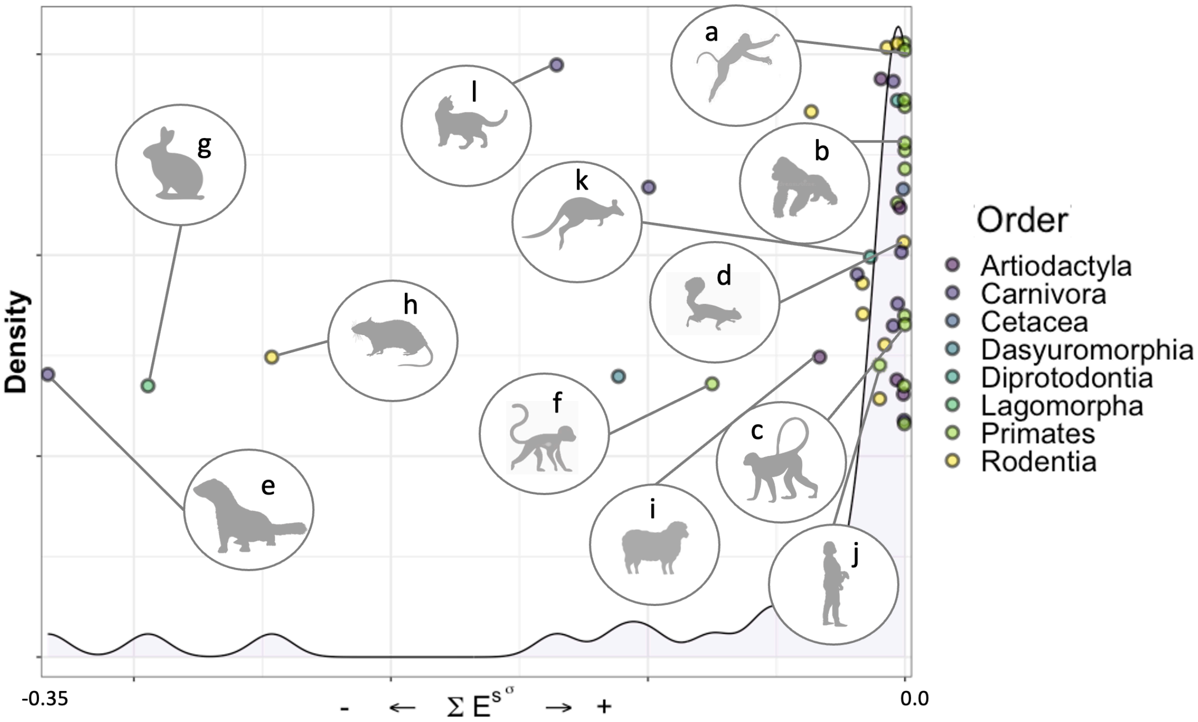

a
b
c
d
e
f
g
h
i
j
k
l
Density
-0.35
0.0
- ← Σ E$^{s^{\sigma}}$ → +
Order
● Artiodactyla
● Carnivora
● Cetacea
● Dasyuromorphia
● Diprotodontia
● Lagomorpha
● Primates
● Rodentia

636 **Figure 3**

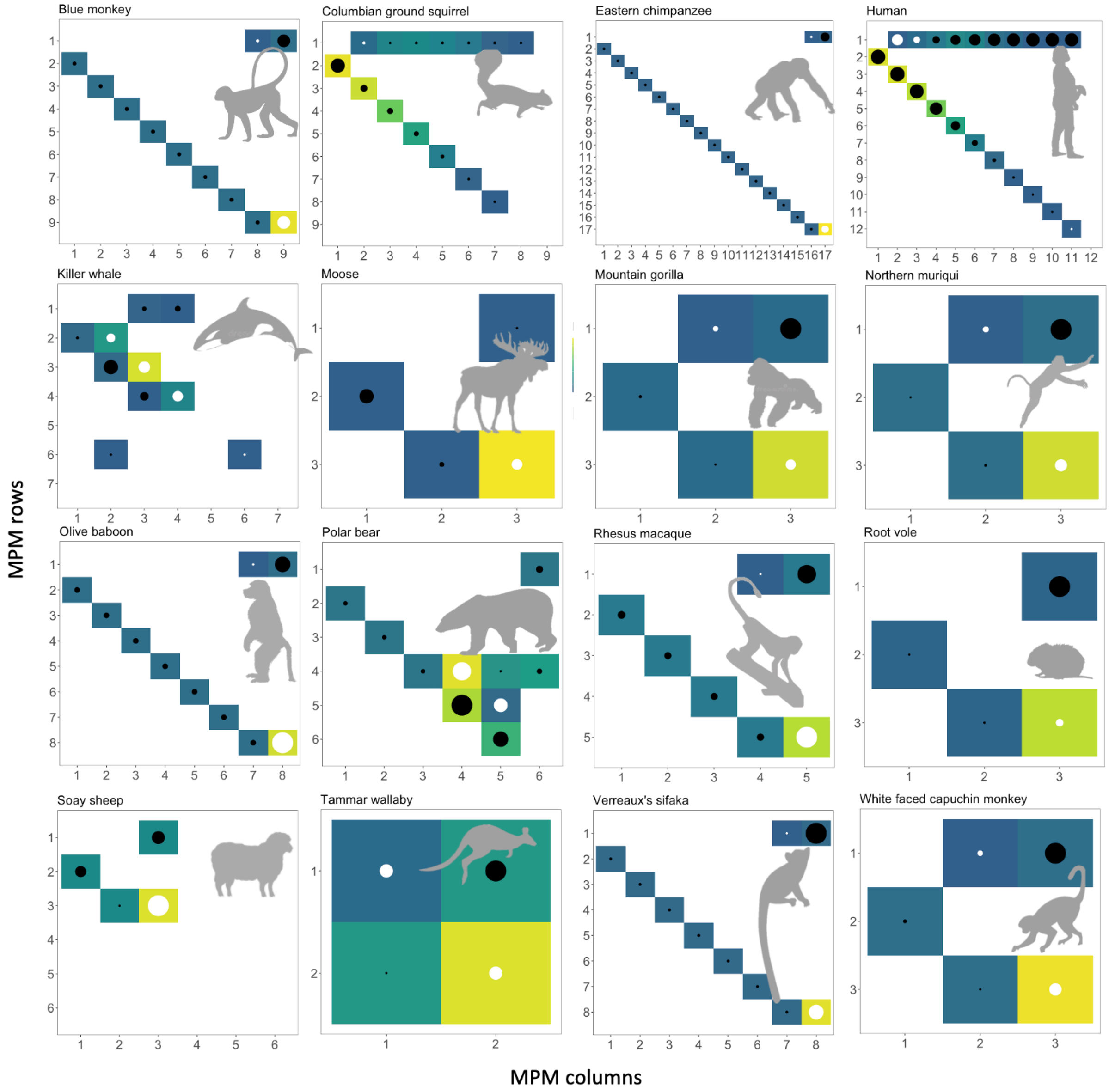

637

638

639

Figure legends

Figure 1. A three-step framework proposed to: Step 1 - allocate species and/or populations on a variance continuum (plot A, dots representing 50 hypothetical species). The variance continuum operates at the between-populations level (see text) and is represented by partitioning the sum of all the stochastic elasticities ($\Sigma E^{S}_{a_{ij}}$) into two compounds: i) sums of stochastic elasticities with respect to the variance ($\Sigma E^{S^{\sigma}}_{a_{ij}}$), and ii) sums of stochastic elasticities with respect to the mean ($\Sigma E^{S^{\mu}}_{a_{ij}}$). The first step of our framework shows the variance compound of the sums of stochastic elasticities forming a continuum where the right-hand side of the plot represents species (or populations) where a perturbation of variance in demographic processes results in weak or no impact on λ_s (yellow dots). The yellow-dotted species (or populations) can be classified as having potentially *buffered life-cycles* – based on all the demographic processes. The left-hand side of the graph represents species (or populations) where a perturbation of the variance in demographic processes results in strong impact on λ_s (blue dots). Thus, the blue-dotted species (or populations) can be classified as having potentially *unbuffered life cycles* – based on all the demographic processes. The vertical axis delineates the values of the density distribution function, indicating the number of species/populations at each value of $\Sigma E^{S^{\sigma}}_{a_{ij}}$. The placement of data points (species/populations) along the horizontal axis corresponds to their calculated values of $\Sigma E^{S^{\sigma}}_{a_{ij}}$ and is arranged linearly, while the breadth along the y-axis is solely for improved visual comprehension. Step 2 - Access the linear selection pressures for individual species or populations at within-species level (see text) (plot B). Step 2 displays the elasticities of the deterministic population growth rate (λ_t) for a hypothetical population of wolf and reveals the linear selection gradients, and which demographic processes are the most influential for λ_t. Step 3 - Access the nonlinear selection pressures at the within-species level (see text) (plot

C). In the third step self-second derivatives for the corresponding demographic processes from step 2 are displayed.

Figure 2. Results for step 1 of our framework showing the sum of stochastic elasticities with respect to the variance $\Sigma E_{a_{ij}}^{S^{\sigma}}$. The closer the $\Sigma E_{a_{ij}}^{S^{\sigma}}$ is to zero, the weaker the impact of variation in demographic processes on λ_s. The 40 populations from 34 species of mammals from the COMADRE database are ranked into the variance continuum from potentially buffered (right-hand side) to less buffered (left-hand side), since any variation in demographic processes would strongly impact λ_s. Colors represent different taxonomic orders with Primates occupying the right-hand side. Silhouettes: a) *Brachyteles hyphoxantus*, b) *Gorilla beringhei*, c) *Cercopithecus mitis*, d) *Urocitellus columbianus,* e) *Mustela erminea*, f) *Erythrocebus patas*, g) *Lepus americanus*, h) *Rattus fuscipes*, i) *Ovis aries*, j) *Homo sapiens*, k) *Macropus eugenii*, and l) *Felis catus*. The vertical axis delineates the values of the density distribution function, indicating the number of species/populations at each value of $\Sigma E_{a_{ij}}^{S^{\sigma}}$. The placement of data points (species/populations) along the horizontal axis corresponds to their calculated values of $\Sigma E_{a_{ij}}^{S^{\sigma}}$ and is arranged linearly, while the breadth along the y-axis is solely for improved visual comprehension.

Figure 3: Results from steps 2 and 3 of the proposed framework (see Fig. 2B, C). The 16 plots represent populations where the MPMs built by ages were available in the COMADRE database (see text). The color scale represents elasticity values for each of the demographic processes in the MPM, where yellow represents high and blue low elasticity values. No color means elasticity=0. Because the aim of step 2 is to identify the most impacting demographic process within each species' life cycle (the within-populations level, see text) - not to

compare the elasticity values among species - each plot has its own scale (see end of legend). The black dots represent negative self-second derivatives of λ_t - thus concave selection - and the white dots represent positive self-second derivatives of λ_t - thus convex selection. The dot sizes are scaled by the absolute value of self-second derivatives, where the smaller the dot, the closer a self-second derivative is to 0, indicting weak or no nonlinearity. Large dots indicate strong nonlinear selection forces. Scales ($E_{min\text{-}max}$=elasticity minimum and maximum value, $SSD_{min\text{-}max}$=self-second derivative minimum and maximum value): Blue monkey $E_{min\text{-}max}$=0.00-0.52, $SSD_{min\text{-}max}$=-1.25-1.27; Columbian ground squirrel: $E_{min\text{-}max}$=0.00-0.23, $SSD_{min\text{-}max}$=-1.48-0.01; Eastern chimpanzee: $E_{min\text{-}max}$=0.00-0.60, $SSD_{min\text{-}max}$=-4.39-2.59; Human: $E_{min\text{-}max}$=0.00-0.18, $SSD_{min\text{-}max}$=-0.15-0.08; Killer whale: $E_{min\text{-}max}$=0.00-0.55, $SSD_{min\text{-}max}$=-5.72-3.43; Moose: $E_{min\text{-}max}$=0.00-0.55, $SSD_{min\text{-}max}$=-0.66-0.36; Mountain gorilla: $E_{min\text{-}max}$=0.00-0.81, $SSD_{min\text{-}max}$=-1.46-0.28; Northern muriqui: $E_{min\text{-}max}$=0.00-0.72, $SSD_{min\text{-}max}$=-1.17-0.35; Olive baboon: $E_{min\text{-}max}$=0.00-0.54, $SSD_{min\text{-}max}$=-0.57-1.13; Polar bear: $E_{min\text{-}max}$=0.00-0.26, $SSD_{min\text{-}max}$=-0.73-0.54; Rhesus macaque: $E_{min\text{-}max}$=0.00-0.51, $SSD_{min\text{-}max}$=-0.54-0.71; Root vole: $E_{min\text{-}max}$=0.00-0.86, $SSD_{min\text{-}max}$=-2.54-0.22; Soay sheep: $E_{min\text{-}max}$=0.00-0.56, $SSD_{min\text{-}max}$=-0.22-0.40; Tammar wallaby: $E_{min\text{-}max}$=0.00-0.55, $SSD_{min\text{-}max}$=-0.64-0.34; White faced capuchin monkey: $E_{min\text{-}max}$=0.00-0.66, $SSD_{min\text{-}max}$=-2.66-1.21.

Supplementary material – Data available in COMADRE Version 2.0.1 and results from Step 1 of the framework

Table S1. The metadata used in step 1 of our framework and the respective results presented in the main text. The first four columns represent the information from where Matrix Populations Models (MPMs) were extract precisely as presented in COMADRE 2.0.1. Column titles differ from the database as “SpeciesAuthorComadre” is equivalent to “SpeciesAuthor” and “SpeciesName” is equivalent to “SpeciesAccepted” in COMADRE 2.0.1. The remaining columns present the results of step 1, where we present the raw values of $\Sigma E^{S^{\mu}}_{a_{ij}}$ and $\Sigma E^{S^{\sigma}}_{a_{ij}}$, their respective standard deviation, the stochastic population growth rate λ_s, and the number of available matrices (# matrices). For ByAge, “TRUE” was assigned for MPMs built by age or “FALSE” if otherwise.

SpeciesAuthorComadre	**SpeciesName**	**CommonName**	**Order**	**ΣE**
Homo_sapiens_subsp._sapiens	*Homo sapiens sapiens*	Human	Primates	1.003
Alces_alces	*Alces alces*	Moose	Artiodactyla	1.001
Antechinus_agilis	*Antechinus agilis*	Agile antechinus	Dasyuromorphia	1.111
Brachyteles_hypoxanthus	*Brachyteles hypoxanthus*	Northern muriqui	Primates	1.000
Callospermophilus_lateralis	*Callospermophilus lateralis*	Golden-mantled ground squirrel	Rodentia	1.054
Cebus_capucinus	*Cebus capucinus*	White faced capuchin monkey	Primates	1.000
Cercopithecus_mitis	*Cercopithecus mitis*	Blue monkey	Primates	1.000
Eumetopias_jubatus	*Eumetopias jubatus*	Northern sea lion; Steller sea lion	Carnivora	1.005
Felis_catus	*Felis catus*	Feral cat	Carnivora	1.136
Gorilla_beringei	*Gorilla beringei*	Mountain gorilla	Primates	1.000
Hippocamelus_bisulcus	*Hippocamelus bisulcus*	Huemul deer	Artiodactyla	1.002
Lepus_americanus	*Lepus americanus*	Snowshoe hare	Lagomorpha	1.294
Lycaon_pictus	*Lycaon pictus*	African wild dog	Carnivora	1.100
Macaca_mulatta_3	*Macaca mulatta*	Rhesus macaque	Primates	1.000
Macropus_eugenii	*Macropus eugenii*	Tammar wallaby	Diprotodontia	1.013
Marmota_flaviventris_2	*Marmota flaviventris*	Yellow-bellied marmot	Rodentia	1.007
Marmota_flaviventris_3	*Marmota flaviventris*	Yellow-bellied marmot	Rodentia	1.008
Microtus_oeconomus	*Microtus oeconomus*	Root vole	Rodentia	1.000
Mustela_erminea	*Mustela erminea*	Stoat	Carnivora	1.334
Orcinus_orca_2	*Orcinus orca*	Killer whale	Cetacea	1.001
Ovis_aries_2	*Ovis aries*	Soay sheep	Artiodactyla	1.033
Pan_troglodytes_subsp._schweinfurthii	*Pan troglodytes*	Eastern chimpanzee	Primates	1.000
Papio_cynocephalus	*Papio cynocephalus*	Olive baboon	Primates	1.000
Peromyscus_maniculatus_2	*Peromyscus maniculatus*	Deer mouse	Rodentia	1.010
Phocarctos_hookeri	*Phocarctos hookeri*	New Zealand sea lion	Carnivora	1.005
Propithecus_verreauxi	*Propithecus verreauxi*	Verreaux's sifaka	Primates	1.000

Puma_concolor_8	*Puma concolor*	Cougar	Carnivora	NA
Rattus_fuscipes	*Rattus fuscipes*	Bush rat	Rodentia	1.246
Spermophilus_armatus	*Urocitellus armatus*	Uinta ground squirrel	Rodentia	1.016
Spermophilus_armatus_2	*Urocitellus armatus*	Uinta ground squirrel	Rodentia	1.017
Spermophilus_columbianus	*Urocitellus columbianus*	Columbian ground squirrel	Rodentia	1.036
Spermophilus_columbianus_3	*Urocitellus columbianus*	Columbian ground squirrel	Rodentia	1.003
Ursus_americanus_subsp._floridanus	*Ursus americanus*	Florida black bear	Carnivora	1.003
Ursus_arctos_subsp._horribilis_5	*Ursus arctos*	Grizzly bear	Carnivora	1.001
Ursus_maritimus_2	*Ursus maritimus*	Polar bear	Carnivora	1.019
Brachyteles_hypoxanthus_2	*Brachyteles hypoxanthus*	Northern muriqui	Primates	1.000
Cebus_capucinus_2	*Cebus capucinus*	WhiteNAfaced capuchin monkey	Primates	1.000
Chlorocebus_aethiops_2	*Chlorocebus aethiops*	Vervet	Primates	1.075
Erythrocebus_patas	*Erythrocebus patas*	Patas monkey	Primates	1.051
Gorilla_beringei_subsp._beringei	*Gorilla beringei*	Mountain gorilla	Primates	1.000

A unified framework to quantify demographic buffering in natural populations

A manuscript in preparation for submission to ECOLOGY LETTERS
Type of article: METHOD

Gabriel Silva Santos [1,2*], Samuel J L Gascoigne[3*], André Tavares Corrêa Dias[4], Maja Kajin [3,5**♦], Roberto Salguero-Gómez[3♦]

1 National Institute of the Atlantic Forest (INMA), 29650-000, Santa Teresa, Espírito Santo, Brazil. ssantos.gabriel@gmail.com
2 Department of Ecology, Graduate Program in Ecology and Evolution, Rio de Janeiro State University, 524 São Francisco Xavier Street, 20550-900, Maracanã, Rio de Janeiro, Brazil
3 Department of Biology, University of Oxford, South Parks Road, OX1 3RB, Oxford, UK. samuel.gascoigne@pmb.ox.ac.uk, rob.salguero@biology.ox.ac.uk, maja.kajin@biology.ox.ac.uk
4 Department of Ecology, Institute of Biology, Universidade Federal do Rio de Janeiro, Avenida Carlos Chagas Filho 373, 21941-590 Rio de Janeiro, RJ, Brazil. atcdias@gmail.com
5 Department of Biology, Biotechnical Faculty, University of Ljubljana, Večna pot 111, 1000 Ljubljana, Slovenia

[*]Shared first authorship
[**]Corresponding author
[♦]Shared senior authorship

AUTHOR CONTRIBUTIONS: GSS developed the initial concept, performed the statistical analyses, and contributed to the first draft of the manuscript. SJLG developed the initial concept, contributed to the first draft and all other versions of the manuscript, and generated final figures. ATCD co-advised the project and contributed significantly to final versions of the manuscript. MK developed and managed the project, contributed to the first draft and all other versions of the manuscript, and generated final figures. RSG developed and managed the project and contributed to the first draft and all other versions of the manuscript. All authors made substantial contributions to editing the manuscript and further refining ideas and interpretations.

RUNNING TITLE: Demographic buffering framework (32/45 characters)

KEYWORDS: COMADRE Animal Matrix Database, elasticity, life-history evolution, natural selection, second-order derivative, sensitivity, stochasticity, variance.

NUMBER OF WORDS: Abstract – 143/150 words, main text (excluding abstract, acknowledgements, references, table, and figure legends) – 5713/5000 words

NUMBER OF REFERENCES: 57

NUMBER OF TABLES: 1 (in Supplementary Material)

NUMBER OF FIGURES: 3

Abstract (143/150 words)

The Demographic Buffering Hypothesis (DBH) predicts that natural selection reduces the temporal fluctuations in demographic processes (such as survival, development, and reproduction), due to their negative impacts on population dynamics. However, a comprehensive approach that allows for the examination of demographic buffering patterns across multiple species is still lacking. Here, we propose a three-step framework aimed at quantifying demographic buffering. Firstly, we categorize species along a continuum of variance based on the sums of stochastic elasticities. Secondly, we examine the linear selection gradients, followed by the examination of nonlinear selection gradients as the third step. With these three steps, our framework overcomes existing limitations of conventional approaches to quantify demographic buffering, allows for multi-species comparisons, and offers insight into the evolutionary forces that shape demographic buffering. We apply this framework to mammal species and discuss both the advantages and potential of our framework.

Environmental stochasticity plays a pivotal role in shaping organisms' life histories (Bonsall & Klug 2011). Nonetheless, how organisms will cope with the increasing variation in environmental conditions expected under climate change (Boyce *et al.* 2006; Morris *et al.* 2008) is one of the most intriguing questions of ecology and evolution (Sutherland *et al.* 2013). Evolutionary demography offers a wide array of explanations for the evolutionary processes that shape the diversity of demographic responses to environmental stochasticity (Charlesworth 1994; Healy *et al.* 2019; Hilde *et al.* 2020; Pfister 1998; Tuljapurkar *et al.* 2009). The Demographic Buffering Hypothesis (*DBH*, hereafter) (Morris & Doak 2004; Pélabon *et al.* 2020) is based on the fact that long-term stochastic population growth rate can be expressed in terms of the geometric mean of the annual population growth rates (Tuljapurkar 1982). As the geometric mean of λ increases, so does the long-term stochastic population growth rate (λ_s, hereafter). However, increases in variance of λ decrease λ_s (Morris & Doak 2004; Tuljapurkar 1982), and thus population persistence. This theoretical context sets the stage for the DBH. The DBH predicts that life histories are under selection pressure to minimise the negative impacts of environmental variation by constraining the temporal variance of those demographic processes (*e.g.*, survival, development, reproduction) to which population growth rate (*i.e.*, fitness) is most sensitive to (Gaillard & Yoccoz 2003; Pfister 1998). The demographic pattern operating the DBH, *i.e.,* demographic buffering, describes the selection-driven constraint on the temporal variance of the most impacting demographic processes for the population growth rate (Hilde *et al.* 2020; Morris & Doak 2004; Pfister 1998). Here, we focus on the latter - on the emerging pattern of demographic buffering in different animal life histories – rather than on the DBH itself.

A unified approach to unambiguously quantify demographic buffering is still missing. Indeed, identifying demographic buffering remains challenging (Doak *et al.* 2005; Morris & Doak 2004) for at least three reasons. First is the different interpretation of results from correlational analyses (*e.g.*, as in Pfister, 1998). Some authors have used the correlation coefficient as an index to order species' life histories in a continuum ranging from buffered (Spearman's correlation ρ = <0 between the sensitivity of λ to demographic processes and their temporal variance) to labile (ρ = >0), regardless of the fit of the linear regression to more or less scattered data (McDonald *et al.* 2017). In contrast, other researchers interpret the absence of statistical support for demographic buffering as an alternative strategy where variance in demographic process(es) is favoured to track environmental conditions (the so-called Demographic Lability Hypothesis, *DLH* (*e.g.,*Koons et al. 2009; Reed & Slade 2012; Jäkäläniemi et al. 2013; Hilde et al. 2020). However, the increased temporal variance is a necessary but not sufficient condition to constitute demographic lability – the increased temporal variance needs to lead to (often high) change in the demographic process mean value (Le Coeur *et al.* 2022).

The second obstacle to obtain generalisation across species' populations regarding demographic buffering is the hierarchical level at which this phenomenon is typically examined. Some studies base their investigations of demographic buffering on a characteristic drawn from *the entire population model* (*between-populations level*, hereafter) (McDonald *et al.* 2017; Reed & Slade 2012). At the between-populations level, a life history is referred to as demographically buffered if the most important demographic process(es) has(ve) low temporal variance (Le Coeur *et al.* 2022; Hilde *et al.* 2020; Morris & Doak 2004; Pfister 1998). However, to understand how, why, and where demographic buffering occurs – or not– and how buffering patterns might be modified in response to the environment, it is essential to also consider the characteristics of the separate *components of population model* (*within-populations level*, hereafter). Within a population, a given demographic process can be buffered against while another can be labile to the environment (Barraquand & Yoccoz 2013; Jongejans *et al.* 2010; Koons *et al.* 2009). Thus far, studies have focused on either one of the hierarchical levels, however, for a mechanistic understanding of how environmental stochasticity shapes life histories, both between- and within-population levels need to be addressed at the same time.

The third reason limiting a holistic understanding of demographic strategies in stochastic environments are the challenges inherent to examining their underlying mechanisms. Evidence for demographic buffering exists across some long-lived organisms with complex life cycles, (Doak *et al.* 2005; Gaillard & Yoccoz 2003; McDonald *et al.* 2017; Pfister 1998; Rotella *et al.* 2012), but also in short-lived species (Ferreira *et al.* 2013; Pfister 1998; Reed & Slade 2012). Importantly, these patterns of variation do not inform entirely on how the life histories were shaped by natural selection. The beforementioned patterns of variation are represented by *first-order* effects that perturbations in demographic processes cause on the population growth rate (*i.e.,* elasticities). A first order effect informs us regarding the population growth rate's sensitivity to *variation in demographic processes*. While a second-order effect of perturbations in demographic processes reveals the population growth rate's sensitivity to *autocorrelation* (Tuljapurkar 1990). Given so, integrating both, first and second-order effects of perturbations in demographic processes on the population growth rate, allows us to understand the behaviour of the fitness function at the vicinity of the local maxima and/or minima.

When the relationship between fitness and a demographic process is linear, the second-order derivatives of population growth rate with respect to demographic processes equal zero. In such cases, natural selection acts on the mean value of a demographic process (Shyu & Caswell 2014). However, nonzero second derivatives indicate a nonlinear relationship between fitness and a demographic process (either concave if <0, or convex if >0) and thus provide additional and often overlooked characteristics of selection acting on demographic processes – not only their mean values, but also their variances and covariances (Brodie *et al.* 1995; Carslake *et al.* 2008; Shyu & Caswell 2014).

The sign (*i.e.*, >0, =0, <0) of the self-second derivative of λ with respect to demographic processes determines the type of (non)linear selection acting on a demographic process. For instance, a negative self-second derivative for a given demographic process describes a concave form of selection, commonly referred to as the ∩-shaped selection (Caswell 1996, 2001; Shyu & Caswell 2014). This form of selection reduces the temporal variance in said demographic process, thereby providing evidence of demographic buffering. Conversely, a demographic process yielding a positive self-second derivative identifies a convex, or ∪-shaped selection (Caswell 1996, 2001; Shyu & Caswell 2014). Such a selection mechanism acts upon demographic processes amplifying their temporal variance, thus potentially evidencing demographic lability (Le Coeur et al. 2022; Koons et al. 2009). The evidence of lability is only potential, because to constitute demographic lability, the increased variance needs to shift the mean value of a demographic process. The shift in the mean value of a demographic process needs to overweight the negative effect of variance on the population growth rate (Le Coeur *et al.* 2022).

The rich variation in demographic strategies across the Tree of Life is a result of evolutionary processes that have shaped variance in demographic processes through time. In this context, setting demographic buffering into the adaptive landscape context of linear and nonlinear selection enables us to identify and quantify the evolutionary processes that generate said demographic patterns. In this way, one will better understand how increased variability of environmental conditions might act on the existing –and shape novel– demographic strategies. However, we still lack a unified approach to constitute the signatures of demographic buffering.

Here, we present a framework that quantifies demographic buffering. Our framework provides a rich insight into the patterns of temporal variance in demographic processes affected by environmental stochasticity. This framework involves categorizing species or populations along a variance continuum based on the extent to which key demographic processes are buffered by natural selection, thereby limiting their temporal variability. The framework consists of four steps with a mix of well-known methods applied to stage-structured demographic information (*e.g.,* matrix population models [Caswell 2001]; integral projection models [Easterling et al. 2000]). First, we position species or populations on the aforementioned continuum to assess the cumulative effect of the variance in their key demographic processes on population growth rate at the between-populations level (see below). Second, we investigate the presence of linear selection forces operating within the life cycle of each species or population at the within-populations level (below). Third, we explore the impact of non-linear selection forces acting within the life cycle of each species or population, also at the within-populations level. The combination of these three steps provides quantitative evidence for the occurrence of demographic buffering. Step four suggests the further necessary analyses to identify demographic lability.

To demonstrate the applicability of our framework, we apply it to 40 populations of 34 mammal species sourced from the COMADRE database (Salguero-Gómez *et al.* 2016). We showcase how the framework can provide valuable insights into the patterns of demographic buffering across species. The framework offers novel, detailed insights into the selection pressures that act *within* species' life cycles, thus allowing for a thorough understanding of the evolutionary selection forces that shape the patterns of demographic buffering across species. Beyond providing a quantitative, systematic toolset to quantify buffering through three steps, we have also offer an alternative fourth step that briefly outlines how to evidence lability.

A unified framework to assess evidence of demographic buffering

The evidence for demographic buffering has been mainly assessed using Matrix Population Models (MPM; Pfister 1998; Rotella et al. 2012)). However, Integral Projection Models (IPM; Rodríguez-Caro et al. 2020; Wang et al. 2023) can be equally applied for identifying the demographic buffering signatures. Both MPMs and IPMs are stage-structured, discrete-time demographic models (Caswell 2001; Ellner *et al.* 2016). For simplicity, here we focus on MPMs, but note that the same approaches are as equally applicable to IPMs (Doak *et al.* 2021; Griffith 2017). Throughout this manuscript, we refer to demographic processes as both matrix entries a_{ij} (*i.e.,* upper-level parameters) and the vital rates that underline the matrix elements (*i.e.,* lower-level parameters), and note that their conversion is straightforward and described elsewhere (Franco & Silvertown 2004). The framework operates on three steps.

The first step of our framework involves acquiring the relative impact of variation in demographic processes on the stochastic growth rate, λ_s, the so-called stochastic elasticities, E_{ij}^{S} (Haridas & Tuljapurkar 2005) (Figure 1A). The sum of all stochastic elasticities ($\Sigma E_{a_{ij}}^{S}$), can be separated into two components to assess how temporal variance and mean values of each demographic process impact λ_s. The first component represents the *sum of stochastic elasticity of* λ_s *with respect to the variance* $\Sigma E_{a_{ij}}^{S^{\sigma}}$, and the second represents the *sum of stochastic elasticity of* λ_s *with respect to the mean* $\Sigma E_{a_{ij}}^{S^{\mu}}$, where $\Sigma E_{a_{ij}}^{S} = \Sigma E_{a_{ij}}^{S^{\sigma}} + \Sigma E_{a_{ij}}^{S^{\mu}}$ (Haridas & Tuljapurkar 2005). Thus, the summation $\Sigma E_{a_{ij}}^{S^{\sigma}}$ quantifies the summed effect to which the stochastic population growth rate (λ_s) is influenced by changes in the variances of the demographic processes within the population matrix.

A higher sum of stochastic elasticity of λ_s with respect to the variance of demographic processes (*i.e.,* higher absolute value; $|\Sigma E_{a_{ij}}^{S^\sigma}|$) indicates that small changes in the variance of demographic processes would have a substantial impact on λ_s. In other words, the variance of that demographic process is not constrained by selection, indicating absence of demographic buffering. On the other hand, a lower (absolute) stochastic elasticity of λ_s with respect to the variance of a given demographic process suggests that λ_s is less sensitive to such perturbations, or, that variance of such demographic process is being constrained by natural selection, thus pointing to demographic buffering (Haridas & Tuljapurkar 2005; Tuljapurkar *et al.* 2003) (Fig. 1A).

The first step of the framework thus features the between-populations level and places species or populations alongside a continuum. Species exhibiting unconstrained variance in demographic processes (*i.e.,* possibly not buffered, Fig. 1A, blue dots) are positioned on the left-hand side of the continuum. In contrast, species with constrained variance in demographic processes (*i.e.,* possibly buffered, Fig. 1A, yellow dots) are positioned on the right-hand side of the continuum. However, the left-hand side of the continuum does not necessarily imply evidence of demographic lability. This is so because demographic lability is defined as an increase in the *mean value* of a demographic process in response to improved environmental conditions (Le Coeur *et al.* 2022). By examining $\Sigma E_{a_{ij}}^{S^\sigma}$, we can visualize an increase or decrease of the contribution that *variance* of demographic processes has on the long-term population growth rate, while the mean value of a demographic process does not change.

Step 1 of our framework examines the impacts that environmental variation has on the long-term population growth rate, λ_s (Tuljapurkar *et al.* 2003). This means that the resulting variance continuum in this step of the framework is based on how λ_s was affected by variation in the key demographic parameter across all contiguous time periods. However, Haridas & Tuljapurkar (2005) explicitly acknowledge that covariances between demographic processes and serial correlations need to be investigated to diagnose buffering entirely. Our approach does not use covariances neither serial correlation, but rather focuses on the second derivatives of the population growth rate with respect to demographic processes and elucidates how selection is acting on variance (step 3, below).

Steps 2 and 3 of the framework are conducted at the within-populations level. Once species or populations are positioned along the variance continuum regarding the summed effect of variation on λ_s, (step 1), one needs to zoom into each life cycle separately, analysing the selection pressures acting on each one of the demographic processes composing the life cycle (*i.e.,* population model). In doing so, one can inspect the selection pressures that have generated the patterns found in step 1. Step 2 (Fig. 1B) requires obtaining the partial derivatives of the deterministic population growth rate, λ_t, relative to all matrix elements of the MPM of interest (*i.e.,* elasticities of λ_t w.r.t each demographic process in the MPM). Step 2 therefore informs on the impact that each of the demographic processes has on λ_t

Finally, in step 3, one assesses the pattern of nonlinear selection by using the self-second derivatives of λ_t with respect to each demographic process (Fig. 1C). This step reveals the potential nonlinear selection pressures on each of the demographic processes within a life cycle. This step is key to understanding the evolutionary processes (*i.e.,* types of nonlinear selection) that the demographic processes are subjected to. Without understanding the evolutionary processes operating on the demographic processes, the pattern observed in step 1 might be artefactual. (e.g., Lawler et al. 2009)

Steps 2 and 3 of the framework feature selection pressures that have been averaged over the contiguous time periods. This means that the resulting patterns are based on how λ_t (obtained from averaging all sequential MPMs across the duration of the study) would be affected if a demographic process were perturbed. Therefore, steps 2 and 3 are based on a different information than step 1 and can thus complete our understanding of the role of selection pressures on shaping demographic patterns across multiple species.

Another important asset of step 3 above includes the notion that the relative importance (elasticity) of demographic processes themselves changes with changing environment (Stearns 1992). In other words, the extent to which λ_t is sensitive to perturbations in a specific demographic process is *dynamic* (Kroon *et al.* 2000). Thus, the self-second derivatives generate information on how the sensitivity (or elasticity) of λ_t might change. If the sensitivity (or elasticity) of λ_t can change, then it is important to know which demographic processes are most prone to trigger such a change. In the example of a hypothetical wolf species (Fig. 1), this means that if the reproduction of the third age-class individuals (matrix element $a_{1,3}$) decreased, the sensitivity of λ_t to $a_{1,3}$ would increase (square with the largest black dot, Fig. 1C). Consequently, with increased environmental variability, the key demographic process might change from remaining in the fourth age class (matrix element $a_{4,4}$, Fig. 1B) to reproduction of the third age-class (matrix element $a_{1,3}$, Fig. 1C).

Combining the three steps of our framework allows for a quantitative identification of buffering. Steps 2 and 3 offer key insights as to *why* a given species or population is placed on either the buffered or the non-buffered end of the variance continuum. A clear and unequivocal evidence for support towards buffering consists of: (1) a species or population being positioned near the 0 end of the continuum (the right-hand side) in step 1; (2) this species' or populations' life cycle having one or more demographic processes with highest elasticity values in step 2; and (3) the same demographic process displaying the highest elasticity in step 2 with negative self-second derivative values in step 3. In this sense, Figure 1B shows that, for the chosen population of a hypothetical wolf species, the most important demographic process is remaining in the fourth stage (MPM element $a_{4,4}$), as this demographic process results in highest elasticity value (Fig. 1B yellow square). However,

Fig. 1C reveals that $a_{4,4}$ is under little selection pressure for variance reduction. Thus, there is no clear evidence of buffering from the third step of the framework (*i.e.,* no concave selection forces).This way, the lack of concave selection forces on the key demographic process within wolf's life cycle explains why this species is placed on the left-hand side of the variance continuum (Fig. 1A).

Species placed on the non-buffered end of the continuum is a necessary but not sufficient condition for evidence demographic lability. It is key highlighting here that demographic buffering and lability do not represent two extremes of the same continuum. The variance continuum allocates the species or populations from strongly buffered to non-buffered, but to test the for lability, a further step is needed.

Although not our primary goal here, we briefly introduce said step 4. To establish compelling evidence of lability, it is essential to fulfil several further criteria. First, sufficient data across various environments (over time or space) are required to construct reaction norms that depict how a demographic process responds to environmental changes (Morris et al., 2008; Koons et al., 2009), which can be challenging in terms of sufficient and high-quality demographic and environmental data. Second, non-linear relationships between demographic processes and the environment must be established based on the demographic process-environment reaction norms. Lastly, demographic processes where an increase in the mean value has a stronger positive impact on population growth rate than the detrimental effect of increased variance needs to be identified. The latter condition is only met when the demographic process-environment reaction norm takes a convex shape (resembling a "U" shape), as described by Koons et al. (2009) and Morris et al. (2008). However, a study by Barraquand and Yoccoz (2013) reported diverging results in this regard. Importantly, we note that more likely than previously thought (*e.g.,* Pfister 1998), species do not exist as purely buffering or labile, but that within populations, some vital rates may be buffered, other labile, and others insensitive to the environment (*e.g.*, (Doak *et al.* 2005). Deciphering generality in this likely complex pattern should attract much research attention going forward, in our opinion.

Demographic buffering in mammals: a case study using the unified framework

We demonstrate the performance of our framework using 44 MPMs from 34 mammal species. Mammals are of special interest here for two reasons: (1) mammalian life histories have been well studied (Bielby *et al.* 2007; Gillespie 1977; Jones 2011; Stearns 1983); and (2) some of their populations have already been assessed in terms of buffering, particularly for primates (Campos *et al.* 2017; Morris *et al.* 2008, 2011; Reed & Slade 2012; Rotella *et al.* 2012). Together, the well-studied life histories and previous information about the occurrence of buffering in mammals provide the necessary information to make accurate predictions and validate the performance of the proposed framework.

We used Matrix Population Models from 40 out of 139 studies with mammals available in the COMADRE database v.3.0.0 (Salguero-Gómez *et al.* 2016). These 40 populations encompass 34 species from eight taxonomic orders. We included these MPMs in our analyses because they provide values of demographic processes (a_{ij}) for three or more contiguous time periods, thus allowing us to obtain the stochastic elasticity of each $a_{ij.}$ Although we are aware that not all possible temporal variation in demographic processes may have been expressed within this period, we assumed three or more transitions are enough to provide sufficient variation for population comparison. At least three contiguous time periods - a common selection criteria in comparative studies of stochastic demography (Compagnoni *et al.* 2023) - also allowed to test and showcase our framework. Fortunately, several long-lived species, characterized by low variation in their demographic processes, were studied for a long time (*e.g.,* some primates in our dataset have been studied for over 20 years – Morris *et al*. 2011). We removed the populations where either only survival or only reproduction rates were reported, because of the impossibility to calculate the stochastic growth rate. A detailed description of the analysed data and their original sources are available in supplementary material (Supplementary Material, Table S1).

Homo sapiens was included in our analyses because it is the only mammalian species in which second-order derivatives have been applied (Caswell 1996). Therefore, *Homo sapiens* provides an ideal basis for comparisons among species. The data for *Homo sapiens* were gathered from 26 modern populations located in various cities, allowing us to construct a spatiotemporal variance. It is important to note that in this case, we are not working with true temporal variance but rather a variance that encompasses both spatial and temporal aspects.

For steps 2 and 3 of our framework, we utilized a subset of 16 populations (including *Homo sapiens*) whose population projection matrices (MPMs) were organized by age. We specifically selected these populations because their life cycles can be summarized by two main demographic processes: survival and contribution to recruitment of new individuals. The contribution to recruitment can be interpreted as either the mean reproductive output for each age class or an approximation thereof, depending on how the matrices are structured (Ebert 1999). One advantage of using such matrices is that they encompass only two types of demographic processes, namely survival and recruitment, eliminating the need to account for multiple transitions between different life stages.

To perform the step 1 of our framework and obtain the $\Sigma E_{a_{ij}}^{S^{\sigma}}$ (and $\Sigma E_{a_{ij}}^{S^{\mu}}$), we followed Tuljapurkar *et al.* (2003) and Haridas & Tuljapurkar (2005). To perform step 2 of our framework, we calculated the deterministic elasticities of each demographic process extracted using the *popbio* package. All analyses were performed using R version 3.5.1 (R Core team, 2018). Finally, to perform the step 3 of our framework the self-second derivatives were adapted from *demogR* (Jones 2007) following (Caswell 1996) and applied for the mean MPM.

Results

We ranked 40 populations from the 34 identified mammal species according to the cumulative impact of variation in demographic processes on λ_s using the step 1 of our framework (Fig. 2). Additional information (including standard deviations of the elasticity estimates and number of matrices available) is provided in the supplementary material (Table S1). Most of the analysed orders were placed on the low-variance end of the variance continuum (Fig. 2). The smallest contributions of variation in demographic processes (*i.e.,* maximum value of $\Sigma E_{a_{ij}}^{S^{\sigma}}$, note that $\Sigma E_{a_{ij}}^{S^{\sigma}}$ ranges from 0 to -1), suggesting more buffered populations, were assigned to Primates: northern muriqui (*Brachyteles hyphoxantus*, $\Sigma E_{a_{ij}}^{S^{\sigma}} = -0.09 \times 10^{-4} \pm 0.12 \times 10^{-4}$) (mean ± standard deviation) (Fig. 2 silhouette a), mountain gorilla (*Gorilla beringhei*, $\Sigma E_{a_{ij}}^{S^{\sigma}} = -0.24 \times 10^{-4} \pm 0.08 \times 10^{-4}$) (Fig. 2 silhouette b), followed by the blue monkey (*Cercopithecus mitis*, $\Sigma E_{a_{ij}}^{S^{\sigma}} = -0.63 \times 10^{-4} \pm 0.06 \times 10^{-4}$) (Fig. 2 silhouette c). The first non-primate species placed near the low-variance end of the continuum was the Columbian ground squirrel (*Urocitellus columbianus*, Rodentia, $\Sigma E_{a_{ij}}^{S^{\sigma}} = -0.003 \pm 0.002$) (Fig. 2 silhouette d). The species with the highest contribution of variation in demographic processes placed at the high-variance end of the continuum was the stoat (*Mustela erminea*, Carnivora, $\Sigma E_{a_{ij}}^{S^{\sigma}} = -0.35 \pm 0.02$) (Fig. 2 silhouette e). All the 14 primate populations displayed potential evidence of buffering, occupying the right-hand side of the variance continuum, with the exception of the Patas monkey (*Erythrocebus patas*, Primates, $\Sigma E_{a_{ij}}^{S^{\sigma}} = -0.05 \pm 0.03$) (Fig. 2 silhouette f). The snowshoe hare (*Lepus americanus*, Lagomorpha, $\Sigma E_{a_{ij}}^{S^{\sigma}}$

= -0.29 ± 0.16) (Fig. 2 silhouette g) and the Bush rat (*Rattus fuscipes*, Rodentia, $\Sigma E^{S^{\sigma}}_{a_{ij}}$ = -0.25 ± 0.03) (Fig. 2 silhouette h) appear on the high-variance end of the continuum.

As predicted for the steps 2 and 3, we could not observe a clear pattern in support of buffering. This finding means that the demographic processes with the highest elasticity values failed to display strongly negative self-second derivatives (Fig. 3). Particularly for majority of primates - with the lack or minor temporal variation in demographic processes - demographic processes with high elasticities had positive values for the self-second derivatives (indicated by yellow squares with white dots in Fig. 3). Examples of primate species exhibiting high elasticities and positive values for the self-second derivatives and include northern muriqui (*Brachyteles hypoxanthus*), mountain gorilla (*Gorilla beringei*), white-faced capuchin monkey (*Cebus capucinus*), rhesus monkey (*Macaca mulatta*), blue monkey (*Cercopithecus mitis*), Verreaux's sifaka (*Propithecus verreauxi*) and olive baboon (*Papio cynocephalus*) (Fig. 3). This implies that the key demographic processes influencing λ_t are not subject to selective pressure for reducing their temporal variability. However, even though the primates were positioned closer to the low-variance end of the continuum in step 1, the evidence from steps 2 and 3 does not support the occurrence of buffering in the most influential demographic processes.

The killer whale showed similar controversy between step 1 and steps 2-3 results as most primates. In step 1, the killer whale was positioned at the buffered end of the variance continuum (*Orcinus orca*, Cetacea, $\Sigma E^{S^{\sigma}}_{a_{ij}} = -0.70 \times 10^{-4} \pm 1.04 \times 10^{-5}$) (Fig. 2 silhouette not shown). However, steps 2 and 3 show that the three demographic processes in killer whale life cycle with highest elasticity values (matrix elements $a_{2,2}$, $a_{3,3}$ and $a_{4,4}$) are not under selection pressures for reducing their temporal variance, but the opposite (depicted by yellow and green squares with white dots, Fig. 3).

The only primate species exhibiting evidence of buffering in steps 2 and 3 was human. In human, demographic parameters representing survival from first to second age class (matrix element $a_{2,1}$) displayed high elasticities and negative self-second derivatives (depicted as yellow squares with black dots in Fig. 3). Evidence supporting buffering was also found in the Columbian ground squirrel (*Urocitellus columbianus*), where, similar to humans, survival from the first to the second age class (matrix element $a_{2,1}$) showed indications of selection acting to reduce $a_{2,1}$variance. Accordingly, the Columbian ground squirrel was positioned close to the buffered end of the variance continuum in step 1. Hence, the Columbian ground squirrel was the sole species with consistent evidence of buffering across all three steps of the framework.

The Soay sheep (*Ovis aries*) was the species furthest from the buffered end of the variance continuum that enabled to perform steps 2 and 3. For the Soay sheep, remaining in the third age class (matrix element $a_{3,3}$) has the major influence on λ_t and is under selection pressure to have its variance increased. The latter characteristics reveal potential conditions for lability even though the species is placed closer to the buffered end of the variance continuum.

Steps 2 and 3 illustrate the importance of examining buffering evidence on the within-populations level. These two steps of the framework identify the simultaneous acting of concave and convex selection on different demographic processes within a single life cycle. In polar bear (*Ursus maritimus*), the key demographic process (matrix element $a_{4,4}$) is under convex selection, as depicted by a yellow square with a white dot in Fig. 3. However, the demographic process with the second highest elasticity value (matrix element $a_{5,4}$) is under strong concave selection (depicted by a light green square with a black dot in Fig. 3).

By adding step 3 to the framework, another important information was accessed. The high absolute values of self-second derivatives (large dots, either black or white, Fig. 3) indicate where the sensitivity of λ_t to demographic parameters is itself prone to environmental changes. For instance, if the value of $a_{5,4}$ for polar bear increased, the sensitivity of λ_t to $a_{5,4}$ would decrease because the self-second derivative of $a_{5,4}$ is highly negative (depicted by the largest black dot in polar bear MPM). Vice versa holds for the $a_{4,4}$ demographic process, where an increase in the value of $a_{4,4}$ would increase λ_t's sensitivity to $a_{4,4}$, because the self-second derivative of $a_{5,4}$ is highly positive (depicted by the largest white dot in polar bear MPM). Thus, sensitivities (or equally elasticities) of demographic processes with high absolute values for self-second derivatives can easily change..

Discussion

In the Anthropocene, identifying and quantifying mechanisms of species responses to stochastic environments holds crucial importance. This importance is particularly tangible in the context of the unprecedented environmental changes and uncertainties that impact the dynamics and persistence of natural populations (Boyce *et al.* 2006). Correlational demographic analysis, whereby the importance of demographic processes and their temporal variability is examined (Pfister 1998), has attempted to identify how species may buffer against the negative effects of environmental stochasticity. However, these widely used approaches have important limitations (see Introduction and Hilde et al. 2020). One significant limitation is the issue of measurement scale concerning demographic processes (Hilde *et al.* 2020; Morris & Doak 2004). Demographic processes, such as birth rates, death rates, immigration, and emigration, operate at various temporal and spatial scales. The choice of scale at which these processes are measured can impact the outcomes of correlational demographic analysis (Bjørkvoll *et al.* 2016). Our novel framework overcomes said limitations by providing a rigorous approach to quantify demographic buffering (Hilde et al. 2020; Pfister 1998).

Evidencing demographic buffering is not straightforward. Indeed, through the analysis of stochastic population growth rate (λ_s) in our application of the framework to 44 populations of 34 species, we identify the highest density of natural populations near the buffered end of the variance continuum (step 1). However, we show that the same species then fail to exhibit signs of concave (∩-shaped) selection on the key demographic parameters when further analyses are performed averaging the variation across the duration of each study (steps 2 and 3). This finding confirms that placing the species near the buffered end of the variance continuum is *necessary* but not *sufficient* to diagnose demographic buffering. Indeed, buffering occurs when concave selection forces act on the key demographic parameter (Caswell 1996, 2001; Shyu & Caswell 2014).

Combining the three steps into a unified framework is of outmost importance. In steps 2 and 3 of the framework, we find relatively limited overall evidence of buffering in the examination of our 16 (out of 34 in step 1) studied animal species. Step 3 of our framework reveals that the role of natural selection shaping temporal variation in demographic processes is more complex than expected. Indeed, demographic processes within our study populations are often under a mix of convex and concave selection. This mix of selection patterns was already suggested by Doak *et al.* (2005). Here, only two out of 16 mammal species revealed concave selection acting on the key demographic processes (Columbian ground squirrel [*Urocitellus columbianus*], and humans, [*Homo sapiens sapiens*]). These two species were also placed near the buffered end of the variance continuum, therefore meeting all the necessary conditions to diagnose buffering. However, finding 12.5% (two out of 16) species that meet the criteria for demographic buffering is not in concordance with previous studies. Evidence of buffering has been reported across 22 ungulate species (Gaillard & Yoccoz

2003). In the one ungulate we examined, the moose (*Alces alces*), we find only partial support for buffering in adult survival, since this species is placed near the buffered end of the variance continuum in step 1 but does not show concave selection pressures on adult survival in step 2/3, as would be necessary to confirm the occurrence of buffering. It is worth noting that a varying number of matrices per species were employed, ranging from 1 to 21, with an average of 8.1 matrices per species (as shown in Table S1). Naturally, having a greater number of matrices is preferred in such analyses. Furthermore, while the size of matrices (matrix dimensions) does not directly bias the results of our framework in any way – since steps 2 and 3 are shown for all the demographic processes independent of matrix dimension – potential implications of varying matrix dimensions should be further investigated in the future.

Our overall findings reveal varying levels of support for the notion that adult survival in long-lived species tends to be buffered. Indeed, Gaillard *et al.* (1998) found that adult female survival varied considerably less than juvenile survival in large herbivores. This finding was also supported by further studies in ungulates and small rodents (Gaillard & Yoccoz 2003), turtles (Heppell 1998), vertebrates and plants (Pfister 1998), and more recently across nine (out of 73) species of plants (McDonald *et al.* 2017).

When placing our study species along a variance continuum (step 1), primates tend to be located on the buffered end. However, most primates displayed convex –instead of the expected concave– selection on adult survival. Similar results, where the key demographic process failed to display constrained temporal variability, have been reported for long-lived seabirds (Doherty *et al.* 2004). One explanation for the unexpected convex selection on adult survival involves trade-offs, as suggested by (Doak *et al.* 2005). When two demographic parameters are negatively correlated, the variance of population growth rate (λ) can be increased or decreased (Compagnoni *et al.* 2016; Evans & Holsinger 2012). The well-established trade-off between survival and fecundity (Roff & Fairbairn 2007; Stearns 1992) might explain the observed deviation of our results. Because variation in primate recruitment is already constrained by physiological limitations (Campos *et al.* 2017), when adult survival and recruitment are engaged in a trade-off, this trade-off might lead to our unexpected result. Correlations among demographic processes (positive and negative) inherently influence the biological limits of variance (Haridas & Tuljapurkar, 2005). This is because the magnitude of variation in a particular demographic process is constrained by (the variation of) other demographic processes that exert an influence on it. Not surprisingly, correlations among demographic processes have been shown to be strongly subjected to ecological factors (Fay *et al.* 2022). Here, future studies may benefit from deeper insights via cross-second derivatives (Caswell 1996, 2001) to investigate correlations among demographic processes.

Examining the drivers of demographic buffering has become an important piece of the ecological and evolutionary puzzle of demography. As such, quantifying buffering can help us better predict population responses to environmental variability, climate change, and direct anthropogenic disturbances (Boyce *et al.* 2006; McDonald *et al.* 2017; Pfister 1998; Vázquez *et al.* 2017). By setting demographic buffering into a broader and integrated framework, we hope to enhance comprehension and prediction of the implications of heightened environmental stochasticity on the evolution of life history traits. This understanding is crucial in mitigating the risk of extinction for the most vulnerable species.

Acknowledgements

This study was financed in part by the *Coordenação de Aperfeiçoamento de Pessoal de Nível Superior* - Brasil (CAPES) - Finance Code 001. GSS was supported by CAPES and CNPq (301343/2023-3). RS-G was supported by a NERC Independent Research Fellowship

(NE/M018458/1). MK was supported by the European Commission through the Marie Skłodowska-Curie fellowship (MSCA MaxPersist #101032484) hosted by RSG.

Data availability

The demographic data used in this paper are open-access and available in the COMADRE Animal Matrix Database (https://compadre-db.org/Data/Comadre). A list of the studies and species used here is available in Supplementary Material (Table S1). The data and code supporting the results can be accessed here: https://github.com/SamuelGascoigne/Demographic_buffering_unified_framework.

References

Barraquand, F. & Yoccoz, N.G. (2013). When can environmental variability benefit population growth? Counterintuitive effects of nonlinearities in vital rates. *Theor Popul Biol*, 89, 1–11.

Bielby, J., Mace, G.M., Bininda-Emonds, O.R.P., Cardillo, M., Gittleman, J.L., Jones, K.E., *et al.* (2007). The Fast-Slow Continuum in Mammalian Life History: An Empirical Reevaluation. *Am Nat*, 169, 748–757.

Bjørkvoll, E., Lee, A.M., Grøtan, V., Saether, B.-E., Stien, A., Engen, S., *et al.* (2016). Demographic buffering of life histories? Implications of the choice of measurement scale. *Ecology*, 97, 40–47.

Bonsall, M.B. & Klug, H. (2011). The evolution of parental care in stochastic environments. *J Evol Biol*, 24, 645–655.

Boyce, M.S., Haridas, C. V., Lee, C.T., Boggs, C.L., Bruna, E.M., Coulson, T., *et al.* (2006). Demography in an increasingly variable world. *Trends Ecol Evol*, 21, 141–148.

Brodie, E.I., Moore, A. & Janzen, F. (1995). Visualizing and quantifying natural selection. *Trends Ecol Evol*, 10, 313–318.

Campos, F.A., Morris, W.F., Alberts, S.C., Altmann, J., Brockman, D.K., Cords, M., *et al.* (2017). Does climate variability influence the demography of wild primates? Evidence from long-term life-history data in seven species. *Glob Chang Biol*, 23, 4907–4921.

Carslake, D., Townley, S. & Hodgson, D.J. (2008). Nonlinearity in eigenvalue-perturbation curves of simulated population projection matrices. *Theor Popul Biol*, 73, 498–505.

Caswell, H. (1996). Second Derivatives of Population Growth Rate: Calculation and Applications. *Ecology*, 77, 870–879.

Caswell, H. (2001). *Matrix Population Models: Construction, Analysis, and Interpretation*. Sinauer Associates Inc. Publishers, Sunderland, Massachusetts, USA.

Charlesworth, B. (1994). *Evolution in age-structured populations*. second edi. Cambridge University Press.

Le Coeur, C., Yoccoz, N.G., Salguero-Gómez, R. & Vindenes, Y. (2022). Life history adaptations to fluctuating environments: Combined effects of demographic buffering and lability. *Ecol Lett*, 1–13.

Compagnoni, A., Bibian, A.J., Ochocki, B.M., Rogers, H.S., Schultz, E.L., Sneck, M.E., *et al.* (2016). The effect of demographic correlations on the stochastic population dynamics of perennial plants. *Ecol Monogr*, 86, 480–494.

Compagnoni, A., Evers, S. & Knight, T. (2023). Spatial replication can best advance our understanding of population responses to climate. *bioRxiv*, https://doi.org/10.1101/2022.06.24.497542.

Doak, D.F., Morris, W.F., Pfister, C., Kendall, B.E. & Bruna, E.M. (2005). Correctly Estimating How Environmental Stochasticity Influences Fitness and Population Growth. *Am Nat*, 166, E14–E21.

Doak, D.F., Waddle, E., Langendorf, R.E., Louthan, A.M., Isabelle Chardon, N., Dibner, R.R., *et al.* (2021). A critical comparison of integral projection and matrix projection models for demographic analysis. *Ecol Monogr*, 91, e01447.

Doherty, P.F., Schreiber, E.A., Nichols, J.D., Hines, J.E., Link, W.A., Schenk, G.A., *et al.* (2004). Testing life history predictions in a long-lived seabird: A population matrix approach with improved parameter estimation. *Oikos*, 105, 606–618.

Easterling, M.R., Ellner, S.P. & Dixon, P.M. (2000). Size-Specific Sensitivity: Applying a New Structured Population Model. *Ecology*, 81, 694–708.

Ellner, S.P., Childs, D.Z. & Rees, M. (2016). *Data-driven Modelling of Structured Populations. A practical guide to the Integral Projection Model*. Lecture Notes on Mathematical Modelling in the Life Sciences. Springer International Publishing, Cham.

Evans, M.E.K. & Holsinger, K.E. (2012). Estimating covariation between vital rates : A simulation study of connected vs . separate generalized linear mixed models (GLMMs). *Theor Popul Biol*, 82, 299–306.

Fay, R., Hamel, S., van de Pol, M., Gaillard, J.M., Yoccoz, N.G., Acker, P., *et al.* (2022). Temporal correlations among demographic parameters are ubiquitous but highly variable across species. *Ecol Lett*, 25, 1640–1654.

Ferreira, M., Kajin, M., Vieira, M., Zangrandi, P., Cerqueira, R. & Gentile, R. (2013). Life history of a neotropical marsupial: Evaluating potential contributions of survival and reproduction to population growth rate. *Mamm Biol*, 78, 406–411.

Franco, M. & Silvertown, J. (2004). A comparative demography of plants based upon elasticities of vital rates. *Ecology*, 85, 531–538.

Gaillard, J.-M. & Yoccoz, N. (2003). Temporal Variation in Survival of Mammals: a Case of Environmental Canalization? *Ecology*, 84, 3294–3306.

Gillespie, J.H. (1977). Natural Selection for Variances in Offspring Numbers: A New Evolutionary Principle. *Am Nat*, 111, 1010–1014.

Griffith, A.B. (2017). Perturbation approaches for integral projection models. *Oikos*, 126, 1675–1686.

Haridas, C.V. & Tuljapurkar, S. (2005). Elasticities in Variable Environments: Properties and Implications. *Am Nat*, 166, 481–495.

Healy, K., Ezard, T.H.G., Jones, O.R., Salguero-Gómez, R. & Buckley, Y.M. (2019). Animal life history is shaped by the pace of life and the distribution of age-specific mortality and reproduction. *Nat Ecol Evol*, 3, 1217–1224.

Heppell, S.S. (1998). Application of Life-History Theory and Population Model Analysis to Turtle Conservation. *Copeia*, 1998, 367.

Hilde, C.H., Gamelon, M., Sæther, B.-E., Gaillard, J.-M., Yoccoz, N.G. & Pélabon, C. (2020). The Demographic Buffering Hypothesis: Evidence and Challenges. *Trends Ecol Evol*, 35, 523–538.

Jäkäläniemi, A., Ramula, S. & Tuomi, J. (2013). Variability of important vital rates challenges the demographic buffering hypothesis. *Evol Ecol*, 27, 533–545.

Jones, J.H. (2007). demogR: A Package for the Construction and Analysis of Age-structured Demographic Models in R. *J Stat Softw*, 22, 1–28.

Jones, J.H. (2011). Primates and the evolution of long, slow life histories. *Current Biology*, 21, R708–R717.

Jongejans, E., De Kroon, H., Tuljapurkar, S. & Shea, K. (2010). Plant populations track rather than buffer climate fluctuations. *Ecol Lett*, 13, 736–743.

Koons, D.N., Pavard, S., Baudisch, A. & Jessica E. Metcalf, C. (2009). Is life-history buffering or lability adaptive in stochastic environments? *Oikos*, 118, 972–980.

Kroon, H. de, van Groenendael, J. & Ehrlen, J. (2000). Elasticities: A review of methods and model limitations.

McDonald, J.L., Franco, M., Townley, S., Ezard, T.H.G., Jelbert, K. & Hodgson, D.J. (2017). Divergent demographic strategies of plants in variable environments. *Nat Ecol Evol*, 1, 0029.

Morris, W.F., Altmann, J., Brockman, D.K., Cords, M., Fedigan, L.M., Pusey, A.E., *et al.* (2011). Low Demographic Variability in Wild Primate Populations: Fitness Impacts of Variation, Covariation, and Serial Correlation in Vital Rates. *Am Nat*, 177, E14–E28.

Morris, W.F. & Doak, D.F. (2004). Buffering of Life Histories against Environmental Stochasticity: Accounting for a Spurious Correlation between the Variabilities of Vital Rates and Their Contributions to Fitness. *Am Nat*, 163, 579–590.

Morris, W.F., Pfister, C.A., Tuljapurkar, S., Haridas, C. V., Boggs, C.L., Boyce, M.S., *et al.* (2008). Longevity can buffer plant and animal populations against changing climatic variability. *Ecology*, 89, 19–25.

Pélabon, C., Hilde, C.H., Einum, S. & Gamelon, M. (2020). On the use of the coefficient of variation to quantify and compare trait variation. *Evol Lett*, 4, 180–188.

Pfister, C. (1998). Patterns of variance in stage-structured populations: Evolutionary predictions and ecological implications. *Proceedings of the National Academy of Sciences*, 95, 213–218.

Reed, A.W. & Slade, N.A. (2012). Buffering and plasticity in vital rates of oldfield rodents. *Journal of Animal Ecology*, 81, 953–959.

Rodríguez-Caro, R.C., Capdevila, P., Graciá, E., Barbosa, J.M., Giménez, A. & Salguero-Gómez, R. (2020). The demographic buffering strategy has a threshold of effectiveness to increases in environmental stochasticity. *bioRxiv*, 1–41.

Roff, D.A. & Fairbairn, D.J. (2007). The evolution of trade-offs: Where are we? *J Evol Biol*, 20, 433–447.

Rotella, J.J., Link, W.A., Chambert, T., Stauffer, G.E. & Garrott, R.A. (2012). Evaluating the demographic buffering hypothesis with vital rates estimated for Weddell seals from 30 years of mark – recapture data, 162–173.

Salguero-Gómez, R., Jones, O.R., Archer, C.R., Bein, C., de Buhr, H., Farack, C., *et al.* (2016). COMADRE: A global data base of animal demography. *Journal of Animal Ecology*, 85, 371–384.

Shyu, E. & Caswell, H. (2014). Calculating second derivatives of population growth rates for ecology and evolution. *Methods Ecol Evol*, 5, 473–482.

Stearns, S. (1992). *The Evolution of Life Histories*. Oxford University Press, New York, USA.

Stearns, S.C. (1983). The Influence of Size and Phylogeny on Patterns of Covariation among Life-History Traits in the Mammals. *Oikos*, 41, 173.

Sutherland, W.J., Freckleton, R.P., Godfray, H.C.J., Beissinger, S.R., Benton, T., Cameron, D.D., *et al.* (2013). Identification of 100 fundamental ecological questions. *Journal of Ecology*, 101, 58–67.

Tuljapurkar, S., Gaillard, J.-M. & Coulson, T. (2009). From stochastic environments to life histories and back. *Philosophical Transactions of the Royal Society B: Biological Sciences*, 364, 1499–1509.

Tuljapurkar, S., Horvitz, C.C. & Pascarella, J.B. (2003). The Many Growth Rates and Elasticities of Populations in Random Environments. *Am Nat*, 162, 489–502.

Tuljapurkar, S.D. (1982). Population dynamics in variable environments. III. Evolutionary dynamics of r-selection. *Theor Popul Biol*, 21, 141–165.

Tuljapurkar, S. (1990). Population Dynamics in Variable Environments. In: *Lecture notes in Biomathematics*, Lecture Notes in Biomathematics (ed. Levin, S.). Springer Berlin Heidelberg.

Vázquez, D.P., Gianoli, E., Morris, W.F. & Bozinovic, F. (2017). Ecological and evolutionary impacts of changing climatic variability. *Biological Reviews*, 92, 22–42.

Wang, J., Yang, X., Silva Santos, G., Ning, H., Li, T., Zhao, W., *et al.* (2023). Flexible demographic strategies promote the population persistence of a pioneer conifer tree (Pinus massoniana) in ecological restoration. *For Ecol Manage*, 529, 120727.

Figure 1

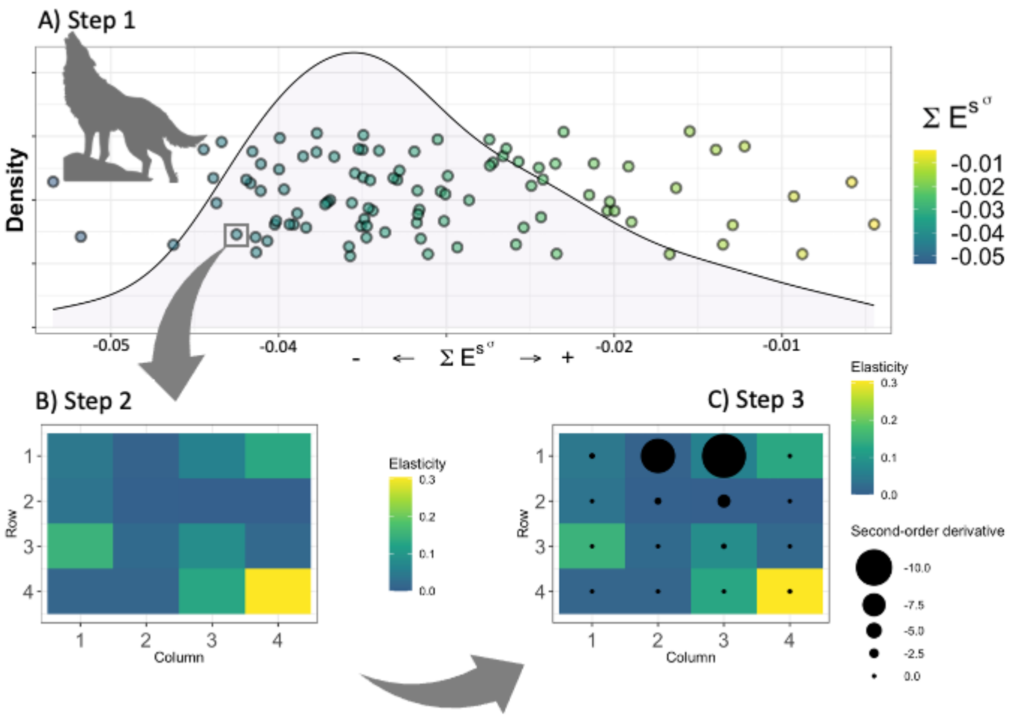
A) Step 1
Density
-0.05
-0.04
-0.02
-0.01
- ← Σ E^sσ → +
Σ E^sσ
-0.01
-0.02
-0.03
-0.04
-0.05
B) Step 2
Row
1
2
3
4
Column
1
2
3
4
Elasticity
0.3
0.2
0.1
0.0
C) Step 3
Row
Column
Elasticity
0.3
0.2
0.1
0.0
Second-order derivative
-10.0
-7.5
-5.0
-2.5
0.0

Figure 2

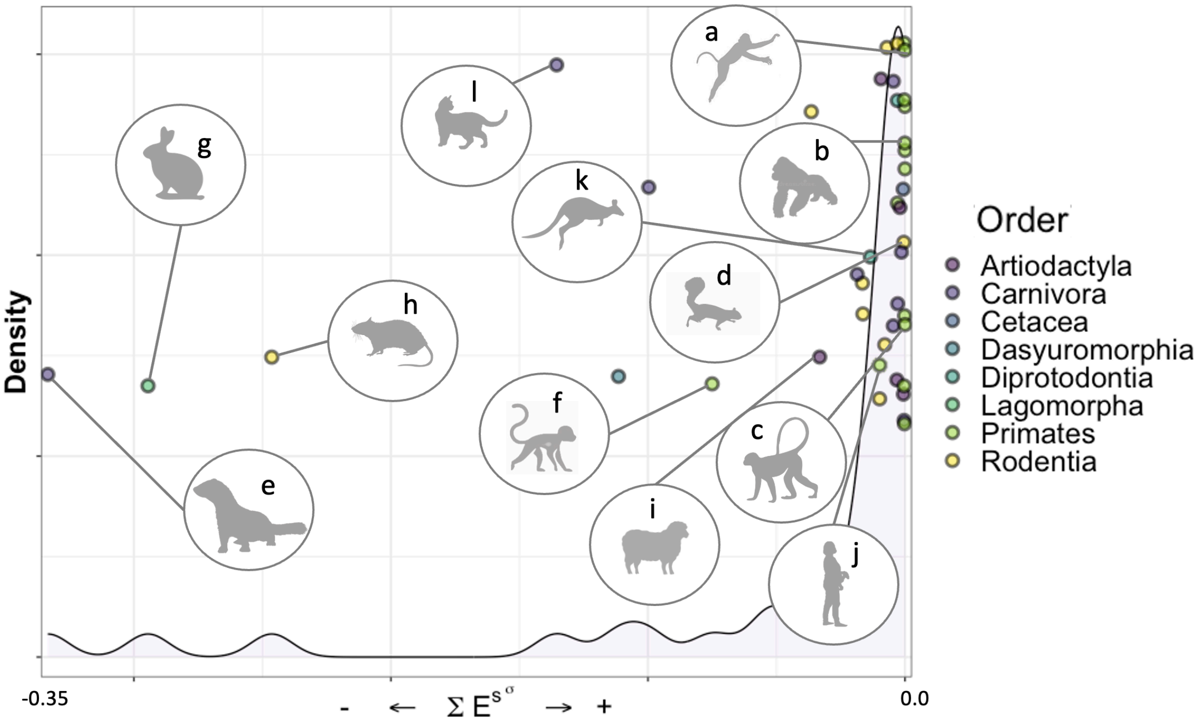
a
b
c
d
e
f
g
h
i
j
k
l
Density
-0.35
0.0
- ← Σ $E^{s^{\sigma}}$ → +
Order
Artiodactyla
Carnivora
Cetacea
Dasyuromorphia
Diprotodontia
Lagomorpha
Primates
Rodentia

Figure 3

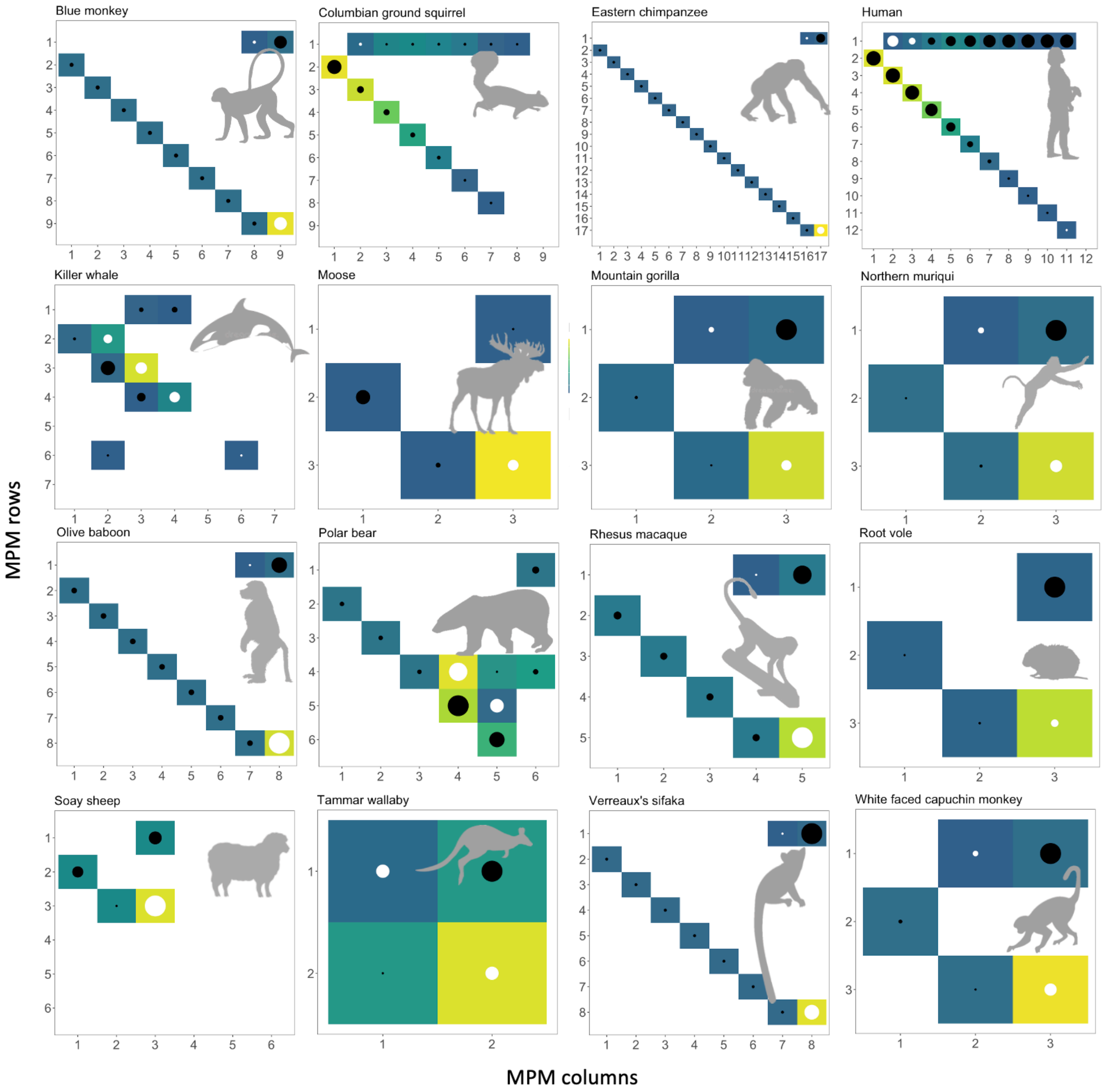
Blue monkey
Columbian ground squirrel
Eastern chimpanzee
Human
Killer whale
Moose
Mountain gorilla
Northern muriqui
Olive baboon
Polar bear
Rhesus macaque
Root vole
Soay sheep
Tammar wallaby
Verreaux's sifaka
White faced capuchin monkey
MPM rows
MPM columns

Figure legends

Figure 1. A three-step framework proposed to: Step 1 - allocate species and/or populations on a variance continuum (plot A, dots representing 50 hypothetical species). The variance continuum operates at the between-populations level (see text) and is represented by partitioning the sum of all the stochastic elasticities ($\Sigma E_{a_{ij}}^{S}$) into two compounds: i) sums of stochastic elasticities with respect to the variance ($\Sigma E_{a_{ij}}^{S^{\sigma}}$), and ii) sums of stochastic elasticities with respect to the mean ($\Sigma E_{a_{ij}}^{S^{\mu}}$). The first step of our framework shows the variance compound of the sums of stochastic elasticities forming a continuum where the right-hand side of the plot represents species (or populations) where a perturbation of variance in demographic processes results in weak or no impact on λ_s (yellow dots). The yellow-dotted species (or populations) can be classified as having potentially *buffered life-cycles* – based on all the demographic processes. The left-hand side of the graph represents species (or populations) where a perturbation of the variance in demographic processes results in strong impact on λ_s (blue dots). Thus, the blue-dotted species (or populations) can be classified as having potentially *unbuffered life cycles* – based on all the demographic processes. The vertical axis delineates the values of the density distribution function, indicating the number of species/populations at each value of $\Sigma E_{a_{ij}}^{S^{\sigma}}$. The placement of data points (species/populations) along the horizontal axis corresponds to their calculated values of $\Sigma E_{a_{ij}}^{S^{\sigma}}$ and is arranged linearly, while the breadth along the y-axis is solely for improved visual comprehension. Step 2 - Access the linear selection pressures for individual species or populations at within-species level (see text) (plot B). Step 2 displays the elasticities of the deterministic population growth rate (λ_t) for a hypothetical population of wolf and reveals the linear selection gradients, and which demographic processes are the most influential for λ_t. Step 3 - Access the nonlinear selection pressures at the within-species level (see text) (plot

C). In the third step self-second derivatives for the corresponding demographic processes from step 2 are displayed.

Figure 2. Results for step 1 of our framework showing the sum of stochastic elasticities with respect to the variance $\Sigma E_{a_{ij}}^{S^{\sigma}}$. The closer the $\Sigma E_{a_{ij}}^{S^{\sigma}}$ is to zero, the weaker the impact of variation in demographic processes on λ_s. The 40 populations from 34 species of mammals from the COMADRE database are ranked into the variance continuum from potentially buffered (right-hand side) to less buffered (left-hand side), since any variation in demographic processes would strongly impact λ_s. Colors represent different taxonomic orders with Primates occupying the right-hand side. Silhouettes: a) *Brachyteles hyphoxantus*, b) *Gorilla beringhei*, c) *Cercopithecus mitis*, d) *Urocitellus columbianus,* e) *Mustela erminea*, f) *Erythrocebus patas*, g) *Lepus americanus*, h) *Rattus fuscipes*, i) *Ovis aries*, j) *Homo sapiens*, k) *Macropus eugenii*, and l) *Felis catus*. The vertical axis delineates the values of the density distribution function, indicating the number of species/populations at each value of $\Sigma E_{a_{ij}}^{S^{\sigma}}$. The placement of data points (species/populations) along the horizontal axis corresponds to their calculated values of $\Sigma E_{a_{ij}}^{S^{\sigma}}$ and is arranged linearly, while the breadth along the y-axis is solely for improved visual comprehension.

Figure 3: Results from steps 2 and 3 of the proposed framework (see Fig. 2B, C). The 16 plots represent populations where the MPMs built by ages were available in the COMADRE database (see text). The color scale represents elasticity values for each of the demographic processes in the MPM, where yellow represents high and blue low elasticity values. No color means elasticity=0. Because the aim of step 2 is to identify the most impacting demographic process within each species' life cycle (the within-populations level, see text) - not to

compare the elasticity values among species - each plot has its own scale (see end of legend). The black dots represent negative self-second derivatives of λ_t - thus concave selection - and the white dots represent positive self-second derivatives of λ_t - thus convex selection. The dot sizes are scaled by the absolute value of self-second derivatives, where the smaller the dot, the closer a self-second derivative is to 0, indicting weak or no nonlinearity. Large dots indicate strong nonlinear selection forces. Scales ($E_{min-max}$=elasticity minimum and maximum value, $SSD_{min-max}$=self-second derivative minimum and maximum value): Blue monkey $E_{min-max}$=0.00-0.52, $SSD_{min-max}$=-1.25-1.27; Columbian ground squirrel: $E_{min-max}$=0.00-0.23, $SSD_{min-max}$=-1.48-0.01; Eastern chimpanzee: $E_{min-max}$=0.00-0.60, $SSD_{min-max}$=-4.39-2.59; Human: $E_{min-max}$=0.00-0.18, $SSD_{min-max}$=-0.15-0.08; Killer whale: $E_{min-max}$=0.00-0.55, $SSD_{min-max}$=-5.72-3.43; Moose: $E_{min-max}$=0.00-0.55, $SSD_{min-max}$=-0.66-0.36; Mountain gorilla: $E_{min-max}$=0.00-0.81, $SSD_{min-max}$=-1.46-0.28; Northern muriqui: $E_{min-max}$=0.00-0.72, $SSD_{min-max}$=-1.17-0.35; Olive baboon: $E_{min-max}$=0.00-0.54, $SSD_{min-max}$=-0.57-1.13; Polar bear: $E_{min-max}$=0.00-0.26, $SSD_{min-max}$=-0.73-0.54; Rhesus macaque: $E_{min-max}$=0.00-0.51, $SSD_{min-max}$=-0.54-0.71; Root vole: $E_{min-max}$=0.00-0.86, $SSD_{min-max}$=-2.54-0.22; Soay sheep: $E_{min-max}$=0.00-0.56, $SSD_{min-max}$=-0.22-0.40; Tammar wallaby: $E_{min-max}$=0.00-0.55, $SSD_{min-max}$=-0.64-0.34; White faced capuchin monkey: $E_{min-max}$=0.00-0.66, $SSD_{min-max}$=-2.66-1.21.

Supplementary material – Data available in COMADRE Version 2.0.1 and results from Step 1 of the framework

Table S1. The metadata used in step 1 of our framework and the respective results presented in the main text. The first four columns represent the information from where Matrix Populations Models (MPMs) were extract precisely as presented in COMADRE 2.0.1. Column titles differ from the database as "SpeciesAuthorComadre" is equivalent to "SpeciesAuthor" and "SpeciesName" is equivalent to "SpeciesAccepted" in COMADRE 2.0.1. The remaining columns present the results of step 1, where we present the raw values of $\Sigma E_{a_{ij}}^{S^{\mu}}$ and $\Sigma E_{a_{ij}}^{S^{\sigma}}$, their respective standard deviation, the stochastic population growth rate λ_s, and the number of available matrices (# matrices). For ByAge, "TRUE" was assigned for MPMs built by age or "FALSE" if otherwise.

SpeciesAuthorComadre	**SpeciesName**	**CommonName**	**Order**	$\Sigma E_{a_{ij}}^{S^{\mu}}$	$\Sigma E_{a_{ij}}^{S^{\mu}}$ **(sd)**	$\Sigma E_{a_{ij}}^{S^{\sigma}}$	$\Sigma E_{a_{ij}}^{S^{\sigma}}$ **(sd)**	**# matrices**	λ
Homo_sapiens_subsp._sapiens	*Homo sapiens sapiens*	Human	Primates	1.003	0.003	1.003	0.004	13	1.064
Alces_alces	*Alces alces*	Moose	Artiodactyla	1.001	0.001	1.001	0.001	13	1.205
Antechinus_agilis	*Antechinus agilis*	Agile antechinus	Dasyuromorphia	1.111	0.111	1.111	0.011	2	0.931
Brachyteles_hypoxanthus	*Brachyteles hypoxanthus*	Northern muriqui	Primates	1.000	0.000	1.000	0.000	12	1.051
Callospermophilus_lateralis	*Callospermophilus lateralis*	Golden-mantled ground squirrel	Rodentia	1.054	0.054	1.054	0.055	9	2.052
Cebus_capucinus	*Cebus capucinus*	White faced capuchin monkey	Primates	1.000	0.000	1.000	0.000	11	1.021
Cercopithecus_mitis	*Cercopithecus mitis*	Blue monkey	Primates	1.000	0.000	1.000	0.000	14	1.036
Eumetopias_jubatus	*Eumetopias jubatus*	Northern sea lion; Steller sea lion	Carnivora	1.005	0.005	1.005	0.002	2	0.904
Felis_catus	*Felis catus*	Feral cat	Carnivora	1.136	0.136	1.136	0.012	1	1.948
Gorilla_beringei	*Gorilla beringei*	Mountain gorilla	Primates	1.000	0.000	1.000	0.000	21	1.027

Hippocamelus_bisulcus	*Hippocamelus bisulcus*	Huemul deer	Artiodactyla	1.002	0.002	1.002	0.001	1	0.996
Lepus_americanus	*Lepus americanus*	Snowshoe hare	Lagomorpha	1.294	0.294	1.294	0.165	2	0.812
Lycaon_pictus	*Lycaon pictus*	African wild dog	Carnivora	1.100	0.100	1.100	0.008	1	1.500
Macaca_mulatta_3	*Macaca mulatta*	Rhesus macaque	Primates	1.000	0.000	1.000	0.001	12	1.127
Macropus_eugenii	*Macropus eugenii*	Tammar wallaby	Diprotodontia	1.013	0.013	1.013	0.012	7	0.981
Marmota_flaviventris_2	*Marmota flaviventris*	Yellow-bellied marmot	Rodentia	1.007	0.007	1.007	0.006	4	0.890
Marmota_flaviventris_3	*Marmota flaviventris*	Yellow-bellied marmot	Rodentia	1.008	0.008	1.008	0.005	4	0.921
Microtus_oeconomus	*Microtus oeconomus*	Root vole	Rodentia	1.000	0.000	1.000	0.001	14	1.028
Mustela_erminea	*Mustela erminea*	Stoat	Carnivora	1.334	0.334	1.334	0.117	2	1.258
Orcinus_orca_2	*Orcinus orca*	Killer whale	Cetacea	1.001	0.001	1.001	0.001	24	0.999
Ovis_aries_2	*Ovis aries*	Soay sheep	Artiodactyla	1.033	0.033	1.033	0.020	3	1.099
Pan_troglodytes_subsp._schweinfurthii	*Pan troglodytes*	Eastern chimpanzee	Primates	1.000	0.000	1.000	0.001	22	0.982
Papio_cynocephalus	*Papio cynocephalus*	Olive baboon	Primates	1.000	0.000	1.000	0.000	19	1.054
Peromyscus_maniculatus_2	*Peromyscus maniculatus*	Deer mouse	Rodentia	1.010	0.010	1.010	0.005	2	1.107
Phocarctos_hookeri	*Phocarctos hookeri*	New Zealand sea lion	Carnivora	1.005	0.005	1.005	0.003	8	1.023
Propithecus_verreauxi	*Propithecus verreauxi*	Verreaux's sifaka	Primates	1.000	0.000	1.000	0.000	12	0.986
Puma_concolor_8	*Puma concolor*	Cougar	Carnivora	NA	NA	NA	NA	10	1.115
Rattus_fuscipes	*Rattus fuscipes*	Bush rat	Rodentia	1.246	0.246	1.246	0.029	2	1.305
Spermophilus_armatus	*Urocitellus armatus*	Uinta ground squirrel	Rodentia	1.016	0.016	1.016	0.011	4	1.125
Spermophilus_armatus_2	*Urocitellus armatus*	Uinta ground squirrel	Rodentia	1.017	0.017	1.017	0.010	3	1.095

Spermophilus_columbianus	*Urocitellus columbianus*	Columbian ground squirrel	Rodentia	1.036	0.036	1.036	0.025	3	1.009
Spermophilus_columbianus_3	*Urocitellus columbianus*	Columbian ground squirrel	Rodentia	1.003	0.003	1.003	0.006	3	1.200
Ursus_americanus_subsp._floridanus	*Ursus americanus*	Florida black bear	Carnivora	1.003	0.003	1.003	0.003	2	1.020
Ursus_arctos_subsp._horribilis_5	*Ursus arctos*	Grizzly bear	Carnivora	1.001	0.001	1.001	0.001	4	1.026
Ursus_maritimus_2	*Ursus maritimus*	Polar bear	Carnivora	1.019	0.019	1.019	0.007	2	0.941
Brachyteles_hypoxanthus_2	*Brachyteles hypoxanthus*	Northern muriqui	Primates	1.000	0.000	1.000	0.000	12	1.111
Cebus_capucinus_2	*Cebus capucinus*	WhiteNAfaced capuchin monkey	Primates	1.000	0.000	1.000	0.000	11	1.059
Chlorocebus_aethiops_2	*Chlorocebus aethiops*	Vervet	Primates	1.075	0.075	1.075	0.087	5	1.187
Erythrocebus_patas	*Erythrocebus patas*	Patas monkey	Primates	1.051	0.051	1.051	0.038	5	1.128
Gorilla_beringei_subsp._beringei	*Gorilla beringei*	Mountain gorilla	Primates	1.000	0.000	1.000	0.000	21	1.053

A unified framework to identify demographic buffering in natural populations

A manuscript in preparation for submission to ECOLOGY LETTERS
Type of article: METHOD

Gabriel Silva Santos [1,2*], Samuel J L Gascoigne[3*], André Tavares Corrêa Dias[4], Maja Kajin [3,5**♦], Roberto Salguero-Gómez[3♦]

1 National Institute of the Atlantic Forest (INMA), 29650-000, Santa Teresa, Espirito Santo, Brazil. ssantos.gabriel@gmail.com
2 Department of Ecology, Graduate Program in Ecology and Evolution, Rio de Janeiro State University, 524 São Francisco Xavier street, 20550-900, Maracanã, Rio de Janeiro, Brazil
3 Department of Biology, University of Oxford, South Parks Road, OX1 3RB, Oxford, UK. samuel.gascoigne@pmb.ox.ac.uk, rob.salguero@biology.ox.ac.uk, maja.kajin@biology.ox.ac.uk
4 Department of Ecology, Institute of Biology, Universidade Federal do Rio de Janeiro, Avenida Carlos Chagas Filho 373, 21941-590 Rio de Janeiro, RJ, Brazil. atcdias@gmail.com
5 Department of Biology, Biotechnical Faculty, University of Ljubljana, Večna pot 111, 1000 Ljubljana, Slovenia

[*]Shared first authorship
[**]Corresponding author
♦Shared senior authorship

AUTHOR CONTRIBUTIONS: GSS developed the initial concept, performed the statistical analyses and contributed to the first draft of the manuscript. SJLG developed the initial concept, contributed to the first draft and all other versions of the manuscript and generated final figures. ATCD co-advised the project and contributed significantly to final versions of the manuscript. MK developed and managed the project, contributed to the first draft and all other versions of the manuscript and generated final figures. RSG developed and managed the project and contributed to the first draft and all other versions of the manuscript. All authors made substantial contributions to editing the manuscript and further refining ideas and interpretations.

RUNNING TITLE: Demographic buffering framework (31/45 words)

KEYWORDS: COMADRE Animal Matrix Database, elasticity, life-history evolution, natural selection, second-order derivative, sensitivity, stochasticity, variance.

NUMBER OF WORDS: Abstract – 146/150 words, main text (excluding abstract, acknowledgements, references, table and figure legends) – 5398/5000 words

NUMBER OF REFERENCES: 64

NUMBER OF TABLES: 1 (in Supplementary Material)

NUMBER OF FIGURES: 3

Abstract (146/150 words)

The Demographic Buffering Hypothesis (DBH) predicts that natural selection reduces the temporal fluctuations in demographic processes (such as survival, development, and reproduction), due to their negative impacts on population dynamics. However, a comprehensive approach that allows for the examination of demographic buffering patterns across multiple species is still lacking. Here, we propose a three-step framework aimed at identifying and quantifying demographic buffering. Firstly, we categorize species along a continuum of variance based on their stochastic elasticities. Secondly, we examine the linear selection gradients, followed by the examination of nonlinear selection gradients as the third step. With these three steps, our framework overcomes existing limitations of conventional approaches to identify and quantify demographic buffering, allows for multi-species comparisons, and offers insight into the evolutionary forces that shape demographic buffering. We apply this framework to mammal species and discuss both the advantages and potential of our framework.

Environmental stochasticity plays a pivotal role in shaping organisms' life histories (Bonsall & Klug 2011). Nonetheless, how organisms will cope with the increasing variation in environmental conditions expected under climate change (Boyce *et al.* 2006; Morris *et al.* 2008) is one of the most intriguing questions of ecology and evolution (Sutherland *et al.* 2013). Evolutionary demography offers a wide array of explanations for the evolutionary processes that shape the diversity of demographic responses to environmental stochasticity (Charlesworth 1994; Pfister 1998; Tuljapurkar *et al.* 2009; Healy *et al.* 2019; Hilde *et al.* 2020). The Demographic Buffering Hypothesis (*DBH*, hereafter) (Morris & Doak 2004; Pélabon *et al.* 2020) predicts a negative relationship between the contribution of a demographic processes (*e.g.*, survival, development, reproduction) to the population growth rate (λ) and their temporal variance (Pfister 1998). The emerging demographic strategy, demographic buffering, accommodates variance of demographic processes to cope with the otherwise negative effects of stochastic environments on λ (Pfister 1998; Morris & Doak 2004; Hilde *et al.* 2020).

A unified approach to unambiguously quantify demographic buffering is still missing. Indeed, identifying demographic buffering remains challenging (Morris & Doak 2004; Doak *et al.* 2005) for at least three reasons. First is the different interpretation of results from correlational analyses (*e.g.*, as in Pfister, 1998). Some authors have used the correlation coefficient as an index to order species' life histories in a continuum ranging from buffered (Spearman's correlation ρ = <0 between the sensitivity of λ to demographic processes and their temporal variance) to labile (ρ = >0, regardless of the "scatterness" around the regression (McDonald *et al.* 2017). In contrast, other researchers interpret the absence of statistical support for demographic buffering as an alternative strategy where variance in demographic process(es) is favoured to track environmental conditions (the so-called Demographic Lability Hypothesis (*DLH*, hereafter; *e.g.,*(Koons *et al.* 2009; Reed & Slade 2012; Jäkäläniemi *et al.* 2013; Hilde *et al.* 2020).

The second obstacle to obtain generalisation across species' populations regarding demographic buffering is the hierarchical level at which this phenomenon is typically examined. Some studies base their investigations of demographic buffering on the *whole* life history at the level of species or populations (*interspecific level*, hereafter), focusing on the one demographic process that is the most influential for λ (Reed & Slade 2012; McDonald *et al.* 2017). At the interspecific level, a life history is referred to as demographically buffered if the most important demographic process has low temporal variance (Pfister 1998; Morris & Doak 2004; Hilde *et al.* 2020; Le Coeur *et al.* 2022). Thus, the associated strategy is commonly decided based on a *single* demographic process (*e.g*., adult survival), ignoring the selection pressures on the rest of the demographic processes within the life cycle. However, to understand how, why, and where demographic buffering occurs –or not– and how buffering patterns might be modified in response to the environment, it is essential to also consider the features *within* a single species' life cycle (*intraspecific level*, hereafter). Within a single life cycle one demographic process can be buffered against while another can be labile to the environment – supporting the DLH (Koons *et al.* 2009; Jongejans *et al.* 2010; Barraquand & Yoccoz 2013). Thus, for a mechanistic understanding of how environmental stochasticity shapes life histories, both inter- and intra-specific levels need to be addressed.

The third reason limiting a holistic understanding of demographic strategies in stochastic environments are the challenges inherent to examining their underlying mechanisms. Evidence for demographic buffering exists across some long-lived organisms with complex life cycles, (Pfister 1998; Gaillard & Yoccoz 2003; Doak *et al.* 2005; Rotella *et al.* 2012; McDonald *et al.* 2017), but also in short-lived species (Pfister 1998; Reed & Slade 2012; Ferreira *et al.* 2013). Importantly, these patterns of variation do not inform on how the life histories were shaped by natural selection. To do so, one would need to identify the type (linear or nonlinear) and strength of selection acting on demographic processes. Linear selection acts on changing *the mean* value of a demographic process via a linear function between the fitness and the demographic process. In contrast, nonlinear selection acts on *the variance* of demographic processes either increasing it, decreasing it, or increasing/decreasing *the covariance* between two demographic processes (Brodie et al. 1995; Carslake et al. 2008).

The sign of the self-second derivative of λ determines the type of nonlinear selection acting on a demographic process. For instance, a negative self-second derivative for a given demographic process describes a concave form of selection, commonly referred to as the ∩-shaped selection (Caswell 1996, 2001; Shyu & Caswell 2014). This form of selection reduces the temporal variance in said demographic process, thereby providing support for the DBH. Conversely, a demographic process yielding a positive self-second derivative identifies a convex, or U-shaped selection (Caswell 1996, 2001; Shyu & Caswell 2014). Such a selection mechanism acts upon demographic processes amplifying their temporal variance, thus supporting the DLH (Koons *et al.* 2009; Le Coeur *et al.* 2022). The cross-second derivatives (not discussed here, see Caswell 1996, 2001 for further details) quantify selection pressures acting on the strength of correlation among different demographic processes.

The rich variation in demographic strategies across the Tree of Life is a result of evolutionary processes that have shaped variance in demographic processes through time. In this context, setting demographic buffering into the adaptive landscape context of linear and nonlinear selection enables us to identify and quantify the evolutionary processes that generate said demographic patterns. In this way, one will better understand how increased variability of environmental conditions might act on the existing –and shape novel– demographic strategies. However, we still lack a unified approach to quantify DBH.

Here, we present a framework that identifies and quantifies demographic buffering. Our framework provides a thorough analysis of temporal variance in demographic processes affected by environmental stochasticity. This framework involves categorizing species or populations along a variance continuum based on the extent to which key demographic processes are buffered by natural selection, thereby limiting their temporal variability. The framework consists of four steps with a mix of well-known methods applied to stage-structured demographic information (*e.g.,* matrix population models [Caswell 2001]; integral projection models [Easterling et al. 2000]). First, we position species or populations on the aforementioned continuum to assess the cumulative effect of the variance on their key demographic processes at the interspecific level (see below). Second, we investigate the presence of linear selection forces operating within the life cycle of each species or population at the intraspecific level (below). Third, we explore the impact of non-linear selection forces acting within the life cycle of each species or population, also at the intraspecific level. The combination of these three steps provides quantitative evidence for/against the DBH, while in step four we describe how to test the DLH.

To demonstrate the applicability of our framework, we apply it to 40 populations of 34 mammal species sourced from the COMADRE database (Salguero-Gómez *et al.* 2016). We showcase how the framework can provide valuable insights into the patterns of demographic buffering across species. The framework offers novel, detailed insights into the selection pressures that act *within* species' life cycles, thus allowing for a thorough understanding of the evolutionary selection forces that shape the patterns of demographic buffering across species. Beyond providing a quantitative, systematic toolset to test the DBH through three steps, we have also offer an alternative fourth step that briefly outlines how to test for the DLH.

A unified framework to assess evidence of DBH

The evidence for demographic buffering has been mainly assessed using Matrix Population Models (Pfister 1998; Rotella *et al.* 2012). However, Integral Projection Models (IPM; Rodríguez-Caro et al. 2020; Wang et al. 2023) can be equally applied for identifying the demographic buffering signatures. Both MPMs and IPMs are stage-structured, discrete-time demographic models (Caswell 2001; Ellner *et al.* 2016). For simplicity, here we focus on MPMs, but note that the same approaches are as equally applicable to IPMs (Griffith 2017; Doak *et al.* 2021). Throughout this manuscript, we refer to demographic processes as both matrix entries a_{ij} (*i.e.,* upper-level parameters) and the vital rates that underline the matrix elements (*i.e.,* lower-level parameters), and note that their conversion is straightforward and described elsewhere (Franco & Silvertown 2004). The framework operates on three steps:

The first step of our framework involves acquiring the relative contribution of each demographic process to the stochastic growth rate, λ_s, the so-called stochastic elasticities, E^S_{ij} (Tuljapurkar *et al.* 2003) (Figure 1A). The sum of all stochastic elasticities $(\Sigma E^S_{a_{ij}})$, can be separated into two components to assess how temporal variance and mean values of each demographic process contributes to λ_s. The first component represents the *sum of stochastic elasticity of* λ_s *with respect to the variance* $\Sigma E^{S^\sigma}_{a_{ij}}$, and the second represents the *sum of stochastic elasticity of* λ_s *with respect to the mean* $\Sigma E^{S^\mu}_{a_{ij}}$, where $\Sigma E^S_{a_{ij}} = \Sigma E^{S^\sigma}_{a_{ij}} + \Sigma E^{S^\mu}_{a_{ij}}$. Thus, the summation $\Sigma E^{S^\sigma}_{a_{ij}}$ quantifies the extent to which the stochastic population growth rate (λ_s) is influenced by changes in the variances of the demographic processes within the population matrix.

A higher sum of stochastic elasticity of λ_s with respect to the variance (*i.e.,* higher absolute value; $|\Sigma E^{S^\sigma}_{a_{ij}}|$) indicates that small changes in the variance of demographic processes would have a substantial impact on λ_s. In other words, the variance of that demographic process is not constrained by selection, supporting the DLH. On the other hand, a lower (absolute) stochastic elasticity of λ_s with respect to the variance suggests that λ_s is less sensitive to such perturbations, or, that variance of such demographic process is being constrained by natural selection, supporting the DBH (Tuljapurkar *et al.* 2003; Haridas & Tuljapurkar 2005) (Fig. 1A).

The first step of the framework thus features the interspecific level and places species or populations alongside a continuum. Species exhibiting unconstrained variance in the most important demographic process (*i.e.,* not buffered/potentially DLH suggesting, Fig. 1A, blue dots) are positioned on the left-hand side of the continuum. In contrast, species with constrained variance in the most important demographic process (*i.e.,* supporting the DBH, Fig. 1A, yellow dots) are positioned on the right-hand side of the continuum. However, the left-hand side of the continuum does not necessarily imply evidence of demographic lability. This is so because demographic lability is defined as an increase in the *mean value* of a demographic process in response to improved environmental conditions (Le Coeur *et al.* 2022). By examining $\Sigma E_{a_{ij}}^{S^{\sigma}}$, we can visualize an increase or decrease in *variance* of demographic processes, while the mean value of a demographic process does not change. The right-hand side (near 0 values for $\Sigma E_{a_{ij}}^{S^{\sigma}}$) supports the DBH, while the opposite end represents the lack of support for the DBH, and potentially support for the DLH. However, to undoubtedly provide support for the DLH, further investigation of demographic parameters is needed, as described below.

Step 1 of our framework examines the impacts that environmental variation has on the long-term population growth rate, λ_s (Tuljapurkar *et al.* 2003). This means that the resulting variance continuum in this step of the framework is based on how λ_s was affected by variation in the key demographic parameter across all contiguous time periods.

Steps 2 and 3 of the framework are conducted at the intraspecific level. Once species or populations are positioned along the variance continuum regarding the most important demographic process for λ_s, (step 1), one needs to zoom into each life cycle separately, analysing the selection pressures acting on each one of the demographic processes composing the life cycle. In doing so, one can inspect the selection pressures that have generated the patterns found in step 1. Step 2 (Fig. 1B) requires obtaining the partial derivatives of the deterministic population growth rate, λ_t, relative to all matrix elements of the MPM of interest (*i.e.,* elasticities of λ_t w.r.t each demographic process in the MPM). Step 2 therefore informs on the strength of the natural selection on each of the demographic processes.

Finally, in step 3, one assesses the pattern of nonlinear selection by using the self-second derivatives of λ_t with respect to each demographic process (Fig. 1C). This final step reveals the potential nonlinear selection pressures on all the demographic processes within a life cycle, rather than only the most important one. This final step is key to understanding the evolutionary processes (*i.e.,* types of nonlinear selection) that the demographic processes are subjected to. Without understanding the evolutionary processes operating on the demographic processes, the pattern observed in step 1 might be artefactual. Moreover, step 1 is founded on the assumption that the importance of a demographic process, as indicated by its elasticity, remains unchanged over time. However, stochastic environments can substantially alter elasticity patterns throughout a life cycle (e.g., Lawler et al. 2009).

Steps 2 and 3 of the framework feature selection pressures that have been averaged over the contiguous time periods. This means that the resulting patterns are based on how λ_t (obtained from averaging all sequential MPMs across the duration of the study) would be affected if a demographic process were perturbed. Therefore, steps 2 and 3 are based on a different information than step 1, and can thus complete our understanding of the role of selection pressures on shaping demographic patterns across multiple species.

Another important asset of step 3 above includes the notion that the relative importance (elasticity) of demographic processes themselves changes with changing environment (Stearns 1992). In other words, the extent to which λ_t is sensitive to perturbations in a specific demographic process is *dynamic* (Kroon, Hans *et al.* 2000). Thus, the self-second derivatives generate information on how the sensitivity (or elasticity) of λ_t – based on which the entire variance continuum of species is produced in step 1 – might change. If the sensitivity (or elasticity) of λ_t can change, then it is important to know which demographic processes are most prone to trigger such a change. In the example of a hypothetical wolf species (Fig. 1), this means that if the reproduction of the third age-class individuals (matrix element $a_{1,3}$) decreased, the sensitivity of λ_t to $a_{1,3}$ would increase (square with the largest black dot, Fig. 1C). Consequently, with increased environmental variability, the key demographic process used to place this species onto the variance continuum in step 1 might change from remaining in the fourth age class (matrix element $a_{4,4}$, Fig. 1B) to reproduction of the third age-class (matrix element $a_{1,3}$, Fig. 1C).

Combining the three steps of our framework allows for the clear, quantitative, holistic identification of evidence to support (or reject) the DBH. Steps 2 and 3 offer key insights as to *why* a given species or population is placed on either the buffered or the non-buffered (potentially labile) end of the variance continuum. A clear and unequivocal evidence for support towards the DBH consists of: (1) a species or population being positioned near the 0 end of the continuum (the right-hand side) in step 1; (2) this species' or populations' life cycle having one or more demographic processes with highest elasticity values in step 2; and (3) the same demographic process displaying the highest elasticity in step 2 with negative self-second derivative values in step 3. In this sense, Figure 1B shows that, for the chosen population of a hypothetical wolf species, the most important demographic process is remaining in the fourth stage (MPM element $a_{4,4}$), as this demographic process results in highest elasticity value (Fig. 1B yellow square). However, Fig. 1C reveals that $a_{4,4}$ is under little selection pressure for variance reduction. Thus, there is no evidence for DBH from the third step of the framework (*i.e.,* no concave selection forces), therefore, the lack of concave selection forces on the key demographic process within wolf's life cycle explains why this species is placed on the left-hand side of the variance continuum (Fig. 1A).

Species placed on the non-buffered end of the continuum is the first but not last step to evidence demographic lability. Indeed, locating a species on the non-buffered end of the variance continuum is a necessary but not sufficient condition for evidence in favour of the DLH. It is key highlighting here that demographic buffering and lability do not represent two extremes of the same continuum. The variance continuum allocates the species or populations from strongly buffered to non-buffered, but to test the DLH, a further step is needed.

Although not our primary goal here, we briefly introduce said step 4. To establish compelling evidence for or against the DLH, it is essential to fulfil several criteria. First, sufficient data across various environments (over time or space) are required to construct reaction norms that depict how a demographic process responds to environmental changes (Morris et al., 2008; Koons et al., 2009). Second, non-linear relationships between demographic processes and the environment must be established based on these reaction norms. Lastly, to identify demographic processes where an increase in the mean value has a stronger positive impact on population growth rate than the detrimental effect of increased variance. This latter condition is only achieved when the vital rate-environment reaction norm is convex (U-shaped; Morris et al. 2008; Koons et al. 2009). Importantly, we note that more likely than previously thought (*e.g.,* Pfister 1998), species do not exist as purely buffering or labile, but that within species, some vital rates may be buffered, other labile, and others insensitive to the environment (*e.g.*, Doak et al. 2005). Deciphering generality in this likely complex pattern should attract much research attention going forward, in our opinion.

Demographic buffering in mammals: a case study using the unified framework

We demonstrate the performance of our framework using 44 MPMs from 34 mammal species. Mammals are of special interest here for two reasons: (1) mammalian life histories have been well studied (Gillespie 1977; Stearns 1983; Bielby *et al.* 2007; Jones 2011); and (2) some of their populations have already been assessed in terms of buffering, particularly for primates (Morris *et al.* 2008, 2011; Reed & Slade 2012; Rotella *et al.* 2012; Campos *et al.* 2017). Together, the well-studied life histories and previous information about the occurrence of buffering in mammals provide the necessary information to make accurate predictions and validate the performance of the proposed framework.

We used Matrix Population Models from 40 out of 139 studies with mammals available in the COMADRE database v.3.0.0 (Salguero-Gómez *et al.* 2016). These 40 populations encompass 34 species from eight taxonomic orders. We included these MPMs in our analyses because they provide values of demographic processes (a_{ij}) for three or more contiguous time periods, thus allowing us to obtain the stochastic elasticity of each a_{ij}. Although we are aware that not all possible temporal variation in demographic processes may have been expressed within this period, we assumed three or more transitions are enough to provide sufficient variation for population comparison. At least three contiguous time periods - a common selection criteria in comparative studies of stochastic demography (Compagnoni *et al.* 2023) - also allowed to test and showcase our framework. Fortunately, several long-lived species, characterized by low variation in their demographic processes, were studied for a long time (*e.g.,* some primates in our dataset have been studied for over 20 years – Morris *et al*. 2011). We removed the populations where either only survival or only reproduction rates were reported, because of the impossibility to calculate the stochastic growth rate. A detailed description of the analysed data and their original sources are available in supplementary material (Supplementary Material, Table S1).

Homo sapiens was included in our analyses because it is the only mammalian species in which second-order derivatives have been applied (Caswell 1996). Therefore, *Homo sapiens* provides an ideal basis for comparisons among species. The data for *Homo sapiens* were gathered from 26 modern populations located in various cities, allowing us to construct a spatiotemporal variance. It is important to note that in this case, we are not working with true temporal variance but rather a variance that encompasses both spatial and temporal aspects.

For steps 2 and 3 of our framework, we utilized a subset of 16 populations (including *Homo sapiens*) whose population projection matrices (MPMs) were organized by age. We specifically selected these populations because their life cycles can be summarized by two main demographic processes: survival and contribution to recruitment of new individuals. The contribution to recruitment can be interpreted as either the mean reproductive output for each age class or an approximation thereof, depending on how the matrices are structured (Ebert 1999). One advantage of using such matrices is that they encompass only two types of demographic processes, namely survival and recruitment, eliminating the need to account for multiple transitions between different life stages.

To perform the step 1 of our framework and obtain the $\Sigma E_{a_{ij}}^{S^{\sigma}}$ (and $\Sigma E_{a_{ij}}^{S^{\mu}}$), we followed Tuljapurkar *et al.* (2003). To perform step 2 of our framework, we calculated the deterministic elasticities of each demographic process extracted using the *popbio* package. All analyses were performed using R version 3.5.1 (R Core team, 2018). Finally, to perform the step 3 of our framework the self-second derivatives were adapted from *demogR* (Jones 2007) following Caswell 1996 and applied for the mean MPM.

Results

We ranked 40 populations from the 34 identified mammal species according to the cumulative impact of variation in demographic processes on λ_s using the step 1 of our framework (Fig. 2). Additional information is provided in the supplementary material (Table S1). Most of the analysed orders were placed on the low-variance end of the variance continuum (Fig. 2). The smallest contributions of variation in demographic processes (*i.e.,* maximum value of $\Sigma E_{a_{ij}}^{S^\sigma}$, note that $\Sigma E_{a_{ij}}^{S^\sigma}$ ranges from 0 to -1), suggesting more buffered populations, were assigned to Primates: northern muriqui (*Brachyteles hyphoxantus*, $\Sigma E_{a_{ij}}^{S^\sigma}$ = -0.09 × 10^{-4} ± 0.12 × 10^{-4}) (mean ± standard deviation) (Fig. 2 silhouette a), mountain gorilla (*Gorilla beringhei*, $\Sigma E_{a_{ij}}^{S^\sigma}$ = -0.24 × 10^{-4} ± 0.08 × 10^{-4}) (Fig. 2 silhouette b), followed by the blue monkey (*Cercopithecus mitis*, $\Sigma E_{a_{ij}}^{S^\sigma}$ = -0.63 × 10^{-4} ± 0.06 × 10^{-4}) (Fig. 2 silhouette c). The first non-primate species placed near the low-variance end of the continuum was the Columbian ground squirrel (*Urocitellus columbianus*, Rodentia, $\Sigma E_{a_{ij}}^{S^\sigma}$ = -0.003 ± 0.002) (Fig. 2 silhouette d). The species with the highest contribution of variation in demographic processes placed at the high-variance end of the continuum was the stoat (*Mustela erminea*, Carnivora, $\Sigma E_{a_{ij}}^{S^\sigma}$ = -0.35 ± 0.02) (Fig. 2 silhouette e). All the 14 primate populations supported the DBH, occupying the right-hand side of the variance continuum, with exception of the Patas monkey (*Erythrocebus patas*, Primates, $\Sigma E_{a_{ij}}^{S^\sigma}$ = -0.05 ± 0.03) (Fig. 2 silhouette f). The snowshoe hare (*Lepus americanus*, Lagomorpha, $\Sigma E_{a_{ij}}^{S^\sigma}$ = -0.29 ± 0.16) (Fig. 2 silhouette g) and the Bush rat (*Rattus fuscipes*, Rodentia, $\Sigma E_{a_{ij}}^{S^\sigma}$ = -0.25 ± 0.03) (Fig. 2 silhouette h) appear on the high-variance end of the continuum.

As predicted for the steps 2 and 3, we could not observe a clear pattern in support of the DBH. This finding means that the demographic processes with the highest elasticity values failed to display strongly negative self-second derivatives (Fig. 3). Particularly for majority of primates - with the lack or minor temporal variation in demographic processes - demographic processes with high elasticities had positive values for the self-second derivatives (indicated by yellow squares with white dots in Fig. 3). Examples of primate species exhibiting high elasticities and positive values for the self-second derivatives and include northern muriqui (*Brachyteles hypoxanthus*), mountain gorilla (*Gorilla beringei*), white-faced capuchin monkey (*Cebus capucinus*), rhesus monkey (*Macaca mulatta*), blue monkey (*Cercopithecus mitis*), Verreaux's sifaka (*Propithecus verreauxi*) and olive baboon (*Papio cynocephalus*) (Fig. 3). This implies that the key demographic processes influencing λ_t are not subject to selective pressure for reducing their temporal variability. However, even though the primates were positioned closer to the low-variance end of the continuum in step 1, the evidence from steps 2 and 3 does not support DBH.

The killer whale showed similar controversy between step 1 and steps 2-3 results as most primates. In step 1, the killer whale was positioned at the buffered end of the variance continuum (*Orcinus orca*, Cetacea, $\Sigma E_{a_{ij}}^{S^{\sigma}} = -0.70 \times 10^{-4} \pm 1.04 \times 10^{-5}$) (Fig. 2 silhouette not shown). However, steps 2 and 3 show that the three demographic processes in killer whale life cycle with highest elasticity values (matrix elements $a_{2,2}$, $a_{3,3}$ and $a_{4,4}$) are not under selection pressures for reducing their temporal variance, but the opposite (depicted by yellow and green squares with white dots, Fig. 3).

The only primate species exhibiting DBH evidence in steps 2 and 3 was human. In human, demographic parameters representing survival from first to second age class (matrix element $a_{2,1}$) displayed high elasticities and negative self-second derivatives (depicted as yellow squares with black dots in Fig. 3). Evidence supporting the DBH was also found in the Columbian ground squirrel (*Urocitellus columbianus*), where, similar to humans, survival from the first to the second age class (matrix element $a_{2,1}$) showed indications of selection acting to reduce its variance. Accordingly, the Columbian ground squirrel was positioned close to the buffered end of the variance continuum in step 1. Hence, the Columbian ground squirrel was the sole species with consistent DBH support across all three steps of the framework.

The Soay sheep (*Ovis aries*) was the species furthest from the buffered end of the variance continuum that enabled to perform steps 2 and 3. For the Soay sheep, remaining in the third age class (matrix element $a_{3,3}$) has the major influence on λ_t and is under selection pressure to have its variance increased. The latter characteristics reveal conditions for the DLH support even though the species is placed closer to the buffered end of the variance continuum.

Steps 2 and 3 illustrate the importance of examining DBH evidence on the intraspecific level. These two steps of the framework identify the simultaneous acting of concave and convex selection on different demographic processes but within a single life cycle. In polar bear (*Ursus maritimus*), the key demographic process (matrix element $a_{4,4}$) is under convex selection, as depicted by a yellow square with a white dot in Fig. 3. However, the demographic process with the second highest elasticity value (matrix element $a_{5,4}$) is under strong concave selection (depicted by a light green square with a black dot in Fig. 3).

By adding step 3 to the framework, another important information was added. The high absolute values of self-second derivatives (large dots, either black or white, Fig. 3) indicate where the sensitivity of λ_t to demographic parameters is itself prone to environmental changes. For instance, if the value of $a_{5,4}$ for polar bear increased, the sensitivity of λ_t to $a_{5,4}$ would decrease because the self-second derivative of $a_{5,4}$ is highly negative (depicted by the largest black dot in polar bear MPM). Vice versa holds for the $a_{4,4}$ demographic process, where an increase in the value of $a_{4,4}$ would increase λ_t's sensitivity to $a_{4,4}$, because the self-second derivative of $a_{5,4}$ is highly positive (depicted by the largest white dot in polar bear

MPM). Thus, sensitivities (or equally elasticities) of demographic processes with high absolute values for self-second derivatives can easily change - potentially changing the key demographic process used for allocating species into the variance continuum in step 1 of the framework.

Discussion

In the Anthropocene, identifying and quantifying mechanisms of species responses to stochastic environments holds crucial importance. This importance is particularly tangible in the context of the unprecedented environmental changes and uncertainties that impact the dynamics and persistence of natural populations (Boyce *et al.* 2006). Correlational demographic analysis, whereby the importance of demographic processes and their temporal variability is examined (e.g., Pfister 1998), has attempted to identify how species may buffer against the negative effects of environmental stochasticity. However, these widely used approaches have important limitations (see Introduction and Hilde et al. 2020). Our novel framework overcomes said limitations by providing a rigorous approach to test the demographic buffering hypothesis (DBH; Pfister 1998; Hilde et al. 2020).

Evidencing demographic buffering is not straightforward. Indeed, through the analysis of stochastic population growth rate (λ_s) in our application of the framework to 44 populations of 34 species, we identify the highest density of natural populations near the buffered end of the variance continuum (step 1), indicating possible support for the DBH. However, we show that the same species then fail to exhibit signs of concave (∩-shaped) selection on the key demographic parameters when further analyses are performed averaging the variation across the duration of each study (steps 2 and 3). This finding confirms that placing the species near the buffered end of the variance continuum is *necessary* but not *sufficient* to test the DBH. Indeed, buffering occurs when concave selection forces act on the key demographic parameter (Caswell 1996, 2001; Shyu & Caswell 2014).

Combining the three steps into a unified framework is of outmost importance. In steps 2 and 3 of the framework, we find relatively limited overall support for the DBH in the examination of our 16 (out of 34 in step 1) studied animal species. Step 3 of our framework reveals that the role of natural selection shaping temporal variation in demographic processes is more complex than expected by the DBH alone. Indeed, demographic processes within our study populations are often under a mix of convex and concave selection. This mix of selection patterns was already suggested by Doak *et al.* (2005). Here, only two out of 16 mammal species revealed concave selection acting on the key demographic processes (Columbian ground squirrel [*Urocitellus columbianus*], and humans, [*Homo sapiens sapiens*]). These two species were also placed near the buffered end of the variance continuum, therefore meeting all the necessary conditions to diagnose clear support in favour of DBH. However, finding 12.5% (two out of 16) species that meet the criteria for demographic buffering is not in concordance with previous studies. Support for the DBH has been reported across 22 ungulate species (Gaillard & Yoccoz 2003). In the one ungulate we examined, the moose (*Alces alces*), we find only partial support for DBH in adult survival, since this species is placed near the buffered end of the variance continuum in step 1 but does not show concave selection pressures on adult survival in step 2/3, as predicted by the DBH.

Our overall findings reveal varying levels of support for the notion that adult survival in long-lived species tends to be buffered. Indeed, Gaillard *et al.* (1998) found that adult female survival varied considerably less than juvenile survival in large herbivores. This finding was also supported by further studies in ungulates (Gaillard & Yoccoz 2003), turtles (Heppell 1998), vertebrates and plants (Pfister 1998), and more recently across nine (out of 73) species of plants (McDonald *et al.* 2017).

When placing our study species along a variance continuum (step 1), primates tend to be located on the buffered end. However, most primates displayed convex –instead of the expected concave– selection on adult survival. Similar results, where the key demographic process failed to display constrained temporal variability, have been reported for long-lived seabirds (Doherty *et al.* 2004). One explanation for the unexpected convex selection on adult survival involves trade-offs, as suggested by Doak et al. (2005). When two demographic parameters are negatively correlated, the variance of population growth rate (λ) can be increased or decreased (Evans & Holsinger 2012; Compagnoni *et al.* 2016). The well-established trade-off between survival and fecundity (e.g., Stearns 1992; Roff & Fairbairn 2007) might explain the observed concave selection signatures on late fecundity and convex selection on adult survival. Because variation in primate recruitment is already constrained by physiological limitations (Campos *et al.* 2017), when adult survival and recruitment are engaged in a trade-off, this trade-off might lead to our unexpected result. Here, future studies may benefit from deeper insights via cross-second derivatives (Caswell 1996, 2001) to investigate correlations among demographic processes.

Examining the drivers of demographic buffering has become an important piece of the ecological and evolutionary puzzle of demography. As such, testing the DBH can help us better predict population responses to environmental variability, climate change, and direct anthropogenic disturbances (Pfister 1998; Boyce *et al.* 2006; McDonald *et al.* 2017; Vázquez *et al.* 2017). By setting the DBH into a broader and integrated framework, we hope to enhance comprehension and prediction of the implications of heightened environmental stochasticity on the evolution of life history traits. This understanding is crucial in mitigating the risk of extinction for the most vulnerable species.

Acknowledgements

This study was financed in part by the *Coordenação de Aperfeiçoamento de Pessoal de Nível Superior* - Brasil (CAPES) - Finance Code 001. GSS was supported by CAPES and CNPq

(301343/2023-3). RS-G was supported by a NERC Independent Research Fellowship (NE/M018458/1). MK was supported by the European Commission through the Marie Skłodowska-Curie fellowship (MSCA MaxPersist #101032484) hosted by RSG.

Data availability

The demographic data used in this paper are open-access and available in the COMPADRE Plant Matrix Database (v. 5.0.1; https://compadre-db.org/Data/ Compadre). A list of the studies and species used here is available in Supplementary Material (Table S1). If the manuscript is accepted, the data and code supporting the results will be archived on Zenodo. The data and code specific DOI will then be included in our "Data availability" statement.

References

Barraquand, F. & Yoccoz, N.G. (2013). When can environmental variability benefit population growth? Counterintuitive effects of nonlinearities in vital rates. *Theor Popul Biol*, 89, 1–11.

Bielby, J., Mace, G.M., Bininda-Emonds, O.R.P., Cardillo, M., Gittleman, J.L., Jones, K.E., *et al.* (2007). The Fast-Slow Continuum in Mammalian Life History: An Empirical Reevaluation. *Am Nat*, 169, 748–757.

Bonsall, M.B. & Klug, H. (2011). The evolution of parental care in stochastic environments. *J Evol Biol*, 24, 645–655.

Boyce, M.S., Haridas, C. V., Lee, C.T., Boggs, C.L., Bruna, E.M., Coulson, T., *et al.* (2006). Demography in an increasingly variable world. *Trends Ecol Evol*, 21, 141–148.

Brodie, E.I., Moore, A. & Janzen, F. (1995). Visualizing and quantifying natural selection. *Trends Ecol Evol*, 10, 313–318.

Campos, F.A., Morris, W.F., Alberts, S.C., Altmann, J., Brockman, D.K., Cords, M., *et al.* (2017). Does climate variability influence the demography of wild primates? Evidence from long-term life-history data in seven species. *Glob Chang Biol*, 23, 4907–4921.

Carslake, D., Townley, S. & Hodgson, D.J. (2008). Nonlinearity in eigenvalue-perturbation curves of simulated population projection matrices. *Theor Popul Biol*, 73, 498–505.

Caswell, H. (1996). Second Derivatives of Population Growth Rate: Calculation and Applications. *Ecology*, 77, 870–879.

Caswell, H. (2001). *Matrix Population Models: Construction, Analysis, and Interpretation*. Sinauer Associates Inc. Publishers, Sunderland, Massachusetts, USA.

Charlesworth, B. (1994). *Evolution in age-structured populations*. second edi. Cambridge University Press.

Le Coeur, C., Yoccoz, N.G., Salguero-Gómez, R. & Vindenes, Y. (2022). Life history adaptations to fluctuating environments: Combined effects of demographic buffering and lability. *Ecol Lett*, 1–13.

Compagnoni, A., Bibian, A.J., Ochocki, B.M., Rogers, H.S., Schultz, E.L., Sneck, M.E., *et al.* (2016). The effect of demographic correlations on the stochastic population dynamics of perennial plants. *Ecol Monogr*, 86, 480–494.

Compagnoni, A., Evers, S. & Knight, T. (2023). Spatial replication can best advance our understanding of population responses to climate. *bioRxiv*, https://doi.org/10.1101/2022.06.24.497542.

Doak, D.F., Morris, W.F., Pfister, C., Kendall, B.E. & Bruna, E.M. (2005). Correctly Estimating How Environmental Stochasticity Influences Fitness and Population Growth. *Am Nat*, 166, E14–E21.

Doak, D.F., Waddle, E., Langendorf, R.E., Louthan, A.M., Isabelle Chardon, N., Dibner, R.R., *et al.* (2021). A critical comparison of integral projection and matrix projection models for demographic analysis. *Ecol Monogr*, 91, e01447.

Doherty, P.F., Schreiber, E.A., Nichols, J.D., Hines, J.E., Link, W.A., Schenk, G.A., *et al.* (2004). Testing life history predictions in a long-lived seabird: A population matrix approach with improved parameter estimation. *Oikos*, 105, 606–618.

Easterling, M.R., Ellner, S.P. & Dixon, P.M. (2000). Size-Specific Sensitivity: Applying a New Structured Population Model. *Ecology*, 81, 694–708.

Ellner, S.P., Childs, D.Z. & Rees, M. (2016). Data-driven Modelling of Structured Populations.

Evans, M.E.K. & Holsinger, K.E. (2012). Estimating covariation between vital rates : A simulation study of connected vs . separate generalized linear mixed models (GLMMs). *Theor Popul Biol*, 82, 299–306.

Ferreira, M., Kajin, M., Vieira, M., Zangrandi, P., Cerqueira, R. & Gentile, R. (2013). Life history of a neotropical marsupial: Evaluating potential contributions of survival and reproduction to population growth rate. *Mamm Biol*, 78, 406–411.

Franco, M. & Silvertown, J. (2004). A comparative demography of plants based upon elasticities of vital rates. *Ecology*, 85, 531–538.

Gaillard, J.-M. & Yoccoz, N. (2003). Temporal Variation in Survival of Mammals: a Case of Environmental Canalization? *Ecology*, 84, 3294–3306.

Gillespie, J.H. (1977). Natural Selection for Variances in Offspring Numbers: A New Evolutionary Principle. *Am Nat*, 111, 1010–1014.

Griffith, A.B. (2017). Perturbation approaches for integral projection models. *Oikos*, 126, 1675–1686.

Haridas, C.V. & Tuljapurkar, S. (2005). Elasticities in Variable Environments: Properties and Implications. *Am Nat*, 166, 481–495.

Healy, K., Ezard, T.H.G., Jones, O.R., Salguero-Gómez, R. & Buckley, Y.M. (2019). Animal life history is shaped by the pace of life and the distribution of age-specific mortality and reproduction. *Nat Ecol Evol*, 3, 1217–1224.

Heppell, S.S. (1998). Application of Life-History Theory and Population Model Analysis to Turtle Conservation. *Copeia*, 1998, 367.

Hilde, C.H., Gamelon, M., Sæther, B.-E., Gaillard, J.-M., Yoccoz, N.G. & Pélabon, C. (2020). The Demographic Buffering Hypothesis: Evidence and Challenges. *Trends Ecol Evol*, 35, 523–538.

Jäkäläniemi, A., Ramula, S. & Tuomi, J. (2013). Variability of important vital rates challenges the demographic buffering hypothesis. *Evol Ecol*, 27, 533–545.

Jones, J.H. (2007). Journal of Statistical Software, 22.

Jones, J.H. (2011). Primates and the evolution of long, slow life histories. *Current Biology*, 21, R708–R717.

Jongejans, E., De Kroon, H., Tuljapurkar, S. & Shea, K. (2010). Plant populations track rather than buffer climate fluctuations. *Ecol Lett*, 13, 736–743.

Koons, D.N., Pavard, S., Baudisch, A. & Jessica E. Metcalf, C. (2009). Is life-history buffering or lability adaptive in stochastic environments? *Oikos*, 118, 972–980.

Kroon, Hans, D., van Groenendael, J. & Ehrlen, J. (2000). Elasticities: A review of methods and model limitations.

Lawler, R.R., Caswell, H., Richard, A.F., Ratsirarson, J., Dewar, R.E. & Schwartz, M. (2009). Demography of Verreaux's sifaka in a stochastic rainfall environment. *Oecologia*, 161, 491–504.

McDonald, J.L., Franco, M., Townley, S., Ezard, T.H.G., Jelbert, K. & Hodgson, D.J. (2017). Divergent demographic strategies of plants in variable environments. *Nat Ecol Evol*, 1, 0029.

Morris, W.F., Altmann, J., Brockman, D.K., Cords, M., Fedigan, L.M., Pusey, A.E., *et al.* (2011). Low Demographic Variability in Wild Primate Populations: Fitness Impacts of Variation, Covariation, and Serial Correlation in Vital Rates. *Am Nat*, 177, E14–E28.

Morris, W.F. & Doak, D.F. (2004). Buffering of Life Histories against Environmental Stochasticity: Accounting for a Spurious Correlation between the Variabilities of Vital Rates and Their Contributions to Fitness. *Am Nat*, 163, 579–590.

Morris, W.F., Pfister, C.A., Tuljapurkar, S., Haridas, C. V., Boggs, C.L., Boyce, M.S., *et al.* (2008). Longevity can buffer plant and animal populations against changing climatic variability. *Ecology*, 89, 19–25.

Pélabon, C., Hilde, C.H., Einum, S. & Gamelon, M. (2020). On the use of the coefficient of variation to quantify and compare trait variation. *Evol Lett*, 4, 180–188.

Pfister, C. (1998). Patterns of variance in stage-structured populations: Evolutionary predictions and ecological implications. *Proceedings of the National Academy of Sciences*, 95, 213–218.

Reed, A.W. & Slade, N.A. (2012). Buffering and plasticity in vital rates of oldfield rodents. *Journal of Animal Ecology*, 81, 953–959.

Rodríguez-Caro, R.C., Capdevila, P., Graciá, E., Barbosa, J.M., Giménez, A. & Salguero-Gómez, R. (2020). The demographic buffering strategy has a threshold of effectiveness to increases in environmental stochasticity. *bioRxiv*, 1–41.

Roff, D.A. & Fairbairn, D.J. (2007). The evolution of trade-offs: Where are we? *J Evol Biol*, 20, 433–447.

Rotella, J.J., Link, W.A., Chambert, T., Stauffer, G.E. & Garrott, R.A. (2012). Evaluating the demographic buffering hypothesis with vital rates estimated for Weddell seals from 30 years of mark – recapture data, 162–173.

Salguero-Gómez, R., Jones, O.R., Archer, C.R., Bein, C., de Buhr, H., Farack, C., *et al.* (2016). COMADRE: A global data base of animal demography. *Journal of Animal Ecology*, 85, 371–384.

Shyu, E. & Caswell, H. (2014). Calculating second derivatives of population growth rates for ecology and evolution. *Methods Ecol Evol*, 5, 473–482.

Stearns, S. (1992). *The Evolution of Life Histories*. Oxford University Press, New York, USA.

Stearns, S.C. (1983). The Influence of Size and Phylogeny on Patterns of Covariation among Life-History Traits in the Mammals. *Oikos*, 41, 173.

Sutherland, W.J., Freckleton, R.P., Godfray, H.C.J., Beissinger, S.R., Benton, T., Cameron, D.D., *et al.* (2013). Identification of 100 fundamental ecological questions. *Journal of Ecology*, 101, 58–67.

Tuljapurkar, S., Gaillard, J.-M. & Coulson, T. (2009). From stochastic environments to life histories and back. *Philosophical Transactions of the Royal Society B: Biological Sciences*, 364, 1499–1509.

Tuljapurkar, S., Horvitz, C.C. & Pascarella, J.B. (2003). The Many Growth Rates and Elasticities of Populations in Random Environments. *Am Nat*, 162, 489–502.

Vázquez, D.P., Gianoli, E., Morris, W.F. & Bozinovic, F. (2017). Ecological and evolutionary impacts of changing climatic variability. *Biological Reviews*, 92, 22–42.

Wang, J., Yang, X., Silva Santos, G., Ning, H., Li, T., Zhao, W., *et al.* (2023). Flexible demographic strategies promote the population persistence of a pioneer conifer tree (Pinus massoniana) in ecological restoration. *For Ecol Manage*, 529, 120727.

Figure 1

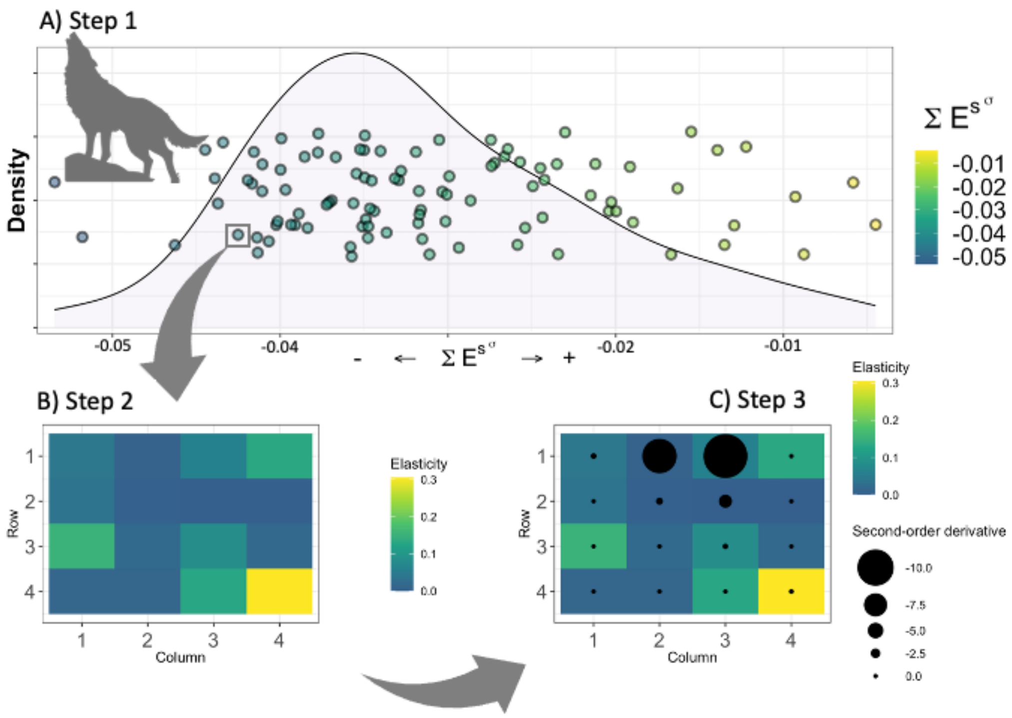
A) Step 1
Density
-0.05
-0.04
-0.02
-0.01
- ← Σ E^s^σ → +
Σ E^s^σ
-0.01
-0.02
-0.03
-0.04
-0.05
B) Step 2
Row
1
2
3
4
Column
1
2
3
4
Elasticity
0.3
0.2
0.1
0.0
C) Step 3
Row
1
2
3
4
Column
1
2
3
4
Elasticity
0.3
0.2
0.1
0.0
Second-order derivative
-10.0
-7.5
-5.0
-2.5
0.0

Figure 2

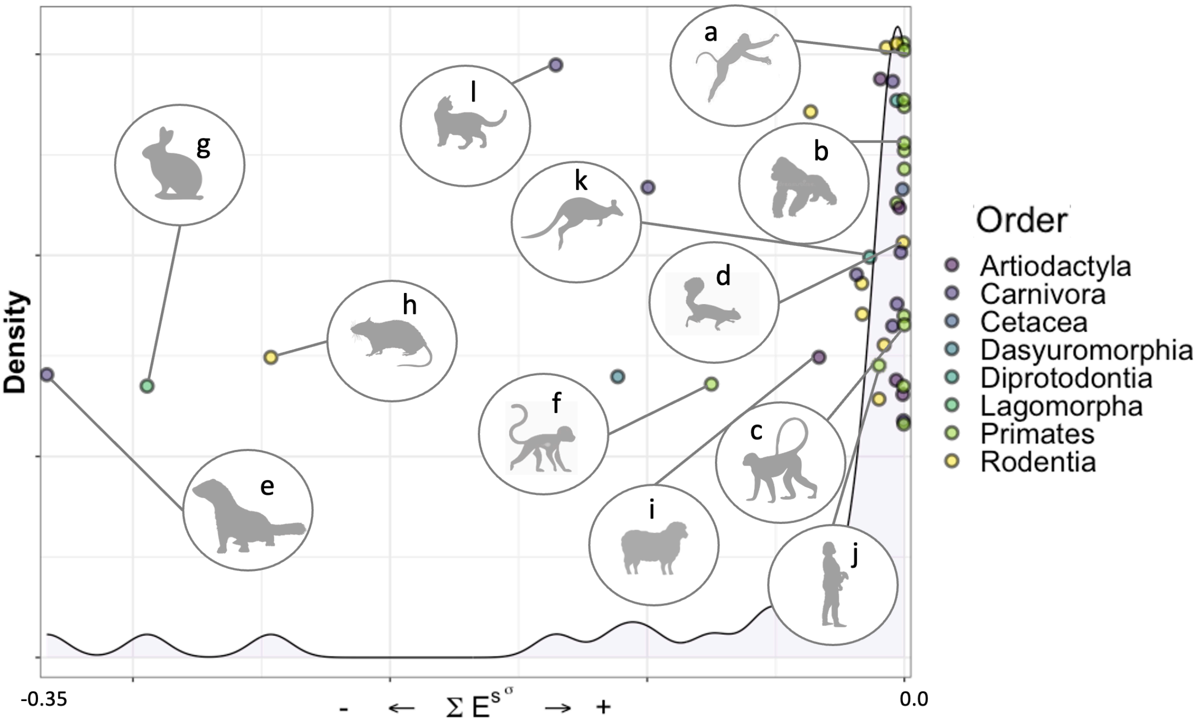
Density
-0.35
0.0
- ← Σ E$^{s^{\sigma}}$ → +
a
b
c
d
e
f
g
h
i
j
k
l
Order
Artiodactyla
Carnivora
Cetacea
Dasyuromorphia
Diprotodontia
Lagomorpha
Primates
Rodentia

Figure 3

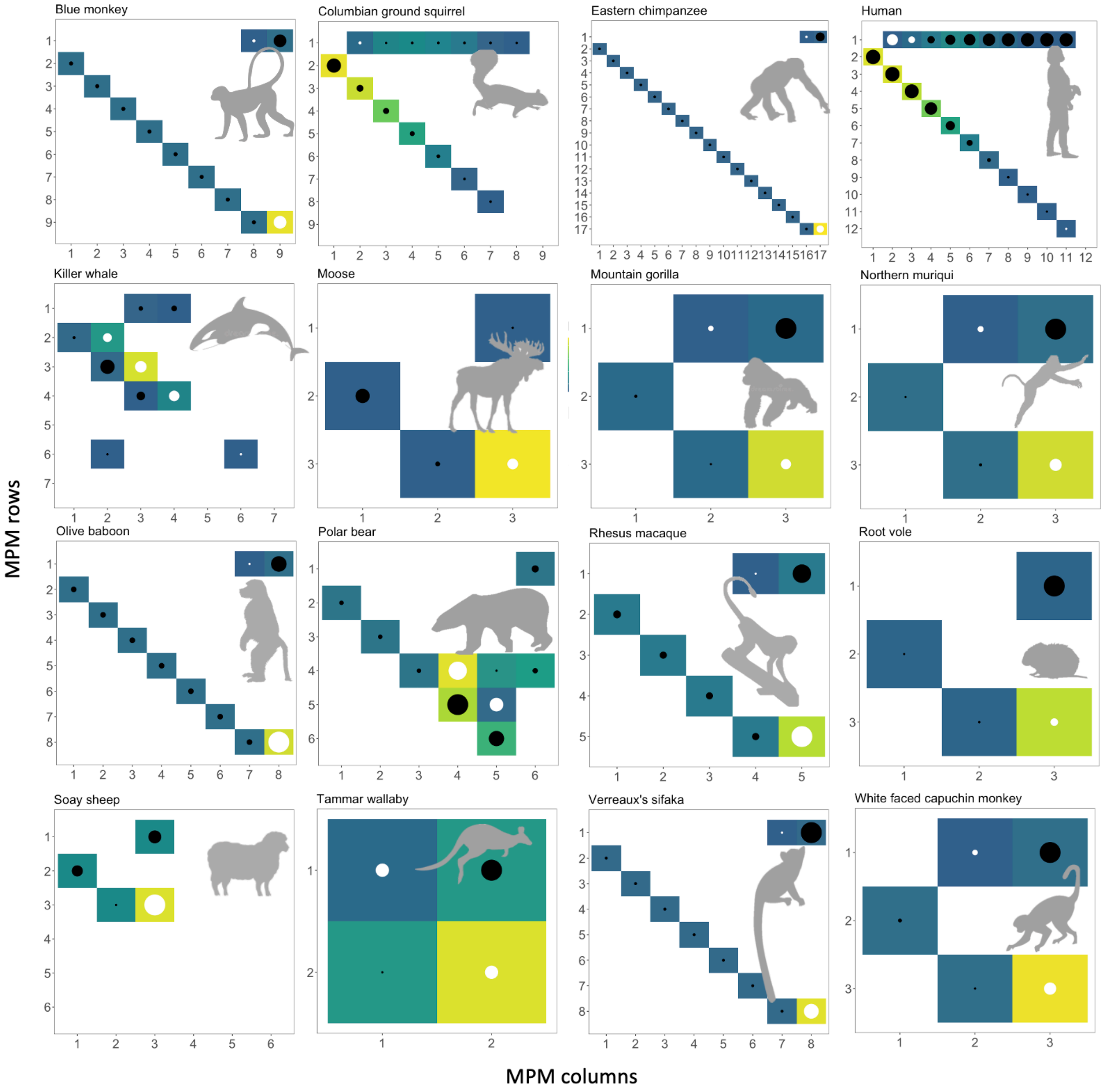
Blue monkey
Columbian ground squirrel
Eastern chimpanzee
Human
Killer whale
Moose
Mountain gorilla
Northern muriqui
Olive baboon
Polar bear
Rhesus macaque
Root vole
Soay sheep
Tammar wallaby
Verreaux's sifaka
White faced capuchin monkey
MPM rows
MPM columns

Figure legends

Figure 1. A three-step framework proposed to: Step 1 - allocate species and/or populations on a variance continuum (plot A, dots representing 50 hypothetical species). The variance continuum operates at the interspecific level (see text) and is represented by partitioning the sum of all the stochastic elasticities ($\Sigma E^{S}_{a_{ij}}$) into two compounds: i) sums of stochastic elasticities with respect to the variance ($\Sigma E^{S^{\sigma}}_{a_{ij}}$), and ii) sums of stochastic elasticities with respect to the mean ($\Sigma E^{S^{\mu}}_{a_{ij}}$). The first step of our framework shows the variance compound of the sums of stochastic elasticities forming a continuum where the right-hand side of the plot represents species (or populations) where a perturbation of variance of the most important demographic process results in weak or no impact on λ_s (yellow dots). The yellow-dotted species (or populations) can be classified as having *buffered life-cycles (supporting the DBH)* – based on the most important demographic process for the λ_s. The left-hand side of the graph represents species (or populations) where a perturbation of the variance of the most important demographic process results in strong impact on λ_s (blue dots). Thus, the blue-dotted species (or populations) can be classified as having *unbuffered life cycles (potentially supporting DLH,* see text) – based on the most important demographic process for the λ_s. The jitter applied on the y-axis has no biological meaning. Step 2 - Access the linear selection pressures for individual species or populations at intraspecific level (see text) (plot B). Step 2 displays the elasticities of the deterministic population growth rate (λ_t) for a hypothetical population of wolf and reveals the linear selection gradients. Step 3 - Access the nonlinear selection pressures at the intraspecific level (see text) (plot C). In the third step self-second derivatives for the corresponding demographic processes from step 2 are displayed.

Figure 2. Results for step 1 of our framework showing the sum of stochastic elasticities with respect to the variance $\Sigma E^{S^{\sigma}}_{a_{ij}}$ increase caused by a perturbation in the most relevant demographic process. The 40 populations from 34 species of mammals from the COMADRE database are ranked into the variance continuum from strongly buffered (right-hand side, supporting the DBH) to more variable, less buffered (left-hand side, potentially supporting the DLH, see text). Colors represent different taxonomic orders with Primates occupying the right-hand side. Silhouettes: a) *Brachyteles hyphoxantus*, b) *Gorilla beringhei*, c) *Cercopithecus mitis*, d) *Urocitellus columbianus,* e) *Mustela erminea*, f) *Erythrocebus patas*, g) *Lepus americanus*, h) *Rattus fuscipes*, i) *Ovis aries*, j) *Homo sapiens*, k) *Macropus eugenii*, and l) *Felis catus*. The jitter applied on the y-axis has no biological meaning.

Figure 3: Results from steps 2 and 3 of the proposed framework (see Fig. 2B, C). The 16 plots represent populations where the MPMs built by ages were available in the COMADRE database (see text). The color scale represents elasticity values for each of the demographic processes in the MPM, where yellow represents high and blue low elasticity values. No color means elasticity=0. Because the aim of step 2 is to identify the most important demographic process within each species' life cycle (the intraspecific level, see text) - not to compare the elasticity values among species - each plot has its own scale (see end of legend). The black dots represent negative self-second derivatives of λ_t - thus concave selection - and the white dots represent positive self-second derivatives of λ_t - thus convex selection. The dot sizes are scaled by the absolute value of self-second derivatives, where the smaller the dot, the closer a self-second derivative is to 0, indicting weak or no selection. Large dots indicate strong selection forces. Scales ($E_{\text{min-max}}$=elasticity minimum and maximum value, $SSD_{\text{min-max}}$=self-second derivative minimum and maximum value): Blue monkey $E_{\text{min-max}}$=0.00-0.52, $SSD_{\text{min-max}}$=-1.25-1.27; Columbian ground squirrel: $E_{\text{min-max}}$=0.00-0.23, $SSD_{\text{min-max}}$=-1.48-0.01;

Eastern chimpanzee: $E_{min-max}$=0.00-0.60, $SSD_{min-max}$=-4.39-2.59; Human: $E_{min-max}$=0.00-0.18, $SSD_{min-max}$=-0.15-0.08; Killer whale: $E_{min-max}$=0.00-0.55, $SSD_{min-max}$=-5.72-3.43; Moose: $E_{min-max}$=0.00-0.55, $SSD_{min-max}$=-0.66-0.36; Mountain gorilla: $E_{min-max}$=0.00-0.81, $SSD_{min-max}$=-1.46-0.28; Northern muriqui: $E_{min-max}$=0.00-0.72, $SSD_{min-max}$=-1.17-0.35; Olive baboon: $E_{min-max}$=0.00-0.54, $SSD_{min-max}$=-0.57-1.13; Polar bear: $E_{min-max}$=0.00-0.26, $SSD_{min-max}$=-0.73-0.54; Rhesus macaque: $E_{min-max}$=0.00-0.51, $SSD_{min-max}$=-0.54-0.71; Root vole: $E_{min-max}$=0.00-0.86, $SSD_{min-max}$=-2.54-0.22; Soay sheep: $E_{min-max}$=0.00-0.56, $SSD_{min-max}$=-0.22-0.40; Tammar wallaby: $E_{min-max}$=0.00-0.55, $SSD_{min-max}$=-0.64-0.34; White faced capuchin monkey: $E_{min-max}$=0.00-0.66, $SSD_{min-max}$=-2.66-1.21.

Supplementary material – Data available in COMADRE Version 2.0.1 and results from Step 1 of the framework

Table S1. The metadata used in step 1 of our framework and the respective results presented in the main text. The first four columns represent the information from where Matrix Populations Models (MPMs) were extract precisely as presented in COMADRE 2.0.1. Column titles differ from the database as “SpeciesAuthorComadre” is equivalent to “SpeciesAuthor” and “SpeciesName” is equivalent to “SpeciesAccepted” in COMADRE 2.0.1. The remaining columns present the results of step 1, where we present the raw values of $\Sigma E^{S^{\mu}}_{a_{ij}}$ and $\Sigma E^{S^{\sigma}}_{a_{ij}}$, their respective standard deviation, the stochastic population growth rate λ_s, and the number of available matrices (# matrices). For ByAge, “TRUE” was assigned for MPMs built by age or “FALSE” if otherwise.

SpeciesAuthorComadre	**SpeciesName**	**CommonName**	**Order**	$\Sigma E^{S^{\mu}}_{a_{ij}}$	$\Sigma E^{S^{\mu}}_{a_{ij}}$ **(sd)**	$\Sigma E^{S^{\sigma}}_{a_{ij}}$	$\Sigma E^{S^{\sigma}}_{a_{ij}}$ **(sd)**	**# matrices**	λ
Homo_sapiens_subsp._sapiens	*Homo sapiens sapiens*	Human	Primates	1.003	0.003	1.003	0.004	13	1.064
Alces_alces	*Alces alces*	Moose	Artiodactyla	1.001	0.001	1.001	0.001	13	1.205
Antechinus_agilis	*Antechinus agilis*	Agile antechinus	Dasyuromorphia	1.111	0.111	1.111	0.011	2	0.931
Brachyteles_hypoxanthus	*Brachyteles hypoxanthus*	Northern muriqui	Primates	1.000	0.000	1.000	0.000	12	1.051
Callospermophilus_lateralis	*Callospermophilus lateralis*	Golden-mantled ground squirrel	Rodentia	1.054	0.054	1.054	0.055	9	2.052
Cebus_capucinus	*Cebus capucinus*	White faced capuchin monkey	Primates	1.000	0.000	1.000	0.000	11	1.021
Cercopithecus_mitis	*Cercopithecus mitis*	Blue monkey	Primates	1.000	0.000	1.000	0.000	14	1.036
Eumetopias_jubatus	*Eumetopias jubatus*	Northern sea lion; Steller sea lion	Carnivora	1.005	0.005	1.005	0.002	2	0.904
Felis_catus	*Felis catus*	Feral cat	Carnivora	1.136	0.136	1.136	0.012	1	1.948
Gorilla_beringei	*Gorilla beringei*	Mountain gorilla	Primates	1.000	0.000	1.000	0.000	21	1.027
Hippocamelus_bisulcus	*Hippocamelus bisulcus*	Huemul deer	Artiodactyla	1.002	0.002	1.002	0.001	1	0.996
Lepus_americanus	*Lepus americanus*	Snowshoe hare	Lagomorpha	1.294	0.294	1.294	0.165	2	0.812
Lycaon_pictus	*Lycaon pictus*	African wild dog	Carnivora	1.100	0.100	1.100	0.008	1	1.500
Macaca_mulatta_3	*Macaca mulatta*	Rhesus macaque	Primates	1.000	0.000	1.000	0.001	12	1.127
Macropus_eugenii	*Macropus eugenii*	Tammar wallaby	Diprotodontia	1.013	0.013	1.013	0.012	7	0.981

Marmota_flaviventris_2	*Marmota flaviventris*	Yellow-bellied marmot	Rodentia	1.007	0.007	1.007	0.006	4	0.890
Marmota_flaviventris_3	*Marmota flaviventris*	Yellow-bellied marmot	Rodentia	1.008	0.008	1.008	0.005	4	0.921
Microtus_oeconomus	*Microtus oeconomus*	Root vole	Rodentia	1.000	0.000	1.000	0.001	14	1.028
Mustela_erminea	*Mustela erminea*	Stoat	Carnivora	1.334	0.334	1.334	0.117	2	1.258
Orcinus_orca_2	*Orcinus orca*	Killer whale	Cetacea	1.001	0.001	1.001	0.001	24	0.999
Ovis_aries_2	*Ovis aries*	Soay sheep	Artiodactyla	1.033	0.033	1.033	0.020	3	1.099
Pan_troglodytes_subsp._schweinfurthii	*Pan troglodytes*	Eastern chimpanzee	Primates	1.000	0.000	1.000	0.001	22	0.982
Papio_cynocephalus	*Papio cynocephalus*	Olive baboon	Primates	1.000	0.000	1.000	0.000	19	1.054
Peromyscus_maniculatus_2	*Peromyscus maniculatus*	Deer mouse	Rodentia	1.010	0.010	1.010	0.005	2	1.107
Phocarctos_hookeri	*Phocarctos hookeri*	New Zealand sea lion	Carnivora	1.005	0.005	1.005	0.003	8	1.023
Propithecus_verreauxi	*Propithecus verreauxi*	Verreaux's sifaka	Primates	1.000	0.000	1.000	0.000	12	0.986
Puma_concolor_8	*Puma concolor*	Cougar	Carnivora	NA	NA	NA	NA	10	1.115
Rattus_fuscipes	*Rattus fuscipes*	Bush rat	Rodentia	1.246	0.246	1.246	0.029	2	1.305
Spermophilus_armatus	*Urocitellus armatus*	Uinta ground squirrel	Rodentia	1.016	0.016	1.016	0.011	4	1.125
Spermophilus_armatus_2	*Urocitellus armatus*	Uinta ground squirrel	Rodentia	1.017	0.017	1.017	0.010	3	1.095
Spermophilus_columbianus	*Urocitellus columbianus*	Columbian ground squirrel	Rodentia	1.036	0.036	1.036	0.025	3	1.009
Spermophilus_columbianus_3	*Urocitellus columbianus*	Columbian ground squirrel	Rodentia	1.003	0.003	1.003	0.006	3	1.200
Ursus_americanus_subsp._floridanus	*Ursus americanus*	Florida black bear	Carnivora	1.003	0.003	1.003	0.003	2	1.020
Ursus_arctos_subsp._horribilis_5	*Ursus arctos*	Grizzly bear	Carnivora	1.001	0.001	1.001	0.001	4	1.026
Ursus_maritimus_2	*Ursus maritimus*	Polar bear	Carnivora	1.019	0.019	1.019	0.007	2	0.941
Brachyteles_hypoxanthus_2	*Brachyteles hypoxanthus*	Northern muriqui	Primates	1.000	0.000	1.000	0.000	12	1.111
Cebus_capucinus_2	*Cebus capucinus*	WhiteNAfaced capuchin monkey	Primates	1.000	0.000	1.000	0.000	11	1.059
Chlorocebus_aethiops_2	*Chlorocebus aethiops*	Vervet	Primates	1.075	0.075	1.075	0.087	5	1.187
Erythrocebus_patas	*Erythrocebus patas*	Patas monkey	Primates	1.051	0.051	1.051	0.038	5	1.128
Gorilla_beringei_subsp._beringei	*Gorilla beringei*	Mountain gorilla	Primates	1.000	0.000	1.000	0.000	21	1.053